The role of the novel demethylase KERS complex in fungal development and secondary metabolism

Betim Karahoda MSc, BSc

Maynooth University
National University of Ireland Maynooth

Thesis submitted to Maynooth University for the degree of Doctor of Philosophy

October 2018

Supervisor:

Dr. Ozgur Bayram,

Fungal Genetics & Secondary Metabolism Laboratory,

Biology Department,

Maynooth University,

Maynooth, Co. Kildare

Head of Department:

Prof. Paul Moynagh

Table of Contents

Declaration of Authorship iv
Acknowledgements v
Abbreviations vi
Summary ix

Chapter 1 1

Introduction 1

1.1 Eukaryotic chromatin structure 2
1.2 Control of gene expression by chromatin remodeling 4
1.3 Post-translational modifications of histones 5
1.4 Chromatin Modifiers 7
1.4.1 Histone acetyltransferases 7
1.4.2 Histone deacetylases 8
1.4.3 Histone methyltransferases 9
1.4.4 Histone demethylases 11
1.5 Fungi as model organisms for studying eukaryotic biology 17
1.5.1 Filamentous fungi 18
1.5.2 *Aspergillus nidulans*; a model organism for fungal development and secondary metabolism 19
1.5.3 *Aspergillus flavus*: Producer of carcinogenic aflatoxin 23
1.6 Secondary metabolism in filamentous fungi 25
1.7 Role of chromatin in fungal development and secondary metabolite production 27
1.8 Aim of this project 30

Chapter 2 31

Materials & Methods 31

2.1 Strains, culture and growth conditions of *A. nidulans* 32
2.2 Strains, culture and growth conditions of *A. flavus* 32
2.3 Protein extraction and Western blotting 33
2.5 Tandem affinity purification (TAP) coupled with liquid chromatography-mass spectrometry 35
2.6 HA and GFP purifications 38
2.7 Trypsin digestion and sample preparation 38
2.10 Southern hybridization 40
2.11 Confocal microscopy 40
2.12 RP-HPLC analysis of aflatoxin production 40
2.14 Purification of RpdA activity and HDAC assay 41
2.15 Generation of plasmid constructs and strains of *A. nidulans* 42
2.15.1 Generation and confirmation of deletion and complementation strains 42
2.15.2 Generation and confirmation of epitope tagged strains; HA, TAP, GFP 45
2.15.3 Generation and confirmation of promoter replacement strains 48
2.15.4 Generation of BIFC plasmids for *in vivo* protein-protein interaction 49
2.16 Generation of plasmid constructs and strains of *A. flavus* 51
2.16.1 Generation and confirmation of *kdmB*Δ and *rpdA*Δ strains 51
2.16.2 Generation and confirmation of complementation strains 52
2.16.3 Generation and confirmation of KdmB::3xHA, KdmB::sGFP strains 53
Table 2.1 DNA Oligonucleotides used in this study for *A. nidulans* work. 55
Table 2.2 Plasmids employed in this study for *A. nidulans* work. 61
Table 2.3 *A. nidulans* strains employed in this study. 63
Table 2.4 DNA Oligonucleotides used in this study for *A. flavus* work. 65
Table 2.5 Plasmids employed in this study for *A. flavus* work. 72
Table 2.6 *A. flavus* strains employed in this study. 73

Chapter 3 Results 74

H3K4 demethylase KdmB bridges cohesin acetylation to the histone deacetylase-ring finger complex for Aspergillus nidulans light responses 74
3.1 KERS is a multi-domain tetrameric chromatin remodeling complex consisting of H3K4me3 demethylase KdmB, cohesin acetyltransferase EcoA, histone deacetylase RpdA and ring finger protein SntB 75
3.2 Physical nuclear interaction of KdmB with EcoA, RpdA, and SntB was confirmed via BIFC 79
3.3 All four KERS complex proteins colocalize within the nucleus 85
3.4 Global regulator of fungal development and secondary metabolism LaeA is not required during KERS assembly 86
3.5 Demethylase KERS complex plays crucial roles in growth, asexual and sexual life-cycles of *A. nidulans* 86
3.5.1 Ring finger protein SntB and RpdA are essential for sexual development 92
3.5.2 Complementation of *kdmB* and *sntB* restored sporulation and cleistothecia formation 96
3.5.3 Osmotic stabilization has a positive-effect on conidiation in KERS mutants 97
3.5.4 Cell wall stress factors negatively affect KERS mutants 99
3.5.5 3-Amino-1,2,4-triazole, camptothecin and benomyl negatively affect KERS mutants 100
3.6 H3K4 demethylase KdmB recruits cohesion factor EcoA to heterodimer RpdA-SntB deacetylase-ring finger protein 103
3.7 Ring finger protein SntB recruits class I histone deacetylase RpdA to heterodimer KdmB-EcoA complex 104
3.8 KdmB prevents EcoA proteasomal-dependent degradation 106
3.9 KdmB is required for EcoA stability 109
3.10 KdmB and SntB do not influence total RpdA HDAC activity 112
3.11 Acetylation of Smc3 homolog SudA 105-106 lysine residues is abolished in *ecoA* down-regulation 114

Chapter 4 Results 118

KERS complex is required for development, secondary metabolism and pathogenicity in Aspergillus flavus 118
4.1 KERS complex is conserved in the aflatoxin producer pathogenic fungus *Aspergillus flavus* 119
4.2 KERS complex is essential for light-dependent asexual conidiation, sclerotia development and stress factor responses 125
4.3 Camptothecin negatively affects *A. flavus* KERS mutants while *kdmB*Δ is more resistant against menadione-mediated oxidative stress 129
4.4 KERS is essential for aflatoxin production and crop contamination 132
4.5 Sclerotia development and aflatoxin production are restored in *kdmB* and *rpdA* complementation strains 138
4.6 KdmB and RpdA are global regulators of secondary metabolism gene clusters in *A. flavus* 140

Chapter 5 148

Discussion 148
5.1 KERS, a novel tetrameric demethylase complex consisting multi-domain subunits, is likely conserved among other eukaryotes 149
5.2 KERS complex has a dual role in fungal development: KdmB-EcoA are negative regulators of sexual development while RpdA-SntB are positive-regulators 153
5.3 The tetrameric KERS complex is assembled via association of the heterodimers KdmB-EcoA and RpdA-SntB 156
5.4 SntB mediates EcoA-proteasomal degradation while KdmB protects its nuclear stability to promote the establishment of chromatid cohesion 157
5.5 KERS complex is conserved in the pathogenic fungus *Aspergillus flavus* with distinctive roles 161
5.6 KdmB and RpdA have opposing roles in the regulation of light-induced development 161
5.7 KERS complex is required for the induction of aflatoxin through the *afl* biosynthetic cluster 162
5.8 KdmB and RpdA are global regulators of secondary metabolism most likely mediated by their *in vivo* HDMA and HDAC activities 163
Reference: 166

Appendix A.....182
Appendix B.....221
Appendix C.....243

Declaration of Authorship

This thesis has not previously been submitted to this, or any other University, for any other degree. This thesis is the sole work of the author with the exception of *A. nidulans* RpdA HDAC activity which was carried out by Dr. Ingo Bauer at Medical University of Innsbruck.

_____

Betim Karahoda MSc., BSc.

Acknowledgements

Firstly, I would like to thank Dr. Ozgur Bayram for giving me the opportunity to conduct my research in his laboratory. I appreciate his great supervision and full support throughout my work and the optimal working conditions he provided.

Special thanks to Dr. Kevin Kavanagh and Dr. David Fitzpatrick for being involved in my thesis committee. I would like to thank Prof. Hubertus Haas for agreeing to become an external examiner for my Ph.D. defence. Many thanks to Dr. Paul Dowling for his help in proteomics analysis.

I wish to thank all the members of my department. Caroline Batchelor for training the use of mass spectrometry and Dr. Illona Dix for her help on confocal microscopy studies. Many thanks to administrative staff Theresa Roche, Jean Burbridge and Tina Sidoli O'Connor.

Thanks to all technical staff for their great help particularly Michelle Finnegan, Nicholas Irani, Patricia Colton and Dr. Frances Tinley.

My gratitude goes to Dr. Ozlem S. Bayram for her excellent support with training new methods, helping me on experiments and giving critical advice.

I really appreciate the time with my colleague Dean Frawley. It was always a pleasure working with you and I deeply valued your honesty and I will miss our conversations, lunch and especially €1 coffee breaks. I'd like to thank Nadia Elramli, Leandro Jose De Assis, Hacer Meral and Sibel Seker for pleasant moments in our lab.

I am very thankful to Rose Waldron, Nicola Moloney, Eoin Mulwill, Daragh Cuskelly, Anatte Margalit, Sandra Murphy, Felipe Guapo De Melo, Dearbhlaith Larkin, Dejana Kosanovic, Linan Xu, Lara Manzanares, Maud Sorel and Kevin Goslin for their friendship in the department.

My sincere gratitude goes to Tadgh O Riogain for teaching me the Irish culture, and for his fantastic friendship during my stay in Ireland.

My deepest thanks to my mother Vehibe and father Alifat Karahoda and sisters Fjorda, Belkiz and Bedila for their enormous support during my doctoral study and life. Thanks to my second mother Canan Kaylan and father Ali Riza Kaylan for being such a wonderful parents-in-law.

I'd like to appreciate my brother Alican and Mehtap Kaylan for their continuous support and visits during my research in Ireland.

Finally, I would like to acknowledge my lovely wife Melisa Karahoda for her endless support during challenging times as without her, this achievement would not become possible.

Abbreviations

ATP	Adenosine triphosphate
AF	Aflatoxin
ASPGD	Aspergilli genome database
Bp	Base pair
BSA	Bovine Serum Albumin
cDNA	Complementary deoxyribonucleic acid
COMPASS	Complex Proteins Associated with Set1
ºC	Degree Celsius
Δ	Deletion
DNA	Deoxyribonucleic acid
DEPC	Diethylpyrocarbonate
DIG	Digoxigenin
DMSO	Dimethyl sulfoxide
EDTA	Ethylenediaminetetraacetic acid
FAD	Flavine adenine dinucleotice
GFP	Green fluorescent protein
GMM	Glucose minimal media
h	Hour
HA	Human influenza hemagglutinin
HAT	Histone acetyltransferase
HDAC	Histone deacetylase
HDMT	Histone demethylase
HP1	Heterochromatin protein 1
HMT	Histone methyltransferase
HRP	Horseradish peroxidase
IgG	Immunoglobulin
Jarid	JMJ–AT-rich interacting domain
K	Lysine
kb	Kilo base pairs
kDa	Kilo Daltons
LB	Luria Bertani
LC	Liquid Chromatography
LSD	Lysine-Specific Demethylase

M	Molar (mol/l)
MS	Mass spectrometry
mAU	milli Absorbance Unit
mRNA	Messenger Ribonucleic Acid
MT	Methyltransferase
µ	micro
ml	millilitre
mm	millimetre
mM	millimolar
Min	minute
nm	nanometre
NRPS	Non-ribosomal peptide synthetase
ORF	Open reading frame
PKS	Polyketide synthase
ROS	Reactive oxygen species
RT-PCR	Reverse-transcriptase polymerase chain reaction
RP-HPLC	Reversed-phase High Performance Liquid Chromatography
SAM	s-adenosyl methionine
Sc	Sclerotia
SDS	Sodium dodecyl sulphate
SDS-PAGE	Sodium dodecyl sulphate polyacrylamide gel electrophoresis
SM	Secondary metabolism
sGFP	synthetic green fluorescent protein
ST	Sterigmatocystin
TAE	Tris:acetate:EDTA
TAP	Tandem affinity purification
TEV	tobacco etch virus
TFA	Trifluoroacetic acid
TSA	Trichostatin A
Tris	tris(hydroxymethyl)aminomethane
UV	Ultraviolet
UTR	Untranslated region
WT	Wild type

Summary

Filamentous fungi can be found almost everywhere around the world including soil and food sources. They are capable of producing various secondary metabolites (SM) such as penicillin and carcinogenic mycotoxins. Aflatoxin B1 is the most notorious mycotoxins causing liver cancer which is produced by a filamentous fungus *Aspergillus flavus*. Although it has been shown at the genetic level that chromatin regulation is critical for controlling the expression of SM genes in fungi, a mechanistic view is not well-understood. In this work, a novel tetrameric histone modifying complex ("KERS" complex), containing JARID1-type H3K4 demethylase KdmB, putative cohesin acetyltransferase (EcoA), a class I type histone deacetylase RpdA and a ring finger protein StnB was discovered in model organism *Aspergillus nidulans* and pathogenic fungus *Aspergillus flavus*. Protein similarity analysis revealed that the KERS subunits are conserved from yeast to complex eukaryotes and mammals. The KERS complex couples chromatin regulation of SM gene clusters, fungal development, pathogenicity, and mycotoxin production. The KERS complex assembles in the nucleus and affects the expression of several gene clusters. The first part of this thesis addresses the role of KERS complex in *A. nidulans*. *ecoA* and *rpdA* are essential for *A. nidulans* viability. To study the functions of EcoA and RpdA in fungal light responses, promoters were replaced with tuneable Tet-ON constructs. KdmB and EcoA depletions resulted in increased sexual development indicating their role as negative-regulators of cleistothecia formation, while the loss of RpdA, and SntB completely abolished cleistothecia development presenting them as positive-regulators of sexual development. It was also shown that KdmB is required for EcoA protein stability, while SntB mediates EcoA proteasomal degradation to control nuclear levels. Post-translational modification analysis revealed that EcoA down-regulation results in the abrogation of conserved cohesin subunit yeast Smc3 ortholog SudA acetylation. Interdependence studies revealed that KdmB acts as a scaffold for binding EcoA to the heterodimer RpdA-SntB, whereas SntB recruits RpdA to

the KdmB-EcoA heterodimer. Interestingly, SntB is required for the recruitment of RpdA to the KdmB-EcoA heterodimer, however, RpdA HDAC activity does not require functional SntB or KdmB.

The second part of this work focuses on the role of KERS complex on pathogenic fungus *A. flavus*. The KERS complex was found to be conserved in *A. flavus,* comprising tetrameric KdmB, EcoA, RpdA, and SntB subunits. Similar to *A. nidulans*, *ecoA* was found to be essential for viability in *A. flavus*. In contrast with *A. nidulans*, *rpdA* was deleted successfully in pathogenic fungi. Developmental assays showed that both *kdmB* and *rpdA* are required for sclerotia production, aflatoxin biosynthesis and crop seed contamination in *A. flavus* through the *nsdC*, *nsdD* and *afl* pathways respectively. KdmB/RpdA affected the transcript levels of nearly 80% of the analysed secondary metabolism backbone gene clusters required for the transcription of polyketide synthetases (PKSs), non-ribosomal peptide synthetases (NRPSs) and dimethylallyl tryptophan synthetases (DMATs). It was also shown that both KdmB and RpdA regulate tri-methylation of H3K4me3 and H3K9me3 residues, while RpdA mainly acts on H3K14ac residues as well as H3K36me3. Hence, chromatin modifiers, KdmB and RpdA, are essential for fungal development, aflatoxin production and are key global regulators of SM gene clusters.

The findings in this thesis provide insight into how chromatin modifier protein complexes can have broad effects on growth, development and natural product biosynthesis by regulating epigenetic marks. These results suggest that similar epigenetic mechanisms mediated by the KERS complex are likely conserved in eukaryotes, including pathogenic fungi. Thus, this study will provide support for the development of new strategies to reduce mycotoxin contamination, crop spoilage, disease and to improve yields of valuable fungal natural drugs which will benefit the pharmaceutical industry and improve economic growth.

Chapter 1

Introduction

1.1 Eukaryotic chromatin structure

DNA is the building blocks of cells and is organized within nucleosomes which form the eukaryotic chromatin architecture. 146 bp of DNA is wrapped around two sets of four core histone proteins, namely H2A, H2B, H3 and H4. Each histone octamer is linked with linker histone H1, forming the nucleosome, which becomes folded into higher-order structures (Ausio, 2006, Libertini et al., 1988). Chromatin structure enables highly dense DNA to be extensively packed in a more compact and dense shape, thus preventing possible DNA damage, regulating gene expression and assisting the cell cycle (Venkatesh and Workman, 2015). More densely packed chromatin regions are known as heterochromatin and less densely regions which are accessible for RNA polymerases are termed as euchromatin (Gottesfeld and Carey, 2018). Heterochromatin regions are usually associated with silent DNA regions that are not transcribed (Grunstein and Gasser, 2013). For instance, centromere regions regulate precise segregation of chromosomes during the cell cycle. Additionally, telomeres are also heterochromatin DNA regions which are crucial for chromosome stability and DNA replication (Franzke et al., 2015, Fortuny and Polo, 2018). As opposed to heterochromatin, euchromatin regions are usually associated with actively transcribed genomic regions, easily accessible by certain RNA polymerases for transcription of genes (Lindsay, 2007). Positively charged histones provide an energy in the form of electrostatic interaction to aid the negatively charged DNA folding within the nucleus, thus, nucleic acids are packed into much smaller sizes as a result of DNA coiling (Figure 1.1) (Chandler and Wolffe, 1999). With the advances of electron microscopy technology, there is a better understanding on how histone octamers form hundreds of thousands of nucleosomes to generate repeating histone-containing units in the chromatin fibre (Finch et al., 1975).

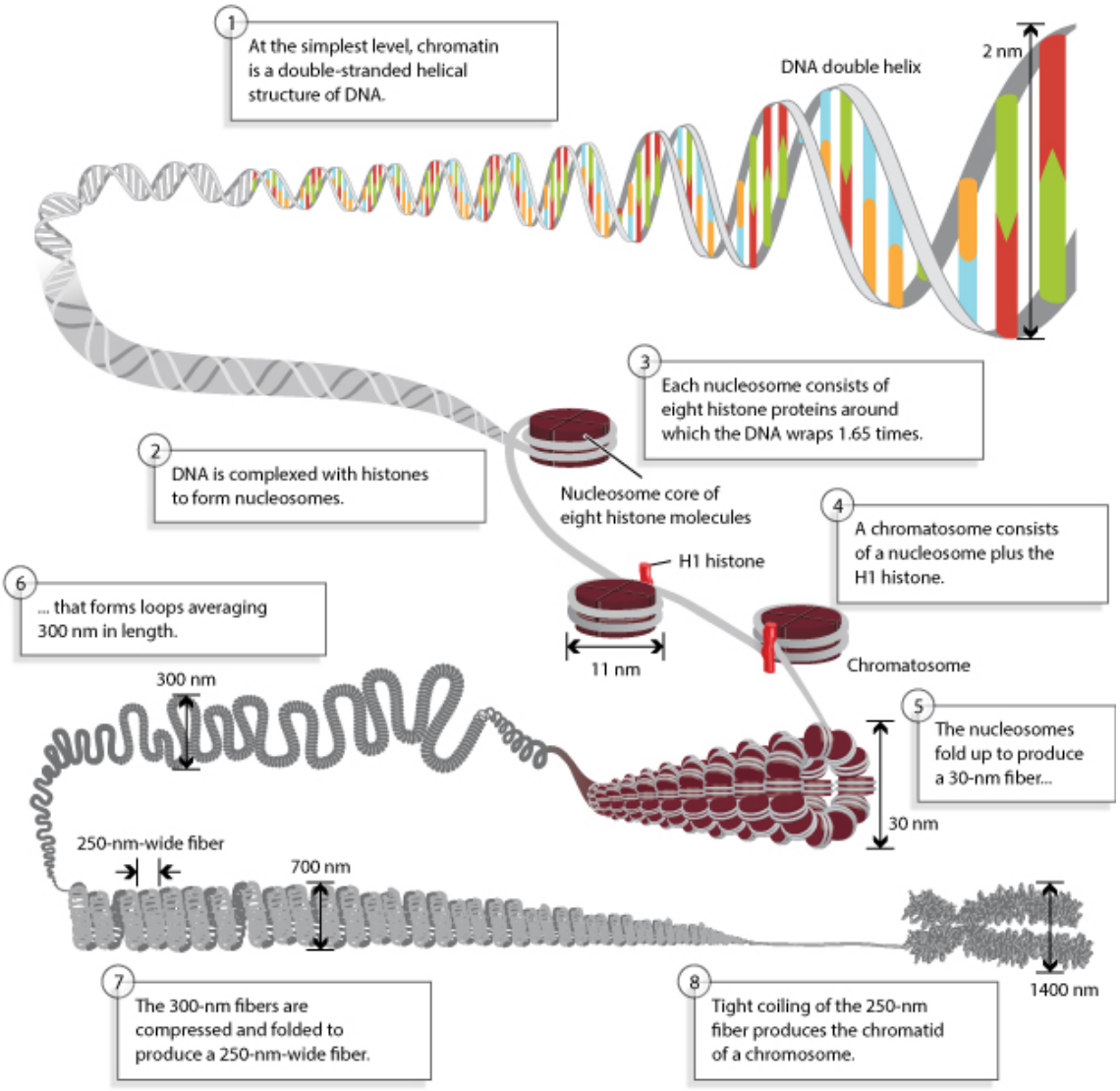

Figure 1.1. From double-stranded helical DNA molecule to chromatid structure. Long eukaryotic genomic nucleic acids possess a dynamic mechanism to pack-up DNA into chromosomes via histones. Positively charged histones condense negatively charged DNA molecules within nuclei to form the chromatin architecture. DNA wraps around eight histone proteins 1.65 times, forming the nucleosome. Groups of nucleosomes by the aid of the linker H1 form chromatin, thus shaping the chromatid of a chromosome (Luger et al., 1997).

1.2 Control of gene expression by chromatin remodeling

DNA accessibility can be regulated in various distinctive ways which are not necessarily mutually exclusive but can cooperate to potentially increase the exposure of DNA for DNA-binding proteins and transcription factors (Travers et al., 2012). ATP-dependent complexes use ATP hydrolysis to disrupt and alter the physical association of histones from DNA molecules. These complexes contain the ATPase subunit required for the hydrolysis reaction which belongs to the SNF2 superfamily of proteins that are divided into two main groups, namely SWI2/SNF2 and the SWI (Zhang et al., 2017). These ATPase subunits are highly conserved from yeast to *Drosophila* and human (Vignali et al., 2000a). Additionally, transcription factors like forkhead box protein A1 (FOXA1) and GATA4 can act on inaccessible chromatin regions to foster loosening of heterochromatin to generate more accessible structures for other transcription factors (Li et al., 2007). Histone chaperons play vital roles in the control of the supply of available histones cooperating with chromatin remodelers during histone deposition. These chaperones are responsible for nucleosome assembly which functions at multiple steps during nucleosome formation. Asf1, CAF-1, and Rtt106 mediate the transport of newly synthesized histone H3–H4 into the nucleus, HIRA and Daxx coordinate replication-independent nucleosome assembly of H3.3-H4 as well as deposition of H3.3-H4 at telomeres (Burgess and Zhang, 2013). Histone variants, other than canonical histones are replication-independent molecules which are present during whole stages of the cell cycle and are required for nucleosome stability and chromatin fibre dynamics (Ausio, 2006).

1.3 Post-translational modifications of histones

Epigenetic regulation contributes to gene activation or repression by initiating or maintaining stable patterns of histone modifications with respect to the environmental signals (Vu et al., 2018). Such modifications can occur on histone N-terminal tail residues which protrude from the nucleosome (Allshire and Ekwall, 2015, Bannister and Kouzarides, 2011). Aberrant histone modifications have been attributed to several disorders and carcinogenesis (Singh et al., 2018, Mochizuki et al., 2017, Nebbioso et al., 2018). Covalent histone post-translational modifications (PTMs) include methylation, acetylation, phosphorylation, ubiquitylation and sumoylation. The chromatin structure can be altered by such modifications resulting in gene silencing or induction. For instance, most histone acetylation sites occur on lysines 9, 14, 18, 23 or 56 located usually at or near promoter regions (Tvardovskiy et al., 2015). Acetylation of histone lysine residues is related to gene activation rendering chromosomal domains more accessible (Deckert and Struhl, 2001). Histone lysine residues can also be mono, di or tri-methylated at their arginine or lysine residues. The most common methylations can occur at histone arginine 2 and lysine 4, 9, 27, 36 and 79 sites. Methylation of H3K4 residue is generally linked with gene activation, while methylation of H3K9 residue is linked with gene repression (Rose and Klose, 2014). Histone phosphorylation mediates the response to DNA damage as well as chromatin remodeling for other nuclear processes (Clayton et al., 2000). In mammals, these modifications occur at serine 139 of the H2AX variant histone which is known as γH2AX. In yeast, similar phosphorylation occurs at serine 129 of H2A. During a mutation leading to the transition of the serine residue to a non-phosphorylatable alanine residue, DNA-damage hypersensitivity increases against agents such as phleomycin and methyl methane-sulphonate (MMS), emphasizing the γH2AX role in DNA repair. This type of modification occurs in all phases of the cell cycle as a response to DNA-damage pathways (Rossetto et al., 2012).

Ubiquitination is an ATP-dependent reaction involving multiple enzymes such as the ubiquitin-activating enzyme (E1), ubiquitin-conjugating enzyme (E2) and ubiquitin-protein isopeptide ligase (E3). H2A and H2B mono-ubiquitination catalysed by these enzymes are important for the regulation of many processes such as transcription initiation, transcription elongation, silencing and DNA repair (Weake and Workman, 2008). Histone ubiquitination processes are reversible where certain ubiquitin-specific proteases can remove these marks by the process known as deubiquitination (Wang et al., 2018). It has been shown that ubiquitination such as H2B monoubiquitination can be a pre-requisite for H3K4 and H3K79 methylation by the Set1 mediated COMPASS complex (Weake and Workman, 2008). Additionally, H2B ubiquitination was shown to affect di- and tri-methylation of H3K4 and H3K79 residues (Weake and Workman, 2008). Members of the small ubiquitin-related modifier (SUMO) protein family are responsible for the sumoylation of histone residues which have similar processes as ubiquitination. It was shown that sumoylation is associated with transcription repression where histone deacetylases and heterochromatin protein1 (HP1) are recruited to all core histones (Shiio and Eisenman, 2003). In another study performed using *Saccharomyces cerevisiae* as a model organism, sumoylation was shown to negatively affect gene expression, mostly occurring at telomeres (Nathan et al., 2006). Sumoylation was shown to have dynamic interplay with histone acetylation and ubiquitination serving as a negative histone modification blocking the occurrence of activating modifications. Histone glycosylation is another less studied histone PTM which targets unique histone residues to bridge nutrient-sensing O-GlcNAc glycosylation with epigenetic regulation (Dehennaut et al., 2014). Histone mono- or poly-ADP-ribosylation is required for DNA repair, replication, and transcription processes. This reversible PTM process can occur in all core histones which mediate nucleosome structure dynamics (Messner and Hottiger, 2011).

1.4 Chromatin Modifiers

1.4.1 Histone acetyltransferases

Histone acetylation is carried out by a protein family called histone acetyl-transferases (HATs) which can occur either at nuclei or in the cytoplasm (Voss and Thomas, 2018). Chromatin regions targeted by HATs enable DNA to be exposed and easily accessible for certain transcription factors required for the initiation of gene expression. For instance, some of the housekeeping genes such as ß-globin loci, which need to be frequently expressed during all stages of growth are acetylated across a broad chromatin domain (Litt et al., 2001). Other examples include male *Drosophila* X chromosome H4K16 acetylation (Gu et al., 1998). Usually, HATs are recruited by multi-subunit transcription factor complexes to the target sites on the chromatin regions. In yeast, HAT complexes can co-ordinately target specific loci with the activators such as VP16, Gcn4, Gal4 and Hap4 (Steger et al., 1998, Eberharter et al., 1998). Such multimeric complex subunits are also conserved in human. Yeast SAGA and NuA4 HAT-containing complexes are recruited by Tra1, which is a TRRAP human ortholog (McMahon et al., 2000). Genome target regions of HAT complexes depends on the type of activators/repressors that are recruited by (Deckert and Struhl, 2001). For instance, SAGA is directed to local H3 acetylation near promoters by VP16, while H4 acetylation occurs in broad acetylation of H4 over 3 kb domain by VP16 recruiting NuA4 complex (Vignali et al., 2000b). Not only are HATs required for transcription initiation by acetylating promoter regions, but they may also assist transcription elongation by facilitating RNA polymerase passage through DNA regions (John et al., 2000). Some early genes in eukaryotes are regulated by HATs and kinases synergistically where certain phosphorylation cascades are required for HAT targeting. An example includes the phosphorylation of serine 10 on H3 followed by acetylation of H3K14 on the same histone tail (Clayton et al., 2000).

Histone acetyltransferases can be classified as “writer” enzymes due to the fact that they can add acetyl residues onto histone residues (Gillette and Hill, 2015).

1.4.2 Histone deacetylases

Histone deacetylases (HDACs) are a superfamily of enzymes which target acetylated histone marks for deacetylation, thus, down-regulating gene expression at the chromatin level (Trojer et al., 2003, Seto and Yoshida, 2014). Since HDACs remove the acetylated histone residues, they can be classified as “eraser” enzymes (Seto and Yoshida, 2014). HDACs fall into two main families, namely Class I HDACs and Class II HDACs. Rpd3 is an example of a Class I HDAC which is highly conserved among eukaryotes, sharing homology with HDAC1, 2, 3, and 8. This class of highly expressed HDACs can act on all histone substrates which retain a highly conserved deacetylase domain. Class I HDACs 1 and 2 share similarity and can act together in some of the chromatin-modifying complexes such as the Sin3, NuRD, CoREST and PRC2 complexes (Yang and Seto, 2003, Meier and Brehm, 2014). Unlike HDAC8, HDAC3 was also shown to be present as a part of the chromatin binding complexes like the N-CoR–SMRT (Yang and Seto, 2008).

Class I HDACs play essential roles during the early development stages of mice. HDAC1 mutant mice cannot survive and show severe proliferation defects and growth retardation (Montgomery et al., 2007). *rpdA* was shown to be essential for growth and development of filamentous fungi *Aspergillus nidulans* and *Aspergillus fumigatus*, whereas deletion of this gene does not cause lethality in budding yeast *Saccharomyces cerevisiae* emphasizing its distinct functional role in yeast (Tribus et al., 2010). It was shown that the RpdA C-terminal is required for its catalytic activity and nuclear localization. Plant-pathogenic fungus *Cochliobolus carbonum* virulence is mediated by another Class I HDAC HosA homologue HDC1, where mutations diminish pathogenicity against maize plants (Baidyaroy et al., 2001). HDACs can be inhibited by a metabolite known as trichostatin A

(TSA), produced by *Streptomyces sp*. This metabolite serves as a potential anticancer drug, which was shown to delay germination and reduce growth and sporulation of pathogenic fungus *A. fumigatus*, making RpdA a promising target for antifungal drug development (Bauer et al., 2016).

1.4.3 Histone methyltransferases

Histone methyltransferases (HMTases) fall into an enzyme family which catalyses the addition of methyl groups onto histone lysine or arginine residues from the *S*-adenosylmethionine (SAM) donor (Murray, 1964). The three classes belonging to the histone methyltransferase family are SET-domain containing proteins, DOT1-like proteins and arginine N-methyltransferase proteins (Trievel, 2004). The first two methyltransferase classes can methylate lysine residues and N-methyltransferase proteins can methylate arginine residues. (Feng et al., 2002, Bannister and Kouzarides, 2011). All three methyltransferase classes have been shown to be capable of methylating histones within chromatin, as well as free histones and non-histone proteins (Huang and Berger, 2008). The first characterized SET-domain methyltransferases were in *Drosophila* SU(VAR)3-9, the Polycomb-group protein E(Z) and the trithorax-group protein TRX (Jones and Gelbart, 1993, Tschiersch et al., 1994). These proteins consist of evolutionary conserved SET and chromatin-associated “chromo” domains. For instance, SUV39H1 or Suv39h proteins are mammalian H3K9 HMTases which are SET-domain-dependent required for heterochromatin formation (Rea et al., 2000). Approximately 130 residues accounting for SET-domain catalytic activity is required for the addition of methyl groups from SAMs as well as recognition and binding to histones. H3K4 methyltransferase CclA is a member of a conserved COMPASS complex required for the regulation of growth and secondary metabolite production in human pathogen *Aspergillus fumigatus* (Palmer et al., 2013). In

cancer patients, mutations in HMTases have been reported resulting in deleterious effects (Meyer et al., 2017). Similarly, overexpression of HMTases were shown to cause diseases (Chen et al., 2018). HMTases and heterochromatin protein 1 (HP1) mutually target H3K9 residues for full repression of transcription of certain genes. The stability of heterochromatin structure is maintained by binding HP1 to H3K9me3. For instance, it was revealed that HP1 is required for the recruitment of HMTases SUV39H1 to H3K9 histone marks by physical interaction in yeast (Yamamoto and Sonoda, 2003). HP1 contains a conserved histone-binding region namely a chromo shadow domain essential for H3K9me3 recognition which maintains full transcription repression and telomere stability (Mishima et al., 2013). Histone methylations were once thought to be irreversible until the discovery of the first H3K4me3 lysine-specific demethylase 1A, LSD1 or KDM1A (Shi et al., 2004). In general, histone acetylation corresponds to the activation of transcription while deacetylation results in gene repression. In comparison to acetylation and deacetylation, methylation has rather mixed and dual function with either activation or repression of SM gene expression (Figure 1.2). Nevertheless, like HATs, HMTases are also considered as "writer" enzymes.

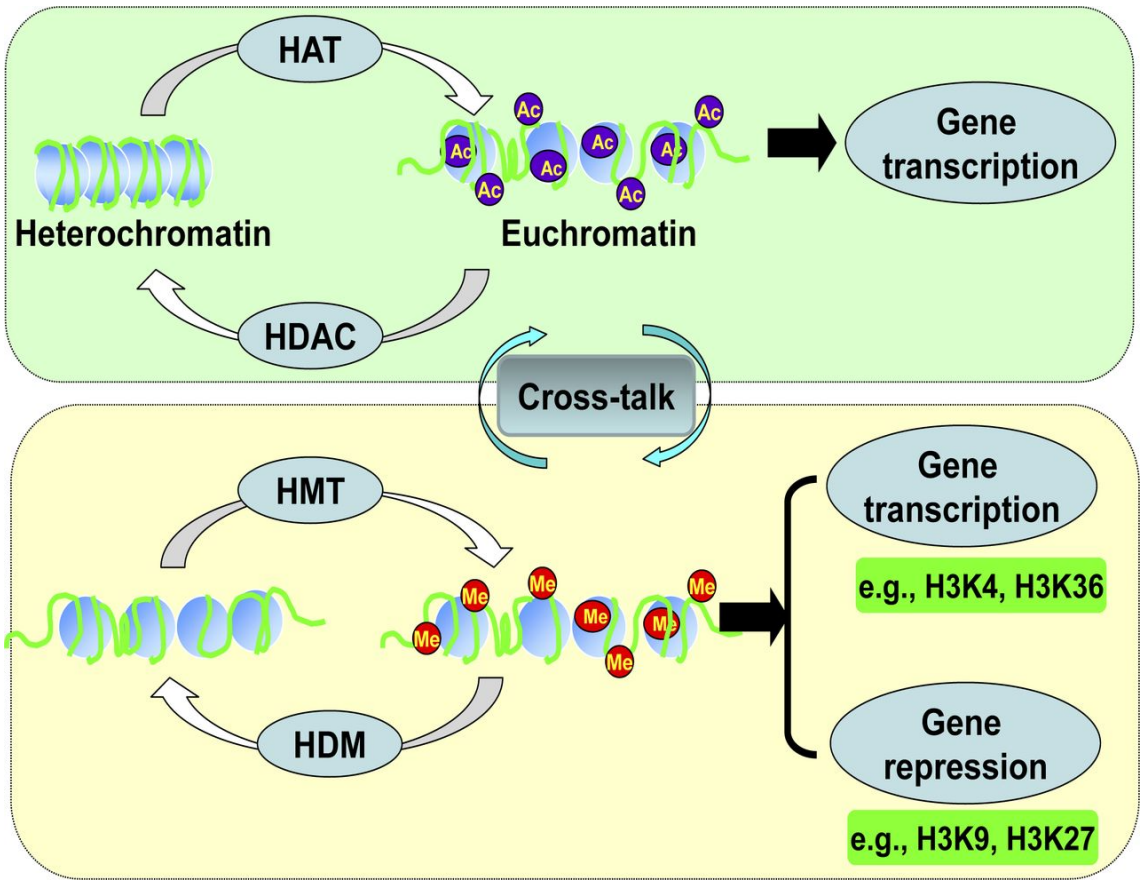

Figure 1.2 The general overview of the processes during histone acetylation and methylation in chromatin biology. Acetylation is usually required for the activation of gene expression, while methylation is histone context-dependent where H3K4 methylation is related to euchromatin formation i.e. activation, H3K9 methylation is related to heterochromatin formation i.e. gene repression (Yao and Li, 2015).

1.4.4 Histone demethylases

Histone demethylases are a group of conserved enzymes required for the removal of histone mono-, di- or tri-methylated lysine or mono-methylated arginine residues. Two families of histone demethylases have been discovered, containing catalytic domains for demethylation activity: the amine oxidases and jumonji C (JmjC) domain-containing, iron-dependent dioxygenases (Tsukada et al., 2006, Whetstine et al., 2006, Cloos et al., 2006). Amine

oxidases use flavin adenine dinucleotide (FAD) as a cofactor while jumonji family demethylases are 2-oxoglutarate-dependent demethylases (Shi et al., 2004, Tsukada et al., 2006). These enzymes are highly conserved from yeast to human consisting of multi-domain regions required for chromatin recognition, methylated histone-binding and catalytic activity (Weaver et al., 2018, Pedersen and Helin, 2010) (Figure 1.3). Plant homeodomain (PHD) fingers and Tudor domains are commonly found in histone demethylases. Other domains include ARID (AT-rich interaction domain), SWIRM (Swi3p, Rsc8p and Moira domain), TPR (tetratricopeptide repeat region) and ZF (Zinc finger) DNA binding domain. The ZF domain is important for demethylase catalytic activity as well as for cofactor binding (Tsukada et al., 2006). TPR, Tudor and PHD domains are considered as "reader" domains as they are not required for catalytic activity of histone demethylases (Weaver et al., 2018). KDM5 H3K4 demethylases contain two PHD domains that are capable of recognizing both unmethylated H3K4 and methylated H3K4 residues, suggesting that these demethylases can identify both their substrate and their products for demethylation reaction (Klein et al., 2014, Gillette and Hill, 2015). Thus, since demethylases are capable of carrying the catalytic reaction for the removal of methyl groups from histones, they are often classified as "eraser" enzymes (Gillette and Hill, 2015).

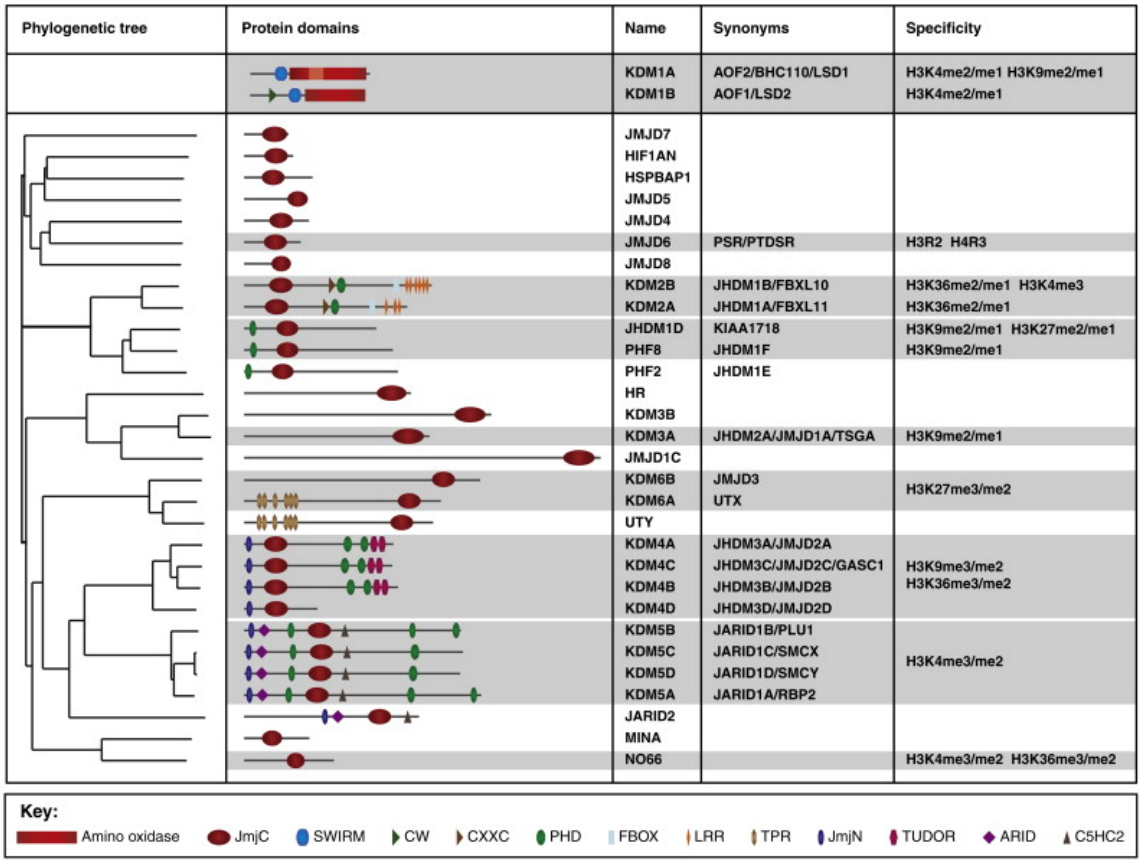

Figure 1.3 Two classes of histone demethylases in humans and phylogenetic tree of JmjC domain containing enzymes. Many histone demethylases possess multi-domain structures necessary for the enzymatic activity, cofactor-binding, histone recognition, and DNA-binding. KDM5 family enzymes catalyse the demethylation of H3K4 di- and tri- methylated residues. (Pedersen and Helin, 2010).

Interestingly, it was shown that demethylases can also scan DNA regions non-specifically for possible target sites. KDM1A was found to interact randomly with DNA regions for scanning and activating the enzyme *in vivo* (Pilotto et al., 2015, Kim et al., 2015). Although these multi-domain enzymes are capable of reading and scanning target regions and can act individually for histone demethylation, recent proteomics data suggest that many characterized demethylases can be recruited by or physically interact with other large protein

complexes during demethylation processes (Figure 1.4). For instance, CoREST is a highly conserved protein complex found in many eukaryotes which not only contains histone demethylase activity by KDM1A but also contains a histone deacetylase enzyme essential for transcription repression (Forneris et al., 2006, Ouyang et al., 2009). This complex was considered a repressive protein complex due to the fact that they act on active histone marks such as removing methyl groups from actively transcribed H3K4me1/2 regions. However, studies also suggested that KDM1A may distinctly interact with another protein complex with an androgen receptor (AR) by targeting repressive histone PTM marks H3K9me1/2 to switch to a transcriptionally active state (Metzger et al., 2005). It was soon discovered that the KDM1A switch from repressive mode to activating mode was a result of a splice variant of KDM1A, known as KDM1A+8a which can interact with the SVIL protein targeting H3K9me1/2 marks (Laurent et al., 2015). Additionally, some demethylases lacking reader domains could still target unmodified histone marks via their Tudor domains by interacting with other protein partners containing multiple functional PHD domains. Examples include vertebrate demethylase complexes KDM5A/JARID1A/RBP2 and KDM5B/JARID1B/PLU1 as well as the repressive deacetylase complex SIN3 (Klose et al., 2006, Klein et al., 2014, van Oevelen et al., 2008). Some initially non-functional demethylases rely on phosphorylating activity of other kinases in order to become fully active. For instance, H3K9me2 demethylase KDM7C/PHF2/JHDM1E becomes active once phosphorylated by PKA which enables the demethylase to interact with another DNA binding protein ARID5B for targeting chromatin regions (Baba et al., 2011).

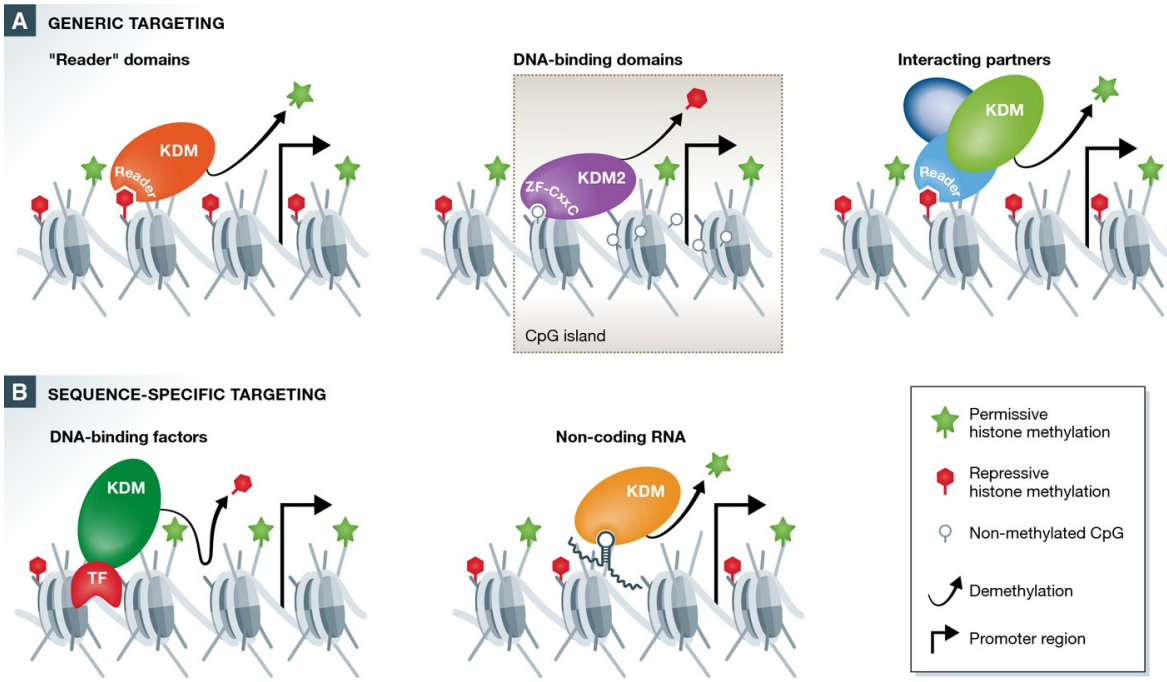

Figure 1.4 Demethylases can act individually or as large protein complexes to modify histone residues. **(A)** Demethylases can scan random regions by their reader domains or by the aid of protein complexes containing multiple-reader domains. **(B)** DNA-binding transcription factors, protein complexes or non-coding RNAs can direct histone demethylases to specific locations on the chromatin. Both pathways can either activate or repress transcription regulation (Dimitrova et al., 2015).

In some other cases, demethylases function alongside SCF E3 ubiquitin ligases for polyubiquitination and proteasomal degradation to control histone demethylase protein levels during appropriate developmental stages (Han et al., 2014, Van Rechem et al., 2011). For instance, Jhd2 is polyubiquitinated by the E3 ligase Not4 for proteasomal degradation in yeast (Huang et al., 2015). Apart from the examples of demethylases interacting with HDACs, KDM6 was shown to interact with MLL H3K4 histone methyltransferase for gene activation. While KDM6 removes repressive H3K27me2/3 marks, SET-containing MLL

methylate H3K4, a dual mechanism for activating and repressing chromatin regions (Issaeva et al., 2007, Cho et al., 2007).

H3K4 methylation usually occurs at promoter and enhancer regions enabling transcription up-regulation which can be altered by KDM5 family demethylases. Recent studies have shown that rather than a repressive role for transcription, these H3K4me demethylases are required to maintain the normal levels of transcription by regulating H3K4me levels at promoter and enhancer regions (Outchkourov et al., 2013). For instance, although H3K4me2/3 marks are transcription activating marks, the same PTM marks are negative transcription marks in enhancer chromatin loci, suggesting dual roles of KDM5 demethylases for switching on/off gene regulation (Kidder et al., 2014). Histone demethylases not only play a role in epigenetic regulation for the cell cycle, development, proliferation, DNA damage response, and chromosome organisation but also they are found to demethylate non-histone related proteins to achieve similar responses. For instance, KDM1A was shown to demethylate P53 which results in alteration of its interaction with 53BP1, a cell cycle regulator (Huang et al., 2007). The same demethylase can remove methyl groups from transcription factor E2F1 as a response to DNA damage by stabilizing E2F1 which in turn leads to apoptosis via induction of E2F1 target genes (Kontaki and Talianidis, 2010, Xie et al., 2011).

In *Drosophila* and *C. elegans*, KDM5 was shown to function during developmental stages. For instance, mutations in the JmjC domain of H3K4 demethylase RBP-2 (retinoblastoma binding protein related 2) result in defective vulva formation in *C. elegans* (Christensen et al., 2007). Mutations in the *Drosophila* counterpart Lid2 (little imaginal discs), a member of the TrxG (trithorax group) of genes maintaining the transcriptional activity of HOX (homeotic) genes, resulted in larval lethality as well as developmental defects (Gildea et al., 2000). In yeast, Jhd2 is responsible for the regulation of genome-wide

transcription levels and control of nucleosome turnover and occupancy as well as mitotic rDNA condensation (Ramakrishnan et al., 2016, Ryu and Ahn, 2014). It was also shown that PHD-H2A interaction was essential for transcriptional regulatory functions of Jhd2 (Huang et al., 2015). Furthermore, PHD finger domain is required for Jhd2 chromatin association and stability is maintained by the JmjN-terminal domain (Huang et al., 2010).

1.5 Fungi as model organisms for studying eukaryotic biology

Fungi and complex eukaryotes have common biochemical pathways which make fungal systems good systems for resolving similar mechanisms in higher eukaryotes. Moreover, some of the medically important fungal organisms have been used to treat certain microbial infections, and many others have contributed to food and agriculture (Brooks, 1949, Alazi and Ram, 2018). Moulds, mushrooms, lichens, rusts, smuts and yeasts fall into this kingdom. Fungi are ubiquitously found throughout the environment and are considered to be large reservoirs for producing various types of natural products known as secondary metabolites (Kobayashi et al., 2007). It is estimated that around 1.5 million fungal species exist in nature and 100,000 have been described so far (Dang et al., 2005, Choi and Kim, 2017). The genome size of typical fungi are around 30-40 Mbp which make them easier for genetic manipulations and transformations due to their genome sizes being smaller than most higher eukaryotes (Meyer, 2008). Dikarya is the sub-kingdom of fungi which hosts almost 98% of known fungi comprising Ascomycota and Basidiomycota phyla (Heitman, 2011). Several Ascomycota species are well-known and thoroughly studied organisms in laboratory research. For instance, genomes of many *Penicillium*, *Neurospora*, *Saccharomyces*, *Schizosaccharomyces* and *Aspergilli* species have been sequenced and they have been widely studied model organisms since they are capable of producing many types of beneficial as well as toxic natural products (Bills and Gloer, 2016). Some of these natural

products have been used as pharmaceutically useful drugs such as penicillin whereas others such as sterigmatocystin or the more toxic compound aflatoxin have been devoted to fungal pathogenicity causing diseases (Hedayati et al., 2007, Kumar et al., 2016). Approximately 10% of known fungi have been classified as being pathogenic to plants, animals or humans (Ziaee et al., 2018). For instance, *Aspergillus fumigatus* is a widely studied organism due to its occurrence in immunocompromised patients causing aspergillosis (van der Linden et al., 2013). *Candida albicans* is another fungus which can colonize and affect patient's gastrointestinal and genitourinary tracts causing candidiasis (Nobile and Johnson, 2015). Despite the presence of many beneficial uses of certain fungi in food biotechnology, pathogenic fungi can cause crop spoilage and mycotoxin contamination leading to massive crop losses each year. Mycotoxins produced by these fungi cause disease in animals and humans when contaminated crops are consumed (Hedayati et al., 2007).

1.5.1 Filamentous fungi

Filamentous fungi can be found almost everywhere around the world, especially in soil or food. They are also commonly found on decaying food or vegetables and can survive in extremely harsh environmental conditions (Powers-Fletcher et al., 2016, Chavez et al., 2015). They are able to grow as vegetative hyphae and can switch between asexual and sexual life cycles. Moulds can be easily grown in laboratory conditions using simple or more complex media and crop seeds (Christensen et al., 2012). They can be selected using various types of selective agents such as vitamins as the auxotrophic markers, or antifungal drugs like antibiotics (Eckert et al., 1999). Fungal optimal growth temperature ranges between 4ºC to 40ºC degrees with an average of 30ºC as the optimal. During favourable conditions, they can germinate and grow rapidly forming white hyphae in the first 24 h, which grows into darker spores with the age of the colony (Adams et al., 1998). In the human host, *Aspergilli*

species can grow within 1-3 weeks causing several types of diseases related to aspergillosis with the most common species being *A. fumigatus*, *A. niger* and *A. flavus* (Powers-Fletcher et al., 2016).

1.5.2 *Aspergillus nidulans*; a model organism for fungal development and secondary metabolism

A. nidulans has been a widely studied organism for understanding fungal cell biology (Goldman and Kafer, 2004). This fungus can undergo three distinct differentiation (Yu, 2010). Spores can germinate to form hyphae and mycelia during vegetative growth (Dynesen and Nielsen, 2003). Both asexual and sexual life-cycles require vegetative growth of hyphae initially. Asexual reproduction occurs in the presence of illumination forming conidial spores from conidiophores which are required for long-term viability as well as spore invasiveness. Thick-walled hyphal cells, alternatively known as foot cells, play major roles in conidiophore formation (Jung et al., 2014). After formation of the foot cells, hyphae aggregates start forming aerial stalks which further create multinucleate vesicles. On top of these vesicles, two types of uninucleate reproductive cells are produced; the metulae and the phialides. Continuous mitotic reproduction of phialides form bunches of conidia spores attached to conidiophores which can be released and dispersed via the air (Adams et al., 1998).

Conidiation is light-induced asexual development regulated by signalling cascades comprising transcription factors required for spore induction (Ruger-Herreros et al., 2011). *brlA* is a conidiation activating gene which encodes the zinc finger transcription factor BrlA (Bristle), which must be expressed in order to activate other genes required for asexual sporulation (Lee and Adams, 1994). Prior to *brlA* expression, the activation of *fluG, flbA,*

flbB, flbC, flbD, and flbE upstream elements are required for the initiation of asexual sporulation (Adams et al., 1998, Lee and Adams, 1996, Alkhayyat et al., 2015). BrlA is required for conidiophore formation and *abaA* (Abacus) activation. *brlA* mutants were shown to lack conidiophore formation, a prerequisite for conidia production (Adams et al., 1988). *abaA*, activated by BrlA, is required for the induction of conidia inducing regulators in the middle phases of the conidiation process during 10-12 h growth phase. *abaA* mutants are not able to undergo asexual reproduction, suggesting a key role of this transcription activator for phialide differentiation and asexual sporulation (Clutterbuck, 1969). AbaA activates *wetA* expression required for conidia pigmentation, and WetA subsequently activates conidium-specific gene expression during activation of late conidia-inducing genes (Andrianopoulos and Timberlake, 1994). VosA is another regulator which couples trehalose biogenesis and conidia activation by repressing *brlA* via feedback regulation for the maturation of conidia (Figure 1.5). Recently, novel regulator AslA for conidia production was discovered in *A. nidulans*. It was shown that AslA is an upstream element of *blrA* up-regulation required for conidiation start-up (Kim et al., 2017).

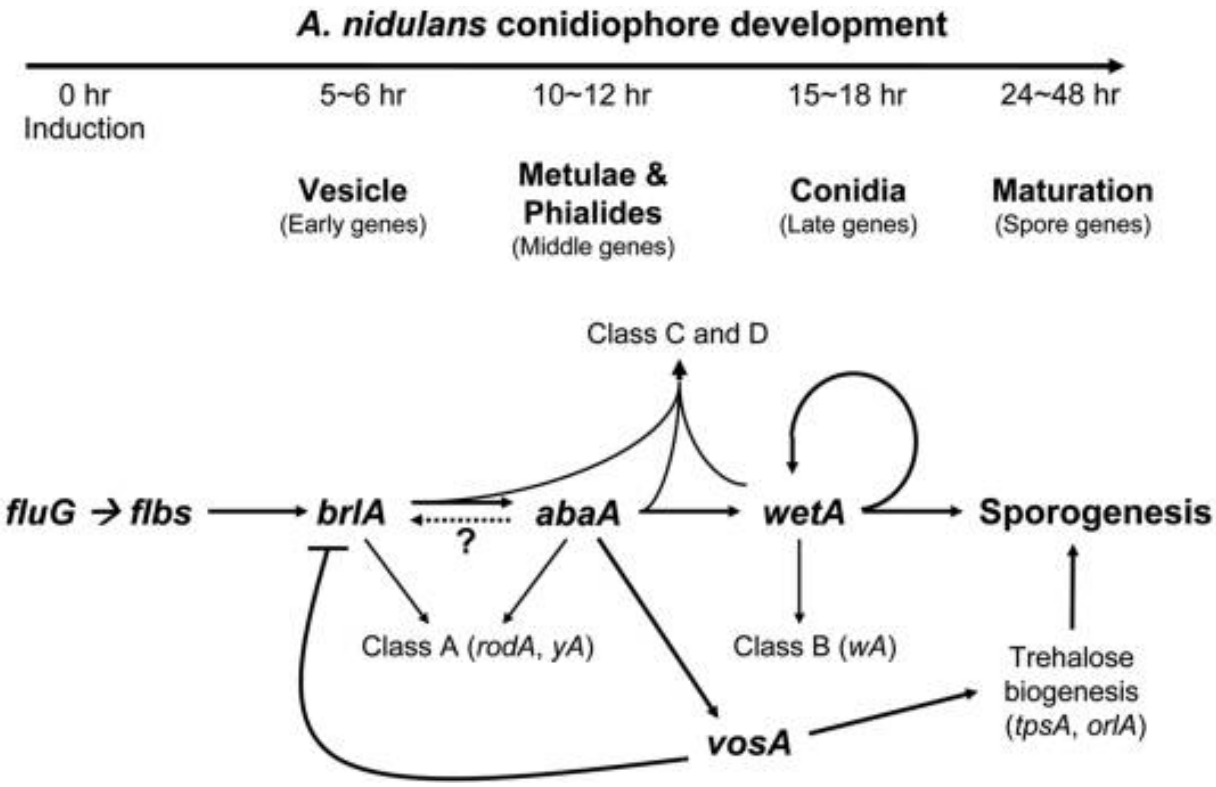

Figure 1.5 Activation of asexual conidiation in *A. nidulans* begins with conidia activating signalling cascades involving transcription factors and activators such as *fluG*, *brlA*, *abaA*, *wetA* and *vosA*. BrlA and AbaA are key regulators of conidia formation (Yu, 2010).

Unlike asexual development, the sexual life-cycle is more complicated and dynamically regulated in *A. nidulans*, which requires highly specialized differentiated cells (Vienken and Fischer, 2006). Genetic recombination in *Aspergilli* species occurs through sexual reproduction from which initially four meiotic ascospore progeny are produced and further mitotic division of these result in eight ascospore progeny within each ascus. Fused hyphae develop cleistothecia surrounded by Hulle cells within fruiting bodies which contain asci (Dyer and O'Gorman, 2012). Since *A. nidulans* is a homothallic species, it can enter sexual reproduction without the need for a compatible partner for crossing. However, this does not necessarily mean that they cannot outcross (Paoletti et al., 2007).

Highly conserved *velvet* family proteins *veA*, *velB*, *velC, vosA,* and *laeA* play essential roles in development and mycotoxin production in *Aspergilli* species (Sarikaya-Bayram et al., 2015) (Figure 1.6). During vegetative growth, VeA-VelB heterodimers are required for sexual development and sterigmatocystin (ST) production by physically interacting with LaeA, a global regulator of secondary metabolism containing a methyltransferase domain (Bayram et al., 2008b, Bayram and Braus, 2012). LaeA is required for the formation of highly specialized types of Hulle cells which play roles in nursing developing fruiting bodies during the dark conditions (Sarikaya Bayram et al., 2010). It was shown that VelC is a positive regulator of sexual development and is required for normal levels of cleistothecia production in *A. nidulans* (Park et al., 2014). In addition to this, a cryptochrome/photolyase-encoding gene, *cryA*, was shown to be a negative regulator of sexual development, repressing fruiting body formation when appropriate environmental conditions are not met (Bayram et al., 2008a). Velvet proteins regulate *A. nidulans* development and SM production by synchronizing with the light receptor phytochrome. Nuclear velvet protein VeA binds to phytochrome, however, in the absence of light, VeA translocates into the nucleus forming a VeA-VelB heterodimer upon its phosphorylation by the MAPK AnFus3 promoting sexual development (Stinnett et al., 2007, Bayram and Braus, 2012). VipC and VapB are nuclear heterodimeric methyltransferases which form the membrane-bound VapA-VipC-VapB complex. Upon release of the heterodimer methyltransferase VipC-VapB into the nucleus, they interact with VeA, inhibiting its nuclear accumulation which negatively regulates sexual development and secondary metabolism and activates asexual differentiation by reducing repressive K3K9me3 levels (Sarikaya-Bayram et al., 2014).

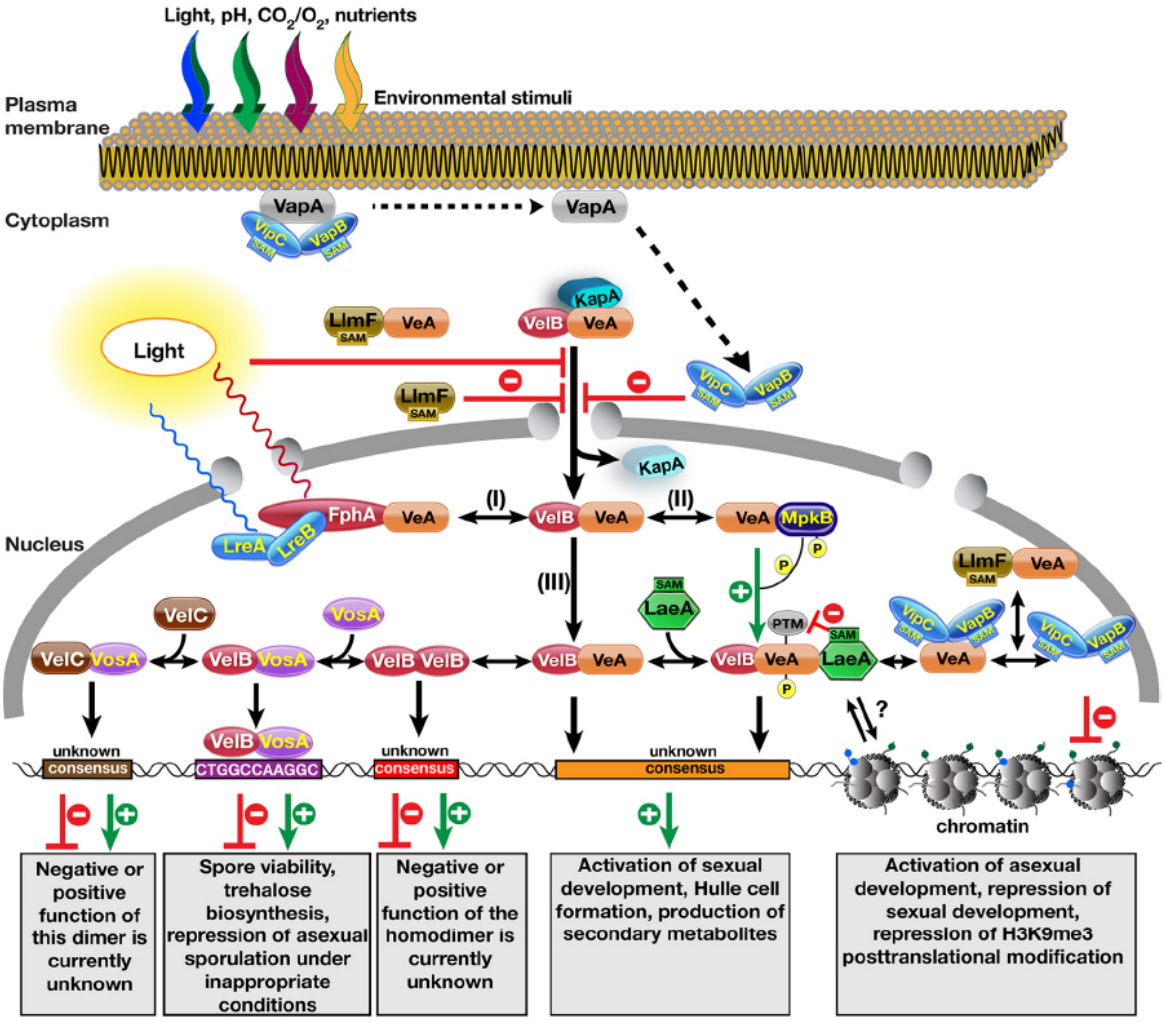

Figure 1.6 A dynamic model illustrating molecular complexes formed by the velvet family proteins and methyltransferases for the control of development and secondary metabolite production as a response to environmental signals in the model fungus *A. nidulans* (Sarikaya-Bayram et al., 2015).

1.5.3 *Aspergillus flavus*: Producer of carcinogenic aflatoxin

The filamentous fungus *Aspergillus flavus* is a plant and human pathogen that is predominantly found in soil as spores or sclerotia structures and is capable of producing a carcinogenic mycotoxin known as aflatoxin (Hedayati et al., 2007). It can contaminate oil-rich seeds such as corn, maize or peanuts during pre or post-harvest (Mitchell et al., 2016).

Every year, approximately $1 billion of economic loss is caused due to aflatoxin contamination in the US alone (Amare and Keller, 2014). Furthermore, it is estimated that around five billion people are susceptible to this fungal poison's threat (Faustinelli et al., 2016). Once aflatoxin is consumed, it is metabolized by the liver, generating reactive epoxide intermediates which create mutations in the tumour suppressor gene *p53*, resulting in liver cancer (Hsu et al., 1991). Among the different types of aflatoxins, B1 is known to be the most toxic carcinogenic compound. *A. flavus* is also an allergen leading to allergic bronchopulmonary aspergillosis in several species. For instance, it can cause Stonebrood (Aspergillosis larvae apium) in honeybees (Scully and Bidochka, 2005, Foley et al., 2014). During favourable conditions, *A. flavus* sporulates producing conidia, while sclerotia, aggregates of hyphal tissue, are formed during starvation to protect the fungus from harsh environmental conditions. The *A. flavus* genome (37Mb) encodes approximately 12,000 functional genes in 8 chromosomes (Rokas et al., 2007). The asexual reproduction mechanism of *A. flavus* is similar to model organism *A. nidulans*. *blrA* and *abaA* play essential roles in the light-stimulated induction of asexual regulatory genes (Cary et al., 2017). The sexual life-cycle, however, is quite different in *A. flavus*. Sclerotia may harbour sexual ascospore depending on the field they occur, although previously it was thought that sclerotia can contain ascospore only in special laboratory conditions (Horn et al., 2016, Horn et al., 2009, Horn et al., 2014). Since *A. flavus* is heterothallic, they contain two mating type alleles *MAT1-1* and *MAT1-2* (Ramirez-Prado et al., 2008). The crosses between individual mating types promote the induction of indehiscent ascospore-bearing ascocarps within the sclerotia structure. However, sclerotia formation does not require two mating types as they can be produced when favourable conditions are met to survive harsh environment (Horn et al., 2009, Horn et al., 2014). Although there is not much information provided for the *A. flavus* sclerotia regulatory mechanism, it was shown that transcription factors NsdC and NsdD are essential for sclerotia formation as well as conidiophore

development (Horn et al., 2016). *A. nidulans* nuclear complexes VeA, velB, and LaeA were found to be conserved in *A. flavus* which mediate development as well as SM production in pathogenic fungus (Chang et al., 2013). LaeA is a negative regulator of VeA and is required for seed pathogenesis. In addition to LaeA, VeA was also shown to be an important factor for seed colonization (Amaike and Keller, 2009).

1.6 Secondary metabolism in filamentous fungi

Development and secondary metabolism are co-dependent, balanced and tightly regulated in filamentous fungi (Calvo et al., 2002). Tremendous research has been performed so far to characterize and study the regulatory mechanisms of secondary metabolite biosynthesis as well as to discover novel metabolites produced by fungi (Gerke and Braus, 2014). Melanins, colourful pigments of the spores, sclerotia and other differentiated structures are the most evident natural products produced by fungi which serve as plant or animal survival factors for UV protectants, antigrowth deterrents, or ROS scavengers. Phytotoxins and mycotoxins are virulence factors produced by fungi, causing a severe and economic loss in agriculture crops (Ahn and Walton, 1997, Bennett and Klich, 2003, Scheu and Simmerling, 2004, Pitkin et al., 2000). Secondary metabolite genes for the biosynthesis of natural products are clustered in fungal genomes (Osbourn, 2010). Penicillin, sterigmatocystin, and aflatoxin gene clusters are widely studied due to their industrially important nature. Both carcinogenic sterigmatocystin and aflatoxin clusters are found in many *Aspergilli* species. Sterigmatocystin, a precursor of aflatoxin, is regulated by a transcription factor and an activator AflR in both *A. nidulans* and *A. flavus* which share common biosynthetic pathways (Yu et al., 1996). *aflR* encodes the binuclear zinc cluster ($Zn(II)_2Cys_6$) transcription factor essential for mycotoxin production (Fernandes et al., 1998). Upstream signalling mechanisms for sterigmatocystin and aflatoxin production involve many regulatory

pathways as a response to environmental factors such as nutrients, hormones and environmental stresses (Yu and Keller, 2005). These signals can be translated to the nucleus by mitogen-activated protein kinase (MAPK) cascades and the cAMP-mediated PkaA cascade for the activation of CreA (carbon metabolism), AreA (nitrogen metabolism) and PacC (pH sensor) regulators (Yu and Keller, 2005, Atoui et al., 2008, Bayram et al., 2009). Mycotoxin productions can be regulated by G-proteins FadA and FlbA through multiple downstream signalling cascades (Hicks et al., 1997). Sterigmatocystin production was found to be completely lost in a *flbA* mutant and FlbA is required for the inactivation of FadA to promote development and SM production (Hicks et al., 1997, Lee and Adams, 1994). It was also shown that FlbA is required for the activation of AlfR for the induction of sterigmatocystin biosynthesis (Hicks et al., 1997). A similar mechanism is also conserved in *A. parasiticus* and *A. flavus* species, with FadA being a negative regulator of aflatoxin biosynthesis. Protein kinase A, PkaA, functions downstream of the FlbA/FadA pathway and is required for normal induction of fungal development and sterigmatocystin production. PkaA acts as a negative regulator of mycotoxin production by inhibiting LaeA, which is essential for sterigmatocystin, penicillin and lovastatin production (Bok and Keller, 2004). Similarly, a small GTP-binding protein (RasA) negatively regulates sterigmatocystin production via *aflR* expression (Shimizu et al., 2003). Velvet protein VeA is also required for mycotoxin production and *aflR* expression in *A. nidulans* (Kato et al., 2003). Furthermore, VeA is conserved and essential for aflatoxin production and sclerotia development in both *A. flavus* and *A. parasiticus* (Cary et al., 2007, Calvo et al., 2004). Penicillin biosynthesis is also dependent on VeA, in which VeA is required for the activation of *acvA*, a delta- (L-alpha-aminoadipyl)-L-cysteinyl-D-valine synthetase (Kato et al., 2003). It is estimated that around 50 gene clusters correspond to secondary metabolite production in *A. nidulans* (Andersen et al., 2013). In *A. flavus*, most likely there are more than 56 gene clusters which correspond to secondary metabolite production, however, the exact number

is still unknown (Umemura et al., 2013). Apart from aflatoxin, *A. flavus* is capable of producing a neural mycotoxin aflatrem, cyclopiazonic acid, piperazine and a cosmetic product kojic acid (Gallagher and Wilson, 1979, Parrish et al., 1966). Despite the biosynthetic pathways of many of these secondary metabolites being well-studied, the epigenetic control mechanisms are still uncertain.

1.7 Role of chromatin in fungal development and secondary metabolite production

Epigenetics play fundamental roles in growth and development from yeast to human (Grunstein and Gasser, 2013). Fungal development and SM production are tightly regulated and quick epigenetic responses are needed for survival against environmental stress responses (Gacek and Strauss, 2012). In fungi, many secondary metabolite gene clusters are found to be located at the sub-telomeric regions suggesting that there must be epigenetic regulation for the activation and repression of certain gene clusters to adapt to a changing environment (Brakhage, 2013, Bok et al., 2009, Rokas et al., 2018). It is also known that the location of gene clusters is a key determining factor for their expression levels being controlled by the state of chromatin structural tension. Several studies have been carried out to prove this phenomenon by transforming gene clusters to different locations on the genome and to analyse their expression level shifts. For instance, a member of the aflatoxin gene cluster in *A. parasiticus*, *ver-1*, was around 500-fold down-regulated when the chromosomal location of this gene was re-located to a different region. On the other hand, chromosomal relocation of *nor-1* caused total loss of expression in two different positions emphasizing the importance of allelic location for the normal expression of secondary metabolism biosynthetic clusters (Liang et al., 1997, Chiou et al., 2002). Chromatin remodellers LaeA, CclA, ClrD, and HepA have been previously shown to play major roles in mediating the activity of secondary metabolism gene clusters (Bok et al., 2009, Palmer et al., 2013). LaeA,

the global regulator of fungal development and secondary metabolism has always been under investigation for whether it is capable of altering post-translational modifications on histone residues due to the fact that LaeA has an S-adenosyl-L-methionine (SAM) domain which is a characteristic feature of methyltransferases, transferring a methyl group from the ubiquitous SAM to either nitrogen, oxygen or carbon atoms (Bok and Keller, 2004). This hypothesis is still not proven yet, however, it is thought that epigenetic marks may be affected in *laeA* mutants which show reduced SM production and increased levels of H3K9 methylation (Bok et al., 2006, Reyes-Dominguez et al., 2010). Normally a *laeA* mutant is unable to produce sterigmatocystin or aflatoxin, however, simultaneous deletions of HDACs and *laeA* were shown to partially recover sterigmatocystin production, suggesting LaeA may have direct or indirect roles on H3K9 acetylation levels (Shwab et al., 2007). Additionally, lack of *laeA* was shown to reduce the pathogenicity of *A. fumigatus* in murine models by reducing the expression levels of SM biosynthetic genes (Sugui et al., 2007). Furthermore, many HDAC inhibitors have been shown to increase SM production by affecting H3K9 acetylation levels which are usually present abundantly in SM gene clusters (Shwab et al., 2007). Penicillin production was positively affected in an HDAC HdaA (Shaaban et al., 2010) deletion. H3K9me3 marks are abundant at heterochromatin regions and they are substrates for heterochromatin protein 1 (HP-1) binding. In fact, HP-1 is essential for heterochromatin formation and for maintaining full transcription repression (Kwon and Workman, 2011). The *A. nidulans* HP-1 homolog, HepA, plays a key role in mediating H3K9me3 repression. It was shown that the deletion of *hepA* resulted in activation of several SM gene clusters emphasizing the repressive role of this protein (Reyes-Dominguez et al., 2010). Another key epigenetic regulator of secondary metabolism biosynthetic gene clusters is a macromolecular protein complex containing the Set1 methyltransferase COMPASS which acts on H3K4 residues (Palmer et al., 2013). Deletion of Set1 *cclA* methyltransferase encoding gene of *A. nidulans* caused significant alteration of the secondary metabolite

profile as well as activation of additional eight metabolites such as monodictyphenone (MDP), emodin and four emodin analogs (Bok et al., 2009). However, deletions of other subunits of the COMPASS complex did not have the same effects. ChIP analysis indicated that H3K4me2/3 marks were reduced which were mostly present at promoter regions of secondary metabolism clusters (Bok et al., 2009).

1.8 Aim of this project

Chromatin modifier complexes play essential roles in proliferation, survival and cellular pathways by regulating histone post-translational modifications epigenetically. Proper transcriptional regulation of fungal development, mycotoxin production, and pathogenicity can be regulated by histone marks. However, mechanism of chromatin control of development and secondary metabolism in fungi is poorly understood. Recently, an H3K4 demethylase, KdmB, was proposed to be a key player of fungal secondary metabolism in *A. nidulans*. Therefore, it was intriguing to know how KdmB controls fungal secondary metabolism and development. The first aim of this thesis was to characterize the protein complexes where KdmB is involved. The second aim of the thesis was to examine how these protein complexes influence the fungal development and secondary metabolite production.

In this thesis, a novel tetrameric histone demethylase complex comprising KdmB-EcoA-RpdA-SntB (KERS complex) was discovered by using various affinity purification methods coupled with Mass Spectrometry (MS) and extensively studied in the model organism *A. nidulans* and pathogenic fungus *A. flavus*.

Overall, this work serves to understand how fungal development, secondary metabolite production, and pathogenicity is controlled at chromatin level by providing a mechanistic view of the functions of the KERS complex using *A. nidulans* and *A. flavus*. By doing so, this study will help to control mycotoxin contamination, reduce crop spoilage, reduce disease and improve the yield of valuable fungal natural drugs which will support the pharmaceutical industry and economic growth.

Chapter 2

Materials & Methods

2.1 Strains, culture and growth conditions of *A. nidulans*

Oligonucleotides (Sigma) and plasmids used in this study are listed in Table 2.1 and Table 2.2. Strains used in this study are listed in Table 2.3. *A. nidulans* AGB551 was used as a host strain for genetic manipulations. Fungal strains were grown in GMM (glucose minimal media): 1 % D-glucose, 1x AspA (70 mM $NaNO_3$, 7 mM KCl, 11.2 mM KH_2PO_4, pH 5.5), 2 mM $MgSO_4$, 1x trace elements (76 µM $ZnSO_4$, 178 µM H_3BO_3, 25 µM $MnCl_2$, 18 µM $FeSO_4$, 7.1 µM $CoCl_2$, 6.4 µM $CuSO_4$, 6.2 µM Na_2MoO_4, 174 µM EDTA). When needed, complete media (GMM with 0.1% yeast extract, 0.2% peptone, 0.1% tryptone and required supplements) was used as a rich culture. For selective media either pyrithiamine (100 µg/ml) or nourseothricin (100 µg/ml) were added where necessary. Biotin (0.02 $\mu g \cdot ml^{-1}$), uracil (50 $\mu g \cdot ml^{-1}$), pyridoxine (0.05 $\mu g \cdot ml^{-1}$) were used as supplements when required. Stress-inducing agents for growth tests of mutant strains supplemented into GMM agar plates were as following; 0.3 µg/ml benomyl for microtubule-stress, 0.3 mM 3-amino 1.2.4 triazol (3-AT) for amino-acid starvation, 1 M KCl, 1 M NaCL, 1.2 M sorbitol for inducing osmotic stress and SDS (0.005%), congo red (20 µg/ml) for inducing cell wall stress. Culture and transformation procedures of *A. nidulans* and *E. coli* used in this study were performed as previously described (Punt and van den Hondel, 1992; Sarikaya Bayram et al., 2010).

For bacterial transformation, DH5α or MACH1 (Invitrogen) *E. coli* competent strains were used to create recombinant plasmids as described previously (Bayram *et al*., 2008b). LB media was supplemented with ampicillin (100 µg/ml) where required.

2.2 Strains, culture and growth conditions of *A. flavus*

Plasmids and oligonucleotides used in this study are listed in Table 2.4 and 2.5 respectively. *Aspergillus flavus* strains used in this study are listed in Table 2.6. For spore cultivation, strains were grown in GMM glucose minimal media with required supplements at 30°C in

1% glucose as the carbon source and nitrate as the nitrogen source. Uracil (50 μg·ml^{-1}) and phleomycin (100 μg/ml) were supplemented when required. For phenotypic analysis, 5μl ($5x10^3$ spores) of spore suspensions were spot inoculated onto petri dishes. Asexual conidiation was quantified at the end of 4 days grown in Potato Dextrose Agar (PDA) supplemented with uridine, uracil under light conditions at 30°C. 0.5 cm diameter of agar surface was removed and resuspended in 500 μl PBS solution prior to counting spores on haemocytometers. For sclerotia analysis, spore suspensions were spot inoculated onto Wickerham medium (Chang et al., 2012) for 21 days under the dark conditions at 30°C. Sclerotia quantification was performed by manually counting the surface of each petri dish. For aflatoxin production, 5μl ($5x10^3$ spores) were spot inoculated onto YES agar medium (20 g yeast extract, 150 g sucrose, 1 g $MgSO_47H_2O$, 20 g agar) for 7 days in the absence of light at 30°C. Stress-inducing agents for growth tests of WT and deletion strains were as following; 0.3 μg/ml Benomyl and 0.1 μg/ml Nocodazole for microtubule-stress, SDS (0.005%), Congo Red (20 μg/ml) and Calcoflour (5 μg/ml) for inducing cell wall stress, CPT (75 μM), Menadione (0.06 mM) and H_2O_2 (2 mM) for inducing oxidative stress.

2.3 Protein extraction and Western blotting

Strains grown in GMM or complete media for 24h at 30°C (for *A. flavus*) and 37°C (for *A. nidulans*) were filtered and washed with PBS using miracloth before harvesting mycelia in liquid nitrogen. Grinded mycelia were lysed using lysis buffer B300; 50 mM Tris [pH 7.6], 300 mM NaCl, 1 mM EDTA, 0.1% NP-40, 10% glycerol, 1 mM dithiothreitol. For nuclear enrichment experiments, nuclei were isolated as described previously (Palmer et al., 2008). The amount of proteins were measured by Bradford assay. 100 μg of total protein was loaded into an SDS-PAGE for whole cell-lysate analysis. For nuclear protein detection, 10 μg of protein was loaded into gels. For primary and secondary antibodies, the following conditions

were used; 1:1000 dilution of Mouse monoclonal α-GFP (Santa Cruz, sc-9996), 1:1,000 dilution of α-HA (Sigma, H9658), 1:2,000 dilution of Goat α-mouse (BioRad, 1706516), rabbit polyclonal α-SkpA (raised in Genescript) 1:2,000 and 1:2,000 Goats α-Rabbit (BioRad, 1706515) antibodies were used in 5% non-fat milk in TBS (0.1% Tween-20). Luminata Crescendo (Millipore, WBLUR0100) was used as a Western HRP substrate. Membrane images were captured by a G-Box (Syngene) and later were stripped off in stripping buffer (Ponceau S Reagent 0.2%, TCA 3%) overnight for SkpA or H3 control experiments. For *A. nidulans* nuclear isolation, approximately $2x10^6$ spores were inoculated onto GMM media for 24 h at 37ºC submerged culture. For *A. flavus* nuclear isolation, approximately $2x10^6$ spores were inoculated into complete media with required supplements for 24 h at 30ºC submerged culture. Solutions and extraction protocol were performed as described previously (Soukup and Keller, 2013). Antibodies (1:2,000 dilution in blocking solution) used for histone PTMs were as following; α-H3 (Abcam; AB1791), α-H3K4me3 (Active Motif; 39159), α-H3K9 (Abcam; ab8899), α-H3K36me3 (Abcam; ab9050), α-H3K9ac (Merck; 07-352), α-H3K14ac (Merck; 07-353).

2.4 RNA extraction and quantitative real time PCR analysis

100 mg of mycelia were collected and mRNA was isolated according to the 'RNeasy Plant Mini Kit' manufacturer's protocol (Qiagen). mRNA was quantified using 'Qubit RNA BR Assay Kit' Protocol (Thermo Fisher). cDNA was synthesised from 1μg of total mRNA using the 'Transcriptor First Strand cDNA Synthesis Kit' (Roche). qPCR reaction mixtures were prepared using LightCycler 480 SYBR Green I Master mix and a LightCycler 480 qPCR (Roche) was used to determine gene expression levels. Beta-tubulin (*benA*) control was used

as a housekeeping gene. Bar charts represent the mean data of two combined biological replicates and 6 combined technical replicates per strain.

2.5 Tandem affinity purification (TAP) coupled with liquid chromatography-mass spectrometry

2.5.1 IgG Immobilization onto NHS-activated magnetic beads

5.0 mg of IgG (Sigma, I4506) was dissolved in 3 ml Coupling Buffer (50 mM Borate) and vortexed vigorously. 300 µl magnetic beads were added into 1.5 ml microcentrifuge tubes and supernatant was discarded using DynaMag™-2 Magnet (ThermoFisher, 12321D). Magnetic beads were washed with Wash Buffer A (1 ml of ice-cold 1 mM HCl) and vortexed gently for 15 seconds. Then, supernatant was discarded using DynaMag™-2 Magnet. 300 µl protein solution (IgG in Coupling Buffer) was added to the magnetic beads and vortexed for 30 seconds. Tubes were incubated at room temperature by rotation for 2 h, vortexed vigorously every 5 minutes for 15 seconds during the first 30 minutes of incubation. Then, tubes were vortexed every 15 minutes. At the end of 2 hours of incubation, beads were collected and supernatant was saved into another tube for future quality control. Samples were washed with 1 ml Wash Buffer B (0.1M glycine, pH 2.0) and vortexed for 15 seconds. Beads were collected and supernatant was removed. This step was repeated one more time. Then, 1 ml ultrapure water was added to the beads and vortexed for 15 seconds. Beads were collected and supernatant was discarded. 1 ml of Quenching Buffer was added to the beads, vortexed for 30 seconds and incubated at room temperature on a rotator for 2 h. Then, beads were collected and supernatant was removed. This step was repeated using ultrapure water and 1 ml Storage Buffer was added to the tubes and mixed well. Beads were collected and supernatant was discarded. This step was repeated two additional times. 300 µl storage buffer was added to the beads, mixed well and stored at 4 ºC for up to 6 months resulting in the final concentration of the IgG-coupled magnetic beads as 10 mg/ml. Optionally, 10 µl

of IgG-coupled magnetic beads was run in SDS PAGE and the presence of IgG subunits with silver staining was checked for quality analysis.

2.5.2 Preparation of cell lysate & TAP tag protein purification

Preparation of buffers used in TAP method were as previously described (Bayram et al., 2012). TAP-tagged fungal strains were inoculated in 800 ml liquid media and grown at 37 ºC/200 g for 24 h. Next day, mycelia were collected using miracloth and washed three times with harvest solution (1x PBS, 100 µM PMSF, 1% DMSO). Remaining liquid was carefully removed by squeezing mycelia using paper towels prior to breaking mycelia down with the help of mortar/pestle in liquid nitrogen. Grounded mycelia were immediately collected and stored in precooled 15 ml falcon tubes and kept in liquid nitrogen. SS34 tubes were pre-cooled for each strain and around 30 ml grounded mycelia product was added to each tube. Protease inhibitors, phosphatase inhibitors and DTT were added to the buffer B250. 12 ml of this buffer was added into each SS34 tube and vortexed vigorously. Tubes were kept on ice for about 10 min. At the end of mixing, tubes were centrifuged at 20,000 g at 4 ºC for 20 min. During centrifugation, 15 ml falcon tubes for each sample were pre-cooled on ice. 50 µl of IgG-coupled NHS magnetic beads was added into a microfuge tube and 1 ml B250 buffer was added to wash the beads. Beads were collected and supernatant was discarded using DynaMag™-2 Magnet (Cat; 12321D, ThermoFisher). Resuspended beads in 200 µl buffer were directly used for the next step. At the end of centrifugation, 12-15 ml supernatant from SS34 tubes was pipetted into pre-cooled falcon tubes and magnetic beads were added into the protein extract and incubated at 4 ºC for 3-4 hours on a rotator. By the end of the incubation period, wash buffers (WB250, and WB150 with protease/phosphatase inhibitors, DTT and PMSF) were prepared. TCB (TEV cleavage buffer (TEV-CB: 25 ml Tris-HCl pH 8.0, 150 mM NaCl, 0.1 % NP 40, 0.5 mM EDTA, 1 mM DTT)) buffer contained only DTT and PMSF. At the end of the 3-4 h incubation, beads were collected and supernatant was

discarded using DynaMag™-15 Magnet (Cat; 12301D, ThermoFisher) for 15 mL tube. 14 mL WB250 was added and mixed by inverting. Beads were collected and supernatant was discarded. This time beads were washed with 14 ml WB150. Next, 10 ml TCB was applied into each sample and mixed carefully. Beads were collected and supernatant was discarded. 1 ml TCB was added to resuspend the beads and solutions were transferred into new 1.5 mL microfuge tubes. 20 µl (200 U) TEV-protease was added to beads and incubated at 4 ºC overnight on a rotating platform. Next day, CBB (25 mM Tris-HCl pH 8.0, 150 mM NaCl, 1 mM Mg acetate, 1 mM imidazole, 2 mM $CaCl_2$, 10 mM β mercaptoethanol) was prepared by adding $CaCl_2$ and B-mercaptoethanol prior to the calmodulin binding step. 50 µl MagnaZoom calmodulin magnetic beads (Cat; 20162002-1, bioworld) was added to 1 ml CBB in 1.5 mL microfuge. Beads were washed and supernatant was discarded. Finally, beads were resuspended in 200 µl CBB. Supernatant from the TEV-treated samples were collected and were added directly into 6 ml of CBB in a 15 ml falcon tube as well as 7 µl of 1 M $CaCl_2$. 200 µl CBB containing calmodulin magnetic beads were added into the same 15 ml falcon tube and incubated for 2-3 h at 4 ºC on a rotator. At the end of incubation, beads were collected and supernatant was removed using DynaMag™-15 Magnet. Beads were washed with 1 ml CBB and transferred into new 1.5 ml microfuge tubes. Next, beads were washed with 1 ml CBB, mixed well by inverting. Supernatant was discarded and this step was repeated 3 additional times. Protein bound beads were directly used for trypsin digestion in the next step.

2.6 HA and GFP purifications

For *A. nidulans*, strains were grown in GMM liquid cultures for 24 h at 37°C at 180 g. For *A. flavus*, strains were grown in complete liquid media for 24 h at 30°C at 180 g. After harvesting and grinding, mycelia were lysed with lysis buffer supplemented with DTT, protease and phosphatase inhibitors. Lysis buffer (B300) was used with the addition of DTT, protease and phosphatase inhibitors (1.5 ml/l 1 M DTT, Complete Protease Inhibitor Cocktail EDTA-free (Roche), 3 ml/l 0.5 M Benzamidine, 10 ml/l phosphatase inhibitors (100 mM NaF, 50 mM NaVanadate, 800 mM β glycerolephosphate) and 10 ml/l 100 mM PMSF). Protein extracts and magnetic beads were incubated at 4°C for approximately 2 h on a rotator prior to trypsin digestion.

2.7 Trypsin digestion and sample preparation

Trypsin digestion protocol for TAP, HA and GFP magnetic beads were performed as described in the manufacturer's ProteaseMAX protocol (Promega, V5111). Trypsin digested magnetic beads were discarded, peptides were precipitated and concentrated using speedy-vac and lastly subjected to Zip-Tip C_{18} (ZTC18S096) purification as described in manufacturer's protocol. Purified peptides were solubilized in Q-Exactive loading buffer (2% acetonitrile, 0.5% TFA in dH_2O) and sonicated for 2 min. Finally, samples were run in a Q Exactive™ Hybrid Quadrupole-Orbitrap™ Mass Spectrometer to detect multiprotein complexes. To analyse multiprotein complexes, MS/MS data processing and identification was performed with Proteome Discoverer 1.3 (Thermo Scientific) and the Discoverer Daemon 1.3 (Thermo Scientific) proteomic software and organism-specific taxon-defined protein databases. AGB551 strain was used as a control to eliminate non-specific protein contaminants in HA and TAP purifications.

2.8 Proteomics analysis and peptide identification

Protein samples were analysed using a Q-Exactive mass spectrometer coupled to a Dionex RSLCnano (Thermo Scientific, Waltham, MA, USA). Peptides were separated using a 2% to 40% gradient of acetonitrile (A: 0.1 % FA, B: 80 % acetonitrile, 0.1 % FA) over 65 min at a flow rate of 250nl/min. The Q Exactive was operated in the data dependent mode, collecting a full MS scan from 300–1650m/z at 70K resolution and an AGC target of $1e^6$. The 10 most abundant ions per scan were selected for MS/MS at 17.5K resolution and AGC target of $1e^5$ and intensity threshold of 1K. Maximum fill times were 10msec and 100msec for MS and MS/MS scans respectively with a dynamic exclusion of 60sec. Samples were analysed using 25 NCE (normalized collisional energy) with 20% stepped energy.

Peptide identification using Proteome Discoverer 1.4 was performed using the Sequest HT (SEQUEST HT algorithm, licence Thermo Scientific, registered trademark University of Washington, USA) and searched against the UniProtKB-SwissProt database (taxonomy: *A. nidulans* and *A. flavus* respectively). The following search parameters were used for protein identification: (1) peptide mass tolerance set to 10 ppm, (2) MS/MS mass tolerance set to 0.02 Da, (3) up to two missed cleavages were allowed, (4) carbamidomethylation set as a fixed modification and (5) methionine oxidation (+15.99492 Da) /acetylation (+42.0106 Da)/phosphorylation (+79.96633 Da) set as a variable modification.

2.9 Protein alignment and ortholog analysis

Data was obtained using basic local alignment tool (BLAST; https://blast.ncbi.nlm.nih.gov/Blast.cgi) with *A. nidulans* and *A. flavus* KERS protein sequences as reference. Listed orthologs correspond to the proteins of highest scores

obtained from the most significant alignments while values represent percentages of identification of protein sequence

2.10 Southern hybridization

Southern blot hybridization experiments were carried out using the Roche DIG Nucleic Acid Detection Kit (Roche, 11175041910). Amplification of either 5'UTR or 3'UTR regions (each yielding approximately 1.2 kbp) used as probes were carried out using the non-radioactive digoxigenic (DIG) labelling kit (Roche, 11093657910).

2.11 Confocal microscopy

Strains expressing sGFP and mRFP were grown in Lab-Tek chambered Coverglass W/CVT (Thermo Scientific, 155360) in 400 µl GMM for 16 h at 29ºC. For *A. flavus* experiments, DRAQ5 (BioStatus Limited, DR50050) with 1:10,000 dilution was used for nuclear staining 30 minute prior to imaging under microscope. Microscopic images were captured using Olympus FV1000 confocal microscopy in 60x magnification.

2.12 RP-HPLC analysis of aflatoxin production

To analyse aflatoxin levels from culture media, approximately 2 cm of agar cores were removed from the centre of culture plates and were subjected to chloroform extraction to collect the organic phase. Samples were dried under speedy-vac and resuspended in methanol for HPLC analysis. To analyse aflatoxin from infected peanuts, one infected peanut seed for each strain was collected and incubated for 30 min with 6 ml

chloroform:dH_2O (v/v) at 4ºC. Samples were centrifuged at 4000 g for 15 min at 4ºC. Organic phase was transferred into microfuge tube. Chloroform was dried out under speedy-vac and samples were resuspended in methanol prior to HPLC analysis. 3 biological replicates were prepared for each experiment. The same procedure was repeated twice. WT was adjusted to 100%.

2.13 Pathogenicity tests

Pathogenicity assays were performed similar to previously described (Christensen et al., 2012). Skins of raw peanut seeds were peeled off, washed with ethanol for 5 min and rinsed with sterile water for 5 min. Rinsing step was repeated three more times and then seeds were let air dry for 30 min under sterile cabinet. Ten peanut seeds were placed into sterile 50 ml centrifuge tubes and incubated with $5x10^3$ conidia spores in PBS for 30 min on shaker at room temperature. Non-infected peanut seeds were used as mock. Ten infected peanut seeds for each strain and mock were placed onto sterile cellulose paper and covered with petri dish. Samples were incubated at 30ºC under the dark condition for five days.

2.14 Purification of RpdA activity and HDAC assay

IgG pull-downs were performed as described by Bayram et al., (2012) with minor modifications. Strains were grown in shaking culture for 14 h at 37 °C at a density of 5 x 10 6 conidia per ml in GMM with appropriate supplementation (3 flasks - 250 ml each). Lyophilized mycelia (approx. 1.2-1.5 g each) were ground to powder in a MixerMill (Gretsch) and resuspended in 6 ml of buffer B250 per g dry weight. After centrifugation (40,000 x g for 30 min at 4 °C), fungal extracts were batched with 300 µl of IgG Sepharose (GE Healthcare) at 4 °C for 2-3 h on a rotator. After washing, elution was performed by

TEV cleavage over night at 4 °C in TCB including 10 % glycerol. Eluates were aliquoted, snap frozen in liquid nitrogen and kept at -80 °C until further usage. Enzymatic activity of enriched RpdA complexes was measured in triplicates using [H-3]-acetate prelabelled chicken histones as substrate as described (Trojer et al., 2003). Briefly, 30 µl of the IgG eluate were mixed with 20 µl of WB150 and 10 µl of labelled histones and subsequently incubated for 60 min at 25 °C.

2.15 Generation of plasmid constructs and strains of *A. nidulans*

2.15.1 Generation and confirmation of deletion and complementation strains

pUC19 (Sigma, D3404) was used as a recipient plasmid to generate plasmid constructs for *A. nidulans* transformation. *Sma*I site was digested and used to integrate DNA fragments. *A. nidulans* A4 (FGSC stock centre) genomic DNA was used as template for the amplification of PCR fragments. All DNA fragments were amplified using Q5 High Fidelity DNA Polymerase kit (New England Biolabs). *Taq* polymerase was used to verify positive colonies after each bacterial transformation.

For deletion cassettes of *kdmB* and *sntB*, a ~2.0kbp *ptrA* fragment was released from pME3024 circular plasmid by *Sfi*I digestion. Approximately 1.2kbp of upstream and terminator regions (OZG610/611, 612/613 for *kdmB*, OZG752/753 and 754/755 for *sntB*) were amplified with primers containing 16 bp overhang homologous regions with pUC19 and *ptrA* sequence prior to fusing to *ptrA* cassette. Three fragments were then fused into pUC19-*Sma*I region by In-Fusion HD cloning kit (Clontech, 121416) as described in the product user manual. Resulting plasmids were digested by *Swa*I and transformed into recipient AGB551 strain to create ANOB226 (*kdmB*Δ*::ptrA*) and ANOB254 (*sntB*Δ*::ptrA*). Similarly, *kdmB* and *sntB* mutants were constructed with *pyrG* or *pyroA* markers. *pyrG*

cassette was amplified using OZG695/OZG694 oligonucleotides yielding ~1.9kbp fragment. *pyroA* marker was amplified using OZG696/OZG694 oligonucleotides yielding ~1.6kbp fragment. These were fused to *kdmB* and *sntB* flanking regions yielding following deletion plasmids pBK53 (*kdmB*Δ*::AfpyrG*) and pBK128 (*sntB*Δ*::pyroA*), respectively. *kdmB*Δ*::AfpyrG* was amplified (BK337/BK338, yielding ~4.2 kbp) and transformed into AGB551 to create ANBK53. Similarly, *sntB*Δ*::pyroA* was amplified (BK568/BK569, yielding ~3.9 kbp) and transformed into ANBK83.1 to create ANBK112.

To generate complementation strain for *kdmB*Δ*::ptrA*, ~8.4 kbp genomic locus of *kdmB* (BK389/390) was fused into pOSB114 *Swa*I-digested linear plasmid by In-Fusion HD cloning kit yielding pBK74. Similarly, to generate complementation strain for *sntB*Δ*::ptrA*, ~8.4 kbp genomic locus of *sntB* (BK391/396) was fused into pOSB114 SwaI-digested plasmid by In-Fusion HD cloning kit yielding pBK75. The resulting complementation plasmids (pBK74, pBK75) were transformed into *kdmB*Δ*::ptrA and sntB*Δ*::ptrA* recipients respectively. *pyroA*$^{+}$ transformants were selected and the mRNA expression levels of *kdmB* and *sntB* were confirmed by RT-qPCR using gene-specific oligonucleotides.

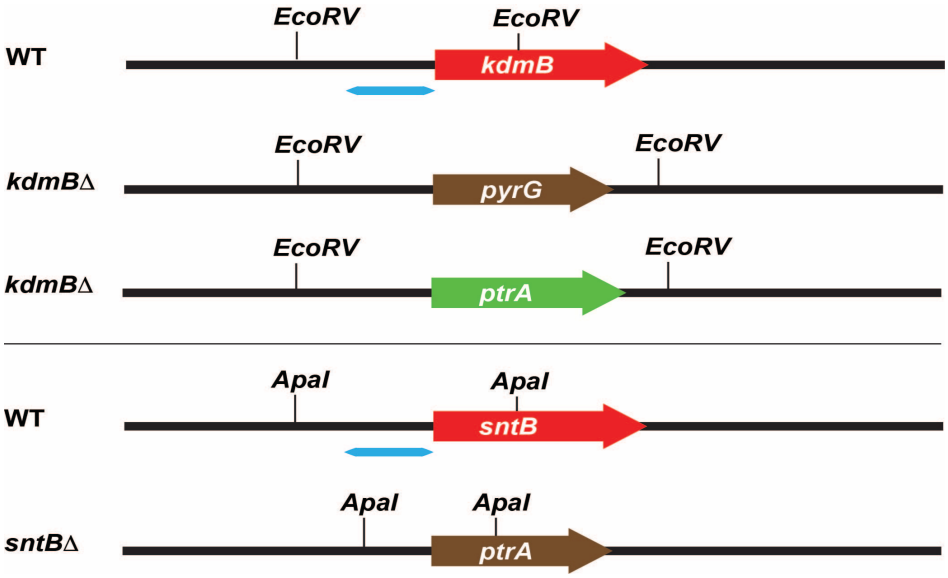
WT
EcoRV
EcoRV
kdmB
kdmBΔ
EcoRV
EcoRV
pyrG
kdmBΔ
EcoRV
EcoRV
ptrA
WT
ApaI
ApaI
sntB
sntBΔ
ApaI
ApaI
ptrA

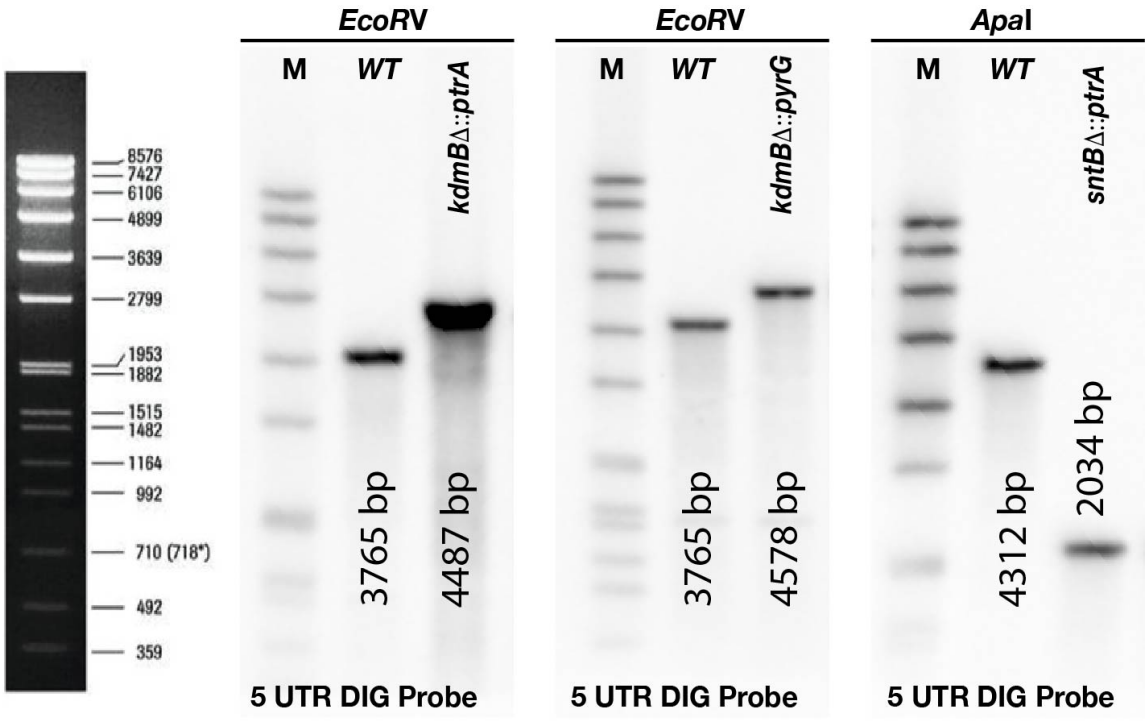
8576
7427
6106
4899
3639
2799
1953
1882
1515
1482
1164
992
710 (718*)
492
359
EcoRV
M
WT
kdmBΔ::ptrA
3765 bp
4487 bp
5 UTR DIG Probe
EcoRV
M
WT
kdmBΔ::pyrG
3765 bp
4578 bp
5 UTR DIG Probe
ApaI
M
WT
sntBΔ::ptrA
4312 bp
2034 bp
5 UTR DIG Probe

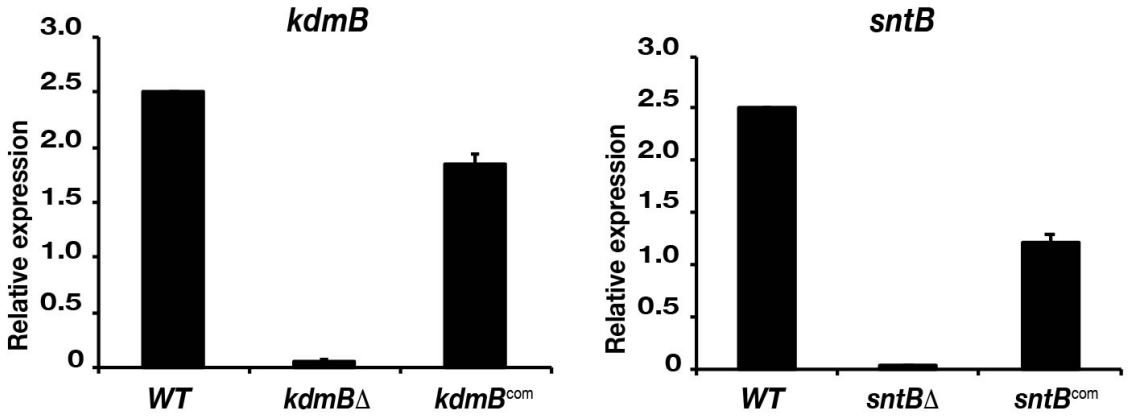
kdmB
Relative expression
3.0
2.5
2.0
1.5
1.0
0.5
0
WT
kdmBΔ
kdmBcom
sntB
Relative expression
3.0
2.5
2.0
1.5
1.0
0.5
0
WT
sntBΔ
sntBcom

Figure 2.1. Confirmation of *kdmB* and *sntB* deletion and complementation strains in *A. nidulans*. *kdmB* and *sntB* deletion strains were confirmed by Southern blot analysis with the digestion strategy in the schematic representation. Blue color indicates the DIG-labelled DNA probe binding region. Approximately 1.2 kbp 5UTR DNA fragment was amplified and detected using DIG-High Prime DNA Labelling and Detection Starter Kit II (Cat. 11585614910). DNA marker for comparison DNA fragments were used from Roche DNA Molecular Weight Marker VII (Cat no: 11209264001). (Lower panel: graphs) RT-qPCR analysis was performed using the total RNA extracted from WT, deletion and complementation strains at the end of 24 h vegetative growth at 37ºC. *benA* was used as a housekeeping gene for relative quantification $2^{\Delta\Delta Ct}$.

In order to create deletion plasmid construct of *laeA*, *Aspergillus fumigatus pyrG* marker was amplified from plasmid pME3858 using OZG694 and OZG695 primers yielding a 1.89 kbp fragment. To create pBK14 (*laeA*Δ*::AfpyrG*), 5' UTR (BK37/BK38) and 3' UTR (BK39/BK40) regions were amplified by using the WT genomic DNA of AGB551 strain. These fragments were fused to *Sma*I-digested pUC19 by using In-Fusion HD Cloning kit, yielding pBK14 from which *laeA*Δ*::AfpyrG* cassette ~4.8 kbp was amplified (BK55/56) and transformed into recipient fungal strain.

2.15.2 Generation and confirmation of epitope tagged strains; HA, TAP, GFP

For the generation of *ctap*, *sgfp* and *3xha* tagged *kdmB*, *ecoA*, *rpdA*, *sntB* strains, a similar strategy was used to create circular plasmid DNA. These epitope tags were fused into upstream and terminator regions of corresponding genes. *ctap-nat*R and *sgfp-nat*R fragments were amplified using OZG916/OZG927 yielding ~1.9kbp and 2.1kbp fragments

respectively. *3xHA-pyrG* fragment was amplified using OZG916/OZG694 oligonucleotides yielding ~2.7 kbp fragment.

In order to create GFP and TAP fusions of KdmB, ORF (open reading frame) of *kdmB* (OZG552/550) and 3'UTR (OZG551/553) were amplified and fused to *ctap-natR* and *sgfp-natR* using fusion PCR (nested oligos OZG548/549), these *kdmB::ctap::natR* and *kdmB::sgfp::natR* PCR products were transformed into WT recipient strain. To construct SntB::cTAP and SntB::sGFP, 1 kb promoter including ORF of *sntB* (OZG1037/1039) and 3'UTR (OZG1040/1041) were amplified and fused to *sgfp* and *ctap* in *Sma*I site of pUC19 leading to plasmids pOB487 (*sntB::sgfp::natR*) and pOB488 (*sntB::ctap::natR*). Cassettes were released by digesting the plasmids with *Pme*I. Similarly, *rpdA* (OZG1033/1034, promoter and ORF, OZG1035/1036 3'UTR) and *ecoA* (OZG1042/1043, promoter and ORF, OZG1044/1045 3'UTR) were amplified and fused to *sgfp* and *ctap* creating the plasmids, pOB485 (*rpdA::sgfp::natR*), pOB486 (*rpdA::ctap::natR*), pOB489 (*ecoA::sgfp::natR*), pOB490 (*ecoA::ctap::natR*).

To create *kdmB::3xha::AfpyrG* fusion plasmid, *kdmB* ORF was amplified using BK27/BK28 oligonucleotides which overhangs complementary to pUC19 from 5' end and GGGSGG linker from 3'end. 3'UTR region of *kdmB* was amplified using BK29/BK30 where BK29 overhangs with *pyrG* from 5' site and BK30 overhangs pUC19 from 3' site. Three fragments were fused into the *Sma*I-site of pUC19 by in-Fusion HD cloning kit. This resulted in plasmid pBK11 which comprises the *kdmB*::3x*ha*::*AfpyrG* fusion cassette when amplified by OZG549/OZG552 oligonucleotides yielding ~5.0 kbp fragment.

To create *ecoA*::*3xha*::*AfpyrG* fusion cassette, OZG1042/BK9 were used to amplify *ecoA* fragment from 5'UTR yielding ~1.77 kbp. *Pme*I site and pUC19 15 bp overhang region were introduced to 5' end of OZG1042. BK8/OZG1045 were used to amplify ~2.2 kbp region of *ecoA* 3'UTR. Similarly, 15 bp overhang sequence of *pyrG* 3'end was introduced

into 5’ end of BK8. *Pme*I and 15 bp overhang sequence of pUC19 was introduced into 5’end of OZG1045. Three fragments were fused into the *Sma*I-site of pUC19 resulting in plasmid pBK3 which comprises the *ecoA*::3x*ha*::*AfpyrG* fusion cassette when digested by *Pme*I restriction enzyme yielding ~6.6 kbp linear fragment.

To create *rpdA*::*3xha*::*AfpyrG* fusion cassette, OZG1033/BK2 were used to amplify *rpdA* fragment from 5’UTR yielding ~2.7 kbp. *Pme*I site and pUC19 15 bp overhang region were introduced to 5’ end of OZG1033. BK5/OZG1036 were used to amplify 806 bp region of *rpdA* 3’UTR. Similarly, 15 bp overhang sequence of *pyrG* 3’end was introduced into 5’ end of BK5. *Pme*I and 15 bp overhang sequence of pUC19 was introduced into 5’end of OZG1036. Three fragments were fused into the *Sma*I-site of pUC19 resulting in plasmid pBK1 which comprises the *rpdA*::3x*ha*::*AfpyrG* fusion cassette when digested by *Pme*I restriction enzyme yielding ~6.2 kbp linear fragment.

To create *sntB*::*3xha*::*AfpyrG* fusion cassette, OZG1037/BK7 were used to amplify *sntB* ORF yielding ~5.9 kbp. *Pme*I site and pUC19 15 bp overhang region were introduced to 5’ end of OZG1037. BK6/OZG1041 were used to amplify ~1.23 kbp region of *sntB* 3’UTR. Similarly, 15 bp overhang sequence of *pyrG* 3’end was introduced into 5’ end of BK6. *Pme*I and 15 bp overhang sequence of pUC19 was introduced into 5’end of OZG1041. Three fragments were fused into the *Sma*I-site of pUC19 resulting in plasmid pBK2 which comprises the *sntB*::3xha::*pyrG* fusion cassette when digested by *Pme*I restriction enzyme yielding ~9.6 kbp linear fragment.

To create *sudA*::*3xha*::*AfpyrG* and *sudA*::*sgfp*::*AfpyrG* fusion cassettes, *3xha::AfpyrG* and *sgfp::AfpyrG* fragments were amplified using OZG916/694 from plasmids pOB430 and pOB435 respectively. To create pBK87, ORF (BK444/BK445) and 3’ UTR (BK435/BK436) regions were amplified by using the WT genomic DNA of A4 strain. These two fragments and *3xha::AfpyrG* were fused to *Sma*I-digested pUC19 by using

In-Fusion HD Cloning kit, yielding pBK87 from which *sudA::3xha::AfpyrG* cassette was amplified (BK446/438) and transformed into recipient fungal strain. Similar strategy was performed to create pBK88. ORF (BK444/BK445) and 3' UTR (BK435/BK436) regions and *sgfp::AfpyrG* were fused to *Sma*I-digested pUC19 by using In-Fusion HD Cloning kit, yielding pBK88 from which *sudA::sgfp::AfpyrG* cassette was amplified (BK446/438) and transformed into recipient fungal strain. *pyrG*+ transformants were selected in the absence of uridine, uracil and epitope tags of *sudA* were confirmed by Southern hybridization. The expression of SudA::sGFP was further confirmed by Western blotting using α-GFP antibody.

2.15.3 Generation and confirmation of promoter replacement strains

In order to generate pOB549, pCH008 was digested by *Pst*I and *Acc65*I to remove *ptrA* marker. OZG1077/11845 was used to amplify *pyroA* cassette (~1.7 kbp) by using pOB508 as a plasmid template. The resulting *pyroA* fragment was fused to *Pst*I/*Acc65*I-digested pCH008 to create pOB549. For generation of *ecoA* (pBK32), *rpdA* (pBK33) Tet-ON-*pyroA* constructs, pOB549 was digested with *Swa*I yielding two fragments for the insertion of upstream and ORF (open reading frame) fragments of *ecoA* and *rpdA*. To generate pBK32, BK127/BK129 were used to amplify ~1.21 kbp fragment of *ecoA* 5'UTR harbouring 16bp pUC19 overhang region from 5' end and 16 bp *pyroA* region from 3' end. Similarly, BK130/BK131 were used to amplify ~1.3 kbp ORF region of *ecoA* harbouring 16 bp homology with Tet-ON sequence at 5' end and 16 bp *sgfp* homology at 3' end. Four linear fragments were mixed and fused into circular plasmid by in-Fusion HD cloning kit. The resulting plasmid resembled *tetO7::Pmin::ecoA::pyroA* cassette when amplified by BK128/BK132 yielding ~6.23 kbp of linear fragment. Similarly, for pBK33 construct, BK133/BK135 were used to amplify ~1.22 kbp fragment of *rpdA* 5'UTR harbouring 16bp

pUC19 overhang region from 5' end and 16 bp *pyroA* region from 3' end. Similarly, BK136/BK137 oligonucleotides were used to amplify ~1.52 kbp ORF region of *rpdA* harbouring 16 bp homology with Tet-ON sequence at 5' end and 16 bp *sgfp* homology at 3' end. Linear fragments harbouring 16 bp homology sequences at 5' and 3' ends were fused to circular plasmid by in-Fusion HD cloning kit. The resulting plasmid resembled *tetO7::Pmin::rpdA::pyroA* cassette when amplified by BK134/BK138 oligonucleotides yielding ~6.56 kbp of linear fragment which was transferred into fungal recipient.

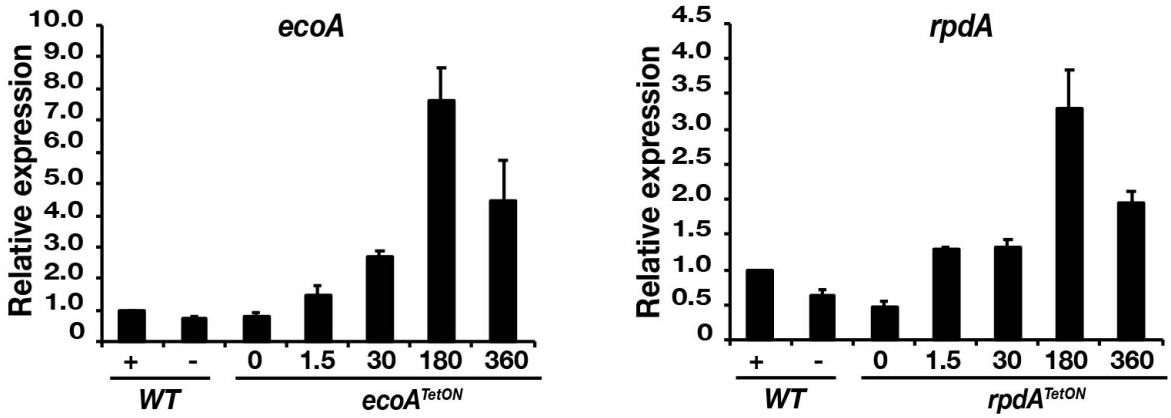

Figure 2.2 Confirmation of promoter replacement strains *ecoA*$^{\text{TetON}}$ and *rpdA*$^{\text{TetON}}$ in *A. nidulans* by RT-qPCR. Relative gene expression analysis was performed using the total RNA extracted from WT, deletion and complementation strains at the end of 24 h submerged medium at 37ºC. *benA* was used as a housekeeping gene for relative quantification $2^{\Delta\Delta Ct}$. + represents doxycycline treated (30µg/ml) WT and – represents untreated WT. Numbers represent the amount of doxycycline (in µg/ml) added to the initial culture.

2.15.4 Generation of BIFC plasmids for *in vivo* protein-protein interaction

For *in vivo* interaction analyses, *n-eyfp* (OZG73/74) and *kdmB* cDNA (OZG670/OZG671) were amplified and cloned into *Swa*I site of pSK353 generating pOB282 plasmid. Similarly, *c-eyfp* (OZG75/76) and *kdmB* cDNA (OZG673/OZG671) were

amplified and cloned into *Swa*I site of pSK353 generating pOB283 plasmid. *rpdA* cDNA was amplified (OZG857/OZG859) and fused to *c-eyfp* (OZG677/OZG388) and combined with n-*eyfp kdmB* (inserted into *PmeI*-digested pOB282) generating plasmid pOB302. *rpdA* cDNA was amplified (OZG858/OZG859) and fused to *n-eyfp* (OZG674/OZG387) and combined with c-*eyfp kdmB* (inserted into *Pme*I-digested pOB283) generating plasmid pOB303. The appropriate *n-eyfp*::*kdmB*, *c-eyfp*::*rpdA* or *n-eyfp*::*rpdA*, *c-eyfp*::*kdmB* fusion constructs were transformed into recipient WT fungal strain to detect *in vivo* KdmB and RpdA interaction.

sntB cDNA was amplified (OZG860/OZG862) and fused to *c-eyfp* (OZG677/OZG388) and combined with n-*eyfp kdmB* (inserted into *PmeI*-digested pOB282) generating plasmid pOB304. *sntB* cDNA was amplified (OZG861/OZG862) and fused to *n-eyfp* (OZG674/OZG387) and combined with c-*eyfp kdmB* (inserted into *Pme*I-digested pOB283) generating plasmid pOB305. The appropriate *n-eyfp*::*kdmB*, *c-eyfp*::*sntB* or *n-eyfp*::*sntB*, *c-eyfp*::*kdmB* fusion constructs were transformed into recipient WT fungal strain to detect *in vivo* KdmB and SntB interaction.

ecoA cDNA was amplified (OZG863/OZG865) and fused to *c-eyfp* (OZG677/OZG388) and combined with n-*eyfp kdmB* (inserted into *PmeI*-digested pOB282) generating plasmid pOB306. *ecoA* cDNA was amplified (OZG864/OZG865) and fused to *n-eyfp* (OZG674/OZG387) and combined with c-*eyfp kdmB* (inserted into *Pme*I-digested pOB283) generating plasmid pOB307. The appropriate *n-eyfp*::*kdmB*, *c-eyfp*::*ecoA* or *n-eyfp*::*ecoA*, *c-eyfp*::*kdmB* fusion constructs were transformed into recipient WT fungal strain to detect *in vivo* KdmB and EcoA interaction.

2.16 Generation of plasmid constructs and strains of *A. flavus*

2.16.1 Generation and confirmation of *kdmB*Δ and *rpdA*Δ strains

In order to create deletion construct of *kdmB* and *rpdA* genes, *Aspergillus fumigatus pyrG* marker was amplified from plasmid pME3858 using OZG694 and OZG695 primers yielding 1.89 kbp fragment. To create pBK22, 5' UTR (BK67/BK69) and 3' UTR (BK70/BK71) regions were amplified by using the WT genomic DNA of NRRL3357 strain. These fragments were fused to *Sma*I-digested pUC19 by using In-Fusion HD Cloning kit, yielding pBK22 from which *kdmB*Δ*::AfpyrG* cassette was amplified (BK68/72) and transformed into recipient fungal strain. Similarly, to create pBK23, 5' UTR (BK73/BK75) and 3' UTR (BK76/BK77) regions were amplified by using the WT genomic DNA of NRRL3357 strain. These fragments were fused to *Sma*I-digested pUC19 by using In-Fusion HD Cloning kit, yielding pBK23 from which *rpdA*Δ*::AfpyrG* cassette was amplified (BK74/78) and transformed into recipient fungal strain. Tjes19.1 (*pyrG*$^{-}$) was used as recipient for DNA transformation into *A. flavus* that was cultured and transformed as previously described (Punt & Hondel, 1992). *pyrG*$^{+}$ transformants were selected in the absence of uridine, uracil and deletion of transcription factors were confirmed by Southern hybridization using DIG-High prime DNA labelling and detection kit (Roche; 11745832910). DIG labelled DNA probes of approximately 1.2 kbp 5' UTR or 3' UTR corresponding regions were amplified by DIG PCR kit (Roche) and used as probe for detections. In addition to Southern blot analysis, deletion of these genes were further confirmed by RT-qPCR analysis showing the absence of these genes in mRNA level.

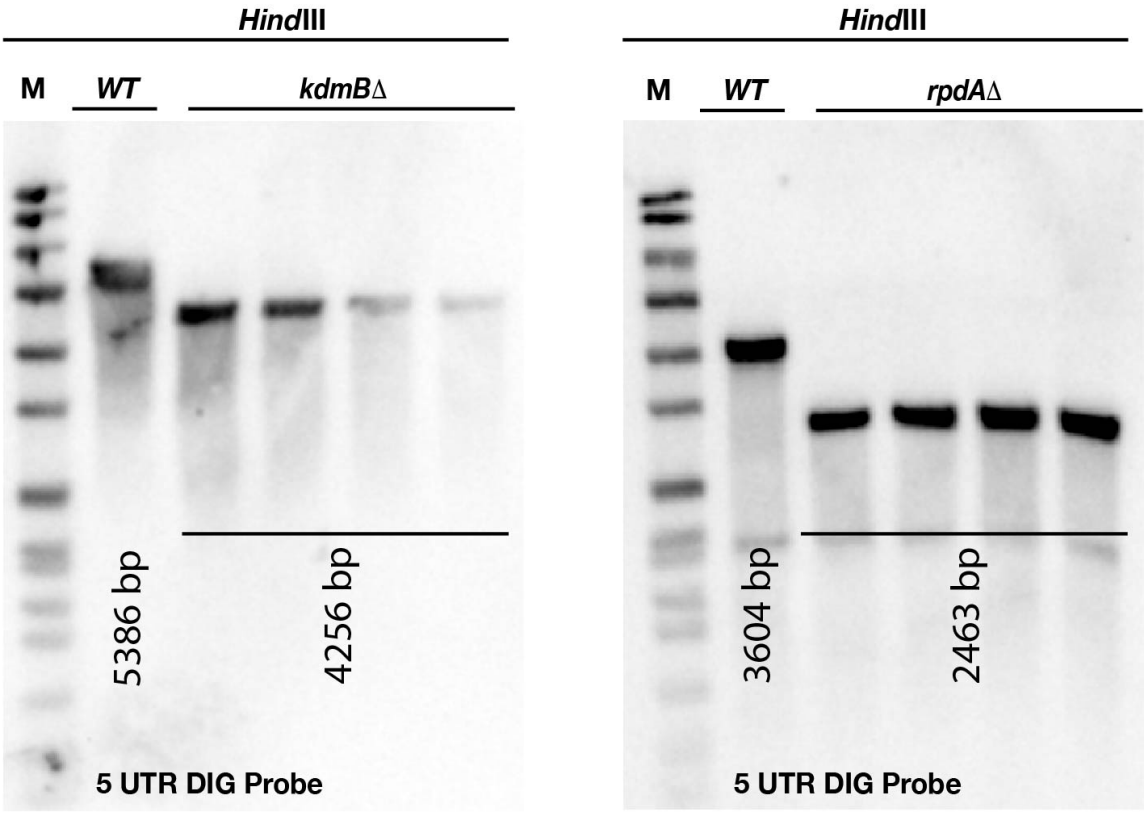

Figure 2.3 Confirmation of *kdmB* and *rpdA* deletion and complementation strains in *A. flavus* by Southern blot analysis. *kdmB* and *rpdA* deletion strains were confirmed by Southern blot analysis. Approximately 1.2 kbp 5UTR DNA fragment was amplified and detected using DIG-High Prime DNA Labelling and Detection Starter Kit II (Cat. 11585614910).

2.16.2 Generation and confirmation of complementation strains

To create complementation strains of *kdmB*Δ, *rpdA*Δ pAN8-1 harbouring phleomycin (*phleO*) resistance cassette, was digested with *Stu*I restriction enzyme. Genomic locus of *kdmB* (BK363/BK364) was amplified and fused to *Stu*I-digested pAN8-1 by using In-Fusion HD Cloning kit, yielding pBK66. Similarly for *rpdA* complementation, genomic locus of *rpdA* (BK365/BK366) was amplified and fused to *Stu*I-digested pAN8-1 by using In-Fusion

HD Cloning kit, yielding pBK67. Approximately 10 µg of plasmid DNA (pBK66, pBK67) were transformed into *kdmB*Δ and *rpdA*Δ deletion strains respectively. *phleO*$^{+}$ transformants were selected and the mRNA expression levels of *kdmB* and *rpdA* were confirmed by RT-qPCR using gene-specific oligonucleotides.

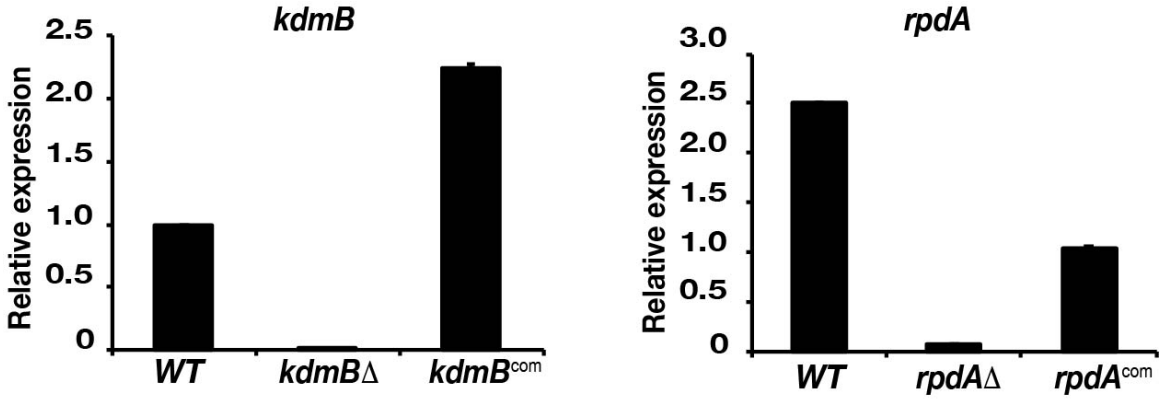

Figure 2.4 Confirmation of *kdmB* and *rpdA* deletion and complementation strains in *A. flavus* by RT-qPCR. Relative gene expression analysis was performed using the total RNA extracted from WT, deletion and complementation strains at the end of 24 h vegetative growth at 30ºC. *benA* was used as a housekeeping gene for relative quantification $2^{\Delta\Delta Ct}$.

2.16.3 Generation and confirmation of KdmB::3xHA, KdmB::sGFP strains

In order to create HA and GFP epitope tagging of KdmB, *3xha::AfpyrG* and *sgfp::AfpyrG* fragments were amplified using OZG916/694 from plasmids pOB430 and pOB435 respectively. To create pBK61, ORF (BK350/BK351) and 3' UTR (BK352/BK353) regions were amplified by using the WT genomic DNA of NRRL3357 strain. These two fragments with *3xha::pyrG* were fused to *Sma*I-digested pUC19 by using In-Fusion HD Cloning kit, yielding pBK61 from which *kdmB::3xha::AfpyrG* cassette was amplified (BK354/355) and transformed into recipient fungal strain. Similar strategy was performed to create pBK62. ORF (BK350/BK351) and 3' UTR (BK352/BK353) regions with *sgfp::AfpyrG* were fused

to *Sma*I-digested pUC19 by using In-Fusion HD Cloning kit, yielding pBK62 from which *kdmB::sgfp::AfpyrG* cassette was amplified (BK354/355) and transformed into recipient fungal strain Tjes19.1 resulting in AFLBK1 and AFLBK2 respectively. *pyrG*$^{+}$ transformants were selected in the absence of uridine, uracil and epitope tags of KdmB were confirmed by Southern hybridization. The expression of KdmB-GFP was further confirmed by Western blotting using anti-GFP antibody (Santa Cruz, sc-9996).

2.17 Statistical analysis

All data was analysed using GraphPad Prism version 7 software. The level of significance was set at $p < 0.05$ (*), $p < 0.01$ (**), $p < 0.001$ and $p < 0.0001$ (****).

Table 2.1 DNA Oligonucleotides used in this study for *A. nidulans* work.

Designation	**Sequence in 5' > 3' direction**
BK2 (rpdA RVS)	CACCGCTACCACCTCCCTCCTTTGCGGCTTCGGGTT
BK5 (rpdA 3UTR FWD)	CCTCCTCTCAGACAGGGACTAGCGCAGCAATTTTGG
BK6 (sntB 3UTR FWD)	CCTCCTCTCAGACAGCTTGGTCGTAGAGAGATCAAG G
BK7 (sntB RVS)	CACCGCTACCACCTCCGGACAGGAGGTTCTTCAGCG
BK8 (ecoA 3UTR FWD)	CCTCCTCTCAGACAGTGGTTTGTGCACAATTGTCATT CG
BK9 (ecoA RVS)	CACCGCTACCACCTCCACTCTCCTTGTAGACATGCCA
BK27 (kdmB-*Sma*I-pUC tail FWD PmeI-site)	TCGAGCTCGGTACCCAGCAAACTCATGTTTACAACC AATG
BK28 (kdmB-3xHA tail RVS)	GATAACCACCGCTACCACCTCCCGCAGTGGCTTCGA CTTCC
BK29 (kdmB 3UTR-pyrG tail FWD)	GCCTCCTCTCAGACAGTTCCATCTGCCTCATTCAACA TC
BK30 (kdmB-*Sma*I-pUC tail RVS PmeI-site)	ACTCTAGAGGATCCCCGTTGGGATATGCAAGGTGTG C
BK37 (laeA 5UTR pUC tail)	TTCGAGCTCGGTACCCAATGAATGGACGAGCACGGG C
BK38 (laeA 5UTR pyrG tail)	GAGCATTGTTTGAGGCCAGCGGCGAAACAGGGTACA A
BK39 (laeA 3UTR pyrG/pyroA tail)	GCCTCCTCTCAGACAGGAGCAAAAGGCGACCACATC C
BK40 (laeA 3UTR pUC19 tail)	ACTCTAGAGGATCCCCCACCGCATCCACATTCATGA AC
BK55 (laeA 5UTR nested)	AATGAATGGACGAGCACGGGC
BK56 (laeA 3UTR nested)	CACCGCATCCACATTCATGAAC
BK127 (5UTR ecoA pUC tail)	aaagctgggtacATTTGGTACTTGCATGGATTAGCGATTG
BK128 (5UTR ecoA nest)	CGCAGTCTTGGACCCATGATG
BK129 (5UTR ecoA pyrG/pyroA tail)	CCTCTCAGACAGATTTCTCCTTTTTGTACTTCTCCCG AG
BK130 (ORF ecoA tet-ON tail)	gcctgagtggccgtttATGCCGTGGACTGTAACAAATTCAT
BK131 (ORF ecoA GFP tail)	cttgctcaccatgtttCTCTCCTTGTAGACATGCCATTC
BK132 (ORF ecoA nest)	ATGCTTGGGCTAGGCTCTTCC

BK133 (5UTR rpdA pUC tail)	aaagctgggtacATTTTATCAACGGAGGAGAGCCAGC
BK134 (5UTR rpdA nest)	TCCAAACCCAGGATGCGAGTG
BK135 (5UTR rpdA pyrG/pyroA tail)	CCTCTCAGACAGATTTTATTTTTGGTAAGTTCGAGGGTAAGG
BK136 (ORF rpdA tet-ON tail)	gcctgagtggccgtttATGGCTTCGGGAACGTCGGG
BK137 (ORF rpdA GFP tail)	cttgctcaccatgtttCGCCGGGCTTCTCAACATATTG
BK138 (ORF rpdA nest)	ATCAAAGCGTCGCTTTGTAAAGCG
BK212 (pyroA control RVS)	CACCACCCTTCAGCATCTGAG
BK213 (pyroA control FWD)	GGTATCAATGTCTCTCAGATGCC
BK214 (kdmB 5UTR OUT)	GAT GGG GTG AAT GGG TTG AAC
BK215 (ecoA 5UTR OUT)	CGCTGCATCCAGAATTGAGCG
BK216 (rpdA 5UTR OUT)	GTCCAGACTTGCTTGTGCAGG
BK217 (sntB 5UTR OUT)	GCAGCACGCTTCACCAGAAC
BK224 (kdmB Rvs cDNA)	ACTTCCGGCTCAGGTTGAC
BK225 (kdmB Fwd cDNA)	CCTGAACCTATGGAGAATACTC
BK226 (ecoA Fwd cDNA)	CACGCATCTGGACGTCTG
BK227 (ecoA Rvs cDNA)	TGGCTGAAAGCTACCTGTTC
BK228 (rpdA Fwd cDNA)	CAGCAGTGACAACCGAGAC
BK229 (rpdA Rvs cDNA)	GTTGTGCTTCTGCGCTAGG
BK230 (sntB Fwd cDNA)	CTACAGGCAGCACACCAG
BK231 (sntB Rvs cDNA)	GTGTCGAGGTCCCAATCG
BK244 (sconC Fwd cDNA)	CCAACTACCTTGACATCAAGC
BK245 (sconC Rvs cDNA)	GATCTGGTCCTCTTCCTCG
BK280 (benA qPCR F)	GATGGCTGCCTCTGACTTC
BK281 (benA qPCR R)	GCATCTGGTCCTCAACCTC
BK333 (kdmB 5UTR pUC tail)	TTCGAGCTCGGTACCCCTTGCAAAGATCAGCTCTGATTCAG

BK334 (kdmB 5UTR pyrG tail)	GAGCATTGTTTGAGGCGTCTTGGGTGCGATAGCTGG
BK335 (kdmB 3UTR pyrG/pyroA tail)	GCCTCCTCTCAGACAGTTCCATCTGCCTCATTCAACATCT
BK336 (kdmB 3UTR pUC tail)	ACTCTAGAGGATCCCCGTTGGGATATGCAAGGTGTGCG
BK337 (kdmB 5UTR nest)	GAGTGGAACCTCTGTTGTGTAC
BK338 (kdmB 3UTR nest)	AGGAGAAGGACATTCTGGGATC
BK389 (kdmB 5UTR F pUC tail compl)	AGCTCGGTACCCATTTTGGATTGAACGAGTTACCATCTAC
BK390 (kdmB 3UTR R pUC tail compl)	CATCTGATGTCCATTTAGTTACAACTCTCGTCACAGAGG
BK391 (sntB 5UTR F pUC tail compl)	AGCTCGGTACCCATTTCACCATCCCACTACGACTGC
BK391new (sntB 5UTR F pUC tail compl)	AGCTCGGTACCCATTTACTACCTACTACCAGCTAGCTG
BK396new (sntB 3UTR R pUC tail compl)	CATCTGATGTCCATTTCCAGGATTGTAGAGGTTTGAGC
BK397 (sntB 5UTR F)	CCCAGTCGATCACTGGGTTAC
BK398 (sntB 3UTR R)	TCGTCGTGCTCTCCTTATCATG
BK433 (sudA 5UTR pUC tail)	TTCGAGCTCGGTACCCCTTCGGCAGAAATGATGAACTCG
BK434 (sudA 5UTR pyrG tail)	GAGCATTGTTTGAGGCCTTGACCTACACGCGAATATGAAG
BK435 (sudA 3UTR pyrG tail)	GCCTCCTCTCAGACAGGATGATGGTGATGATCAGTTCCCT
BK436 (sudA 3UTR pUC tail)	ACTCTAGAGGATCCCCCAGTGATGTTCTCGAGCGATAG
BK437 (sudA 5UTR nest)	CTTCGGCAGAAATGATGAACTCG
BK438 (sudA 3UTR nest)	CAGTGATGTTCTCGAGCGATAG
BK443 (sudA ORF nest)	GAGTCTGTCTCTTTCATCCTTGG
BK444 (sudA 5UTR pUC tail)	TTCGAGCTCGGTACCCGGTTCCGAGCTGCTGATTGG
BK445 (sudA ORF HA tail)	CACCGCTACCACCTCCTGACTTCTGCTCCTCGACAAATTTG
BK446 (sudA 5UTR nest)	GGTTCCGAGCTGCTGATTGG
BK564 (5UTR sntB pUC tail)	TTCGAGCTCGGTACCCCCCAGTCGATCACTGGGTTAC
BK565 (5UTR sntB pyroA tail)	CCAGCATCTGATGTCCCCTCCGACGCGACAAGAAAAG
BK566 (sntB ORF pyroA tail)	GCCTCCTCTCAGACAGGCTCACAAAGGACACTGTTGCTG

BK567 (sntB ORF pUC tail)	ACTCTAGAGGATCCCCTCGTCGTGCTCTCCTTATCATG
BK568 (5UTR sntB nest F)	CCCAGTCGATCACTGGGTTAC
BK569 (ORF sntB nest R)	TCGTCGTGCTCTCCTTATCATG
BK564 (5UTR sntB pUC tail)	TTCGAGCTCGGTACCCCCCAGTCGATCACTGGGTTAC
BK565 (5UTR sntB pyroA tail)	CCAGCATCTGATGTCCCCTCCGACGCGACAAGAAAAG
BK566 (sntB ORF pyroA tail)	GCCTCCTCTCAGACAGGCTCACAAAGGACACTGTTGCTG
BK567 (sntB ORF pUC tail)	ACTCTAGAGGATCCCCTCGTCGTGCTCTCCTTATCATG
BK568 (5UTR sntB nest F)	CCCAGTCGATCACTGGGTTAC
BK569 (ORF sntB nest R)	TCGTCGTGCTCTCCTTATCATG
OZG73	ATGGTGAGCAAGGGCGAGAG
OZG74	GGTGGTGGTGCTGCAAGTGTAGCCATCGTGGCG ATGGAGCGCATGATATAG
OZG75	ATG GCC GAC AAG CAG AAG AAC
OZG76	ACGAGTTCCCACCGGGCCCATCTCAAACATGTGGTTCA GACCT CTGTTTCAG
OZG387	CGTGGCGATGGAGCGCATGATATA
OZG388	GTGGTTCATGACCTTCTGTTTCAGGTC
OZG548 (kdmB-A) for TAP	AGCAAACTCATGTTTACAACCAATG
OZG549 (kdmB-B) for TAP	CTGTGACAGGTACCATGGAAAGTG
OZG550 (kdmB-C) for TAP	CCATCTTCTCTTACCACCGCTACCACCCGCAGTGGCTTCGACTTCCG
OZG551 (kdmB-D) for TAP	CTCTACATGAGCATGCCCTGCCCCTGATTCCATCTGCCTCATTCAACATC
OZG552 (kdmB-E) for TAP	GAAGGACATTCTGGGATCACCG
OZG553 (kdmB-F) for TAP	GTTGGGATATGCAAGGTGTGC
OZG609 (kdmB-A) del	CAGATTGCTTCAGACTGTGTTGC
OZG610 (kdmB-B SwaI)	TTATTTAAATGGCTACTCAATGTACGTTTGC
OZG611 (kdmB-C) del	CGTTACCAATGGGATCCCGTAATCAATTGTCTTGGGTGCGATAGCTGG
OZG612 (kdmB-D) del	GACAGTATAATACAAACAAAGATGCAAGATTCCATCTGCCTCATTCAACATC
OZG613 (kdmB-E SwaI)	TTATTTAAATGAAGGACATTCTGGGATCACCG

OZG670 (kdmB for nyfp)	GCGCTCCATCGCCACGATGGTGGCTCCGGCTGCAATG
OZG671 (kdmB stop for *Swa*I)	atgcgaacccgtATTTTTAAGCGGCCGCAGTGGCTTC
OZG674 (nYFP for pmeI)	GCGCCCGCCATCGTTTATGGTGAGCAAGGGCGAGGAG
OZG677 (cYFP for pmeI)	GCGCCCGCCATCGTTTATGGCCGACAAGCAGAAGAAC
OZG694 (UP2 end of pyrG&pyroA)	CTGTCTGAGAGGAGGCACTGAT
OZG695 (UP3 head for pyrG deletion)	GCCTCAAACAATGCTCTTCA
OZG696 (UP3 head for pyroA deletion)	GGACATCAGATGCTGGATTAC
OZG752 (sntB SwaI 5)	TCGAGCTCGGTACCCATTTAAATCCCAGTCGATCACTGGGTTAC
OZG753 (sntB ptrA 5)	GATCCCGTAATCAATTCCCTCCGACGCGACAAGAAAAG
OZG754 (sntB ptrA 3)	AAACAAAGATGCAAGAGTCGAATACGTCAAACCTATTGA
OZG755 (sntB SwaI 3)	ACTCTAGAGGATCCCCATTTAAATTCGTCGTGCTCTCCTTATCATG
OZG860 (cyfp-sntB)	GAAGGTCATGAACCACATGTCCTCGGATAGGTCACC
OZG861 (nyfp-sntB)	GCGCTCCATCGCCACGATGTCCTCGGATAGGTCACC
OZG862 (sntB-niit stop)	gtatcctcgtcagtTTTCACCACAGCCTGGTGTCGAG
OZG863 (cyfp-ecoA)	GAAGGTCATGAACCACATGCCGTGGACTGTAACAAATTC
OZG864 (nyfp-ecoA)	GCGCTCCATCGCCACGATGCCGTGGACTGTAACAAATTC
OZG865 (ecoA-niit stop)	gtatcctcgtcagtTTTCAACTCTCCTTGTAGACATGC
OZG1033 (rpdA 5 UTR PmeI)	TTCGAGCTCGGTACCCGTTTAAACGCACAGGAAAGGAACACGAAG
OZG1034 (rpdA GFP & TAP fuser)	TACCACCGCTACCACCCTCCTTTGCGGCTTCGGGTTG
OZG1035 (rpdA natR)	CATGCCCTGCCCCTGAGGACTAGCGCAGCAATTTTGG
OZG1036 (rpdA 3 UTR PmeI)	ACTCTAGAGGATCCCCGTTTAAACCTCTCTCCATGTATTGACGCAAG
OZG1037 (sntB 5 UTR PmeI)	TTCGAGCTCGGTACCCGTTTAAACGCCTACCTTGTCTGTCTACTG
OZG1039 (sntB GFP & TAP fuser)	TACCACCGCTACCACCGGACAGGAGGTTCTTCAGCG
OZG1040 (sntB natR)	CATGCCCTGCCCCTGACTTGGTCGTAGAGAGATCAAGG
OZG1041 (sntB 3 UTR PmeI)	ACTCTAGAGGATCCCCGTTTAAACCTAGCTGGATTCTGGAAGCAG

OZG1042 (ecoA 5 UTR PmeI)	TTCGAGCTCGGTACCCGTTTAAACGGAGCGAGCGCG ATGGTTG
OZG1043 (ecoA GFP & TAP fuser)	TACCACCGCTACCACCACTCTCCTTGTAGACATGCCA
OZG1044 (ecoA natR)	CATGCCCTGCCCCTGATGGTTTGTGCACAATTGTCAT TCG
OZG1045 (ecoA 3 UTR PmeI)	ACTCTAGAGGATCCCCGTTTAAACGCATTCCTGAGA AGCCTGTTG
OZG1077 (pyroA 5 for TET plasmid)	cctcggcagatctgcaGGACATCAGATGCTGGATTAC
OZG1184 (pyroA 3 for TET plasmid)	aacaaaagctgggtacATTTAAATCTGTCTGAGAGGAGGCAC TGAT

Table 2.2 Plasmids employed in this study for *A. nidulans* work.

Plasmid	Description	Reference
pUC19	*E. coli* cloning plasmid with *bla* (ampicillin resistance gene) gene	Thermo Fisher
pBK1	*rpdA* (AN4493) *3xha::AfpyrG* cassette with *Pme*I in *Sma*I site of pUC19	This study
pBK2	*sntB* (AN9507) *3xha::AfpyrG* cassette with *Pme*I in *Sma*I site of pUC19	This study
pBK3	*ecoA* (AN10336) *3xha::AfpyrG* cassette with *Pme*I in *Sma*I site of pUC19	This study
pBK11	*kdmB* (AN8211) *3xha::AfpyrG* cassette with *Pme*I in *Sma*I site of pUC19	This study
pBK14	*laeA* deletion cassette with *AfpyrG* in *Sma*I site of pUC19	This study
pBK32	*tetO7::Pmin::ecoA/pyroA* cassette in *Sma*I site of pUC19	This study
pBK33	*tetO7::Pmin::rpdA/pyroA* cassette in *Sma*I site of pUC19	This study
pBK53	*kdmB* deletion cassette with *AfpyrG* in *Sma*I site of pUC19	This study
pBK74	*kdmB* genomic locus in *Swa*I site of pOSB114	This study
pBK75	*sntB* genomic locus in *Swa*I site of pOSB114	This study
pBK87	*sudA* (AN6364) *3xHA::AfpyrG* cassette with *Pme*I in *Sma*I site of pUC19	This study
pBK88	*sudA* (AN6364) *sgfp::AfpyrG* cassette with *Pme*I in *Sma*I site of pUC19	This study
pBK128	*sntB* deletion cassette with *pyroA* in *Sma*I site of pUC19	This study
pOB226	*kdmB* deletion cassette with *ptrA* in *Sma*I site of pUC19	This study
pOB254	*sntB* deletion cassette with *ptrA* in *Sma*I site of pUC19	This study
pOB282	*N-yfp::kdmB* genomic locus in *Swa*I site of pSK353	This study
pOB283	*C-yfp::kdmB* genomic locus in *Swa*I site of pSK353	This study
pOB302	CYFP OZG677/OZG388 + OZG857/OZG859 *rpdA* in *Pme*I site of pOB282A	This study
pOB303	NYFP OZG674/OZG387 + OZG858/OZG859 *rpdA* in *Pme*I site of pOB283A	This study
pOB304	CYFP OZG677/OZG388 + OZG860/OZG862 *sntB* in *Pme*I site of pOB282A	This study
pOB305	NYFP OZG674/OZG387 + OZG861/OZG862 *sntB* in *Pme*I site of pOB283A	This study
pOB306	CYFP OZG677/OZG388 + OZG863/OZG865 *ecoA* in *Pme*I site of pOB282A	This study

pOB307	NYFP OZG674/OZG387 + OZG864/OZG865 *ecoA* in *Pme*I site of pOB283A	This study
pOB430	3X HA with GGGSGG linker *trpC pyrG* in *Sma*I of pUC19	(Manfiolli et al., 2017)
pOB485	*rpdA sgfp::natR* cassette with *Pme*I in *Sma*I site of pUC19	This study
pOB486	*rpdA ctap::natR* cassette with *Pme*I in *Sma*I site of pUC19	This study
pOB487	*sntB sgfp::natR* cassette with *Pme*I in *Sma*I site of pUC19	This study
pOB488	*sntB ctap::natR* cassette with *Pme*I in *Sma*I site of pUC19	This study
pOB489	*ecoA sgfp::natR* cassette with *Pme*I in *Sma*I site of pUC19	This study
pOB490	*ecoA ctap::natR* cassette with *Pme*I in *Sma*I site of pUC19	This study
pOB549	*pyroA* Tet ON with SwaI in pUC19 *Sma*I site	This study
pCH008	Tet-ON module $^{p}tpiA::rtTA2^{S}$ *-M2::cgrA*^{t} *-tetO-*^{p}*min*	(Helmschrott et al., 2013)
pOSB114	*Pme*I::Af*pyroA*::*Swa*I inserted in *Sma*I site of pUC19	Unpublished

Table 2.3 *A. nidulans* strains employed in this study.

Strain	Genotype	Reference
AGB551	*nkuAΔ::argB,pyrG89,pyroA4,veA+*	Bayram et al 2012
ANBK1	*rpdA::3xHA::AfpyrG;nkuAΔ::argB, pyroA4,veA+*	This study
ANBK2	*sntB::3xHA::AfpyrG;nkuAΔ::argB, pyroA4,veA+*	This study
ANBK3	*ecoA::3xHA::AfpyrG;nkuAΔ::argB, pyroA4,veA+*	This study
ANBK5	*kdmB::ctap::natR;nkuAΔ::argB, pyrG89, pyroA4,veA+*	This study
ANBK11	*kdmB::3xHA::AfpyrG;nkuAΔ::argB, pyroA4,veA+*	This study
ANBK32	*tetO7::Pmin::ecoA/pyroA; nkuAΔ::argB,pyrG89,veA+*	This study
ANBK33	*tetO7::Pmin::rpdA/pyroA; nkuAΔ::argB,pyrG89,veA+*	This study
ANBK53	*kdmBΔ::AfpyrG;nkuAΔ::argB, pyroA4,veA+*	This study
ANBK54	*ecoA::ctap::natR, kdmBΔ::ptrA, nkuAΔ::argB, pyrG89, pyroA4,veA+*	This study
ANBK55	*rpdA::ctap::natR, kdmBΔ::ptrA, nkuAΔ::argB, pyrG89, pyroA4,veA+*	This study
ANBK56	*sntB::ctap::natR, kdmBΔ::ptrA, nkuAΔ::argB, pyrG89, pyroA4,veA+*	This study
ANBK61	*sntBΔ::ptrA, kdmBΔ::AfpyrG, nkuAΔ::argB, pyroA4,veA+*	This study
ANBK65	*kdmB::ctap::natR, laeAΔ::pyrG, nkuAΔ::argB, pyroA4,veA+*	This study
ANBK67	*kdmB::ctap::natR, sntBΔ::ptrA, nkuAΔ::argB, pyrG89, pyroA4,veA+*	This study
ANBK68	*ecoA::ctap::natR, sntBΔ::ptrA, nkuAΔ::argB, pyrG89, pyroA4,veA+*	This study
ANBK69	*rpdA::ctap::natR, sntBΔ::ptrA, nkuAΔ::argB, pyrG89, pyroA4,veA+*	This study
ANBK70.1	*kdmBΔ::ptrA; ^{p}kdmB::kdmB::kdmB^{t}-AfpyroA; nkuAΔ::argB, pyrG89, veA+*	This study
ANBK71.2	*sntBΔ::ptrA; ^{p}nii::sntB::nii^{t}-AfpyroA; nkuAΔ::argB, pyrG89, veA+*	This study
ANBK76.1	*sudA::3xHA::AfpyrG;nkuAΔ::argB, pyroA4,veA+*	This study
ANBK77.2	*sudA::sgfp::AfpyrG;nkuAΔ::argB, pyroA4,veA+*	This study
ANBK80	*kdmBΔ::ptrA, rpdA::sgfp::natR, h2A::mRFP::pyroA, nkuAΔ::argB, bioA, veA+*	This study
ANBK81	*kdmBΔ::ptrA, sntB::sgfp::natR, h2A::mRFP::pyroA, nkuAΔ::argB, bioA, veA+*	This study
ANBK82	*kdmBΔ::ptrA, ecoA::sgfp::natR, h2A::mRFP::pyroA, nkuAΔ::argB, bioA, veA+*	This study
ANBK83.1	*kdmBΔ::ptrA, ecoA::3xHA::AfpyrG, nkuAΔ::argB, pyroA4,veA+*	This study

ANBK84.2	*kdmBΔ::ptrA, rpdA::3xHA::AfpyrG, nkuAΔ::argB, pyroA4,veA+*	This study
ANBK85.4	*kdmBΔ::ptrA, sntB::3xHA::AfpyrG, nkuAΔ::argB, pyroA4,veA+*	This study
ANBK86.1	*tetO7::Pmin::ecoA/pyroA, sudA::3xHA::AfpyrG, nkuAΔ::argB, veA+*	This study
ANBK87.2	*tetO7::Pmin::ecoA/pyroA, sudA::sgfp::AfpyrG, nkuAΔ::argB, veA+*	This study
ANBK98	*sntBΔ::ptrA, kdmB::sgfp::natR, h2A::mRFP::AfpyrG, pyroA4 nkuAΔ::argB, veA+*	This study
ANBK99	*sntBΔ::ptrA, ecoA::sgfp::natR, ^{P}biA::h2A::mRFP::pyroA::^{t}biA, pyrG89, nkuAΔ::argB, veA+*	This study
ANBK100	*sntBΔ::ptrA, rpdA::sgfp::natR, ^{P}biA::h2A::mRFP::AfpyrG::^{T}biA, pyrG89, nkuAΔ::argB, veA+*	This study
ANBK101.1	*ecoA::3xHA::AfpyrG, sntBΔ::ptrA, nkuAΔ::argB, pyroA4,veA+*	This study
ANBK102.1	*rpdA::3xHA::AfpyrG, sntBΔ::ptrA, nkuAΔ::argB, pyroA4,veA+*	This study
ANBK103.1	*kdmB::3xHA::AfpyrG, sntBΔ::ptrA, nkuAΔ::argB, pyroA4,veA+*	This study
ANBK107.5	*kdmBΔ::ptrA, sudA::3xHA::AfpyrG, pyroA4, nkuAΔ::argB, veA+*	This study
ANBK112	*sntBΔ::pyroA, kdmBΔ::ptrA, ecoA::3xHA::AfpyrG, nkuAΔ::argB ,veA+*	This study
ANBK113	*kdmB::sgfp::natR;nkuAΔ::argB, pyrG89, pyroA4,veA+*	This study
ANOB302	*^{p}niiA::nyfp::kdmB::niiA^{T}-^{p}niaD::cyfp::rpdA::niaD^{T}, A.f. pyrG; ^{p}gpdA::mrfp::h2A, ^{p}gpdA::natR; pyroA4, pyrG89*	This study
ANOB303	*^{p}niiA::nyfp::rpdA::niiA^{T}-^{p}niaD::cyfp::kdmB::niaD^{T}, A.f. pyrG; ^{p}gpdA::mrfp::h2A, ^{p}gpdA::natR; pyroA4, pyrG89*	This study
ANOB304	*^{p}niiA::nyfp::kdmB::niiA^{T}-^{p}niaD::cyfp::sntB::niaD^{T}, A.f. pyrG; ^{p}gpdA::mrfp::h2A, ^{p}gpdA::natR; pyroA4, pyrG89*	This study
ANOB305	*^{p}niiA::nyfp::sntB::niiA^{T}-^{p}niaD::cyfp::kdmB::niaD^{T}, A.f. pyrG; ^{p}gpdA::mrfp::h2A, ^{p}gpdA::natR; pyroA4, pyrG89*	This study
ANOB306	*^{p}niiA::nyfp::kdmB::niiA^{T}-^{p}niaD::cyfp::ecoA::niaD^{T}, A.f. pyrG; ^{p}gpdA::mrfp::h2A, ^{p}gpdA::natR; pyroA4, pyrG89*	This study
ANOB307	*^{p}niiA::nyfp::ecoA::niiA^{T}-^{p}niaD::cyfp::kdmB::niaD^{T}, A.f. pyrG; ^{p}gpdA::mrfp::h2A, ^{p}gpdA::natR; pyroA4, pyrG89*	This study
ANOB485	*rpdA::sgfp::natR;nkuAΔ::argB, pyrG89, pyroA4,veA+*	This study
ANOB486	*rpdA::ctap::natR;nkuAΔ::argB, pyrG89, pyroA4,veA+*	This study
ANOB487	*sntB::sgfp::natR;nkuAΔ::argB, pyrG89, pyroA4,veA+*	This study
ANOB488	*sntB::ctap::natR;nkuAΔ::argB, pyrG89, pyroA4,veA+*	This study
ANOB489	*ecoA::sgfp::natR;nkuAΔ::argB, pyrG89, pyroA4,veA+*	This study
ANOB490	*ecoA::ctap::natR;nkuAΔ::argB, pyrG89, pyroA4,veA+*	This study

Table 2.4 DNA Oligonucleotides used in this study for *A. flavus* work.

Designation	**Sequence in 5' > 3' direction**
BK67 (5UTR AFLkdmB pUC tail)	TTCGAGCTCGGTACCCagacgatcggtttgctggcac
BK68 (5UTR AFLkdmB nest)	agacgatcggtttgctggcac
BK69 (5UTR AFLkdmB pyrG tail)	GAGCATTGTTTGAGGCgctaatgaggctctggaagtact
BK70 (3UTR AFLkdmB pyrG tail)	GCCTCCTCTCAGACAGttcttaaatgcgacgatctgatcg t
BK71 (3UTR AFLkdmB pUC tail)	ACTCTAGAGGATCCCCtttatttccccctcctatggtgc
BK72 (3UTR AFLkdmB nest)	tttatttccccctcctatggtgc
BK73 (5UTR AFL rpdA pUC tail)	TTCGAGCTCGGTACCCctgggtgttgatatcgacagatg
BK74 (5UTR AFL rpdA nest)	ctgggtgttgatatcgacagatg
BK75 (5UTR AFL rpdA pyrG tail)	GAGCATTGTTTGAGGCcttggatgacaatgtatgagaga g
BK76 (3UTR AFL rpdA pyrG tail)	GCCTCCTCTCAGACAGgctccgctttttagaggcgttta
BK77 (3UTR AFL rpdA pUC tail)	ACTCTAGAGGATCCCCacggtggccatgaccatgtca
BK78 (3UTR AFL rpdA nest)	acggtggccatgaccatgtca
BK182 (AFL kdmB 5UTR OUT)	gccctactggattccttcgg
BK184 (AFL rpdA 5UTR OUT)	gttgtgctcgccttcctcatg
BK212 (pyroA control RVS)	CACCACCCTTCAGCATCTGAG
BK213 (pyroA control FWD)	GGTATCAATGTCTCTCAGATGCC
BK214 (AFLkdmB 5UTR OUT)	GAT GGG GTG AAT GGG TTG AAC
BK216 (rpdA 5UTR OUT)	GTCCAGACTTGCTTGTGCAGG
BK217 (sntB 5UTR OUT)	GCAGCACGCTTCACCAGAAC
BK250 (AFL kdmB cDNA FWD)	CGTGGTGAACCTACATTGGC
BK251 (AFL kdmB cDNA RVS)	CCGGTGTAGAATCGCTTGC
BK254 (AFL rpdA cDNA FWD)	GTCAAGAGCAAGCAGCTCC
BK255 (AFL rpdA cDNA RVS)	GATTGCTCCTGCTGCTCTG
BK274 (AFL h2A cDNA FWD)	CAAGGTCAAGCGTATCACCC

BK275 (AFL h2A cDNA RVS)	GGTTGATGCGTGGCAAGAC
BK276 (AFL skpA cDNA FWD)	CGATGTTAGTCTTGCCTTGC
BK277 (AFL skpA cDNA RVS)	GACCAGATGAAACTCAAGCTG
BK363 (AFL kdmB 5UTR pAN8-1 tail)	cccaagaccgacaagggatagttcgacggtggataacag
BK364 (AFL kdmB 3UTR pAN8-1 tail)	gcgttctggagggaggcggagaagtcatcgtatctctc
BK365 (AFL rpdA 5UTR pAN8-1 tail)	cccaagaccgacaaggcgacctttccgacatatcttgtc
BK366 (AFL rpdA 5UTR pAN8-1 tail)	gcgttctggagggaggagttggaagcgatacgctgttg
BK399 (AFLkdmB ORF pUC tail)	TTCGAGCTCGGTACCCccagtctctgtatgagagaagc
BK400 (AFLkdmB ORF linker tail)	CACCGCTACCACCTCCcaaatcctctgtactgcgatcg
BK401 (AFLkdmB 3UTR pyrG/pyroA tail)	GCCTCCTCTCAGACAGcgctgttttaaagtataatccctatc
BK402 (AFLkdmB 3UTR pUC tail)	ACTCTAGAGGATCCCCgatagttcgacggtggataacag
BK403 (AFLkdmB 5UTR nest)	ccagtctctgtatgagagaagc
BK404 (AFLkdmB 3UTR nest)	gatagttcgacggtggataacag
BK417 (AFLrpdA 5UTR pUC tail)	TTCGAGCTCGGTACCCcgctatcggtgctctctcatac
BK418 (AFLrpdA ORF linker tail)	CACCGCTACCACCTCCtgcctcgctcttggtgggc
BK419 (AFLrpdA 3UTR pyrG tail)	GCCTCCTCTCAGACAGgctccgctttttagaggcgttt
BK420 (AFLrpdA 3UTR pUC tail)	ACTCTAGAGGATCCCCcttgctctgacggacgacaac
BK421 (AFLrpdA 5UTR F)	cgctatcggtgctctctcatac
BK422 (AFLrpdA 3UTR R)	cttgctctgacggacgacaac
BK431 (AFLrpdA F qPCR)	GACGAAGAAGAGAACGCTGC
BK432 (AFLrpdA R qPCR)	GTAGTATCCATGTCATCGTCAG
BK461 (AFLkdmB 5UTR for comp)	cccaagaccgacaagggacccgattacgcctattctgg
BK462 (AFLkdmB 3UTR for comp)	gcgttctggagggagggtttgtggtgtttgtggaaagatag
BK463 (AFLkdmB ORF F pOB110tail)	GCAGACATCACCGTTTatggtggctccggcctcg
BK464 (AFLkdmB ORF R pOB110tail)	GATAGACATGGCGTTTttacaaatcctctgtactgcgatcg
brlA-F (Chang et al., 2012)	TATCCAGACATTCAAGACGCACAG

brlA-R (Chang et al., 2012)	GATAATAGAGGGCAAGTTCTCCAAAG
abaA-F (Chang et al., 2012)	GAGTGGCAGACCGAATGTATGTTG
abaA-R (Chang et al., 2012)	TAGTGGTAGGCATTGGGTGAGTTG
aflR-F (Zhuang et al., 2016)	GCAACCTGATGACGACTGATATGG
aflR-R (Zhuang et al., 2016)	TGCCAGCACCTTGAGAACGATAAG
BK471 (AFLA nsdC cDNA F)	CAGCCATTCTAGCAACCATAAC
BK472 (AFLA nsdC cDNA R)	TCTCGCTCACGATTCTGATC
BK473 (AFLA nsdD cDNA F)	CAATGTACCAAGACGAATACAAG
BK474 (AFLA nsdD cDNA R)	TGTCTCAGCTCGGTTACAAC
aflA-F (Chang et al., 2012)	CCTATAAGTGCTTCAAAGATCGTGATCG
aflA-R (Chang et al., 2012)	CGTACATGGATGACACGTTGTCCCAG
aflC-F (Chang et al., 2012)	CCTATTCTAGCCGCCTTTCTTGAC
aflC-R (Chang et al., 2012)	CATGTTGCCAGATTCCTCATATTCC
aflD-F (Chang et al., 2012)	TGTATGCTCCCGTCCTACTGTTTC
aflD-R (Chang et al., 2012)	TGTAGTCTCCTTAGTCGCTTCATC
aflM-F (Chang et al., 2012)	GCGGAGAAAGTGGTTGAACAGATC
aflM-R (Chang et al., 2012)	CAGCGAACAAAGGTGTCAATAGCC
aflP-F (Chang et al., 2012)	CGATGTCTATCTTCTCCGATCTATTC
aflP-R (Chang et al., 2012)	TCTCAGTCTCCAGTCTATTATCTACC
BK585 (AFLA flbA cDNA F)	CACTGCGCAACAGCTTGG
BK586 (AFLA flbA cDNA R)	GATCGAATCACTTGACATCAAC
BK589 (AFLA flbC cDNA F)	CATGATGAGCCAGTTCAGTTC
BK590 (AFLA flbC cDNA R)	CACCAGTGTGACTGTACATG
BK603_AFCL1F	GGAAGCAAGAGAGATTATCCTC
BK604_AFCL1R	CGAGTGAGTCAATTCCTAGTTC
BK605_AFCL2F	CATGCTGCACAGTGGTATCC
BK606_AFCL2R	CTTCCAGTTCAGTGAACTCTG

BK607_AFCL3F	GGAGATCAGTCCTGAGAAGC
BK608_AFCL3R	CTACTCATGATATCAAAGATGACG
BK609_AFCL4F	CAAGTCAGCATGGTTGACATTC
BK610_AFCL4R	TCGTCGCATCTTGTTCCGAG
BK611_AFCL5F	CCATTCAAAGACGAGAAATGGG
BK612_AFCL5R	CAATGTATCCCACTTGTTAGGTC
BK613_AFCL6F	CAGACTATCTTCGAAACCTCG
BK614_AFCL6R	GACCTGCTGGTCTGTACAG
BK615_AFCL7F	CTCGACCACATTTGAGTTATCG
BK616_AFCL7R	CCTCTTTGCTCTACCAAGCC
BK617_AFCL8F	GTTGATATTCTGAACCCAGATG
BK618_AFCL8R	GGCAGCCAACTCATCAAGG
BK619_AFCL9F	CTACAATGTCCAGCCAATTGAG
BK620_AFCL9R	CCTTCCACTAGCCCTTGG
BK621_AFCL10F	GGATTGGTTGGAGATACTATCG
BK622_AFCL10R	CATCGTAAGTGGCCATGTCC
BK623_AFCL11F	CTGTGATGCCACTCCTTCAG
BK624_AFCL11R	GAATATCCGGTGCATCCTTC
BK625_AFCL12F	CTGATGATGCGAAGTCCACG
BK626_AFCL12R	GATGGAGTCCAAGACAATCC
BK627_AFCL13F	CTAGCGTTATAGTACGGATTGG
BK628_AFCL13R	TGCTAAGGGAGTCAGGCAG
BK629_AFCL14F	GATCAACAATAAAGACCAGGATAG
BK630_AFCL14R	GTAATGAAGTGGTGGATTCCTG
BK631_AFCL15F	CAGTTCCATTCTGGCGGAG
BK632_AFCL15R	GGTGATCAGTCATCGCTCG
BK633_AFCL16F	CAGGGAACTGATACTAAGACC

BK634_AFCL16R	GATCGACCTGCTTTCCACTG
BK637_AFCL18F	GTTGATGCTGGTAAGAAGCG
BK638_AFCL18R	AGGTAGGAGTCGTCAAGTTC
BK639_AFCL19F	GTTTCGCTCGTTAGACCAGG
BK640_AFCL19R	CAGCGACCAGGGTGGTAG
BK641_AFCL20F	CATCGTCAAGTCAGCGCAG
BK642_AFCL20R	CGTCTCTTCGTCTCCGATG
BK643_AFCL21F	CCTGAATCAGGATGATCTAGC
BK644_AFCL21R	GTGATATGCGTAAGTTGTACCTC
BK645_AFCL22F	ACTCCGGACCTGCTACAC
BK646_AFCL22R	AGAAGCTGTATATTCTCTTCCG
BK647_AFCL23F	CAGCGAGCGATATCTGGAG
BK648_AFCL23R	AGGATCGCATTCAAGGCATC
BK649_AFCL24F	CTACTTTCTTGGGCCATTTGG
BK650_AFCL24R	GAGACAGACGGAACACGAG
BK651_AFCL25F	GTTATCAACGATGCAGGGTAC
BK652_AFCL25R	CGGAACATCGGTAACAGAGG
BK653_AFCL26F	CCTGGCCTTGGTGTCTAC
BK654_AFCL26R	GTCCGTAGACATGTTGAGAAG
BK655_AFCL27F	GTGAACAGTCTACATACATACC
BK656_AFCL27R	CAATCCCTCTGGGTCATCG
BK657_AFCL28F	CCATCAACAGAACTAATTCCAG
BK658_AFCL28R	CGTACTAGAAGGATTGACATGG
BK659_AFCL29F	CCGTCGCTACATTCTGTGC
BK660_AFCL29R	GATACCAATGATTGAAGATGGTTC
BK661_AFCL30F	GGATAGAGAGCTTCAGATCAAAG
BK662_AFCL30R	TGGTCAACGGCGATGGATC

BK663_AFCL31F	CTCCCTCATTGAGATATTACGA
BK664_AFCL31R	CAACTCCTTAAAGCAGAGACTC
BK665_AFCL32F	GTCCTTCTCGACAGATCATG
BK666_AFCL32R	CGTGCTGGAAGAGCTGTC
BK667_AFCL33F	GGAAACGAATCTTCCGTCCG
BK668_AFCL33R	ATATTCTCGTACAGCTCCCAC
BK669_AFCL34F	GTGACTCCAGAGGATATCTC
BK670_AFCL34R	TGGCAGAAGCTCTCCATCAC
BK671_AFCL35F	AGTGGATTCGACTTCCAGAC
BK672_AFCL35R	TTCTCTGTGACGAAGGTCTTC
BK673_AFCL36F	CAAGAGCTGTGTCTGCTAATC
BK674_AFCL36R	CTAGCTGCATATTACACCGAAC
BK675_AFCL37F	GTCACAGCAAGATGAGTCAG
BK676_AFCL37R	GGTCTCGGATGCGATTAGAG
BK677_AFCL38F	GATGTTAGCGACAATGCTGAG
BK678_AFCL38R	GAGGTATCCAAGGCAGACAC
BK679_AFCL39F	AGAACGATTGGTTGCAGGATC
BK680_AFCL39R	GCAACGTCGAAGACCTGG
BK681_AFCL40F	CTTCCTCTGCCTCGAAACC
BK682_AFCL40R	CATATTGCTCAGTGGCTCTTG
BK683_AFCL41F	CCTTCAATGATGTACTAAGCCAG
BK684_AFCL41R	GGGTCCCTTGGCGACTTG
BK685_AFCL42F	GACCAGATGCAGGACCAAG
BK686_AFCL42R	GGAATCTCCTGACACATGATG
BK687_AFCL43F	GTGGAGTTATTGCTGACTGAC
BK688_AFCL43R	GACAATATTACCGGTAGGAATAC
BK689_AFCL44F	CTTCCACCTTATGAACCCTAATC

BK690_AFCL44R	CTTGATAGATTCCAGATCACTGAT
BK691_AFCL45F	GTCTAGTGTTGAAAGAGCAGC
BK692_AFCL45R	TGACTGCTTCCACCAATTGC
BK693_AFCL46F	CAGAGGTTGTCGATATGCATG
BK694_AFCL46R	GTAAAGGTACCATGGTTGCTG
BK695_AFCL47F	GTTGACTACGTTAACTCGGTC
BK696_AFCL47R	ACAGGTCCATTGTGGCATCC
BK697_AFCL48F	GATCTCGACGGTGTTCTATC
BK700_AFCL49R	TGCAACCAGCGAATCAACAC
BK701_AFCL50F	CAACGAGACTGGATCCACC
BK702_AFCL50R	TCAGTATGCCAGTTGAACGAC
BK703_AFCL51F	GTATGACCATCTGTGCTGTG
BK704_AFCL51R	GTTGGTCAATGCCACATCTATC
BK705_AFCL52F	GTTTCGAGAGCGGGACATG
BK706_AFCL52R	CTCCATCCATCGTGCTCTC
BK709_AFCL54F	CGTCCTACTTAATCCCACAC
BK710_AFCL54R	CTCGTCCATGACTGTATCTG
BK711_AFCL55F	CAATTCAACCCGAGATTCGAC
BK712_AFCL55R	CTCACAAGGGAGCCAATTATAC

Table 2.5 Plasmids employed in this study for *A. flavus* work.

Plasmid	**Description**	**Reference**
pUC19	*E. coli* cloning plasmid with *bla* (ampicillin resistance gene) gene	Thermo Fisher
pBK22	*kdmB* deletion cassette with *AfpyrG* in *Sma*I site of pUC19	This study
pBK23	*rpdA* deletion cassette with *AfpyrG* in *Sma*I site of pUC19	This study
pBK66	*kdmB* genomic locus in *StuI* site of pAN8-1	This study
pBK67	*rpdA* genomic locus in *StuI* site of pAN8-1	This study
pBK79	*kdmB::sgfp::AfpyrG* cassette in *Sma*I site of pUC19	This study
pBK80	*kdmB::3xha::AfpyrG* cassette in *Sma*I site of pUC19	This study

Table 2.6 *A. flavus* strains employed in this study.

Strain	**Genotype**	**Reference**
NRRL3357	*nku70Δ::argB*	Keller Lab
Tjes19.1	*nku70Δ::argB, pyrG89*	Keller Lab
AFLBK1	*kdmB::3xha::pyrG, nku70Δ*	This study
AFLBK2	*kdmB::sgfp::pyrG, nku70Δ*	This study
AFLBK22	*kdmBΔ::pyrG, nku70Δ*	This study
AFLBK23	*rpdAΔ::pyrG, nku70Δ*	This study
AFLBK6.10	*kdmBΔ::pyrG; kdmB::phleO; nkuAΔ::argB*	This study
AFLBK7.4	*rpdAΔ::pyrG; rpdA::phleO; nkuAΔ::argB*	This study

Chapter 3 Results

H3K4 demethylase KdmB bridges cohesin acetylation to the histone deacetylase-ring finger complex for *Aspergillus nidulans* light responses

3.1 KERS is a multi-domain tetrameric chromatin remodeling complex consisting of H3K4me3 demethylase KdmB, cohesin acetyltransferase EcoA, histone deacetylase RpdA and ring finger protein SntB

Lysine-specific demethylase 1 (LSD1) interaction with the SIN3A/HDAC complex was shown to be the regulator of several cellular signalling pathways such as proliferation, survival, metastasis and the P53 signalling pathway (Yang et al., 2018). KDM5, an H3K4 JARID1 demethylase, was also indicated to interact with the histone deacetylase SIN3B-HDAC complex for the control of regulation of developmental genes (Nishibuchi et al., 2014). In order to investigate possible chromatin modifier complexes in filamentous fungi, *Aspergillus nidulans* was used as a model organism to create endogenous C-terminal epitope tags of KdmB protein with TAP, sGFP and HA (Figures 3.1 and 3.2). KdmB immunoprecipitation was carried out and potential KdmB *in vivo* interacting partners were analysed by liquid chromatography-mass spectrometry (LC-MS^2) method. Proteomics data revealed that KdmB recruited cohesin acetyltransferase EcoA, histone deacetylase RpdA and chromatin binding ring finger protein SntB (Table 3.1). Therefore, the resulting novel demethylase tetrameric complex was named as KERS (KdmB-EcoA-RpdA-SntB) complex. In order to prove if EcoA, RpdA, and SntB are similarly capable of recruiting the KERS complex, the same strategy was used to tag these proteins with three different epitope tags. Indeed, reciprocal tagging and LC-MS^2 analysis of EcoA, RpdA, and SntB purifications further confirmed the bulk presence of the KERS complex. These experiments were performed using nutrient limited culture as well as rich media and similar results were found. Growth temperature shifts from 37ºC to 30ºC did not have any effect on complex formation emphasizing the stable tetrameric complex formation during different growth conditions. The number of unique peptides for all four proteins were significantly high. KdmB, EcoA, RpdA, and SntB were top-interacting partners in every analysed purification. AGB551 and GFP expressing *A. nidulans* strains were used as negative controls.

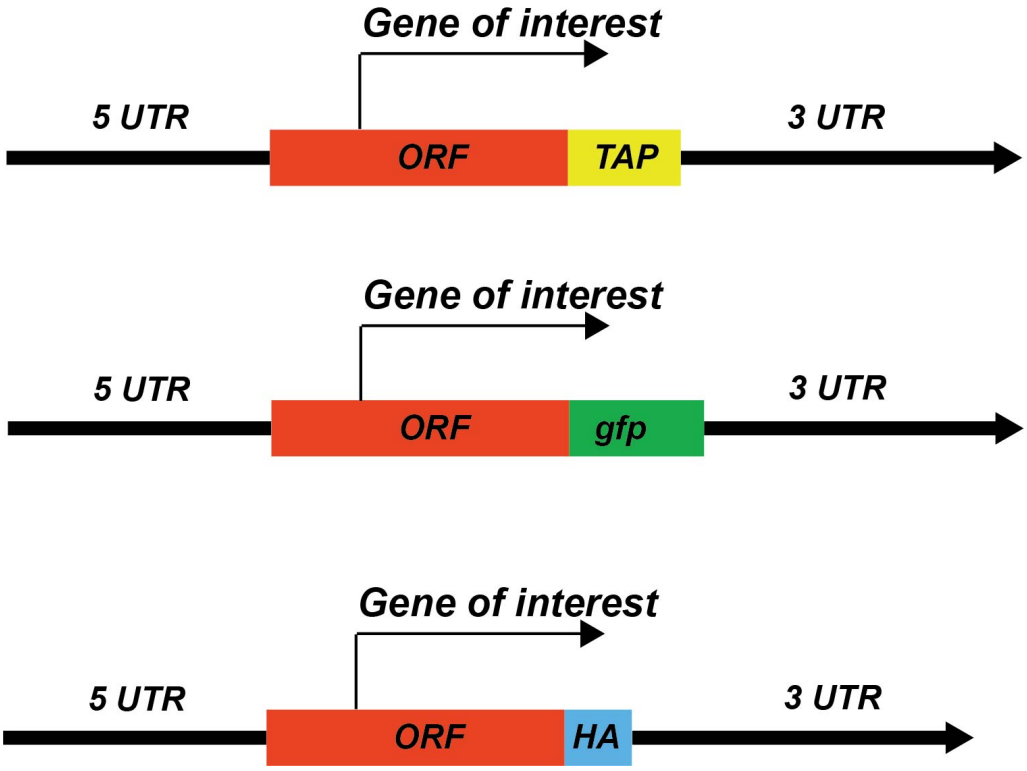

Figure 3.1. Representation of epitope tag strategy of KERS complex proteins. The *Sma*I-digested linear pUC19 plasmid was used as a donor to insert DNA fragments of epitope tags. DNA fragments of 5UTR-ORF and 3UTR were amplified and fused together with the epitope tag and selective marker *nat*R expressing antibiotic nourseothricin or *pyr*G as the auxotrophic marker for uracil. Each tag was fused to the C-terminals of gene open reading frames (ORFs) via the In-Fusion HD cloning kit. TAP, GFP and HA proteins were expressed under each genes native promoters. Selected recombinant strains expressing TAP, GFP and HA were confirmed by Western blot using specific monoclonal mouse antibodies and checked by Mass Spectrometry.

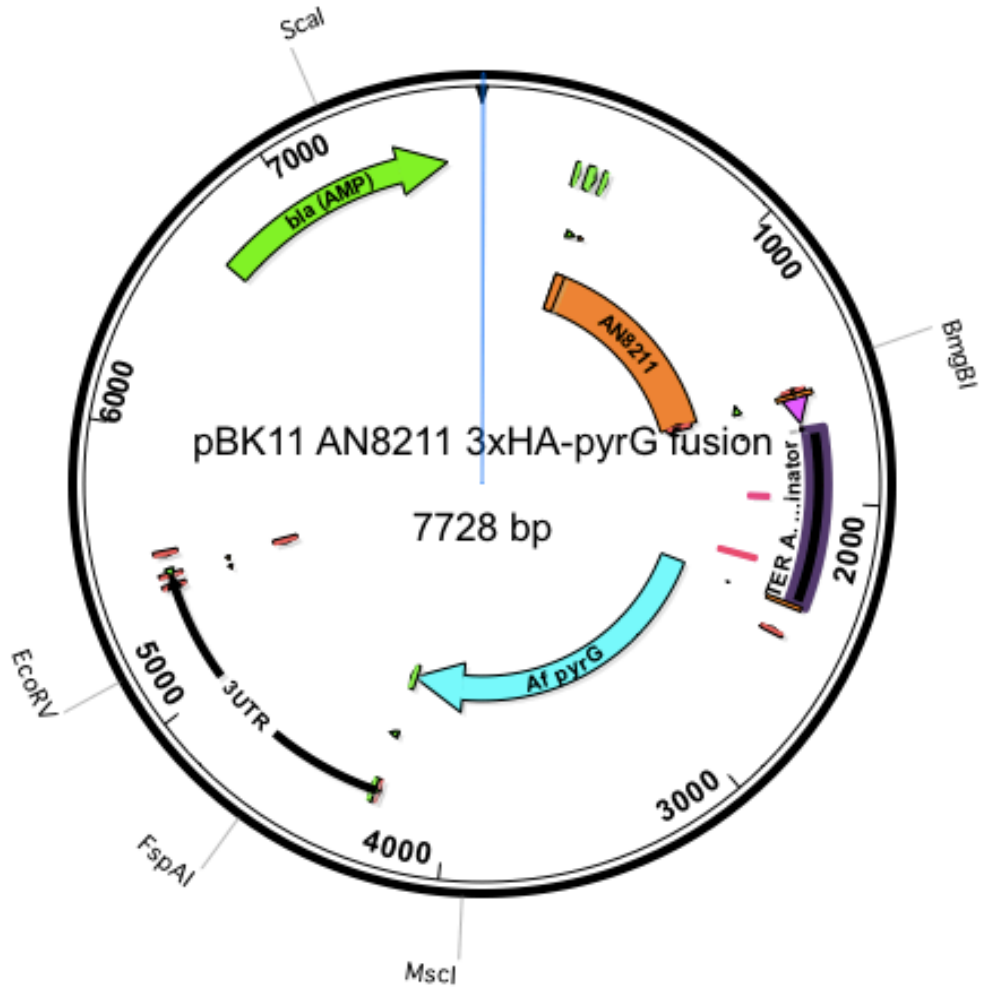

Figure 3.2. An illustration of a plasmid map of KdmB::3xHA circular plasmid construct. 5UTR-ORF and 3UTR regions were selected as homology sequences for introducing DNA cassettes into *A. nidulans* WT strain. For TAP and GFP strains, *nat*R as a selective marker was used. For HA strains, *pyrG* as an auxotrophic marker was used. Plasmids were confirmed by standard PCR by using nested primers to amplify DNA fragments containing 5UTR-ORF-EpitopeTag-Marker-3UTR final amplicon for fungal transformation.

Table 3.1. Discovery of a novel KdmB demethylase complex (KERS complex): KdmB, EcoA, RpdA, and SntB. Interaction partners of KdmB::cTAP, EcoA::cTAP, RpdA::cTAP, SntB::cTAP, KdmB::sGFP, EcoA::sGFP, RpdA::sGFP, SntB::sGFP, KdmB::3xHA, EcoA::3xHA, RpdA::3xHA and SntB::3xHA expressing TAP, HA and GFP fused proteins which were detected by LC-MS/MS analysis. Fungal mycelia were harvested at the end of 24 h vegetative culture at 37ºC. Values are the average of the three independent biological replicates.

IP LC-MS²	TAP			GFP			HA		
	Proteins Identified	#Unique peptides	% Coverage	Proteins Identified	#Unique peptides	% Coverage	Proteins Identified	#Unique peptides	% Coverage
KdmB	**KdmB**	95	60	**KdmB**	68	48	**KdmB**	87	68
	EcoA	25	48	EcoA	8	24	EcoA	18	51
	RpdA	15	37	RpdA	10	18	RpdA	23	43
	SntB	16	36	SntB	15	31	SntB	20	44
EcoA	KdmB	58	50	KdmB	12	10	KdmB	67	53
	EcoA	18	58	**EcoA**	11	31	**EcoA**	23	61
	RpdA	12	24	RpdA	4	8	RpdA	21	43
	SntB	9	24	SntB	2	4	SntB	16	32
RpdA	KdmB	65	50	KdmB	47	40	KdmB	61	50
	EcoA	7	20	EcoA	4	25	EcoA	7	20
	RpdA	30	60	**RpdA**	24	46	**RpdA**	30	60
	SntB	15	33	SntB	13	13	SntB	15	33
SntB	KdmB	71	55	KdmB	43	35	KdmB	80	62
	EcoA	15	49	EcoA	8	22	EcoA	16	48
	RpdA	20	37	RpdA	12	23	RpdA	25	49
	SntB	14	33	**SntB**	15	39	**SntB**	19	43

3.2 Physical nuclear interaction of KdmB with EcoA, RpdA, and SntB was confirmed via BIFC

Moreover, to confirm physical *in vivo* interactions of KdmB with EcoA, RpdA, and SntB, nYFP/cYFP strains with H2A-mRFP were constructed to perform Bimolecular Fluorescence Complementation (BIFC) assays. Cultures were grown in a liquid GMM media with required supplements in microscopic chambers for 16 h at 30ºC. BIFC images clearly showed that KdmB physically interacted with EcoA, RpdA, and SntB within the nucleus (Figure 1B). Red signals (H2A-mRFP) and light green signals (YFP) were overlapped confirming physical interactions of KdmB-EcoA, KdmB-RpdA and KdmB-SntB.

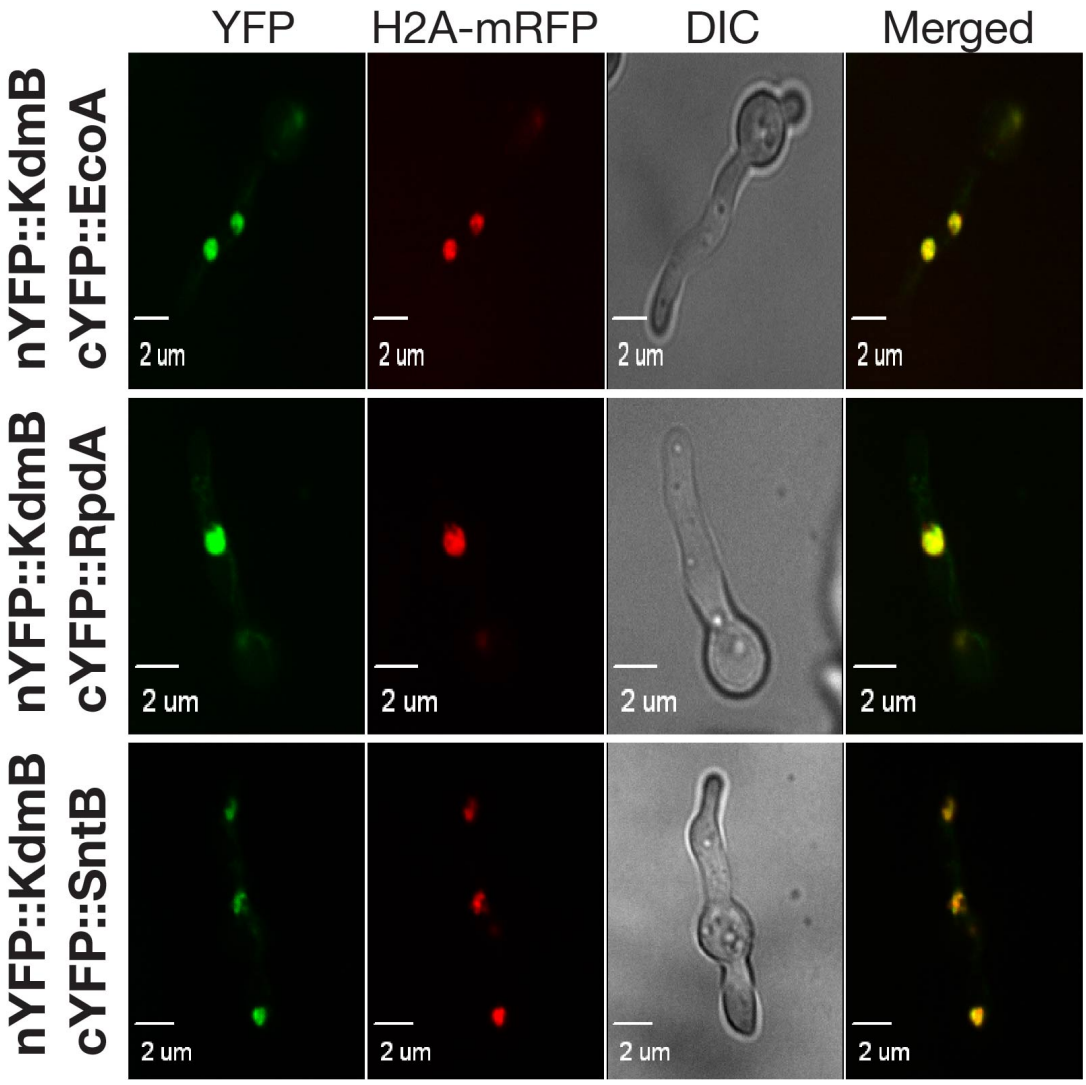

Figure 3.3. Bimolecular fluorescence complementation analysis, verifying subcellular KdmB-EcoA, KdmB-RpdA and KdmB-SntB interactions. The images were captured from vegetative hyphae by fluorescence microscopy at the end of 16 h incubation at 30ºC under illumination. Nuclei are detected by mRFP fused to H2A.

By performing BLAST analysis using protein sequences of the *A. nidulans* KERS complex, it was revealed that KdmB, EcoA, RpdA, and SntB ortholog proteins are conserved from simple fungi to animals and human (Table 3.2). *A. nidulans* KdmB falls into the human KDM5 Jumonji H3K4 demethylase family as previously shown (Gacek-Matthews et al., 2016). Mouse KDM5 is named as Retinoblastoma Protein 2 (RBP2), while fruit fly *Drosophila* KdmB is named as Little Imagine Disk protein (LID). KdmB was shown to have H3K4 demethylase activity capable of removing mono-,di- or trimethylated lysine residues in yeast, *C. elegans*, *D. melanogaster*, mouse and human. It is not clear whether the KdmB ortholog of *A. thaliana* has H3K4 demethylase activity. Similarly, Establishment of Cohesion factor (EcoA) is conserved from yeast to *Drosophila*, mouse and humans. Humans have two EcoA orthologs, ESCO1, and ESCO2 respectively. HDAC RpdA is one of the most conserved proteins across various organisms from yeast to filamentous fungi, plant, *Drosophila*, mouse, and humans. RpdA orthologs have been characterised in these organisms and it has been shown to have global deacetylase activity on histone acetylated lysine residues. Interestingly, the ring finger protein SntB has a similar structure in yeast, filamentous fungi, mouse and humans, all harbouring PHD and E3 protein-ubiquitin ligase domains, however, it is not known if structural protein domain is identical in *A. thaliana*, *C. elegans* or *Drosophila*. The highest KdmB sequence similarity among the orthologs was found to be in filamentous fungi *Neurospora crassa* (57%), followed by plant-pathogen *Magnaporthe oryzae* (55%) and budding yeast *S. cerevisiae* JHD2 demethylase (42%). EcoA was found to be highly conserved in *C. elegans* (63%), followed by *N. crassa* (35%) and *M. oryzae* (35%). RpdA ortholog in *S. cerevisiae* (76%), *N. crassa* (73%) and *M. oryzae*

(65%) have significantly high protein sequence similarities. SntB orthologs sequence similarity was not found to be as high as RpdA. Nevertheless, SntB orthologs were present in all organisms analysed. The highest SntB sequence similarity among the orthologs was found to be in *N. crassa* (47%), and *M. oryzae* (47%) followed by *D. melanogaster* (41%).

Table 3.2. Orthologue analysis of the KdmB complex among various organisms. KdmB, EcoA, RpdA, and SntB are conserved from budding yeast to human. The table was generated by BLAST analysis using *A. nidulans* protein sequences as a reference. Numbers indicated beside ortholog proteins correspond to the percent of protein sequence similarity with respect to *A. nidulans*.

	Fungi								Model Organisms										Human	
	S. cerevisiae		*S. pombe*		*N. crassa*		*M. oryzae*		*A. thaliana*		*C. elegans*		*D. melanogaster*		*M. musculus*		*H. sapiens*	
KdmB	Jhd2	42	Lid2	32	NCU01238	57	MGG_04878	55	F2K11.14	38	RBR-2	32	LidA	31	RBP2	31	KDM5	30
	H3K4 demethylase		H3K4 demethylase		Unknown		Unknown		Unknown		H3K4 demethylase		H3K4 demethylase		H3K4 demethylase, Retinoblastoma protein 2		H3K4 demethylase, (JARID1)	
EcoA	Eco1p	26	Eso1	32	NCU00241	35	hypothetical	35	Ctf7	25	NHR-114	63	EcoA	29	ESCO2	30	ESCO1/2	28
	Cohesin acetylation, Establishment of sister chromatid, essential		Cohesin acetylation, DNA Pol.5 acetylation		Unknown		Unknown		Unknown		Unknown		Cohesin acetylation		Cohesin acetylation, H4K16 acetylation.		Cohesin acetylation, Roberts Syndrome	
RpdA	Rpd3	76	Clr6	63	RPD3	73	RPD3	65	HDA6	59	HDAC1	59	HDAC1	58	HDAC2	56	HDAC2	56
	Histone deacetylase response to oxidative stress		Histone deacetylase		Histone deacetylase		Histone deacetylase		Histone deacetylase		Histone deacetylase		Histone deacetylase		Histone deacetylase		Histone deacetylase	
SntB	Snt2	35	Snt2	34	Snt2	47	MGG_04421	47	AT2G25120	27	lin-49	25	BR140	41	Jade2	29	Jade2	28
	PHD domain protein response to oxidative stress		PHD domain protein		PHD domain protein, affects sporulation/ hyphal/sexual growth		Unknown		Unknown		Unknown		Unknown		E3 ubiquitin-protein ligase		E3 ubiquitin-protein ligase PHD domain protein	

Domain architectures of KdmB and SntB revealed that both proteins have characteristic plant homeodomains (PHD) required for histone-binding and chromatin-mediated gene regulation (Figure 3.4). KdmB contains a Jumonji N domain at its N terminus (between amino acids 74-115), an Arid/Bright domain (164-252), a plant homeodomain and bromo adjacent homology (PHD/BAH) domain (457-537), a Jumonji C domain (629-745), a zinc finger domain (853-912) and a second PHD domain (1323-1367) at the C terminus with a total size of 1717 amino acids. Domain architectures of KERS members clearly present chromatin recognition, binding sites and their catalytic domains involved in demethylation, acetylation and deacetylation (Figure 3.4). EcoA was the smallest member of the tetrameric complex with 401 amino acids. It contains a zinc finger domain (156-193) and acetyl-transferase (AT) (329-390) domains. Histone deacetylase RpdA contains a deacetylase domain (26-424). SntB protein was almost as big as KdmB protein with 1596 amino acids and contains a PHD/BAH domain (235-360), two PHD domains (402-448 and 997-1197) and a SANT domain (728-769) named after common chromatin regulators Swi3-Ada2-N-CoR-TFIIIB of yeast. These results demonstrate that KERS is a novel histone demethylase protein complex which consists of multi-domain proteins bearing classical chromatin binding regions that are present in higher eukaryotes as well as human.

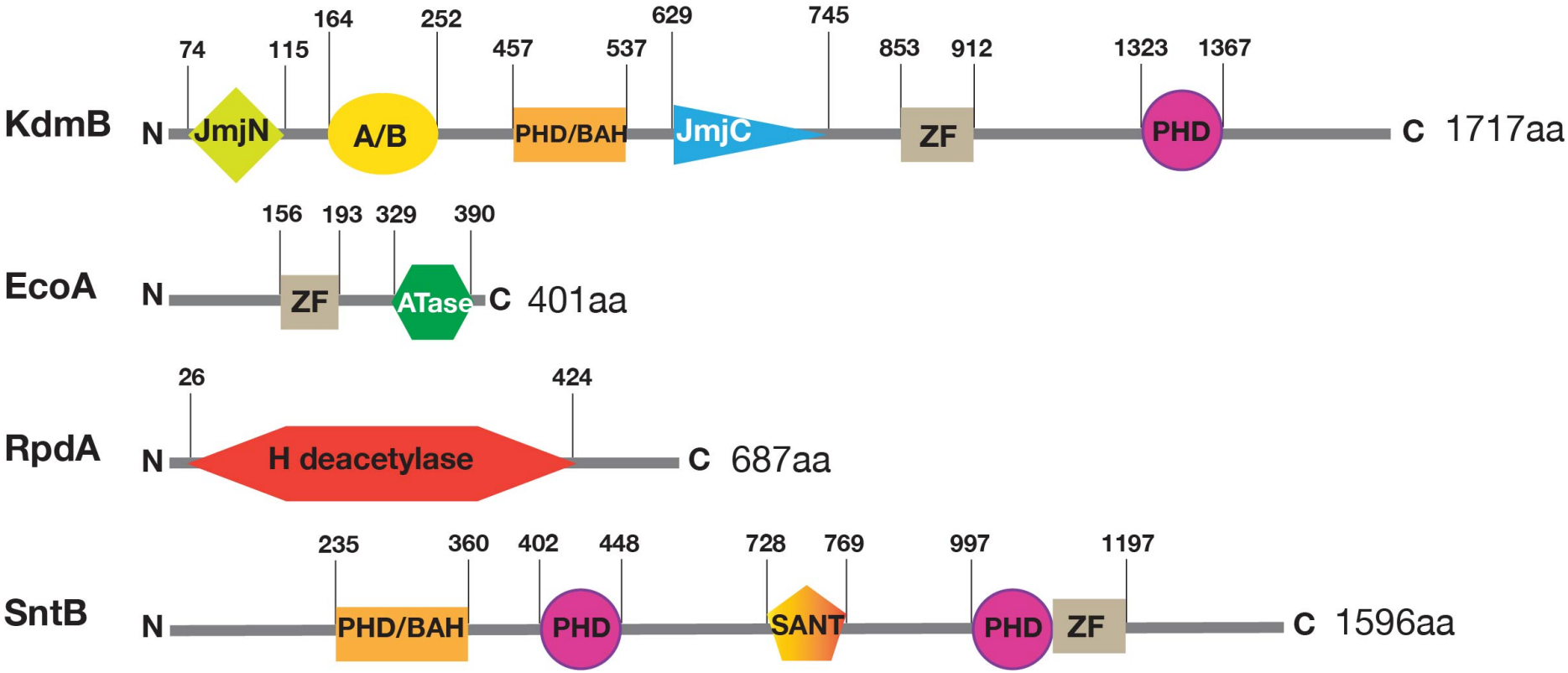

Figure 3.4. Domain architecture of KERS complex members in *A. nidulans*. PHD: Plant homeodomain, ZF: Zinc Finger, A/B: Arid/Bright domain, BAH: Bromo-adjacent homology domain, SANT: Swi3, Ada2, N-Cor, and TFIIIB domain. The sequence positions of each domain were obtained from The National Center for Biotechnology Information (NCBI) protein database. N = N-terminal, C = C-terminal.

3.3 All four KERS complex proteins colocalize within the nucleus

From protein sequence analysis**,** it is clear that KERS consists of multi-domain proteins which have characteristic chromatin recognition and histone-binding sites for their catalytic activities. In order to explore KERS sub-cellular localizations, GFP fused strains were used as hosts to insert H2A-mRFP fragments for histone visualization. The resulting strains expressing both GFP and H2A-mRFP were subjected to confocal microscopy analysis to validate whether these proteins are localized within the nucleus. Interestingly, all members of the complex (green colour) accumulated within the nucleus co-localizing with H2A-mRFP (red colour) suggesting the bulk presence of the complex within the nuclei (Figure 3.5). As can be seen, GFP and mRFP signals merge in all four strains. GFP signals could not be detected in the plasma membrane. Functional KdmB::sGFP, EcoA::sGFP, RpdA::sGFP and SntB::sGFP expressed under their native promoters were only found to be present within the nucleus which is in agreement their involvement in chromatin binding functions.

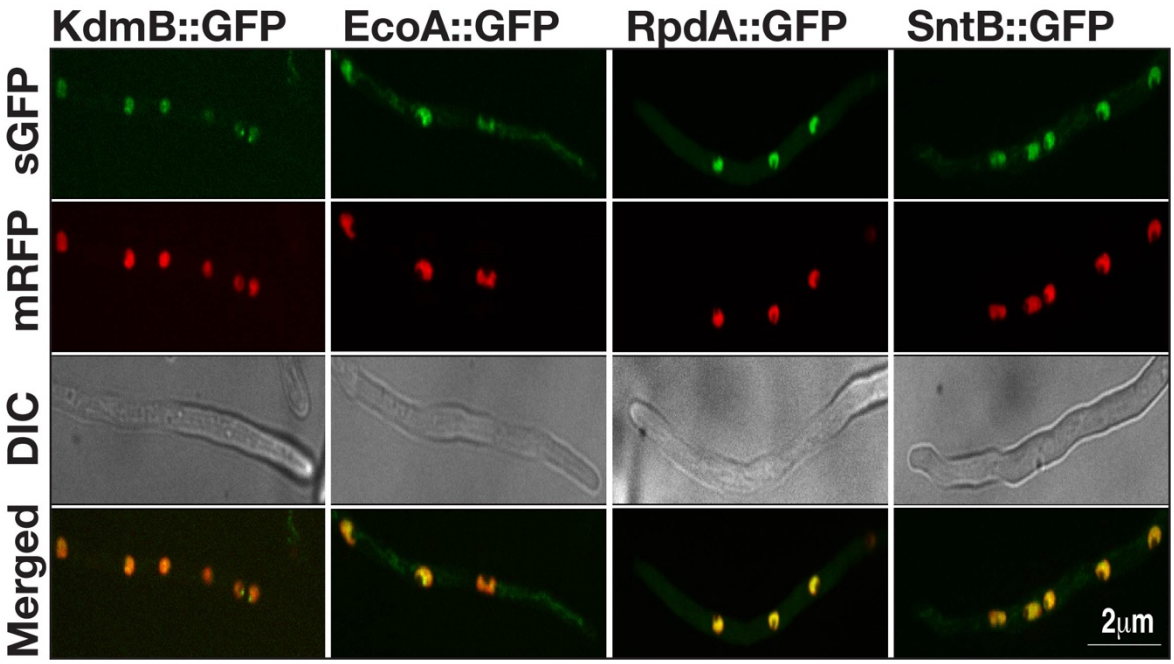

Figure 3.5. Cellular localization of KERS complex proteins. Confocal microscopy analysis of GFP expressing KdmB, EcoA, RpdA, SntB in H2A-mRFP expressing strain and their cellular localization. Images were captured at 60x magnification at the end of 16 h static growth at 30°C in GMM.

3.4 Global regulator of fungal development and secondary metabolism LaeA is not required during KERS assembly

As previously mentioned in Chapter 1, LaeA has always been under investigation for whether it is capable of modifying histone residues due to the fact that LaeA is a methyltransferase domain protein, transferring a methyl group from the ubiquitous SAM to either nitrogen, oxygen or carbon atoms. Although this hypothesis is still not proven yet, it has been shown that epigenetic marks can be affected in *laeA* mutants which show reduced SM production and increased levels of H3K9 methylation (Reyes-Dominguez et al., 2010). In order to elucidate if demethylase KERS complex formation is LaeA-dependent, *laeA* was deleted in the KdmB::cTAP strain to conduct mass spectrometry analysis. KdmB::TAP purification recruited all four proteins forming the tetrameric complex, suggesting that LaeA is not required for KERS complex formation. Furthermore, there was not any significant change in the number of unique peptides or percent coverage of proteins recruited (Data not presented).

3.5 Demethylase KERS complex plays crucial roles in growth, asexual and sexual life-cycles of *A. nidulans*

To more thoroughly investigate the roles of the KERS complex in fungal growth and development, DNA fragments containing 5UTR and 3UTR regions with a *ptrA* marker

replacing the ORFs were introduced into a WT strain to create *kdmB*, *ecoA*, *rpdA,* and *sntB* deletion strains. Although many attempts were made to delete *ecoA* (AN10336) and *rpdA* (AN4493), there were no viable colonies detected at the end of transformations, suggesting that *ecoA* and *rpdA* are essential genes for growth in *A. nidulans* (Graessle et al., 2000). Therefore, doxycycline-dependent promoter replacements of *ecoA* and *rpdA* were performed to down-regulate these proteins to investigate their roles in fungal development (Figure 3.6). Successfully, there were viable colonies present displaying weaker growth with respect to WT and they were selected for further analysis. Multi-well culture plates were used to detect phenotypic effects of $ecoA^{TetON}$ and $rpdA^{TetON}$ strains. Doxycycline with increasing concentrations was supplemented into each well to gradually induce the expressions of *ecoA* and *rpdA*. The absence of inducer and low concentrations of doxycycline (up to 120 μg/ml) resulted in reduced growth and sporulation. Sporulation in $ecoA^{TetON}$ and $rpdA^{TetON}$ strains was found to be partially restored in 180 μg/ml doxycycline supplemented media. Thus, in the subsequent experiments, $ecoA^{TetON}$ and $rpdA^{TetON}$ strains were used without the requirement of an inducer to analyse the consequences of EcoA and RpdA depletion on fungal development. Confirmation of promoter replacement strains was performed by RT-qPCR using total mRNA derived from mycelia cultures grown under GMM supplemented with various doxycycline concentrations (See Chapter 2, Figure 2.2).

kdmB (AN8211) and *sntB* (AN9517) were successfully deleted and viable colonies were selected for subsequent experiments. *kdmB* and *sntB* mutants were verified by Southern hybridization using DIG-labelled probes and RT-qPCR experiment showing the absence of *kdmB* and *sntB* expression (Figure 2.1).

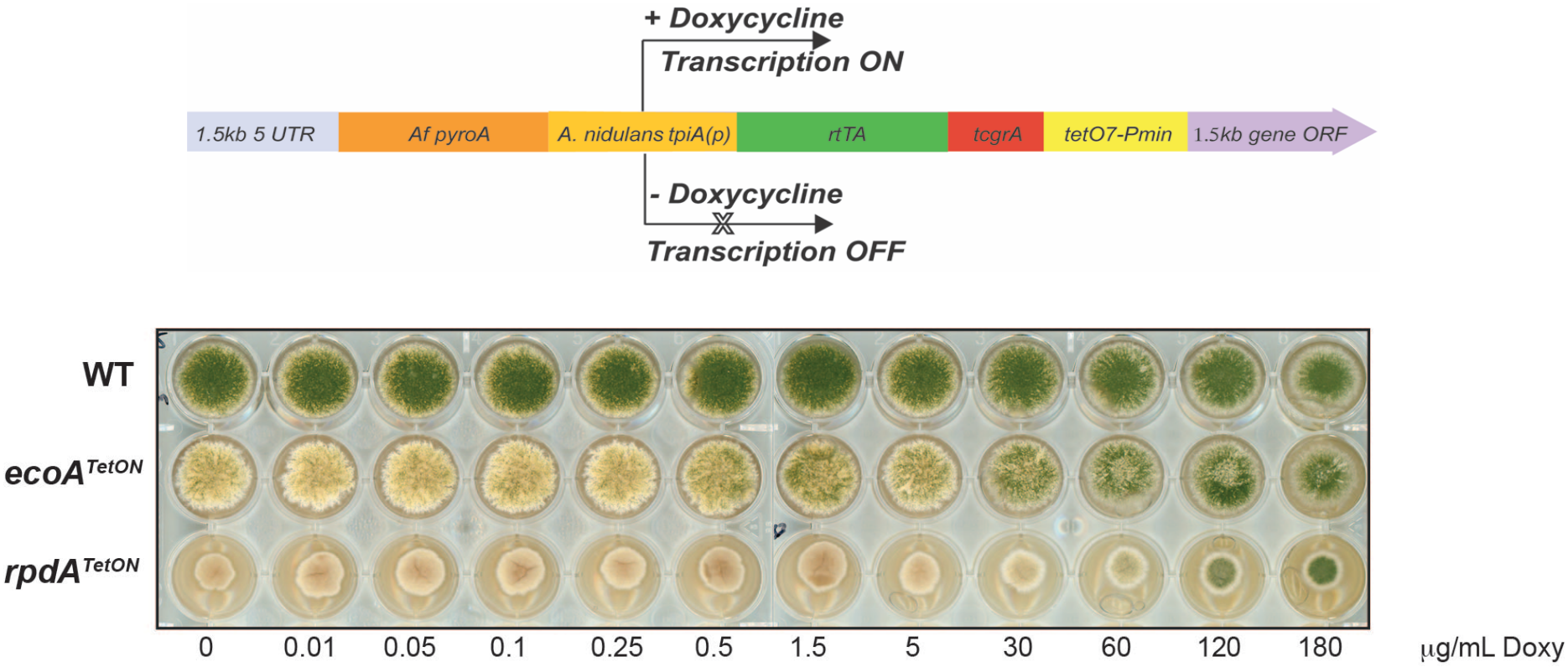

Figure 3.6. Promoter replacement using Tet-ON doxycycline-dependent tuneable promoter. (Upper panel) Schematic representation of doxycycline-dependent promoter region. *A. fumigatus pyroA* marker was used to select successful transformants. (Lower panel) Growth of the WT, *ecoA*^{TetON} and *rpdA*^{TetON} in GMM agar media with required supplements and various concentrations of inducer doxycycline. Cultures were grown for 36 h at 37ºC. *ecoA*^{TetON} and *rpdA*^{TetON} are still able to grow in the absence of inducer suggesting trace levels of *ecoA* and *rpdA* expression are sufficient for survival. Phenotypes of *ecoA*^{TetON} and *rpdA*^{TetON} strains are improved in higher doxycycline concentrations.

All mutants, with the exception of the *ecoA* knock-down strain, showed reduced radial growth. The most drastic inhibition of growth was visible in the *rpdA* down-regulation strain. RpdA depletion resulted in 80% reduced radial growth when compared to the WT strain. There was approximately 30% reduced growth in the *sntB*Δ and double-deletion *kdmB*Δ/*sntB*Δ strains, while the single *kdmB*Δ deletion strain resulted in only 10% reduced radial growth (Figure 3.7B). Interestingly, light-dependent asexual sporulation was drastically reduced in all deletions with the highest reduction being shown in the *sntB* mutant which could sporulate only 10% of WT levels in light conditions. The *kdmB* mutant strain showed 40% less sporulation while *ecoA* and *rpdA* knock-down strains showed 80% and 90% reduced sporulation respectively. A similar result was found when cultures were subjected to growth in the dark conditions. Normally, conidiation is reduced in dark conditions but it should still occur at certain levels. In addition to their single deletions, a *kdmB* and *sntB* double deletion strain was constructed to determine the epistatic role of these proteins. *kdmB/sntB* double deletion and *rpdA* knock-down strains produced conidia only at trace levels. The *kdmB/sntB* deletion phenotype showed that SntB is epistatic to KdmB. Similar sterile phenotype lacking sexual ascospore showing white hyphal mass was visible in double deletion strain under both light and dark condition (Figures 3.7A and 3.7C). Overall, asexual sporulation seemed to be negatively affected in all mutants when compared to WT. Hence, these results certainly imply that the KERS complex is a positive-regulator of light-induced conidiation in *A. nidulans*.

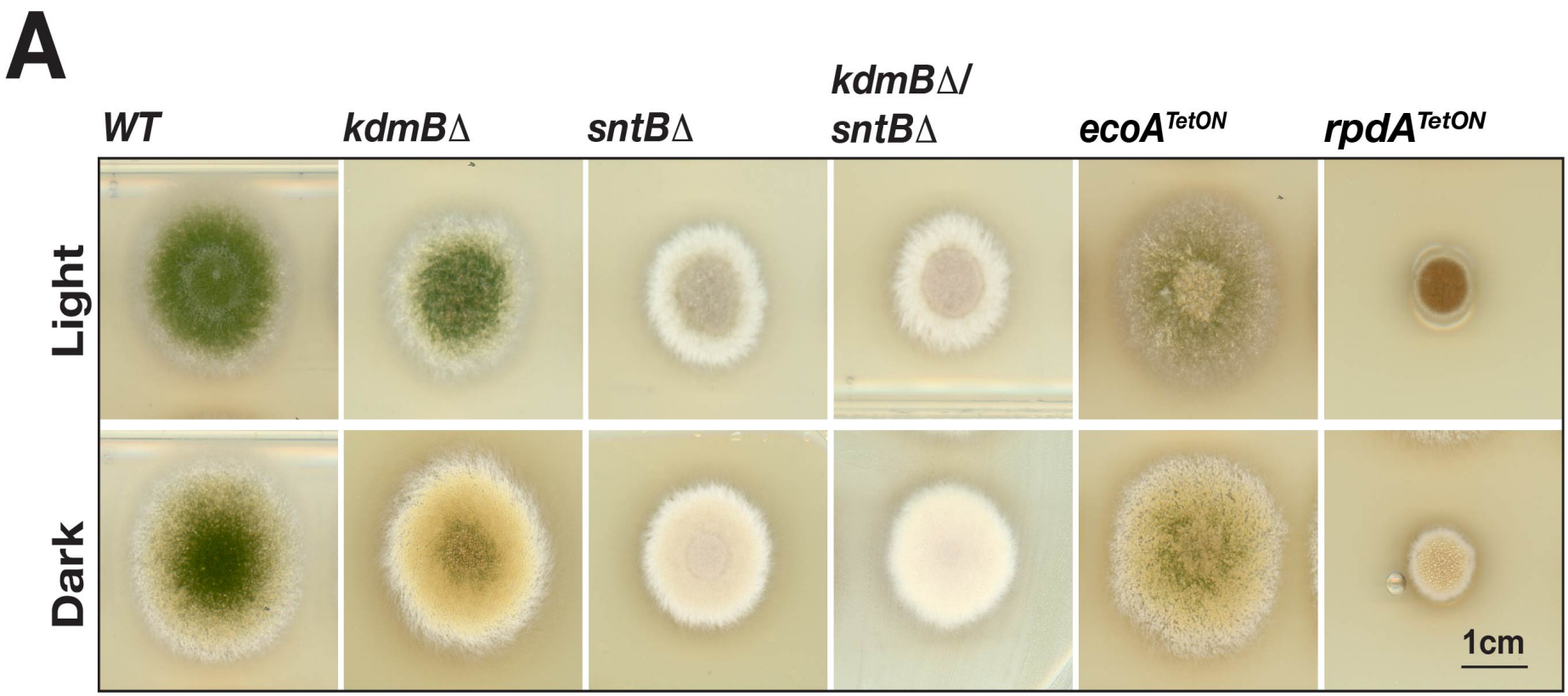
A
WT
kdmBΔ
sntBΔ
kdmBΔ/
sntBΔ
ecoA TetON
rpdA TetON
Light
Dark
1cm

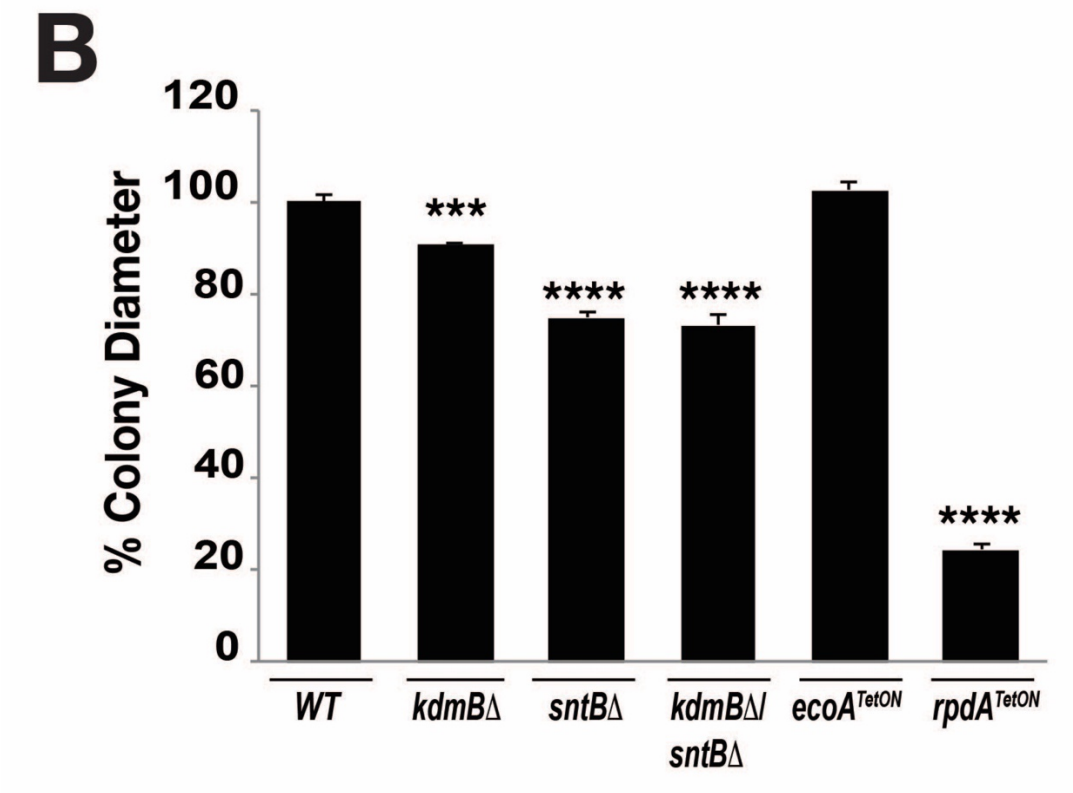

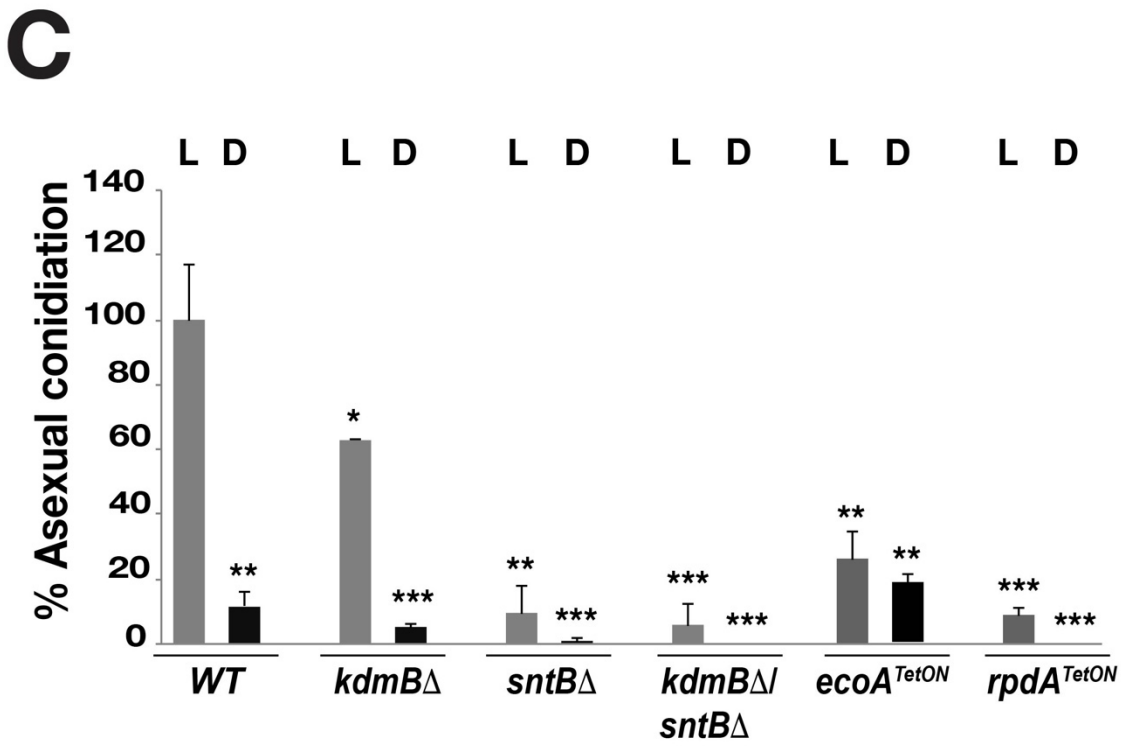

Figure 3.7. The roles of *kdmB*, *ecoA*, *rpdA,* and *sntB* on growth and asexual development of *A. nidulans*. (A) Examination of growth behaviour of WT and mutant strains grown

during light and dark conditions. Approximately $5x10^3$ spores of WT, *kdmB*Δ, *sntB*Δ, *kdmB*Δ/*sntB*Δ, $ecoA^{TetON}$ and $rpdA^{TetON}$ strains were spot inoculated onto GMM with required supplements and grown under light and dark conditions for 3 days at 37°C. (B) For the examination of the radial growth of the WT, *kdmB*Δ, *sntB*Δ, *kdmB*Δ/*sntB*Δ, $ecoA^{TetON}$ and $rpdA^{TetON}$, strains were subject to grow under illumination. Approximately $5x10^3$ spores of WT and the mutant strains were spot inoculated onto GMM with required supplements and grown under illumination for 3 days at 37°C. WT is adjusted to 100%. (C) Percent of asexual conidiation of WT and mutant strains during light and dark conditions. For conidia quantification, 1 cm diameter agar core was removed and resuspended in 200µl PBS. Asexual spores were quantified using microscopic counting chambers. WT grown under the light condition is adjusted to 100% for relative comparison. *sntB* deletion shows blind phenotype where this mutant does not respond to light stimuli lacking normal conidiation. Similarly, *rpdA* down-regulation results in loss of conidiation during both light and dark conditions. Conidia quantifications are the average of the three independent biological replicates. The level of significance is set at $p < 0.05$ (*), $p < 0.01$ (**), $p < 0.001$ and $p < 0.0001$ (****).

3.5.1 Ring finger protein SntB and RpdA are essential for sexual development

Cleistothecia are highly specialized sexual structures of *A. nidulans,* required for genetic exchange and survival during limited sources. These structures are surrounded by nursing cells known as Hulle cells which are required to protect and nourish cleistothecia during full maturation (Bayram and Braus, 2012). Each fruiting body contains one mature cleistothecium embedded within Hulle cells, containing sexual ascospores required for genetic exchange. Each ascospore can propagate and grow when optimal conditions are met. In order to analyse the possible effects of KERS mutant strains during cleistothecia

formation, spores were subjected to grow in GMM during light and dark conditions for five days and phenotypes were analysed. Strikingly, the *sntB* mutant and *rpdA* down-regulation strain caused complete loss of cleistothecia development. In addition to this, Hulle cell could also not be detected in these mutants, suggesting that SntB and RpdA are essential for sexual development in *A. nidulans*. In addition to the total loss of cleistothecia, *rpdA* knock-down radial growth rate was drastically reduced. Similarly, the *kdmB*/*sntB* double deletion strain showed a loss of fruiting body formation (Figure 3.8). The *kdmB* mutation and *ecoA* down-regulation, on the contrary, showed increased levels of fruiting body formation. The *ecoA* knock-down strain resulted in a 400% increase and the *kdmB*Δ produced 50% more fruiting bodies when compared with the WT strain. In summary, *kdmB* and *ecoA* mutants seem to have opposing effects on the *rpdA* and *sntB* mutants during sexual development. KdmB and EcoA act as negative-regulators while RpdA and SntB act as positive-regulators during sexual development in *A. nidulans*.

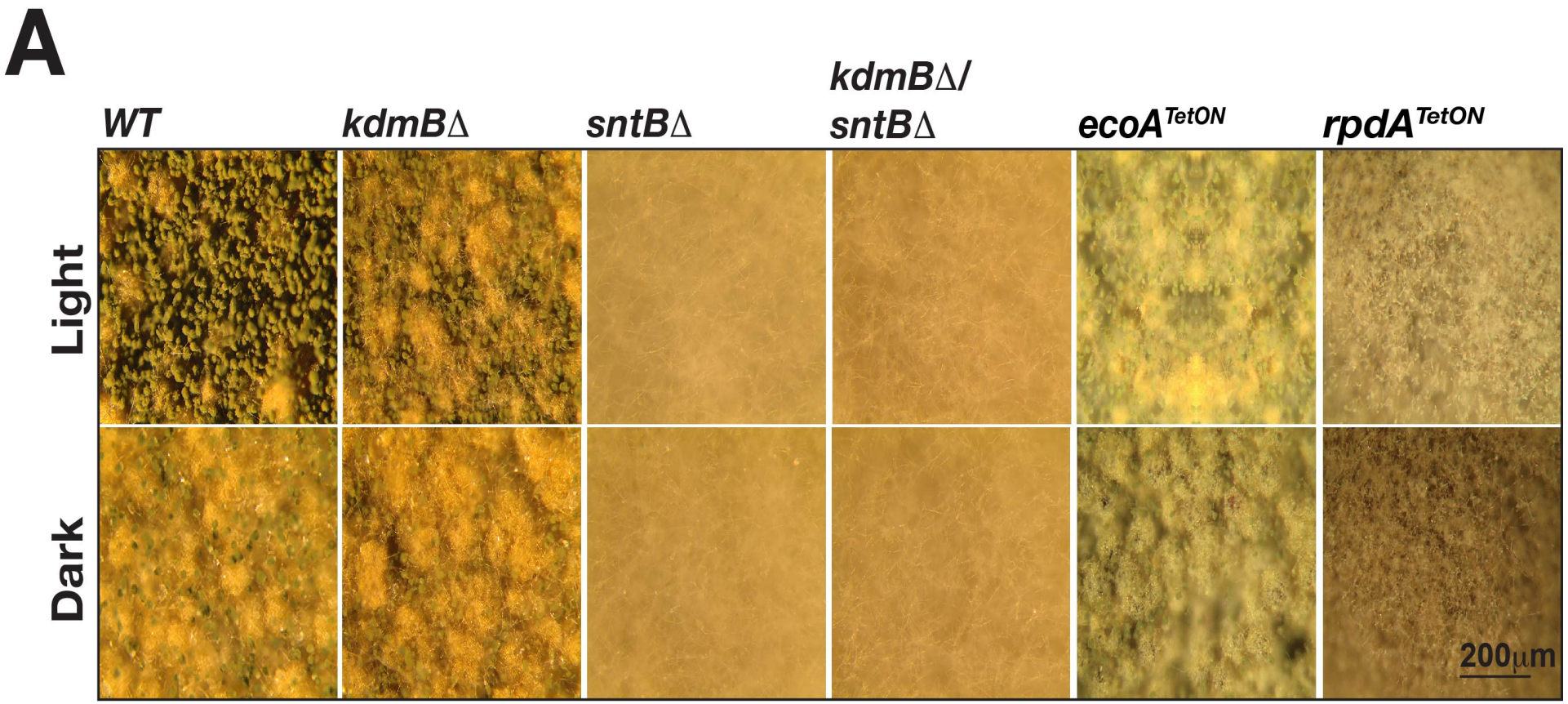
A
WT
kdmBΔ
sntBΔ
kdmBΔ/
sntBΔ
ecoA TetON
rpdA TetON
Light
Dark
200μm

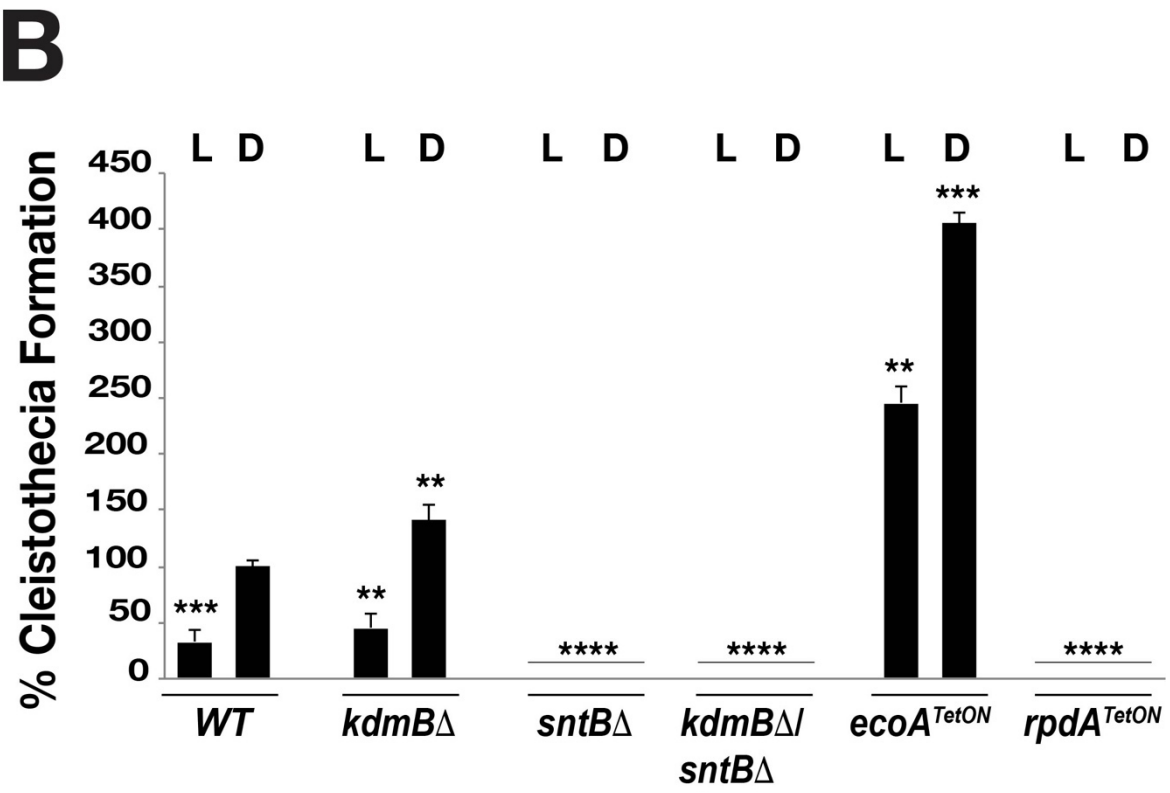

Figure 3.8. Examination of cleistothecia formation in WT and KERS mutants under stereomicroscope (5x). (A) Approximately $5x10^3$ spores of WT, *kdmB*Δ, *sntB*Δ, *kdmB*Δ/*sntB*Δ, *ecoA*^{TetON} and *rpdA*^{TetON} strains were spot inoculated onto glucose minimal media (GMM) containing appropriate supplements and grown under light and dark conditions for 5 days at 37°C. (B) Percent of cleistothecia formation of WT, *kdmB*Δ, *sntB*Δ, *kdmB*Δ/*sntB*Δ, *ecoA*^{TetON} and *rpdA*^{TetON} strains during light and dark conditions. All samples calculation were optimized with respect to the number of fruiting body formation from WT grown under the dark condition which is adjusted to 100%. The number of fruiting body formation was manually calculated using sections of three independent plates. The level of significance is set at $p < 0.05$ (*), $p < 0.01$ (**), $p < 0.001$ and $p < 0.0001$ (****).

3.5.2 Complementation of *kdmB* and *sntB* restored sporulation and cleistothecia formation

kdmB and *sntB* mutant strains were used as hosts for the insertion of the genomic locus of *kdmB* and *sntB* for complementation analysis. *AfpyroA* was used as an auxotrophic marker to select positive colonies. Selected transformants were confirmed by RT-qPCR using cDNA specific oligonucleotides for the amplification of *kdmB* and *sntB* cDNA (Chapter 2, Figure 2.1). Phenotypic spot inoculation assays showed that mutant strains phenotypes were completely restored. Normally, the *sntB* mutant strain was not able to produce sexual structures as well as proper conidiation. However, *sntB* genomic locus insertion completely restored sexual development and conidia production in this mutant strain (Figure 3.9).

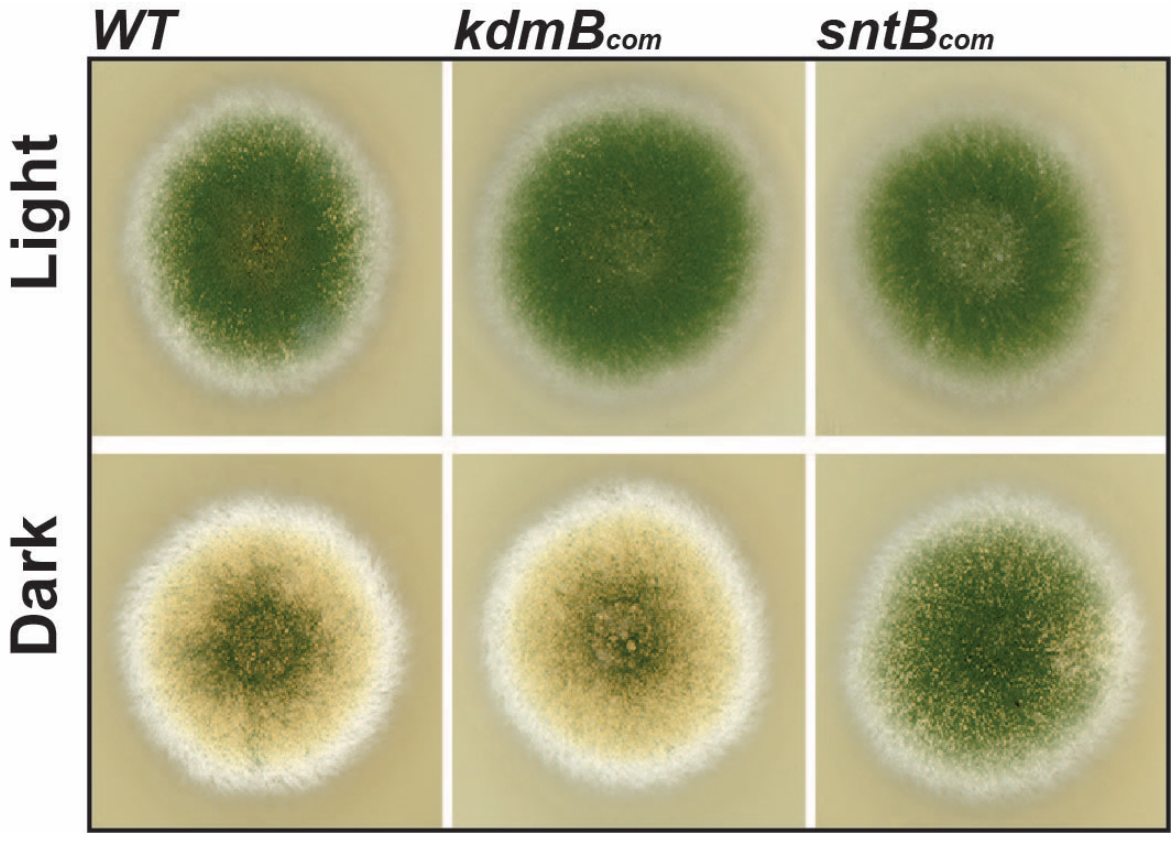

.

Figure 3.9. Sporulation and cleistothecia production is completely restored in *sntB* complementation strain. Ectopic insertion of *kdmB* and *sntB* genomic locus into mutant hosts

were performed by protoplast fusion and *AfpyroA* was used as a selective marker. Approximately $5x10^3$ spores were spot inoculated onto GMM agar media. Images of complementation strains were taken at the end of 3 days grown under light and dark conditions at 37ºC.

3.5.3 Osmotic stabilization has a positive-effect on conidiation in KERS mutants

Chromatin modifier complexes can have genome-wide effects on development likely via involvement in more than one cellular pathway as well as acting as a response to environmental stress factors. Having discovered that KERS plays a major role in conidiation and cleistothecia development, it became interesting to see if this complex has any possible roles against stress-causing agents such as high osmolarity. KCl, NaCl and sorbitol were supplemented into GMM agar plates. *kdmB*Δ, *sntB*Δ, *kdmB*Δ/*sntB*Δ, *ecoA*$^{\text{TetON}}$ and *rpdA*$^{\text{TetON}}$ strains, as well as WT, were centre spot-inoculated with various spore numbers indicated. Normally, conidiation in *sntB*Δ and *rpdA* knock-down strains was drastically reduced when grown on GMM agar plates (Figure 3.7). Additionally, conidiation was also reduced in *kdmB*Δ and *ecoA*^{TetON} strains on GMM agar media. Surprisingly, asexual sporulation was found to be improved in all mutant strains with the most significant increase found in the *sntB* deletion strain. The positive change in conidiation can be seen in all three different osmotic stress agents when applied. Although conidiation was restored in *sntB*Δ and *rpdA*^{TetON} strains under high osmotic stress, fruiting body formation still could not be detected in these strains emphasizing essential roles of RpdA and SntB proteins on sexual development pathways which cannot be recovered by applying osmotic stress. It is very likely that the KERS complex may be involved directly or indirectly in the osmotic regulation pathway in *A. nidulans*.

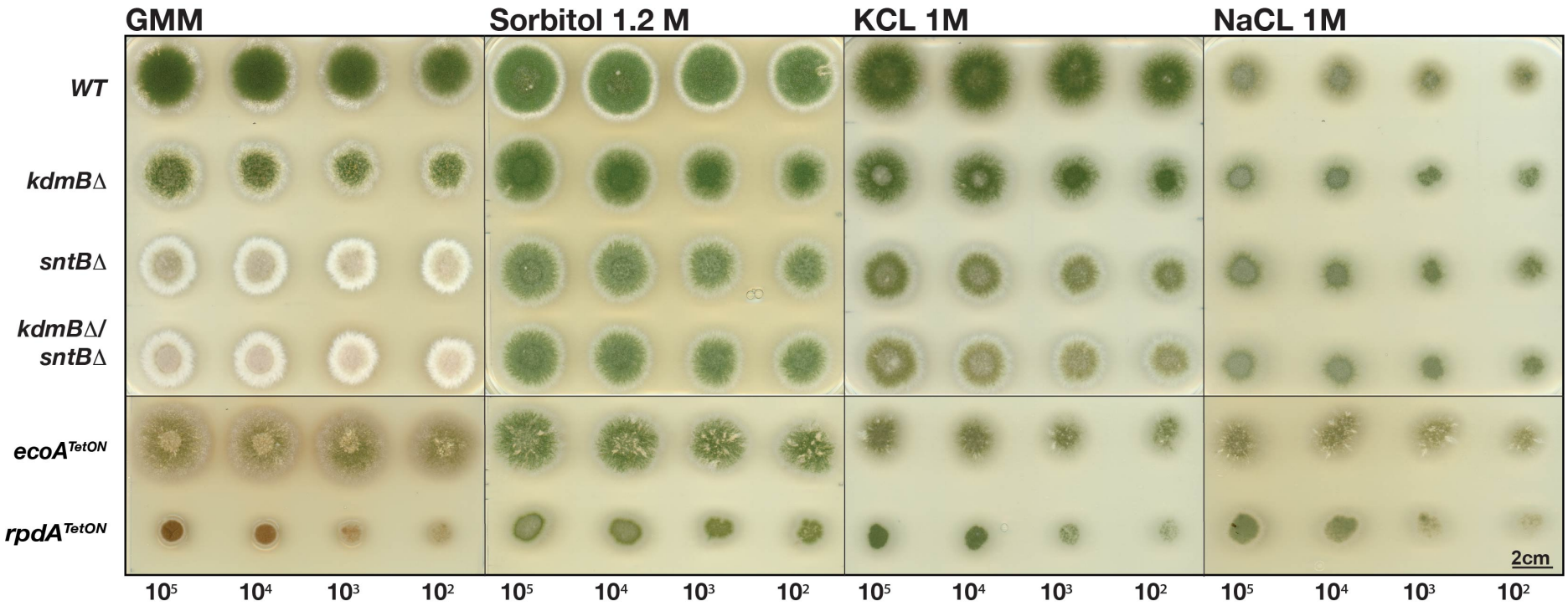

Figure 3.10. High osmolarity restores conidiation in the *sntB* mutant as well as up-regulates conidiation in *ecoA* and *rpdA* knock-down strains. Conidial spores with various numbers, indicated below the figure, were spot-inoculated onto GMM agar with KCl, NaCl and sorbitol, generating high osmolarity. Cultures were grown for 3 days at 37ºC under illumination prior to observation. Phenotypic observations were compared with respect to control medium GMM without any stress-causing agents. The effects of reagents on mutants were correlated with WT strain.

3.5.4 Cell wall stress factors negatively affect KERS mutants

To analyse possible effects of other stress-causing agents on KERS mutants, several chemical factors used in research studies were supplemented into GMM agar plates. In previous studies, sodium dodecyl sulfate (SDS) and Congo red have been used to create cell-wall stress in filamentous fungi (Ram and Klis, 2006, Ram et al., 2004). In order to investigate the role of KERS complex on cell wall stress responses, SDS (0.005%) and Congo red (20µg/mL) were supplemented into GMM media with required supplements and phenotypes were observed at the end of 3 days. Although there was no significant change when SDS was used as a cell wall agent, all KERS mutants showed reduced growth in the presence of congo red. In fact, the *rpdA*^{TetON} strain could not survive in the presence of congo red. Furthermore, the *ecoA*^{TetON} strain exhibited dramatic reductions in growth in the presence of congo red (Figure 3.11). These results suggest that all KERS subunits are equally important during survival against cell-wall agents. The KERS complex is a positive regulator during congo red regulated cell-wall stress which is necessary for the survival against stress factors.

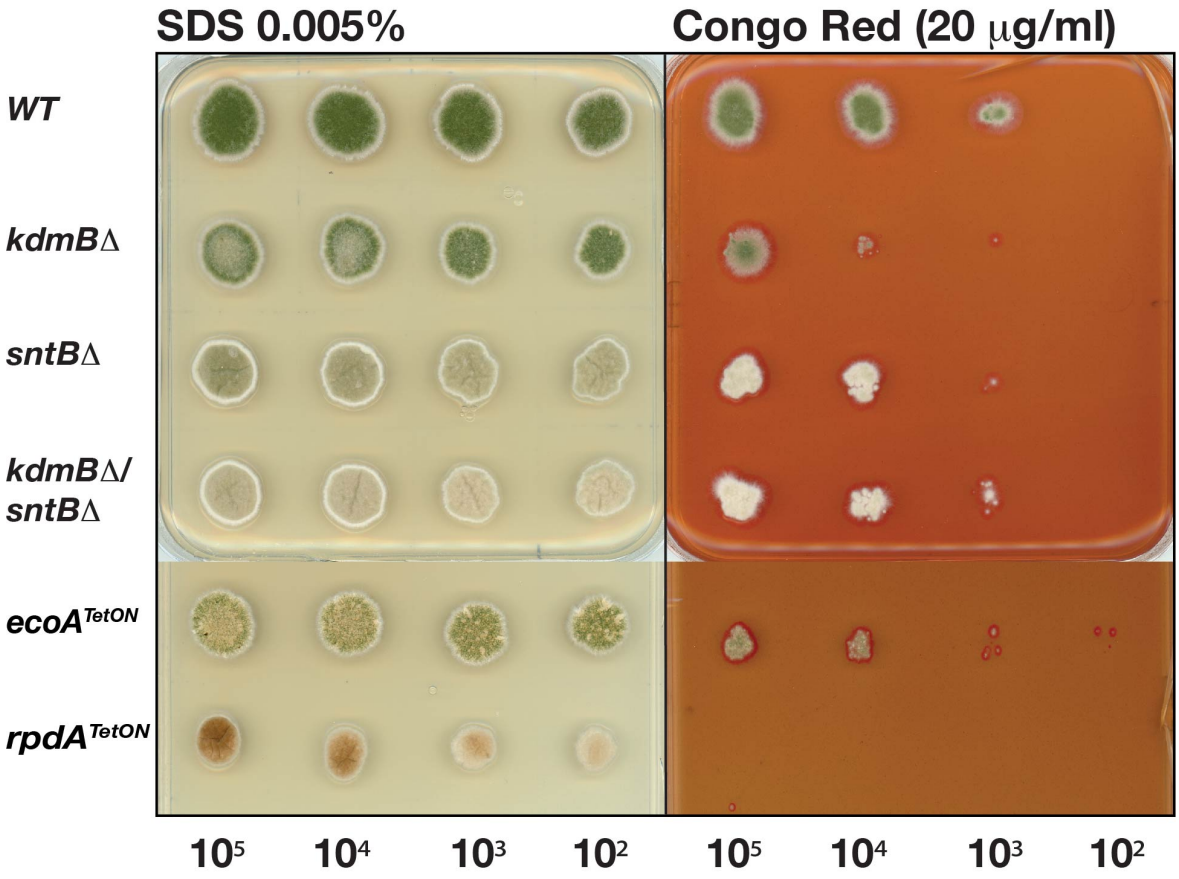

Figure 3.11. The effect of cell wall stress agents on KERS mutants. Conidial spores with 10-fold decreasing numbers were spot-inoculated onto GMM agar supplemented with SDS and Congo Red to generate cell wall stress. Cultures were grown for 3 days at 37ºC under illumination prior to observation.

3.5.5 3-Amino-1,2,4-triazole, camptothecin and benomyl negatively affect KERS mutants

In molecular biology research, 3-Amino-1,2,4-triazole (3-AT) is applied to culture conditions to generate amino acid starvation (Alcazar-Fuoli, 2016). 3-AT leads to histidine depletion and strains cannot survive in culture media in the absence of histidine. In KERS mutants, the addition of 3-AT significantly reduced the growth of the *kdmB*Δ and *rpdA*^{TetON}

strains. 3-AT caused a drastic effect on KERS mutants when compared with WT. There was no visible growth of the *sntB*Δ, *ecoA*^{TetON} and *kdmB*Δ/*sntB*Δ mutants. 3-AT appeared to have a lethal effect on *sntB*Δ, *ecoA*^{TetON} and *kdmB*Δ/*sntB*Δ mutants. Camptothecin (CPT) is a topoisomerase inhibitor widely used as a DNA damage stress agent to study fungal responses (Son et al., 2016). Benomyl, on the other hand, is a fungicide which is toxic to most members of Ascomycota (Zhou et al., 2016). Interestingly, CPT and benomyl resulted in similar phenotypes of the KERS mutants. A significant amount of pigmentation was visible in *kdmB*, *ecoA*^{TetON} and *kdmB*Δ/ *sntB*Δ mutants, emphasizing the activation of certain clusters as a response to stress factors in these mutants while the WT did not have any visible pigmentation produced. In addition to pigmentation, conidiation was highly reduced in the *kdmB* mutant in the presence of benomyl (Figure 3.12). Overall, these results show that the KERS complex plays a role in several distinct stress response pathways such as osmotic, cell-wall, DNA damage and amino acid starvation. Furthermore, these findings present important clues for KERS chromatin binding regions necessary for the regulation of certain biochemical pathways during environmental stresses.

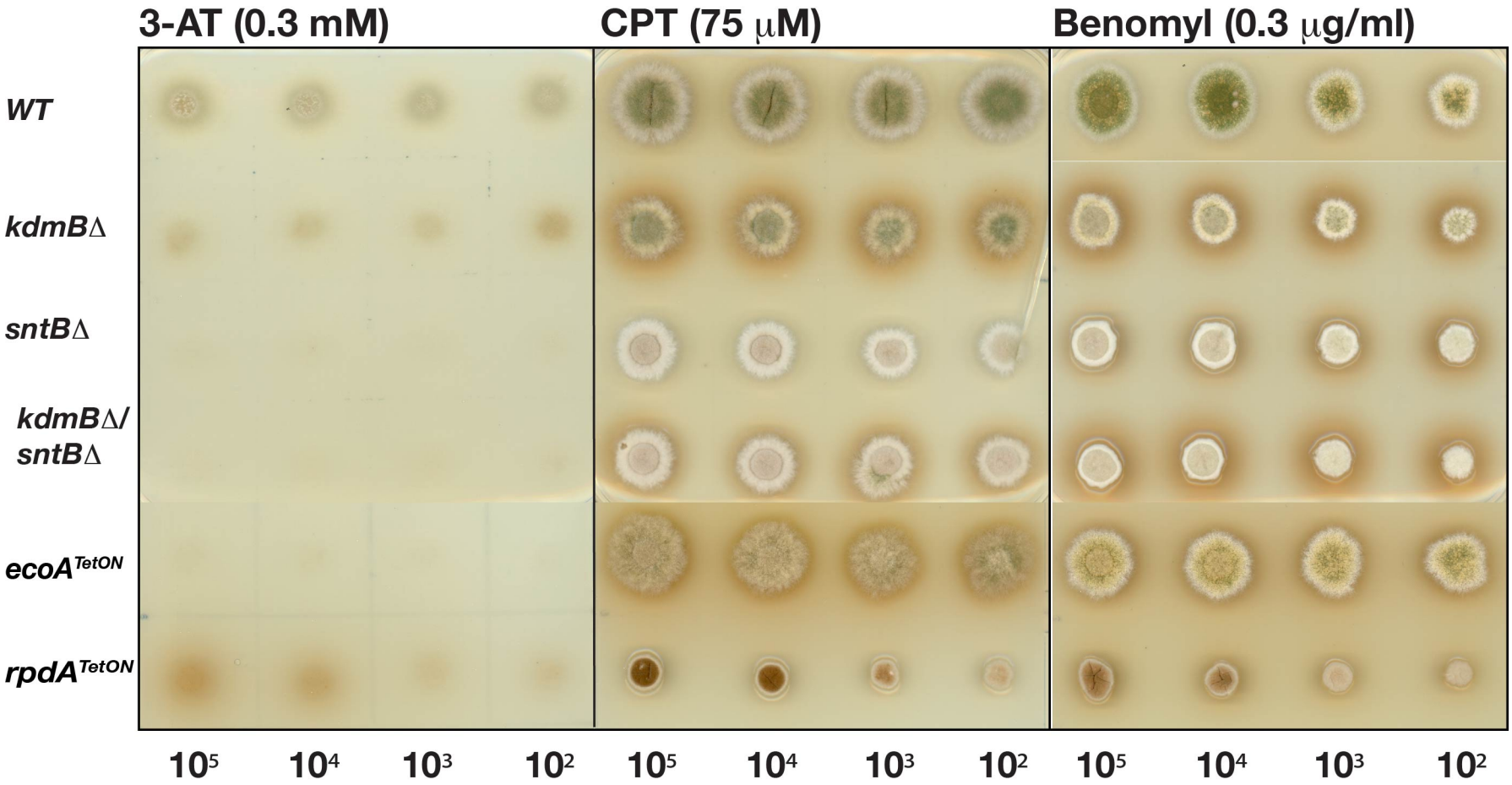

Figure 3.12. The effect of 3-AT, CPT and Benomyl stress agents on KERS mutants. Conidial spores with 10-fold decreasing numbers were spot-inoculated onto GMM agar supplemented with stress agents to observe mutant responses. Cultures were grown for 3 days at 37ºC under illumination prior to observation

3.6 H3K4 demethylase KdmB recruits cohesion factor EcoA to heterodimer RpdA-SntB deacetylase-ring finger protein

Chromatin modifier complexes often interact with other scaffold proteins to target certain genomic regions. Furthermore, such interacting proteins might serve as co-activators or co-repressors for the regulation of complex catalytic activities. In order to analyse *in vivo* complex interdependency of the complex formation, *kdmB* was deleted in EcoA::TAP, RpdA::TAP and SntB::TAP strains. Therefore, the resulting strains were pulled-down and analysed by LC-MS^2 to elucidate the role of KdmB interdependency during complex formation.

Remarkably, in the absence of *kdmB*, RpdA, and SntB could not be detected in the EcoA::TAP purification. EcoA could recruit neither RpdA nor SntB in the KdmB depletion. Interestingly, RpdA::TAP recruited SntB, however, EcoA was not present in the identified proteins. Similarly, SntB::TAP purification recruited RpdA but EcoA could not be detected in the identified protein list. The proteomics analysis revealed that RpdA and SntB form a heterodimer (RpdA-SntB) in the absence of KdmB. These results strongly suggested that H3K4 demethylase KdmB is required for the tetrameric complex formation and essentially it acts as a scaffold by recruiting EcoA to the heterodimer RpdA-SntB for the assembly of the tetrameric KERS complex (Table 3.3).

Table 3.3. LC-MS^2 analysis of EcoA::TAP, RpdA::TAP and SntB::TAP purifications in the *kdmB*Δ strain. Approximately $2x10^6$ conidial spores per ml were inoculated into 800 ml GMM liquid culture and grown for 24 h at 37ºC 220 g. Mycelia were harvested and tandem affinity purification protocol (see Chapter 2) was applied. The same procedure was applied to WT strain which serves as a control sample to filter out non-specific peptide contaminants. Obtained values are the average of the three independent biological replicates.

***kdmB*Δ**

	TAP	#Unique peptides	% Coverage
EcoA	EcoA	19	52
RpdA	RpdA	27	55
	SntB	20	41
SntB	RpdA	28	45
	SntB	19	43

3.7 Ring finger protein SntB recruits class I histone deacetylase RpdA to heterodimer KdmB-EcoA complex

A similar strategy was performed to investigate the role of ring finger protein SntB in the assembly of the tetrameric KERS complex. In order to analyse the role of SntB for complex interdependency, *sntB* was deleted in KdmB::TAP, EcoA::TAP and RpdA::TAP strains. The resulting strains were TAP pulled-down and analysed by mass spectrometry to study the role of SntB for complex assembly.

In the absence of *sntB*, KdmB::TAP could only recruit EcoA, forming a heterodimer demethylase and cohesion factor KdmB-EcoA complex. RpdA could not be detected in the identified proteins in the SntB depletion. Similarly, KdmB was identified in the EcoA-interacting proteins list while RpdA could not be detected. This was further confirmed by RpdA::TAP purification where neither KdmB nor EcoA could be detected in the RpdA-

interacting proteins list suggesting that SntB recruits RpdA to the heterodimer KdmB-EcoA for the assembly of tetrameric KERS complex. Together, these results strongly suggest that ring finger protein SntB is required for tetrameric complex formation and essentially acts as a scaffold by recruiting RpdA into the KERS complex (Table 3.4).

Table 3.4. LC-MS^2 analysis of KdmB::TAP, EcoA::TAP, and RpdA::TAP purifications in the absence of *sntB*. Approximately 2x10^6 conidial spores per ml were inoculated into 800 ml GMM liquid culture and grown for 24 h at 37ºC 220 g. Mycelia were harvested and tandem affinity purification protocol (see Chapter 2) was performed. The same procedure was applied to WT strain which served as a control sample to filter out non-specific peptide bindings. Obtained values are the averages of the three independent biological replicates.

	***sntB*Δ**		
	TAP	#Unique peptides	% Coverage
KdmB	KdmB	94	65
	EcoA	2	8
EcoA	KdmB	35	42
	EcoA	19	50
RpdA	RpdA	29	54

3.8 KdmB prevents EcoA proteasomal-dependent degradation

It was shown earlier in this work that KdmB and SntB are required for tetrameric complex assembly as the depletion of either of these proteins abrogated the recruitment of EcoA and RpdA to the complex. However, it is not clear yet if protein levels of *kdmB*, *ecoA*, *rpdA,* and *sntB* are interdependent. Therefore, KdmB::3xHA, EcoA::3xHA, RpdA::3xHA and SntB::3xHA strains were used to introduce *kdmB* and *sntB* deletion cassettes containing *ptrA* as a selective marker expressing pyrithiamine. *kdmB*Δ*::ptrA* was introduced into EcoA::3xHA, RpdA::3xHA and SntB::3xHA strains. Additionally, *sntB*Δ*::ptrA* was inserted into KdmB::3xHA, EcoA::3xHA, RpdA::3xHA. Immunoblotting analysis using α-HA antibody revealed that the protein expression of KdmB is not SntB-dependent (Figure 3.13A). Full-length KdmB (~196 kDa) was visible in both the WT and *sntB*Δ strain. Consistently, SntB levels were also not affected in the *kdmB* mutant. SntB full-length protein (~186 kDa) could be seen in the WT and in the *kdmB*Δ strain (Figure 3.13B). Furthermore, *rpdA* expression was not affected by the absence of either KdmB or SntB (Figure 3.13C). Full-length RpdA (~78.7 kDa) was clearly detected in the WT, *kdmB* and *sntB* mutants. Surprisingly, EcoA stability was dramatically reduced in the *kdmB*Δ strain while *sntB*Δ did not have any effect over EcoA levels. Full-length EcoA::3xHA normally corresponds to around 47.8 kDa which could not be detected in the KdmB depletion. *sntB* was deleted in EcoA::3xHA, *kdmB*Δ*::ptrA* strain to uncover if EcoA stability could be improved. Previously, SntB was shown to have E3 ubiquitin ligase activity in yeast (Singh et al., 2012). Strikingly, double deletion of *kdmB/sntB* fully restored EcoA protein levels suggesting that the putative E3 ubiquitin ligase SntB may play a role in EcoA proteasome degradation in the absence of KdmB. In order to prove the hypothesis if SntB is involved in EcoA proteasomal degradation, epoxomicin was supplemented into culture media in the *kdmB*Δ strain. Epoxomicin is widely used in research to inhibit proteasome activity *in vivo* which

specifically inhibits proteasomal proteases only (Meng et al., 1999). Notably, EcoA full-length protein was restored in the *kdmB*Δ strain in the presence of epoxomicin, preventing EcoA proteasomal degradation (Figure 3.13D). In essence, EcoA mRNA expression remained stable in *kdmB*Δ, *sntB*Δ and in *kdmB*Δ/*sntB*Δ strains providing critical information that *ecoA* mRNA levels did not change in *kdmB*Δ, *sntB*Δ and in *kdmB*Δ/*sntB*Δ strains (Figure 3.13E). To determine whether EcoA residues are prone to post-translational modifications which lead to its proteasomal degradation, MS analysis was performed using a phosphorylation-sensitive method. In order to detect potential PTMs residues on the EcoA protein sequence, EcoA::3xHA purification was performed in WT, *kdmB*Δ and *kdmB*Δ/*sntB*Δ strains. Remarkably, EcoA S41/45 residues are phosphorylated when KdmB is absent which normally did not appear in WT. Surprisingly, S41/45 phosphorylation disappeared in *kdmB/sntB* double mutant strain (Figure 3.13F). These findings were consistent with immunoblotting assays where EcoA stability was completely lost in KdmB depletion. The EcoA phosphorylated residues S41/45 in the KdmB depletion most likely serves as essential marks for proteasome degradation of EcoA, mediated by SntB.

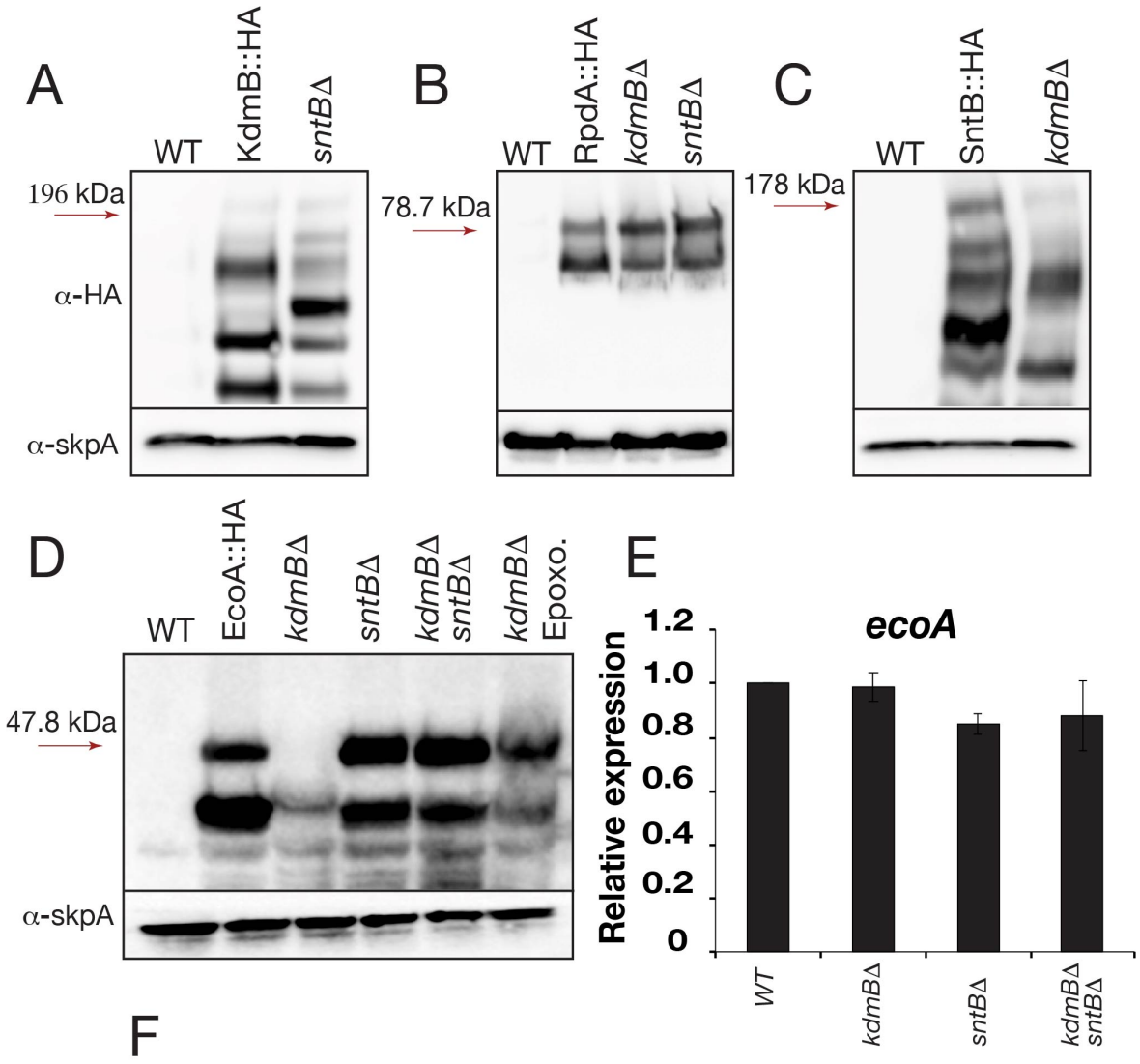

F

LC-MS/MS	Peptides unique to EcoA
EcoA-HA	31 RPAAKKRRVL SDCESDAAEK
*kdmB*Δ	31 RPAAKKRRVL **S**DCE**S**DAAEK
*kdmB*Δ *sntB*Δ	31 RPAAKKRRVL SDCESDAAEK

Figure 3.13. (A-D) Cellular levels of KdmB, EcoA, RpdA, and SntB in the WT, and mutant strains. Fungal cultures were grown in submerged liquid GMM media with required supplements for 24 h at 37ºC. Approximately 100 µg total protein was loaded into 10%

SDS-PAGE gels. Proteins were transferred onto 0.45 μm nitrocellulose Western blotting membrane (Amersham Protran, GE healthcare) overnight at 35V. α-HA monoclonal mouse antibody (Sigma) was used to detect HA-fused proteins, and generic α-SkpA polyclonal rabbit antibody was used to visualize SkpA as a loading control. Proteasome inhibitor epoxomicin (20 μM) was supplemented at the end of 20 h vegetative growth for a further 4 h incubation. **(E)** RT-qPCR mRNA expression analysis of *ecoA* in WT, *kdmB*Δ, *sntB*Δ and in *kdmB*Δ*/sntB*Δ strains. WT was adjusted to 1.0 which was used as a reference point. mRNA was extracted from samples grown in submerged liquid GMM culture with required supplements for 24 h at 37ºC. Relative expression fold-change analysis was performed using $2^{\Delta\Delta Ct}$ formula and *benA* was used as a reference housekeeping gene for normalization. qPCR analyses are the average of the two independent biological replicates and six technical replicates. (F) Analysis of possible PTMs on EcoA residues in WT, *kdmB*Δ and in *kdmB*Δ*/sntB*Δ. Red stars and bold letters represent phosphorylated residues. Underlined amino acids represent peptide coverage in mass spectrometry analysis with high confidence. Low or medium confidence peptides are filtered out from the analysis.

3.9 KdmB is required for EcoA stability

Immunoblot analysis confirmed EcoA proteasomal degradation in the *kdmB*Δ strain while *sntB*Δ restored EcoA stability. Full-length EcoA::3xHA could not be detected in the absence of KdmB, while deletion of *kdmB/sntB* restored and improved full-length EcoA, suggesting that EcoA might be translocated out of the nucleus in the absence of functional KdmB. To investigate cellular localization interdependency of the KERS complex, H2A-mRFP fusion was inserted into *ecoA::sgfp*/*kdmB*Δ, *rpdA::sgfp*/*kdmB*Δ, *sntB::sgfp*/*kdmB*Δ, *kdmB::sgfp*/*sntB*Δ, *ecoA::sgfp/sntB*Δ, *rpdA::sgfp*/*sntB*Δ, and *ecoA::sgfp/ kdmB*Δ*/sntB*Δ

strains. Approximately $5x10^3$ spores were inoculated into 500µl GMM liquid media with required supplements in Lab-Tek® Chamber Slides and incubated overnight at 30ºC for 16h. Confocal microscopy analysis revealed that nuclear localizations of RpdA and SntB were not affected in the absence of KdmB. Similarly, KdmB and RpdA nuclear localizations were not affected in the *sntB*Δ strain. In both cases, sGFP and mRFP signals overlap clearly presenting co-localization of chromatin binding proteins within the nucleus. However, in the *kdmB*Δ strain, EcoA could not be detected within the nucleus (Figure 3.14, Left panel). On the contrary, the *sntB*Δ did not have any effect on EcoA nuclear localization where the green EcoA::sGFP signal was clearly visible (Figure 3.14, Right panel). More interestingly, when *sntB*Δ was inserted into the *ecoA::sgfp*/*kdmB*Δ strain, EcoA::sGFP signal was restored within the nucleus, further confirming previously performed immunoblot analyses. These data suggest that KdmB positively controls EcoA nuclear stability which could be targeted by SntB for proteasomal degradation (Figure 3.14).

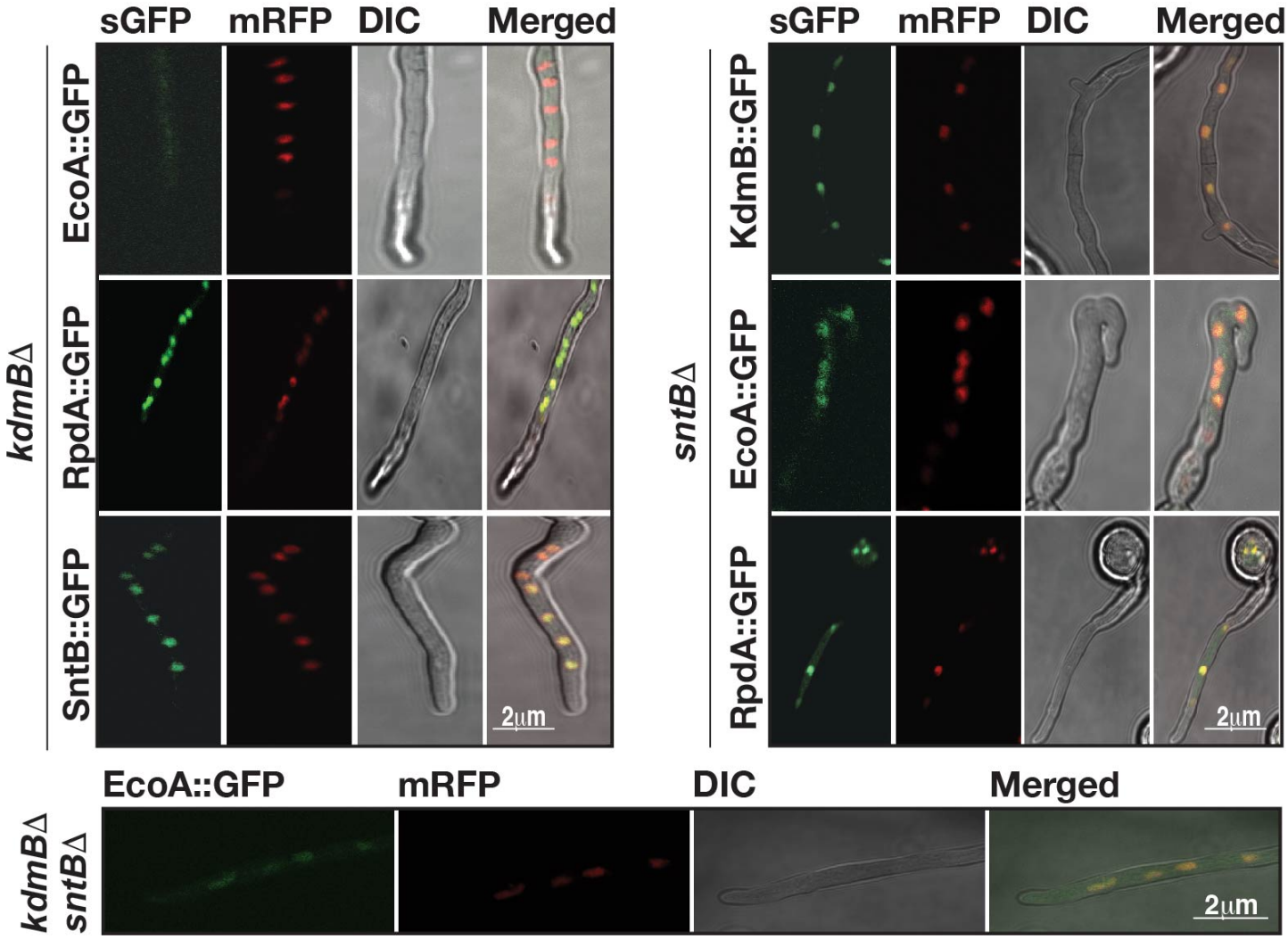
sGFP
mRFP
DIC
Merged
kdmBΔ
EcoA::GFP
RpdA::GFP
SntB::GFP
2μm
sntBΔ
KdmB::GFP
EcoA::GFP
RpdA::GFP
2μm
kdmBΔ sntBΔ
EcoA::GFP
mRFP
DIC
Merged
2μm

Figure 3.14. KdmB-SntB mediates EcoA nuclear stability. Confocal microscopy analysis of GFP-expressing KdmB, EcoA, RpdA, and SntB in H2A-mRFP strains and their cellular localizations in *kdmB* and *sntB* mutants. Images were captured at 60x magnification at the end of 16 h static growth at 30°C in GMM with required supplements.

3.10 KdmB and SntB do not influence total RpdA HDAC activity

Highly conserved SANT domain-containing protein motifs, such as Snt2, N-CoR and SMRT (silencing mediator of retinoid and thyroid receptors) were previously shown to promote Rpd3 deacetylase activity, which are subunits of histone HDAC complexes. Rpd3 activity was shown to be negatively affected in the Snt2 depletion (Yang and Seto, 2008). Proteomic analysis in this work has shown that RpdA is recruited to the demethylase KERS complex through a SntB-mediated mechanism. In the *sntB* mutant, RpdA could not be recruited by KdmB or EcoA. This phenomenon raises an important question of whether RpdA HDAC activity requires functional KdmB or SntB. In order to elucidate the functional dependency of RpdA, an HDAC *in vitro* activity assay was performed (Figure 3.15). Strains were grown in a shaking culture for 14 h at 37 °C at a density of 5 x 10^6 conidia per ml in GMM with required supplements. As described previously in Chapter 2, the enzymatic activity of enriched RpdA complexes was measured in triplicates using [H-3]-acetate prelabelled chicken histones as substrate. 30 µl of the IgG eluate was mixed with 20 µl of WB150 and 10 µl of labelled histones and subsequently incubated for 60 min at 25 °C. IgG pull-downs using SntB or KdmB as bait clearly display HDAC activity, which is indicated by an increase in activity compared to the KdmB pull-down in a *sntB*Δ background (KdmB-T-*sntB*Δ) and the AS6 pull-down with inactive RpdA as bait (Bauer et al., 2016) that can be regarded as background level. As expected from the TAP results, RpdA is lost from the KdmB-T-*sntB*Δ pull-down, which was also demonstrated by proteomics LC-MS^2 analysis (see Table 3.4).

This gives further evidence for the assumption that the counts measured in KdmB-T-*sntB*Δ fractions were not significantly different from the background. In contrast to *sntB* deletion, *kdmB*Δ did not seem to alter the HDAC activity of the remaining SntB complex. This is in line with the fact that SntB recruits RpdA to this complex, as shown before (Table 3.4). HDAC activity in pull-downs using RpdA as bait was generally much higher, which most likely was due to the presence of other RpdA complexes, i.e. RpdA-L and RpdA-S in these fractions. Remarkably, neither *sntB* nor *kdmB* deletion seems to affect overall RpdA HDAC activity *in vitro*.

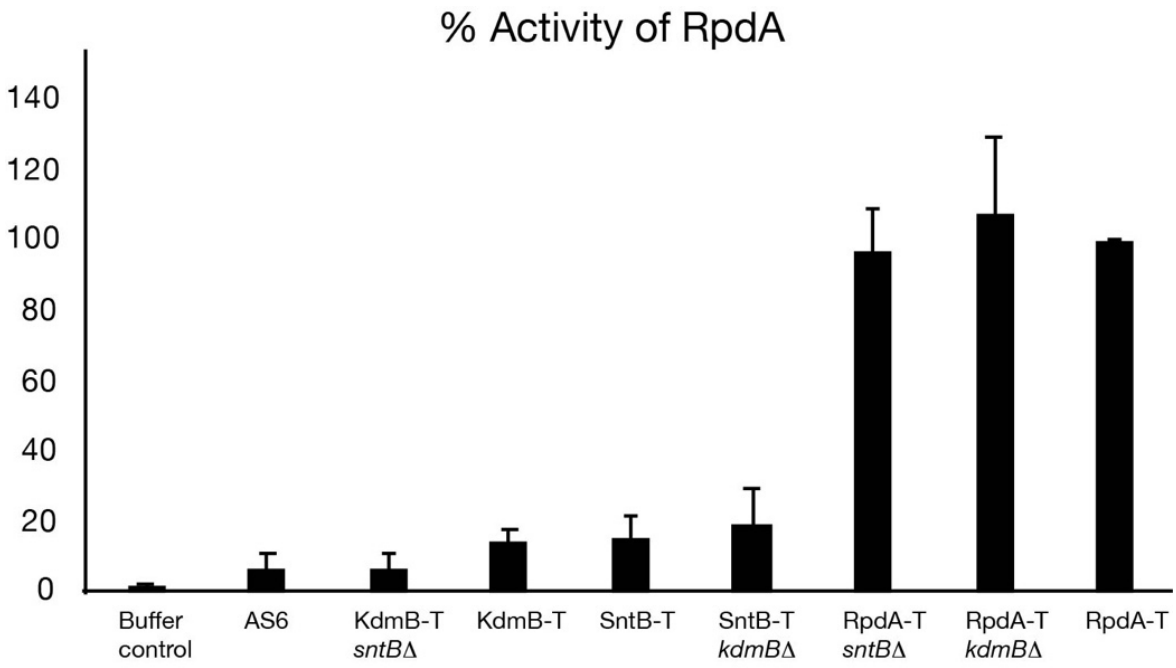

Figure 3.15. RpdA complexes exhibit HDAC activity *in vitro*. Enzymatic activity of enriched RpdA complexes was measured in triplicates using [H-3]-acetate prelabeled chicken histones as substrate as described (Trojer et al., 2003). 30 µl of the IgG eluate was mixed with 20 µl of WB150 and 10 µl of labeled histones and subsequently incubated for 60 min at 25 °C. RpdA-AS6 pull-down represents a nonfunctional TAP-tagged RpdA mutant (6 aa substituted by Ala). All samples were calculated with respect to RpdA::TAP activity which is adjusted to 100%.

3.11 Acetylation of Smc3 homolog SudA 105-106 lysine residues is abolished in *ecoA* down-regulation

In yeast, N-acetyltransferase Eco1 is required for the establishment of sister chromatid cohesion. Eco1 acetylates cohesin complex component SMC3 (SudA homolog in *A. nidulans*) K112/113 residues. A similar mechanism is conserved in complex eukaryotes and humans, where ESCO1 and ESCO2 (human EcoA homologs) acetylate SMC3 on K106/107 residues (Alomer et al., 2017). To investigate the functional role of the KERS complex for the formation of the cohesin complex, a GFP epitope tag was fused to the c-terminal of *sudA* in its native promoter. The resulting strain expressing SudA::GFP was subjected to purification and mass spectrometry analysis. With the objective to see if an EcoA knock-down had any effect on cohesin complex formation, SudA::GFP plasmid constructs harbouring the *pyrG* selective marker were introduced into WT and *ecoA*$^{\text{TetON}}$::*pyroA* strains. Furthermore, a SudA::3xHA construct was inserted into an *ecoA*^{TetON}*::pyroA* strain to study the functional role of EcoA in cohesin acetylation. SudA::GFP pull-downs and mass spectrometry analysis revealed that cohesin subunits are conserved in *A. nidulans* (Figure 3.16A). SudA recruited yeast homologs Smc1, Mcd1, PRP43, TRL1, SSQ1 and TorA. The same complex members of SudA are recruited in the *ecoA*$^{\text{TetON}}$ knock-down strain, suggesting that down-regulation of EcoA did not affect cohesin complex assembly. Eco1 was shown to be responsible for the acetylation of SMC3 conserved lysine 105 and 106 residues in yeast (Rolef Ben-Shahar et al., 2008). It was also shown that Eco1 acetylates cohesin complex subunit Mcd1 (Kim et al., 2002). According to the mass spectrometry analysis in SudA::3xHA purifications, down-regulation of *ecoA* resulted in the absence of acetylated residues in SudA. This is direct evidence that EcoA may directly or indirectly be responsible for acetylating SudA K106/107 residues in filamentous fungi. However, Mcd1

was found to be acetylated in conserved K367 residue in WT and EcoA depletion suggesting that EcoA has no effect on Mcd1 acetylation (Data not presented). It was shown in immunoblotting assays that EcoA stability is positively regulated by KdmB (Figure 3.13D). In order to elucidate the effect of KdmB depletion in SudA K106/107 acetylation residues, SudA::3xHA was inserted into the *kdmB*Δ strain. Interestingly, the *kdmB* mutation did not have any effect on the acetylation of SudA, suggesting that trace levels of nuclear EcoA are sufficient for the acetylation of conserved K106/107 residues (Figure 3.16B). To investigate the nuclear localization of SudA in EcoA depletion, confocal microscopy was performed using SudA::GFP in WT and in the *ecoA*^{TetON} strain. The presence of nuclei was visualized by a nuclear staining method using DRAQ5 dye. As could be seen from Figure 3.16C, the *ecoA*^{TetON} knock-down did not have an effect on SudA nuclear levels. SudA was predominantly present within the nucleus. It was also apparent that cellular SudA::GFP levels were not affected by EcoA down-regulation (Figure 3.16D).

A

SudA-GFP		
Accession	Proteins Identified	#Unique peptides
AN6364	**Smc3**	58
AN2963	Smc1	66
AN7465	Mcd1	23
AN0133	PRP43	22
AN1296	TRL1	30
AN0866	SSQ1	14
AN5982	TorA	12

C

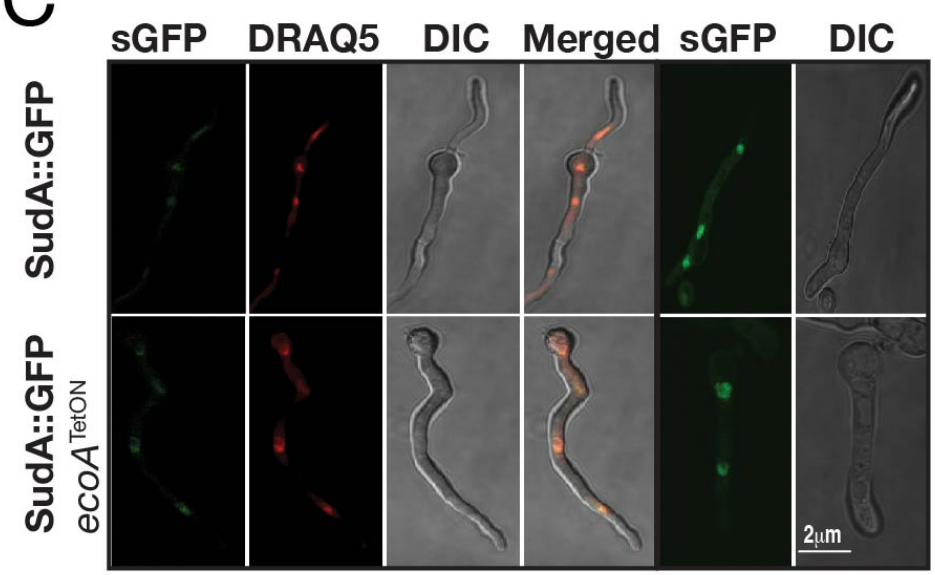

B

LC-MS/MS	Peptides unique to Smc3/SudA
SudA-HA	91 TGKPELVLRR TIGL**KK**DEYT
ecoA^{TetON}	91 TGKPELVLRR TIGLKKDEYT
*kdmB*Δ	91 TGKPELVLRR TIGL**KK**DEYT

D

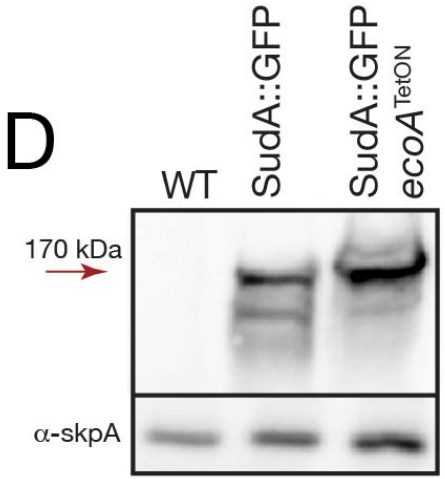

Figure 3.16. EcoA knock-down abolished SudA acetylation. (A) GFP was fused to C-terminal of SudA ORF in its native promoter resulting in the expression of SudA::sGFP both in WT and in the *ecoA*^{TetON} strain. SudA::sGFP pull-downs and LC-MS^2 were performed as in previous experiments. (B) Similarly, HA was fused to the C-terminal of SudA ORF in its native promoter resulting in the expression of SudA::3xHA in WT, *ecoA*^{TetON} and *kdmB*Δ strains. An HA-expressing SudA strain was used for detection of acetylated residues due to resulting in higher coverage of unique peptides. Green stars above bold letters represent acetylated residues. Underlined amino acids represent peptides covered in the LC-MS^2 analysis. (C) Confocal microscopy analysis of GFP expressing SudA in an H2A::mRFP strain and their cellular localization in WT and *ecoA*^{TetON} strain. DRAQ5 (1:10,000) was used for nuclear staining. Images were captured at 60x magnification at the end of 16 h static growth at 30°C in GMM. (D) Western blot analysis of protein levels of SudA::sGFP and SudA::sGFP in an *ecoA*^{TetON} strain. Fungal cultures expressing GFP were grown in submerged liquid GMM culture for 24 h at 37ºC prior to protein extraction. Approximately 100 µg total protein was loaded onto 10% SDS-PAGE gels. α-GFP monoclonal mouse antibody (Santa Cruz, 1:1000 in TBS) was used to detect GFP-fused proteins, while generic α-SkpA polyclonal rabbit antibody was used against SkpA as a loading control.

Chapter 4 Results

KERS complex is required for development, secondary metabolism and pathogenicity in *Aspergillus flavus*

4.1 KERS complex is conserved in the aflatoxin producer pathogenic fungus *Aspergillus flavus*

Secondary metabolism gene clusters are likely regulated by chromatin post-translational modifications as a response to various environmental stimuli such as light, pH, temperature, UV and nutrient conditions. Certain PTMs on the histone tails determine the state of chromatin activation or repression which are regulated by chromatin modifier enzymes such as methyltransferases, acetyl-transferases, demethylases and deacetylases. In the previous chapter, a novel tetrameric demethylase KERS complex is identified in the model organism *Aspergillus nidulans,* showing critical roles for fungal development which possibly can act on certain gene clusters essential for development and secondary metabolism. These findings strongly suggested the hypothesis of whether this complex is also conserved in pathogenic fungus and carcinogenic aflatoxin producer *A. flavus* and if development and SM gene clusters could be regulated by a similar chromatin modifier complex. In order to prove this hypothesis, first, we determined an *A. nidulans* KdmB ortholog (AFLA 006240) in *A. flavus* genome using a BLAST search. *A. flavus* KdmB contains a Jumonji N domain at its N-terminus (between amino acids 74-115), an ARID/Bright domain (141-229), a plant homeodomain and bromo adjacent homology (PHD/BAH) domain (438-518), a Jumonji C domain (610-726), a zinc finger domain (834-893) and a second PHD domain (1306-1352) at the C terminus with a total size of 1704 amino acids (Figure 4.1D). The respective *kdmB* gene was tagged endogenously in native locus with synthetic green fluorescent protein (sGFP) (*kdmB::sgfp*) or human influenza hemagglutinin (HA) (*kdmB::3xha*) epitope tag fusions. Confirmation of full-length (~200kDa) KdmB::GFP expression was carried out in an immunoblotting assay using monoclonal mouse antibody α-GFP (Figure 4.1A). Moreover, KdmB::GFP strain was used to investigate the intracellular localization of KdmB. GFP signals of KdmB overlapped with red-stained nuclei (DRAQ5) and presented predominantly nuclear localization under confocal microscopy in vegetative cells (Figure

4.1B). Having shown the nuclear presence of KdmB, another important aspect was to discover its possible protein interacting partners. Therefore, HA and GFP immunoprecipitations coupled with mass spectrometry were performed using KdmB::3xHA, KdmB::GFP and WT (as a negative control) strains. Interestingly, *A. flavus* KdmB recruited putative cohesin acetyltransferase EcoA, histone deacetylase RpdA and recently characterized BAH/PHD domain transcription factor ring finger protein SntB in both HA and GFP pull-downs as top KdmB interacting proteins. The number of unique peptides for all four proteins were high, suggesting the bulk presence of conserved tetrameric KERS complex formation in the pathogenic fungus (Figure 4.1C). *A. nidulans* KERS complex members have multi-domain protein structures required for chromatin recognition, histone-binding, DNA binding and catalytic activities. Domain architectures of *A. flavus* KERS members clearly emphasized chromatin recognition sites as well as their catalytic domains involved in demethylation, acetylation and deacetylation processes (Figure 4.1D). In light of these results, it is clearly evident that the KERS complex is conserved in the pathogenic fungus *A. flavus* and possesses similar domain architecture unique to chromatin modifier enzymes. EcoA was the smallest member of the tetrameric complex with 385 amino acids which contains a zinc finger domain (141-178) and acetyl-transferase (AT) (314-375) domains. Putative histone deacetylase RpdA contains a deacetylase domain (19-392). SntB protein was large, like the KdmB protein, with 1713 amino acids and contains a PHD/BAH domain (243-368), two PHD domains (410-456 and 1005-1205) and a SANT domain (737-777).

Alignment tool using protein sequences of *A. flavus* KERS complex suggested that all four proteins are highly conserved from yeast to human (Figure 4.1E). The highest KdmB sequence similarity among the orthologs was found to be in *A. fumigatus* (83%), followed by *A. nidulans* KdmB (79%) and *M. oryzae* (54%). EcoA was found to be highly conserved in *A. nidulans* (83%) followed by *A. fumigatus* (82%) and fission yeast *S. pombe* (33%).

Surprisingly, an EcoA ortholog could not be detected in *M oryzae*. RpdA was found to be highly conserved in *A. fumigatus* (97%), *A. nidulans* (78%), *S. cerevisiae* (76%), *M. oryzae* (70%) and human (69%), which were shown to have significantly large protein sequence similarities. The most SntB sequence similarity among the orthologs was found to be in *A. fumigatus* (74%), *A. nidulans* (69%), followed by *M. oryzae* hypothetical protein (47%).

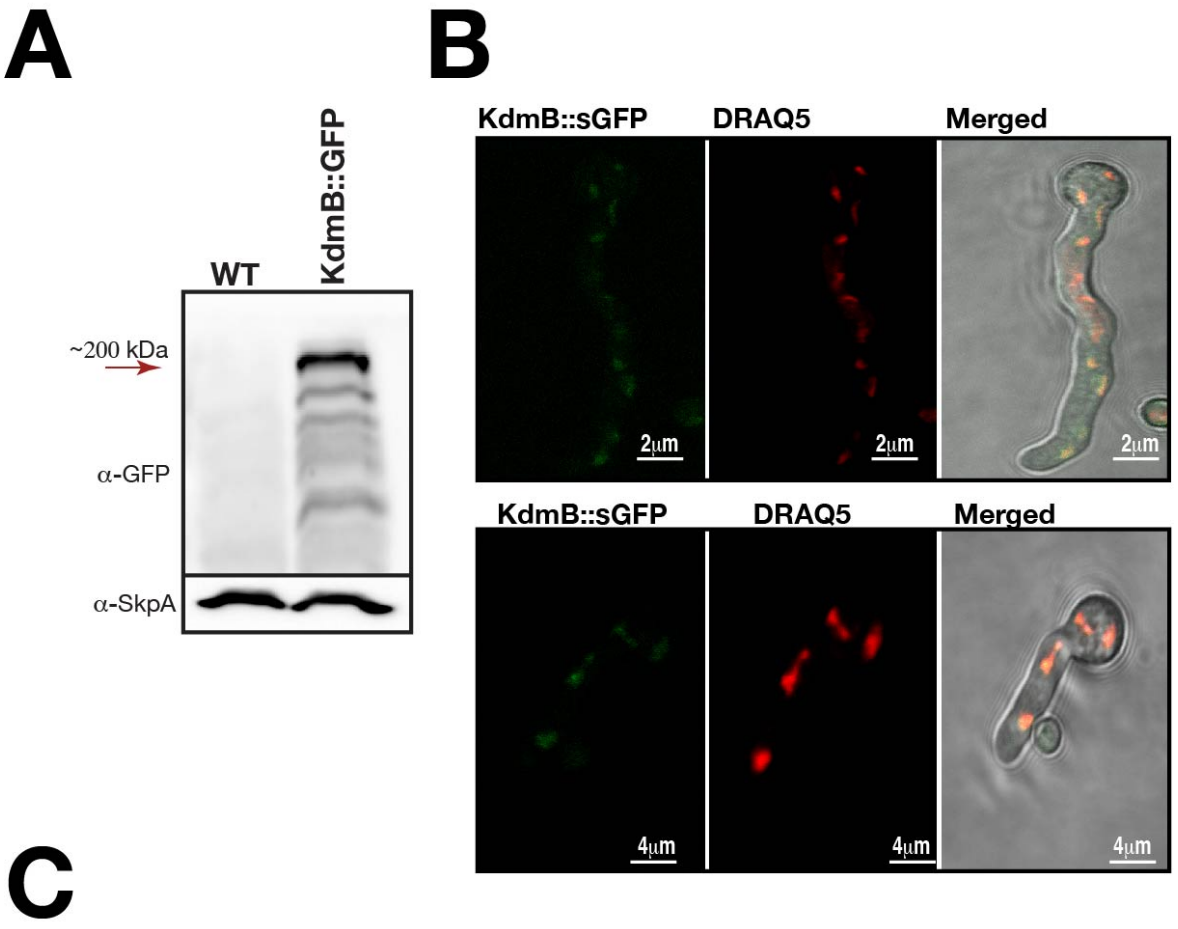

C

KdmB-GFP			KdmB-HA		
Proteins Identified	#Unique peptides	% Coverage	Proteins Identified	#Unique peptides	% Coverage
KdmB	**90**	**64**	**KdmB**	**77**	**62**
EcoA	11	42	EcoA	9	38
RpdA	20	43	RpdA	12	41
SntB	62	51	SntB	56	44

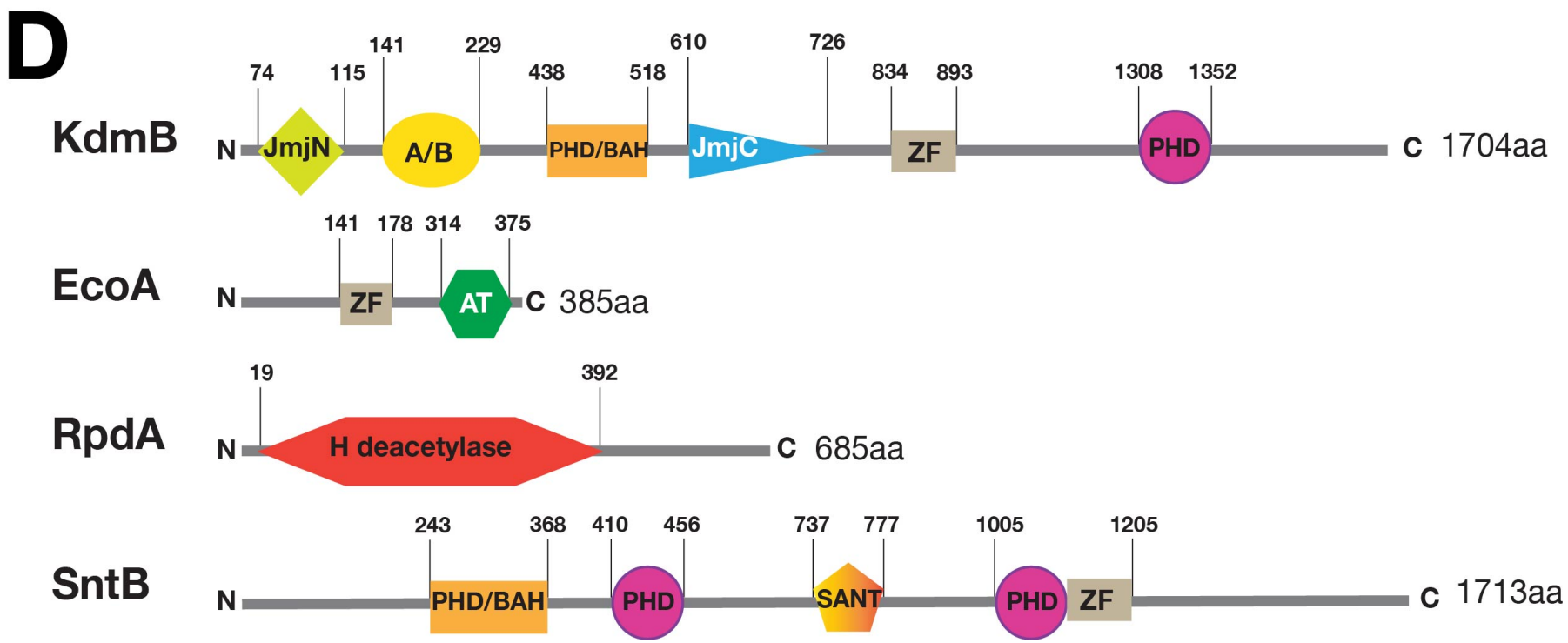
D
KdmB
74
115
141
229
438
518
610
726
834
893
1308
1352
N
JmjN
A/B
PHD/BAH
JmjC
ZF
PHD
C 1704aa
EcoA
141
178
314
375
N
ZF
AT
C 385aa
RpdA
19
392
N
H deacetylase
C 685aa
SntB
243
368
410
456
737
777
1005
1205
N
PHD/BAH
PHD
SANT
PHD
ZF
C 1713aa

E

	Yeast				Pathogenic Fungi				Model Organism		Human	
	S. cerevisiae		*S. pombe*		*A. fumigatus*		*M. oryzae*		*A. nidulans*		*H. sapiens*	
KdmB	Jhd2	40	Lid2	32	PHD TF	83	MGG04878	54	KdmB	79	Kdm5C	28
	H3K4 demethylase		H3K4 demethylase		AFUA_5G03430		Unkown		H3K4 demethylase		lysine-specific demethylase	
EcoA	Eco1	25	Eso1	33	Eco1	82	No similarity	-	AN10336	83	ESCO1/2	28
	sister chromatid cohesion acetyltransferase		putative, sister chromatid cohesion acetyltransferase		AFUA_3G06000		X		putative, sister chromatid cohesion acetyltransferase		Cohesin acetylation, Roberts Syndrome	
RpdA	Rpd3	76	Clr6	64	RpdA	97	RPD3	70	RpdA	78	HDAC1	69
	Histone deacetylase, response to oxidative stress		Class I histone deacetyltransferase		Class I histone deacetyltransferase, Essential		Histone deacetylase		Class I histone deacetyltransferase, Essential		Histone deacetylase I	
SntB	Snt2	29	Snt2	23	Snt2	74	MoSnt2	47	SntB	69	BRD1	29
	DNA-binding E3 ubiquitin-protein ligase		Lid2 complex subunit		PHD domain ring finger protein		PHD/BAH, SANT domain containing		PHD domain ring finger protein		Bromodomain containing protein 1	

Figure 4.1. Demethylase KERS complex is conserved in the pathogenic fungus *Aspergillus flavus*. (A) KdmB::sGFP fusion immunoblotting prepared from a crude extract of vegetative growth at 30°C for 24 h. 100 μg of total protein from WT and KdmB::sGFP strains was loaded onto an SDS-PAGE gel (10%). For GFP detection, α-GFP monoclonal mouse antibody (Santa Cruz Biotech., 1:500 in TBS) was used. α-SkpA polyclonal rabbit antibody (Generic, 1:1000 in TBS + 1% Tween 20) against SkpA as a loading control. (B) Sub-cellular localization of KdmB::sGFP expressed under native promoter. KdmB co-localized in the nucleus. Nuclei staining was performed by incubating samples with 1:10,000 DRAQ5 dye for 30' at room temperature. Confocal microscopy images were produced using 60x magnification (C) Demethylase KERS complex consisting of H3K4me3 demethylase KdmB, acetyltransferase EcoA, histone deacetylase RpdA and ring finger protein SntB is conserved in pathogenic fungus *A. flavus*. Three biological replicates of KdmB::sGFP and KdmB::3xHA strains and WT as a negative control were immunoprecipitated and run in LC-MS^2. The protein list obtained from the WT control was subtracted from KdmB::sGFP and KdmB::3xHA samples to eliminate non-specific peptide binding. See Table 4.1 and 4.2 for all identified proteins list. (D) Domain architecture of multidomain KERS complex proteins of *A. flavus*. Both KdmB and SntB contain a histone-binding plant homeodomain (PHD) protein sequence region that is unique for chromatin recognition and gene regulation. (E) KdmB, EcoA, RpdA, and SntB are conserved across various organisms from yeast to human comprising demethylase, deacetylase, cohesion acetyltransferase and histone-binding domains.

4.2 KERS complex is essential for light-dependent asexual conidiation, sclerotia development and stress factor responses

In *A. nidulans*, KERS complex was shown to be involved in light-regulated asexual conidiation and sexual fruiting body formation (Figures 3.7, 3.8). Furthermore, *ecoA* and *rpdA* are shown to be essential for survival. *ecoA* and *rpdA* knock-downs resulted in phenotypic growth defects. Additionally, cleistothecia formation was found to be up-regulated in the *kdmB* mutant and *ecoA* knock-down, whereas, asexual conidiation and sexual development were found to be totally abolished in the *sntB* mutant strain (See chapter 3). Similar results were shown in *Neurospora crassa*, *Fusarium oxysporum f.sp. melonis* and *A. flavus* where *snt2* deletion caused reduced conidia formation (Denisov et al., 2011, Pfannenstiel et al., 2018). In order to show the possible impact of the KERS complex in *A. flavus* development, deletion DNA constructs were transformed into an *A. flavus* WT *pyrG*$^{-}$ auxotroph strain. *kdmB* and *rpdA* (AFLA_092360) were successfully deleted in *A. flavus*, although *rpdA* was found to be essential for growth in *A. nidulans* and *A. fumigatus* previously (Bauer et al., 2016). Despite performing many attempts to knock-out *ecoA*, no viable colony was detected, suggesting that *ecoA* may be essential for growth in *A. flavus* similar to *A. nidulans*. Surprisingly, light-induced asexual conidiation was shown to be negatively affected in the *rpdA* mutant strain when compared to the WT control in the phenotypic tests performed in PDA media (Figure 4.2A). The percentage of conidiation was drastically reduced by approximately 70% in the *rpdA*Δ strain (Figure 4.2 B). On the contrary, asexual sporulation was slightly increased in the *kdmB*Δ mutant. To determine the affected conidia regulatory genes in *rpdA*Δ and *kdmB*Δ strains, mRNA relative quantification was performed. RT-qPCR mRNA expression analysis of transcription factors required for conidiation suggested that transcription activator *abaA*, *flbA* (developmental regulator) and *flbB* (basic-zipper-type transcription factor) were significantly down-

regulated in the *rpdA* mutant strain. *abaA* was shown to be reduced by almost 50% in the *rpdA* mutant with respect to WT. In particular, *flbA* expression was reduced by 60% in the *rpdA* mutant. *flbA* and *abaA* expressions were reduced in the *kdmB* mutant, however, *flbB* was found to be upregulated resulting in slight induction of sporulation in *kdmB*Δ (Figure 4.2 C). These data suggest that the KERS complex is required for controlled and balanced expression of the asexual sporulation pathway in *A. flavus*.

Sclerotia are the cleistothecia-like vestigial structures of *A. flavus* which have lost their sexual cycle ability throughout evolution, though some recent studies show that they may produce sexual ascospores during exceptionally special conditions (Horn et al., 2016). Like cleistothecia, these structures are induced in the absence of illumination and limited nutrient sources. In order to see the effects of *kdmB* and *rpdA* deletions on the development of *A. flavus*, sclerotia-inducing PDA and WKM plates were inoculated with *kdmB*Δ, *rpdA*Δ and WT strains. Culture plates were incubated in dark conditions at 30ºC to promote sclerotia development. At the end of 21 days, no sclerotia formation was present in either the *kdmB*Δ or *rpdA*Δ mutants (Figure 4.2 A,B). Phenotypical assays clearly demonstrated that, in addition to asexual growth, sclerotia formation is totally abolished in *kdmB*Δ and *rpdA*Δ strains. Sclerotia-inducing genes *nsdC* (C_2H_2 zinc finger protein) and *nsdD* (sexual development factor) were found to be significantly depleted in *kdmB*Δ and *rpdA*Δ strains, emphasizing the inductive role of the KERS complex in sclerotia development (Figure 4.2 D). This finding is in parallel to the recent study performed by using a *sntB* mutant in *A. flavus* which was shown to be unable to produce sclerotia (Pfannenstiel et al., 2018). These results clearly state that the KERS complex positively regulates sclerotia development by affecting certain sclerotia regulatory gene clusters. Unlike *kdmB*, *rpdA* is also required for normal induction of asexual conidiation.

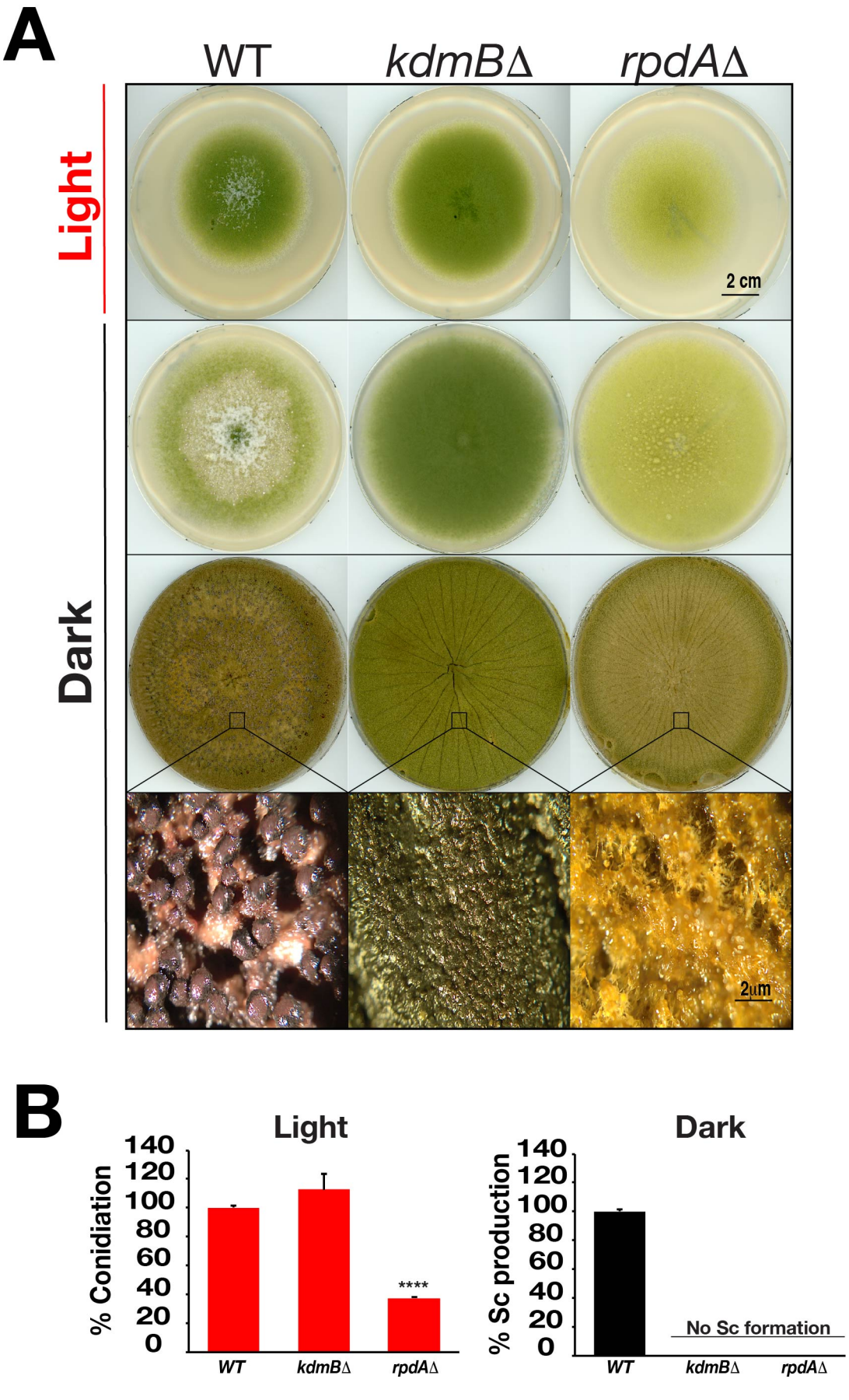
A
WT
kdmBΔ
rpdAΔ
Light
Dark
2 cm
2μm
B
Light
% Conidiation
140
120
100
80
60
40
20
0
****
WT
kdmBΔ
rpdAΔ
Dark
% Sc production
140
120
100
80
60
40
20
0
No Sc formation
WT
kdmBΔ
rpdAΔ

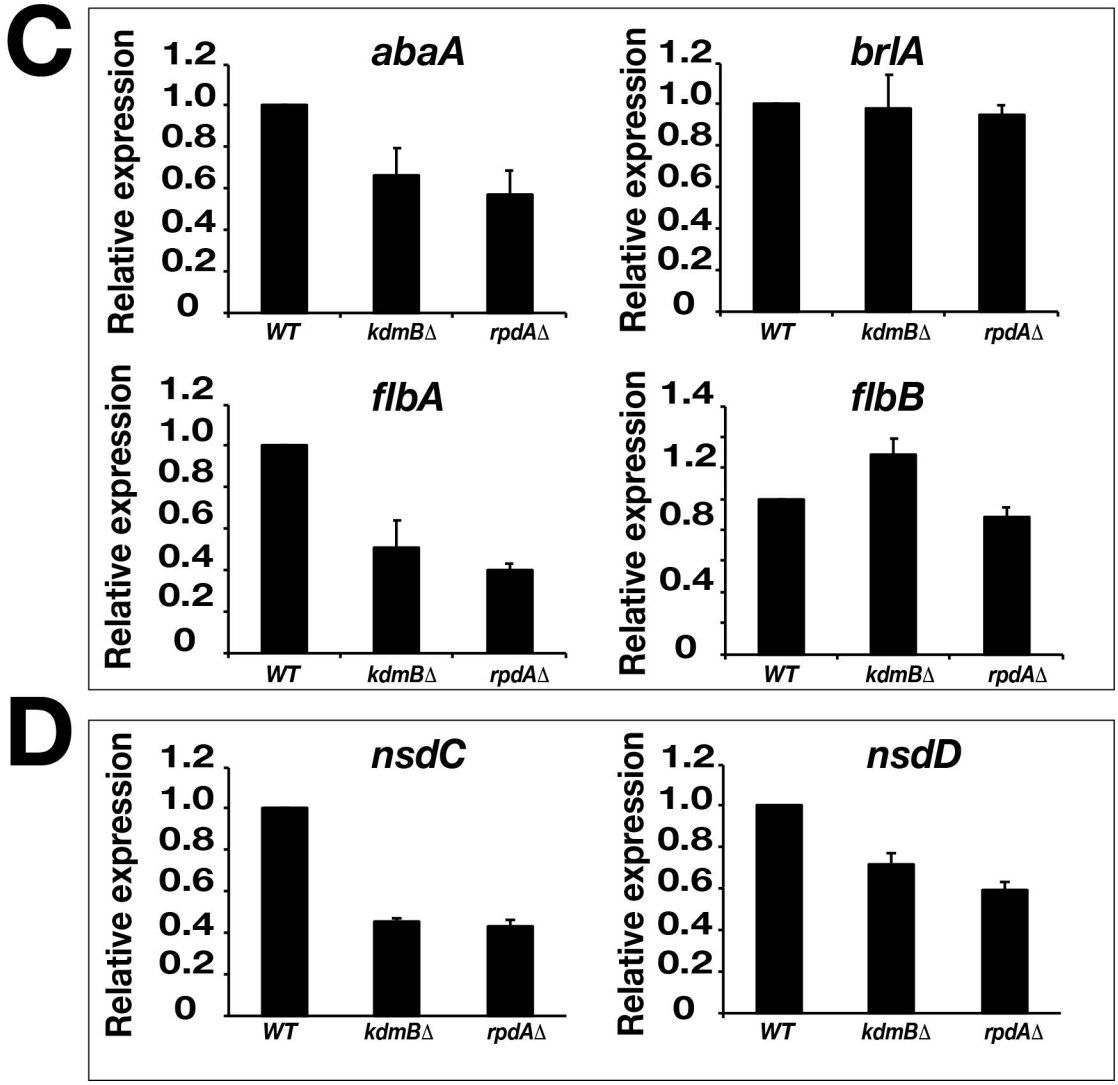

Figure 4.2. KdmB and RpdA are essential for *A. flavus* sclerotia development. **(A)** For conidiation analysis, approximately 5x10^3 spores of WT, *kdmB* and *rpdA* mutants were spot inoculated onto Potato Dextrose Agar (PDA) plates including required supplements and grown for 4 days at 30°C under illumination (upper lane). For sclerotia induction, PDA (5 days) and WKM plates (21 days) including required supplements were incubated in dark conditions at 30°C for the duration indicated in parenthesis. Lower lane shows the stereomicroscopic images of sclerotia (Sc) formation in WT, whereas Sc production was totally abolished in mutant strains. **(B)** Percentages of conidiation and Sc production in WT and deletion strains. Conidia quantification was performed from the PDA plates grown under light conditions. Approximately 1 cm of agar plug was removed and resuspended in

200µl PBS for conidia counting using microscopic counting chambers. Sclerotia counting was performed manually by quantifying sclerotia produced on WKM agar plates under dark conditions. Final values were optimized with respect to WT representing as 100%. All quantifications are the result of three independent biological replicates. **(C)** RT-qPCR expression analysis of conidia regulatory genes *abaA*, *brlA*, *flbA*, *flbB* and sclerotia regulatory genes *nsdC* and *nsdD*. For the analysis of conidia regulatory genes, fungal mycelia grown in complete media with required supplements for 24 h at 30ºC 200 g was shifted onto agar plates. Total mRNA was obtained by harvesting fungal mat grown on PDA plates for 3 days at 30°C under illumination. For the analysis of the mRNA expression profiles of sclerotia regulatory genes, total mRNA was obtained by harvesting fungal mat grown on WKM agar plates for 5 days at 30°C under dark conditions. WT is adjusted to 1.0. RT-qPCR experiments were carried out using two independent biological replicates and nine technical replicates.

4.3 Camptothecin negatively affects *A. flavus* KERS mutants while *kdmB*Δ is more resistant against menadione-mediated oxidative stress

Having seen that KERS is essential for the development of *A. flavus*, it became interesting to see if the demethylase complex also plays a role in the responses to various environmental stress factors. Therefore, various stress factors agents were applied including microtubule, DNA, osmotic, oxidative and cell wall stresses and growth of deletion strains was compared with the WT (Figure 4.3). It can be observed that both *kdmB* and *rpdA* mutants are more susceptible to topoisomerase inhibitor camptothecin (CPT), emphasizing their possible roles in DNA replication during the cell cycle. Interestingly, although the *rpdA*Δ strain did not exhibit any difference in growth on menadione-mediated oxidative stress when compared to WT, the *kdmB*Δ strain was found to be more tolerant. Surprisingly, both mutants and WT

were similarly sensitive to hydrogen peroxide, presenting no exclusive effect. Additionally, we could not detect any effect of benomyl, nocodazole, SDS, congo red and calcofluor on either *kdmB* or *rpdA* mutants when compared to WT (Figure 4.3). Together, these results suggest that not only is KERS essential for development but also that it is also involved in response to certain stress factors.

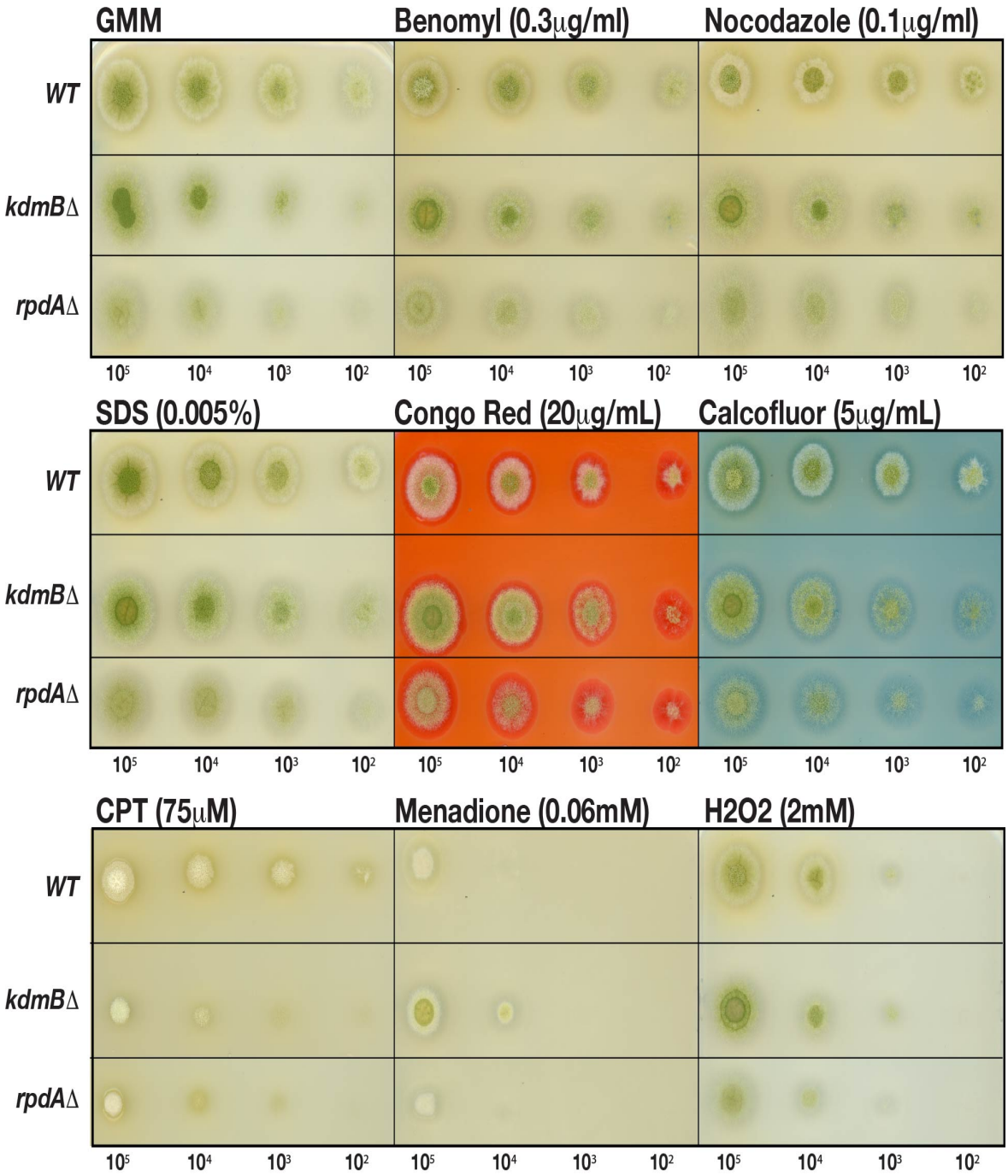

Figure 4.3. The effects of *kdmB* and *rpdA* mutants in response to various stress agents. GMM agar plates including required supplements and various stress-inducing agents for the concentrations indicated were incubated for 3 days under light conditions. Variable spore numbers are indicated at the bottom of images. All phenotypic tests were carried out with three independent biological replicates.

4.4 KERS is essential for aflatoxin production and crop contamination

Sexual development is often linked with SM production in filamentous fungi. In previous studies, production of the aflatoxin precursor sterigmatocystin (ST) was shown to be induced during sexual development (Bayram et al., 2008b). To this end, since it is shown in this work that KERS is essential for sclerotia development, it became essential to see if the chromatin modifier KERS complex is also required for aflatoxin production in plant pathogen *A. flavus*. Therefore, organic extracts of mutants and WT grown on YES agar plates were isolated by a chloroform extraction method. The organic extracts of *kdmB, rpdA* mutants and WT were subjected to reversed-phase HPLC. To detect aflatoxin retention time, aflatoxin B_1 standard (Sigma) was used as a reference point. Based on the HPLC analysis, aflatoxin production was completely abrogated in *kdmB*Δ and *rpdA*Δ strains, while AF production was clearly detected in the WT sample (Figure 4.4A). As can be seen from the chromatogram, aflatoxin B1 standard absorbance could be detected at approximately ~20 min retention time similar to aflatoxin B1 from WT overlapping at that point. *kdmB* and *rpdA* mutants did not have any absorbance signals for aflatoxin B1 emphasizing that these deletions caused total loss of carcinogenic mycotoxin production. Aflatoxin production is regulated by *afl* gene clusters. For this reason, *kdmB*Δ, *rpdA*Δ mutants and WT strain were analysed to determine the expression levels of aflatoxin regulatory genes *aflC*, *aflD*, *aflM* and *aflR* by RT-qPCR. All four genes were significantly down-regulated in both mutants (Figure 4.4B). The most drastic reduction was seen in *aflM* expression. *aflM* in the *kdmB* mutant was shown to be reduced by almost 90% with respect to WT. Similarly, at least 80% *aflM* reduction was seen in the *rpdA* mutant when compared to the WT strain. Therefore, it is likely that KdmB and RpdA play essential roles in aflatoxin production by regulating *afl* cluster genes.

Fungi can cause massive invasions on oil-rich seeds by contaminating with AF and causing loss of agricultural crop products. Sclerotia and AF analyses from culture media

showed promising results which posed an important question whether KdmB and RpdA are required for fungal pathogenicity. Therefore, infection tests using peanut seeds were performed to monitor the influence of *kdmB* and *rpdA* mutants for growth on seeds. We did not see any effect on surface colonization, however, there was no sign of sclerotia production observed in deletion strains while the WT produced premature sclerotia at the end of the 5th day of growth in dark conditions (Figures 3C, 3D). Peanut samples treated with *kdmB*Δ, *rpdA*Δ and WT were used to perform organic extraction for the analysis of aflatoxin levels. The HPLC results from peanut samples demonstrated that samples treated with either *kdmB*Δ or *rpdA*Δ mutant strains did not contain aflatoxin, while samples extracted from peanuts treated with WT gave positive results for aflatoxin B1 production (Figure 3E). All in all, these results underlined the critical role of *kdmB* and *rpdA* in sclerotia development and aflatoxin production. Since SntB was also shown to be required for AF production (Pfannenstiel et al., 2018), the KERS complex is involved in the positive induction of sclerotia and AF biosynthetic regulatory gene clusters. KERS complex is also required for seed contamination with aflatoxin.

A

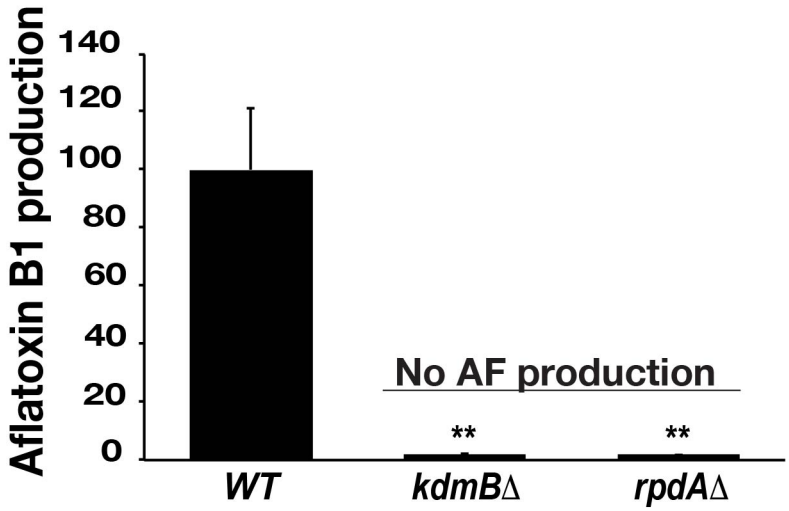
Aflatoxin B1 production
140
120
100
80
60
40
20
0
No AF production
**
**
WT
kdmBΔ
rpdAΔ

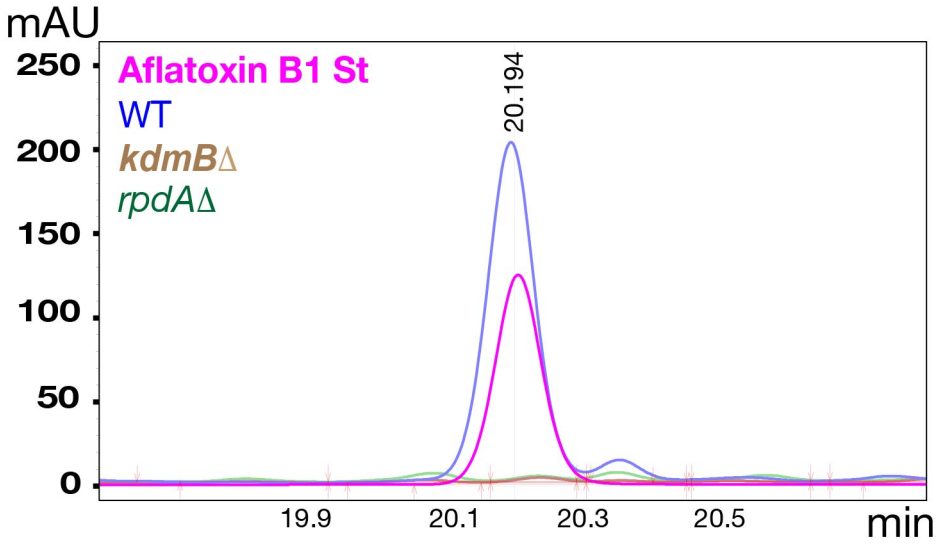
mAU
250
200
150
100
50
0
Aflatoxin B1 St
WT
kdmBΔ
rpdAΔ
20.194
19.9
20.1
20.3
20.5
min

B

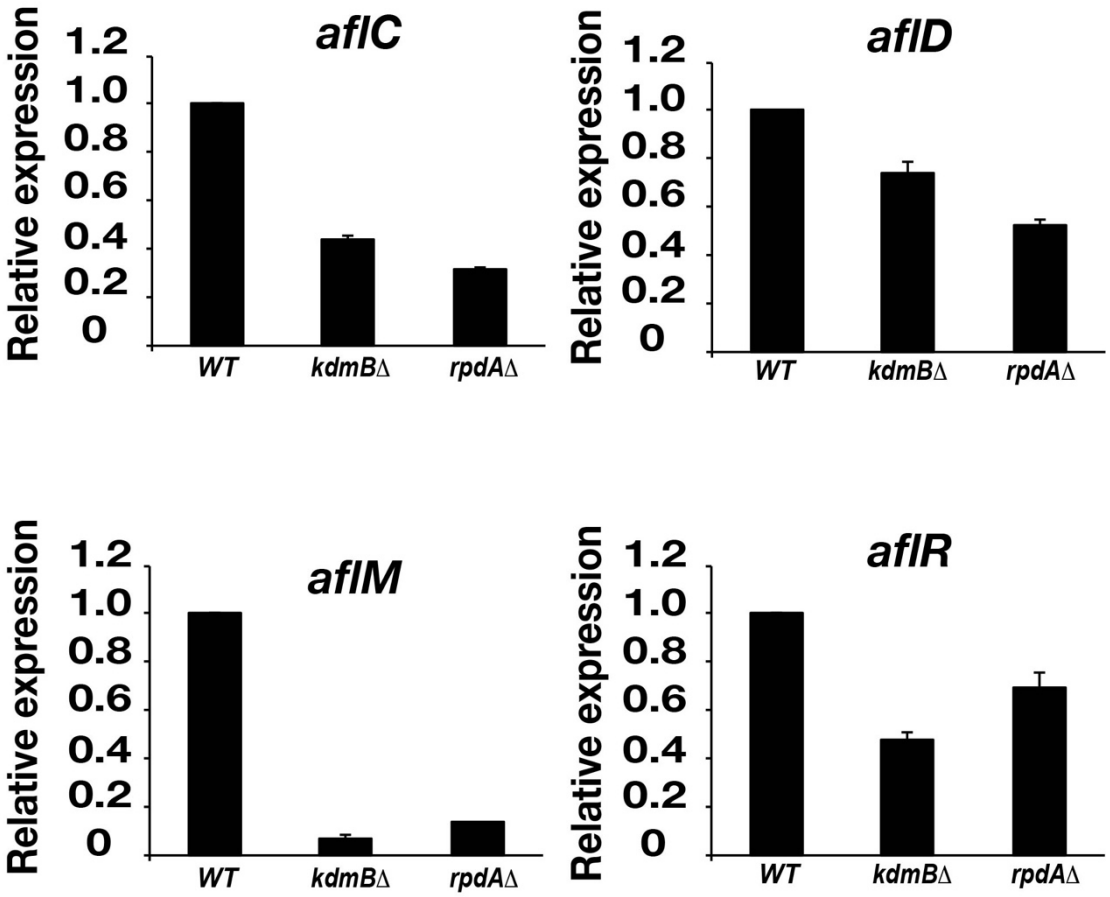
aflC
aflD
aflM
aflR
Relative expression
1.2
1.0
0.8
0.6
0.4
0.2
0
WT
kdmBΔ
rpdAΔ

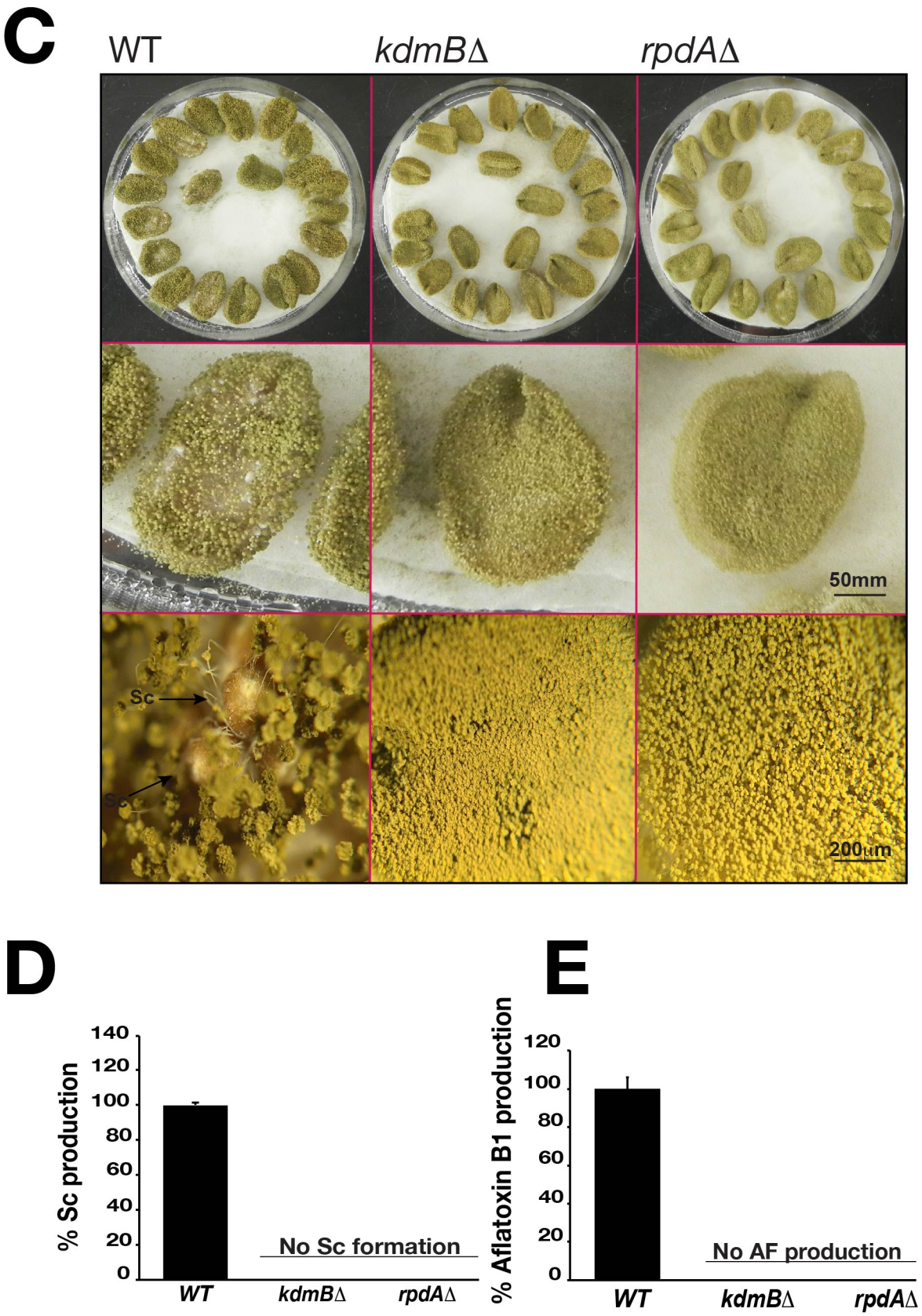
C
WT
kdmBΔ
rpdAΔ
50mm
Sc
Sc
200μm
D
% Sc production
140
120
100
80
60
40
20
0
No Sc formation
WT
kdmBΔ
rpdAΔ
E
% Aflatoxin B1 production
120
100
80
60
40
20
0
No AF production
WT
kdmBΔ
rpdAΔ

Figure 4.4. KdmB and RpdA are essential for aflatoxin production and play vital roles in peanut seed contamination. (A) Aflatoxin B_1 analysis of WT, *kdmB* and *rpdA* mutant strains by reversed-phase HPLC. The organic phase was extracted using chloroform from samples grown on YES agar media including required supplements for 7 days at the dark condition. WT represents 100% production. The lower panel shows the chromatogram of aflatoxin B1 peaks obtained from AFB_1 standard (pink), WT (purple) and *kdmB* (brown), *rpdA* (green) mutants. (B) RT-qPCR expression analysis of the aflatoxin regulatory gene cluster *aflC*, *aflD*, *aflM* and *aflR*. For the analysis of aflatoxin regulatory genes, fungal mycelia grown in complete media with required supplements for 24 h at 30ºC 200 g was shifted onto agar plates. Total mRNA was obtained by harvesting fungal mat grown on YES agar plates for 3 days at 30°C under the dark conditions. 1 μg total DNAase-treated RNA was used for cDNA synthesis. *benA* was used as a reference gene to obtain relative expression levels of mRNA using $2^{\Delta\Delta Ct}$ method. RT-qPCR experiments were performed using two independent biological replicates and nine technical replicates (C) For the pathogenicity tests, peanut seeds were treated with spores of WT strain, *kdmB* and *rpdA* mutants for 5 days at 30ºC in a dark environment. Mock control peanut seeds without any fungal treatment were not included in the figure for simplicity. (D) Sclerotia numbers grown on each peanut were manually counted and adjusted to the WT strain. (E) Aflatoxin analysis was performed by extracting AF from infected peanuts. All values are the average of three independent biological replicates and error bars represent standard errors.

4.5 Sclerotia development and aflatoxin production are restored in *kdmB* and *rpdA* complementation strains

It has been shown that deletions of *kdmB* and *rpdA* result in a complete loss of sclerotia (Sc) development and aflatoxin production (Figures 4.2 and 4.4). In order to confirm the functional roles of KdmB and RpdA, the genomic loci of *kdmB::phleO* and *rpdA::phleO* were inserted into *kdmB*Δ and *rpdA*Δ strains respectively, creating *kdmB*^{com} and *rpdA*^{com}. Complementation of *kdmB* and *rpdA* confirm the roles of functional KdmB and RpdA in *A. flavus* development and aflatoxin production. Sc production is restored by 20% in the *kdmB*^{com} strain, while *rpdA*^{com} restores Sc production around 45% with respect to WT (Figure 4.5A). Similarly, aflatoxin was restored by 130% in *kdmB*^{com}, while *rpdA*^{com} was able to produce 30% aflatoxin levels when compared to WT (Figure 4.5B). The lack of full restoration of sclerotia and aflatoxin might be due to the genomic loci of *kdmB* and *rpdA* being integrated ectopically into *A. flavus* genomic DNA.

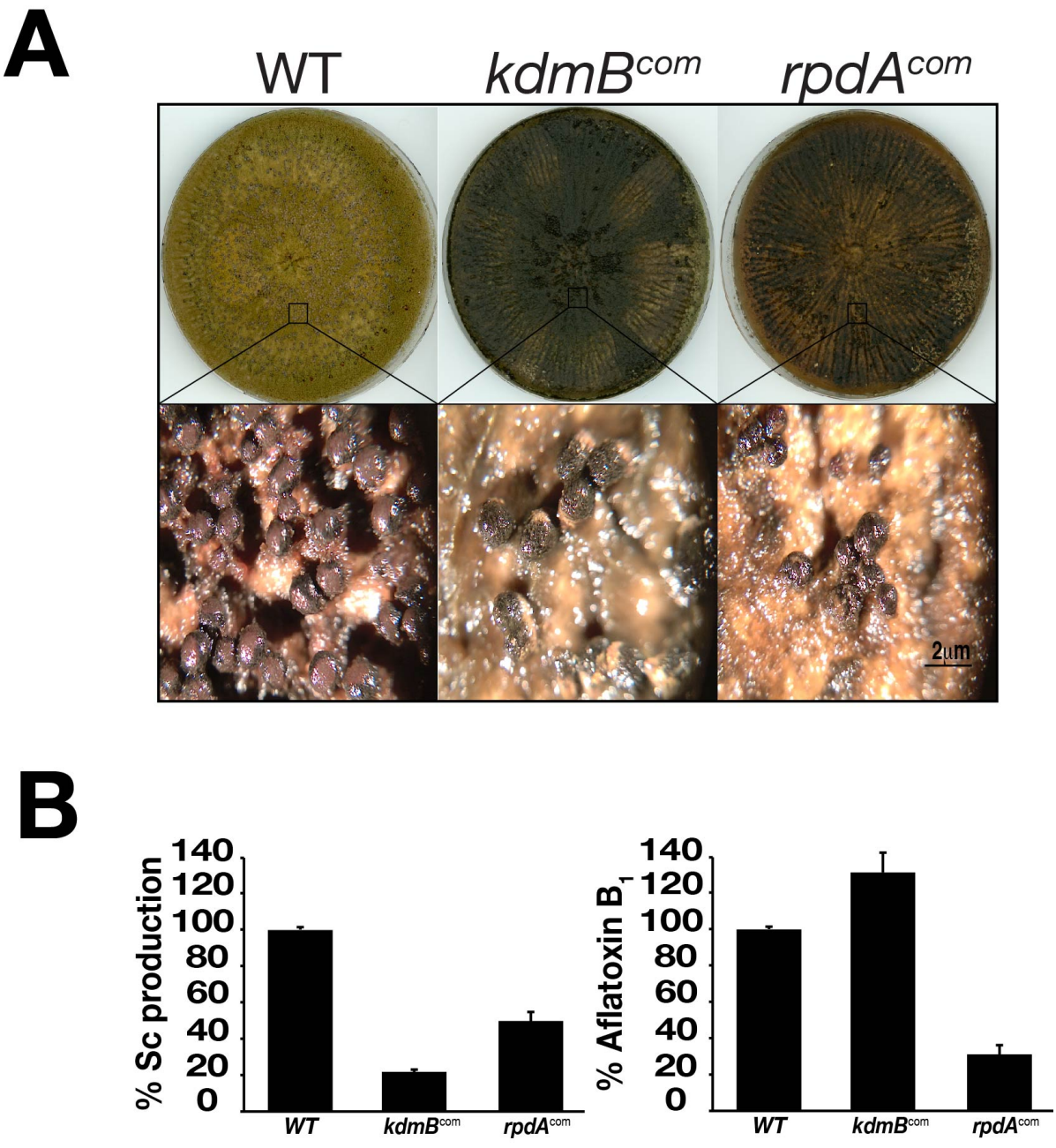

Figure 4.5. Complementation strains *kdmB*^{com} and *rpdA*^{com} recovered sclerotia and aflatoxin production. (A) For sclerotia analysis, WKM plates with required supplements were incubated in the dark conditions at 30°C for 21 days. Lower lane shows the stereomicroscopic images of sclerotia (Sc) formation in WT and complementation strains. (B) Percentages of Sc production in WT and complementation strains. Counting was performed manually by quantifying Sc produced on WKM agar plates. Final values were optimized with respect to WT representing 100%. Aflatoxin B_1 analysis by reversed-phase

HPLC organic phase extracted from culture agar media through chloroform extraction method in WT, *kdmB* and *rpdA* complementation strains. WT represents 100% production. All quantifications are the results of three independent biological replicates and error bars represent standard errors.

4.6 KdmB and RpdA are global regulators of secondary metabolism gene clusters in *A. flavus*

Chromatin modifications play fundamental roles not only during development but also in the regulation of secondary metabolite gene clusters. In pathogenic fungus *Fusarium graminearum*, histone H3K27 methyltransferase KTM6 was shown to be responsible for the activation of SM gene clusters required for mycotoxins, pigments and other SMs (Connolly et al., 2013). In a more recent study, it has been demonstrated that the HDA1-type histone deacetylase is involved in the accumulation of 1,8-dihydroxynaphthalene melanin and ergosterol pathways of phytopathogenic fungi *Magnaporthe oryzae* and increased levels of nivalenol-type trichothecenes in *Fusarium asiaticum,* emphasizing HDACs crucial role in the regulation of production of natural chemicals in pathogenic fungi (Maeda et al., 2017). More recently, a *sntB* deletion was shown to cause total loss of aflatoxin production in *A. flavus* (Pfannenstiel et al., 2018). It is previously mentioned in this thesis that aflatoxin gene clusters are negatively affected in *kdmB* and *rpdA* mutants in *A. flavus*. However, it is important to see if the roles of KdmB and RpdA are more global rather than simply regulating aflatoxin production.

In essence, other SM gene clusters could also be affected in *kdmB*Δ and *rpdA*Δ mutants. Therefore, the Secondary Metabolite Unique Regions Finder (SMURF) tool (https://www.jcvi.org/smurf) was used to determine potential SM gene clusters in *A. flavus*

genome. According to the database, there were 55 predicted backbone genes for SM clusters (Table 4.3). Hence, cDNA oligonucleotides for qPCR analysis were designed for these 55 backbone genes to analyse their gene expression levels in *kdmB*, *rpdA* and WT strains. The expression of 3 out of 55 genes could not be analysed possibly due to their complete absence in the selected growth condition, whereas 52 genes were analysed successfully. Minimum 30% of the change in expression level of backbone genes were considered as either up (Green box) or down-regulated (Red box), while lower than 30% expression differences were considered as similar or equal (Grey box) to WT strain (Figure 4.6A). Strikingly, 41 of the backbone genes required for NPRS (12 up-regulated, 12 down-regulated) and PKS (7 up-regulated, 11 down-regulated) were affected in at least *kdmB*Δ or *rpdA*Δ strains which correspond to approximately 79% of total 52 genes analysed. 11 genes (4 PKSs, 4 NPRSs, 1 dimethylallyl tryptophan synthase, putative 3-oxoacyl carrier protein synthase and 1 hypothetical protein) do not seem to be affected in *kdmB* or *rpdA* mutants. 10 backbone genes (5 NRPS, 4 PKS and 1 DMATS) in total have been drastically down-regulated, whereas only 3 genes (all NRPSp) were highly up-regulated in both mutants when compared to WT, emphasizing KERS complex generally as the positive-regulator of SM backbone genes. Additionally, 25 SM backbone gene expressions (11 NRPS, 11 PKS, 2 DMATS and 1 NRPS/PKS hybrid) were negatively affected, while only 4 genes (all NRPS) were positively affected in the *kdmB*Δ strain, clearly demonstrating an inductive role of H3K4me3 demethylase KdmB. As opposed to *kdmB*Δ, expression of 20 genes was affected positively (11 NRPS, 7 PKS and 2 DMATS), while expression of 12 genes was affected negatively (7 NRPS, 4 PKS and 1 DMATS) in *rpdA*Δ, proposing RpdA more as a repressor rather than inducer on certain SM backbone genes. 20 out of 52 genes were affected only in either *kdmB*Δ or *rpdA*Δ strains exhibiting their unique role on certain SM clusters. All in all, expression profiles of 52 SM backbone genes suggests that the H3K4me3 KdmB demethylase acts mostly as an inducer, while class I histone deacetylase RpdA acts as a

repressor, displaying mostly opposing roles in the regulation of SM production. Nevertheless, 11 genes were found to be regulated by both KdmB and RpdA in similar patterns (Figure 4.6B). Conidial pigmentation is regulated by PKS AFLA_006170 (Cluster 5) which was significantly down-regulated in both mutants. Interestingly, Asparasone A (AFLA_082150), PKS for sclerotia pigmentation (Cluster 27 (Chang et al., 2017)) and PKS/NRPS hybrid enzyme synthesizing leporin (*lepA*, Cluster 23, AFLA_066840 (Cary et al., 2015) are found to be down-regulated in the *kdmB* mutant while there was no significant change in the *rpdA* mutant when compared to WT. Similarly, aflatrem DMATS (AFLA_045490, Cluster 14) is down-regulated in the *kdmB* mutant, while it does not change in the *rpdA* mutant with respect to WT, emphasizing a distinct role of KdmB in the regulation of asparasone A and aflatrem. mRNA expression of NRPS for the biosynthesis of aspergillic acid (AFLA_023020, Cluster 10) and a PKS synthesizing an anti-insectan metabolite aflavarin (Cluster 37, AFLA_108550) are not changed in *kdmB*Δ while they are significantly increased in the *rpdA*Δ strain, indicating repressive roles of RpdA in the production of these metabolites.

Previously, SntB was shown to be a positive regulator of aflavarin, aflatoxin B_1, asparasone A, aflatrem, and kojic acid, and a negative regulator of ditryptophenaline and leporin B (Pfannenstiel et al., 2018). Similarly, KdmB acted as a positive-regulator of asparasone A, aflatrem, AF and leporin backbone gene mRNA levels underlining the common KERS complex functions on the regulation of SMs. RpdA, on the other hand, did not seem to have any effect on aflavarin or asparasone cluster backbone gene expression levels. RpdA seemed to be a positive regulator of aflatoxin and a negative regulator of aspergillic acid and aflavarin. Taken together, KERS complex components KdmB, RpdA, and SntB are positive-regulators of AF production while RpdA and SntB may have opposing roles in aflavarin production.

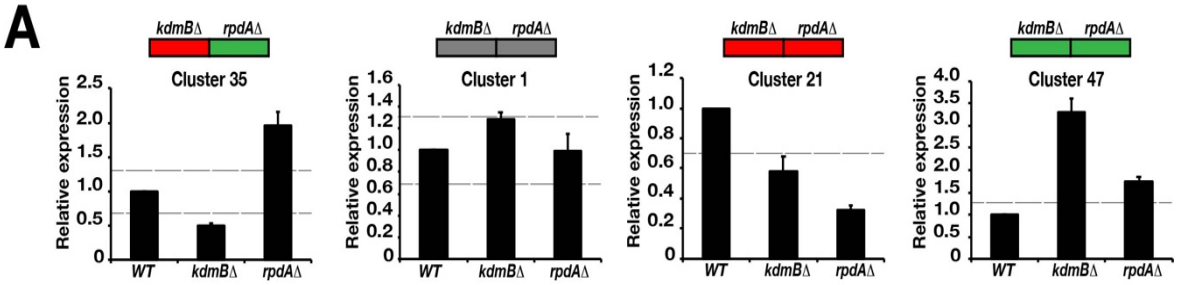

B

C	Accession		kdmBΔ	rpdAΔ
1	AFLA_002900	PKS		
2	AFLA_004450	NRPS		
3	AFLA_005320	PKS		
4	AFLA_005440	NRPS		
5	AFLA_006170	PKS		
6	AFLA_008770	NRPS		
7	AFLA_010010	NRPS		
8	AFLA_010620	NRPS		
9	AFLA_017840	NRPS		
10	AFLA_023020	NRPS		
11	AFLA_028720	NRPS		
12	AFLA_038600	NRPS		
13	AFLA_041610	NRPS		
14	AFLA_045490	DMATS		
15	AFLA_053870	PKS		
16	AFLA_054090	PKS		
18	AFLA_060020	PKS		
19	AFLA_060680	DMATS		
20	AFLA_062860	PKS		
21	AFLA_064240	NRPS		
22	AFLA_064560	NRPS		
23	AFLA_066840	NRPS/PKS		
24	AFLA_069330	NRPS		
25	AFLA_070920	NRPS		
26	AFLA_079400	NRPS		
27	AFLA_082150	PKS		

C	Accession		kdmBΔ	rpdAΔ
28	AFLA_082480	NRPS		
29	AFLA_083250	DMATS		
30	AFLA_084080	DMATS		
31	AFLA_090200	NRPS		
32	AFLA_096770	PKS		
33	AFLA_101700	NRPS		
34	AFLA_104210	PKS		
35	AFLA_105190	NRPS		
36	AFLA_105450	PKS		
37	AFLA_108550	PKS		
38	AFLA_109430	NRPS		
39	AFLA_112840	PKS		
40	AFLA_114820	PKS		
41	AFLA_116220	PKS		
42	AFLA_116600	DMATS		
43	AFLA_116890	PKS		
44	AFLA_118440	NRPS		
45	AFLA_118940	PKS		
46	AFLA_119110	NRPS		
47	AFLA_121520	NRPS		
49	AFLA_128060	PKS		
50	AFLA_128170	NRPS		
51	AFLA_129930	oxoacyl cps		
52	AFLA_135490	NRPS		
54	AFLA_139410	PKS		
55	AFLA_139670	HP		

Figure 4.6. KdmB and RpdA affect the majority of the SM gene clusters either positively or negatively. Complete media with required supplements was inoculated with *kdmB*Δ, *rpdA*Δ and WT spores ($2x10^6$ per ml) and grown for 24 h at 30ºC shaking condition. At the end of the incubation period, mycelia were shifted onto PDA agar plates to induce SM production. Total mRNA was obtained by harvesting fungal mycelia grown on PDA plates for 3 days at 30°C under the dark conditions. 1 µg total DNAase-treated RNA was used for cDNA synthesis. *benA* was used as a reference gene to obtain relative expression levels of

corresponding genes using $2^{\Delta\Delta Ct}$ method. (A) RT-qPCR expression analysis of 52 SM gene clusters which show either up-regulation, down-regulation or no change. Grey box represents no change, the red box represents down-regulation by at least 30% or more and the green box represents at least 30% up-regulation or more. cDNA was obtained from total mRNA extracted from fungal samples grown on PDA plates for 72 h at 30ºC in the dark condition. (B) Heat map expression profiles of 52 SM backbone genes with their accession numbers which belong to either NRPS, PKS, dimethylallyl tryptophan synthase, 3-oxoacyl carrier protein synthase and a hypothetical protein (HP). All values are the average of two independent biological replicates and 6 technical replicates. The error bars represent standard errors. See Appendix C for full description of all backbone gene clusters obtained from SMURF.

4.7 KERS complex regulates *in vivo* histone modifications

In *A. nidulans*, it was shown that KdmB is a Jumonji domain-containing demethylase which specifically targets H3K4me3 residues (Gacek-Matthews et al., 2016). Diversely, Class I histone deacetylase RpdA acts on global acetylated histone residues including H3, and H4 (Tribus et al., 2010). In order to analyse HPTMs regulated by KdmB and RpdA in *A. flavus*, a crude nuclei extraction protocol was carried out to enrich histones of *kdmB*Δ*, rpdA*Δ and WT strains as previously described (Soukup and Keller, 2013). PTM of histones were detected using antibodies specific for histone lysine residues described in Chapter 2. Interestingly, *A. flavus* KdmB is shown to be responsible for the demethylation of not only H3K4me3 but also H3K9me3 residues. Immunoblot band intensities of H3K4me3 and H3K9me3 were increased in the *kdmB*Δ. However, it remains unclear if H3K9me3 demethylation is affected directly or indirectly by KdmB. On the other hand, *kdmB*Δ H3K36me3 band intensities remained similar to WT levels suggesting that this residue is

not targeted by *A. flavus* KdmB. Notably, H3K36me3 levels were increased by 30% in the *rpdA* mutant with respect to WT. Previous studies suggested that RpdA acts on global histone residues including H3K9ac levels which control ST production. Surprisingly, H3K9ac levels did not show any increase in the *rpdA* mutant. However, a drastic increase in H3K14ac residues occurs in the RpdA depletion suggesting that *A. flavus* RpdA mainly targets H3K14ac residues which might correspond to aspergillic acid and aflavarin repression. KdmB depletion did not effect on the analysed acetylation residues of histones in *A. flavus* (Figure 4.7). Presumably, KdmB and RpdA may regulate development, SM production and pathogenicity through targeting H3K4me3, H3K9me3, H3K36me3 and H3K14ac marks.

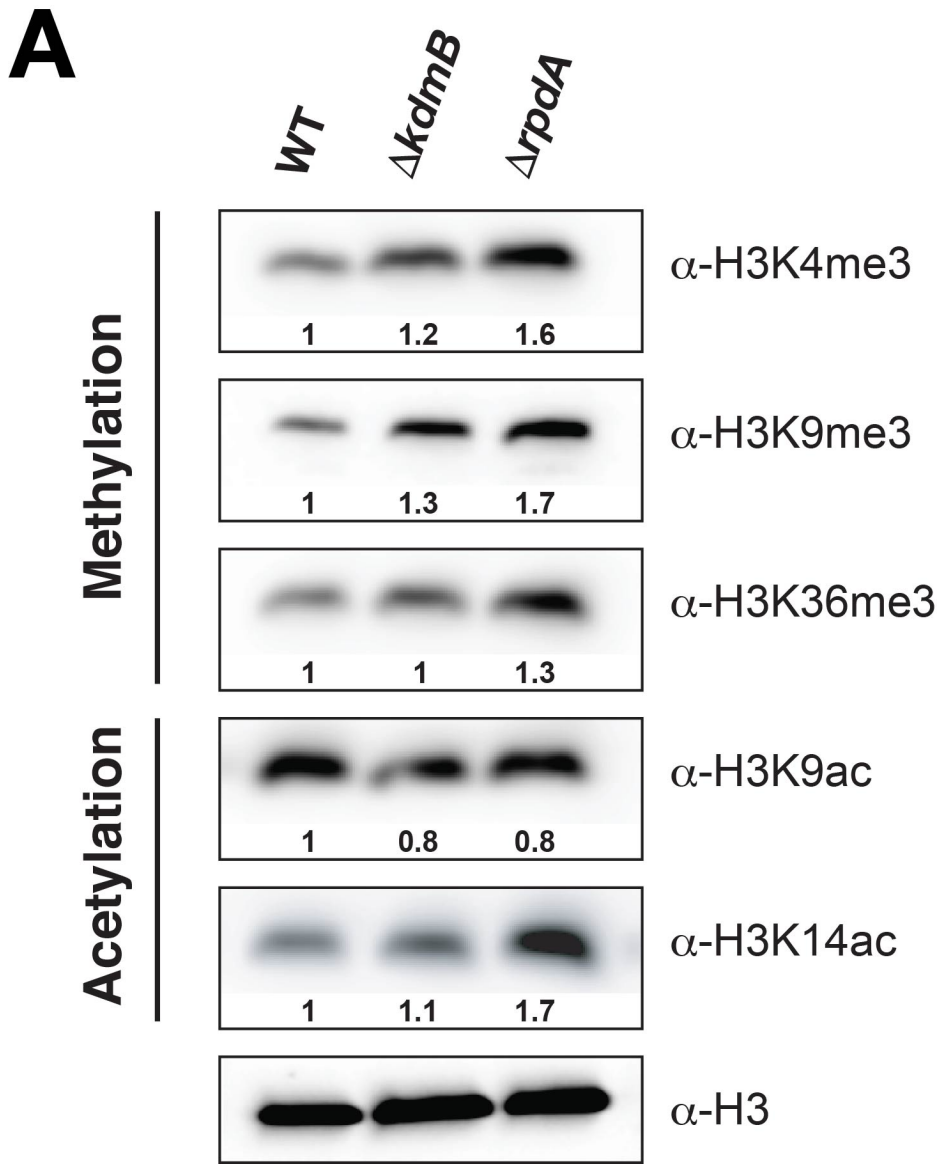

Figure 4.7. KERS complex has *in vivo* HDMA and HDAC activities. Demethylation of histone lysine residues is controlled by KdmB and RpdA, while deacetylation of lysine residues are only RpdA-dependent. Approximately 2x10^6 conidia were inoculated into GMM liquid culture with required supplements and incubated at 30ºC for 48 h. 20 μg nuclear protein extract was loaded onto SDS-PAGE gels (15%). Nuclear proteins were transferred onto 0.2 μm nitrocellulose Western blotting membrane (Amersham Protran, GE healthcare) and fast transfer protocol was applied using the Thermo Scientific™ Pierce™ Power Blotter for 10 minutes. α-H3 polyclonal rabbit antibody (Abcam, 1:5000 in TBS + 1% Tween20) was used to detect H3 levels for standardization. ImageJ software was used for the

quantification of signal intensity. Immunoblot analysis was conducted in two independent biological and three technical replicates for each strain.

Chapter 5

Discussion

5.1 KERS, a novel tetrameric demethylase complex consisting multi-domain subunits, is likely conserved among other eukaryotes

Chromatin modifiers play important roles in proliferation, survival and cellular responses to environmental stimuli by regulating HPTMs at the chromatin level (Chen and Dent, 2014). Transcriptional regulation of fungal development, secondary metabolite production and pathogenicity are likely dependent on certain HPTMs (Gacek and Strauss, 2012). Although various signal transduction pathways controlling the regulation of fungal development and SM production have been discovered, epigenetic level chromatin control by chromatin modifier complexes in the model organism *A. nidulans* or pathogenic fungus *A. flavus* is not yet clarified. In this thesis, the novel chromatin modifying complex KERS, comprising Jarid1-type demethylase KdmB, putative cohesin acetyltransferase EcoA, ring finger PHD domain-containing protein SntB and Class I HDAC RpdA have been discovered and studied extensively in model organism *A. nidulans* and pathogenic fungi *A. flavus*. Discovery of the KERS complex was proved by performing tandem affinity purification (TAP) coupled with mass spectrometry using a KdmB::TAP expressing strain (Table 3.1). Co-purification and analysis of EcoA::TAP, RpdA::TAP and SntB::TAP by LC-MS^2 confirmed the bulk presence of the KERS complex. Similar results were found in HA and GFP reciprocal co-purifications (Table 3.1). *In vivo* physical interactions of KdmB with EcoA, RpdA, and SntB were further supported by BIFC analysis (Figure 3.3). The same complex is also conserved in *A. flavus* which was confirmed by purification of KdmB::3xHA and KdmB::sGFP (Figure 4.1C). Similarly, EcoA, RpdA, and SntB were recruited by KdmB forming the tetrameric complex in the pathogenic fungus.

In *A. nidulans*, it is predicted that there are seven JmjC domain-containing demethylases, two of which have been characterised so far. KdmA, KDM4 family H3K9me2/3 and H3K36me2/3 demethylase were shown to act on between 25% and 30% of

genes during early and late vegetative growth conditions. Furthermore, it was shown that KdmA normally acts as a co-repressor during primary growth and as an inducer during secondary metabolism induction which can equally positively and negatively influence gene expression. The *kdmA* mutant strain did not show any significant phenotypic change under normal conditions, however, when oxidative stress was applied, it caused lethality and sensitivity (Gacek-Matthews et al., 2015). KdmB was studied by the same research group (using *ve1* strain background) and it was found that KDM5-type demethylase KdmB acts on the removal of methyl groups from lysine residues from H3K4me2/3 by mediating transcriptional repression due to the fact that H3K4me2/3-containing nucleosomes are primarily found at promoter regions and are a hallmark of actively transcribed genes. According to ChIP-seq and RNA-seq analyses, ~1750 genes were up-regulated in the *kdmB* deletion. Interestingly, it was also demonstrated that the *kdmB* mutant resulted in the down-regulation of an equal number of genes comprising secondary metabolite gene clusters, suggesting that KdmB is involved in the control of induction of secondary metabolite biosynthetic gene clusters (Gacek-Matthews et al., 2016). Domain analysis of KdmB demonstrates multi-domain protein structure (Figures 3.4 and 4.1D) and previously it was shown to be closely identical to higher eukaryotes than yeast *S. cerevisiae*. Arid/Bright domain does not exist and only one PHD domain is present in yeast, whereas two PHD domains are present together with Arid/Bright region in human and *A. nidulans* (Gacek-Matthews et al., 2016).

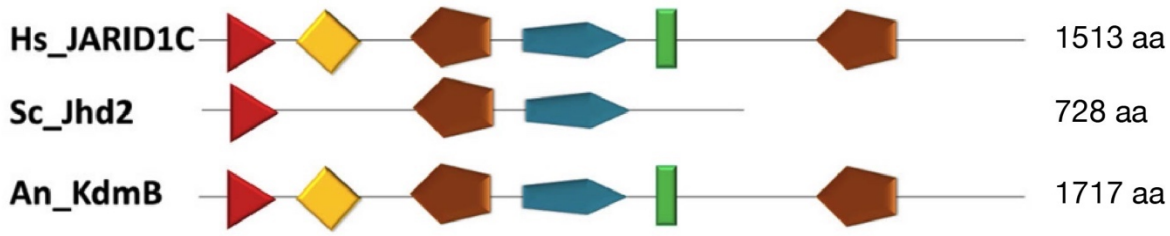

Figure 5.1. Protein domain architecture of KdmB in human, *S. cerevisiae* and *A. nidulans*. Red triangle represents the N-terminal Jmj domain. Yellow box represents Arid/Bright AT-rich interaction α-KG binding domain. The brown pentagonal shape represents PHD classical chromatin binding domain. Blue represents catalytic JmjC domain required for the removal of methyl residues from lysine using Fe^{2+}. Green represents C5HC2 zinc finger domain for binding specificity. Yeast Jhd2 in protein size is at least twice as small as human or *A. nidulans* KdmB (Modified from (Gacek-Matthews et al., 2016)).

In budding yeast, it is estimated that there are a total of five JmjC domain-containing proteins namely Jhd1, Jhd2, Rph1, Ecm5 and Gis1 (Kwon and Ahn, 2011). Jhd1 is KDM2 demethylase which catalyses the removal of methyl groups from H3K36me3. Similarly, Rph1 (KDM4) acts on H3K36me2/3 residues. Although Ecm5 and Gis1 contain the JmjC domain, little is known about their role in mediating global histone PTMs. Ecm5 was shown to physically interact with Snt2 and deacetylase Rpd3 (Baker et al., 2013). Furthermore, in the same study, Ecm5 and Snt2 were shown to be responsible for the recruitment of Rpd3 to a number of promoter regions. Ecm5 and Snt2 were found to target a common set of genes when treated with H_2O_2 stress agent (Kwon and Ahn, 2011). Budding yeast KdmB ortholog *JHD2* encodes H3K4me3 demethylase Jhd2 (KDM5) which inhibits the Nrd1-Nab3-Sen1 (NNS) transcription termination complex and is involved in genetic inhibition of the histone chaperone complexes Spt16-Pob3 (FACT) and Spt6-Spn1 (Lee et al., 2018a). In mammals, there are four KDM5 family members, while *C. elegans* and *Drosophila* have one, RBR2 and LID respectively. All four KDM5 family demethylases play important roles in development. KDM5 was shown to interact with HDACs such as HDAC1 and HDAC4. For instance, H3K4 demethylase Lid (*Drosophila* KDM5) interacts with and inhibits Rpd3. Lid also interacts with FOXO and promotes the activation of oxidative-response genes under oxidative stresses by recruiting HDAC4 to FOXO in order to facilitate FOXO deacetylation which affects FOXO DNA binding (Liu et al., 2014). KDM5 was identified to interact with

two distinct histone deacetylase complexes, the SIN3B-HDAC and the HDAC NuRD, both of which are essential in nucleosome remodelling and controlling developmentally regulated genes (Nishibuchi et al., 2014, Gajan et al., 2016). Human ortholog ESCO1 was found to be associated with Lysine-specific-demethylase 1 (LSD1), required for H3K4 -mono, -di demethylation. In Co-IP experiments, it was shown that ESCO1 also interacts with HDAC1/HDAC2 (Choi et al., 2010). It remains unknown if EcoA directly contributes to histone modification in filamentous fungi. Since we could not obtain a viable *ecoA* deletion strain in *A. flavus*, a knock-down construct may help to investigate its genome-wide effect. The *A. nidulans ecoA*$^{\text{TetON}}$ strain could be used in future studies to study the possible influence of EcoA on histone modifications.

Class I HDACs can form multi-protein complexes to target unique locations across the genome. Apart from previously mentioned Rpd3 complexes in higher eukaryotes and Ecm5-Snt2-Rpd3 in yeast, Rpd3 forms large and small Sin3 complexes in *S. cerevisiae*, Rpd3L and Rpd3S respectively (Yeheskely-Hayon et al., 2013). Rpd3L interacts with Ume1 (DNA-binding protein), Sds3, Sap30 and Pho23 (an inhibitor of growth protein), while Rpd3S is associated with Sin3, Ume1, Eaf3 (Chromodomain protein) and Rco1 (Plant homeodomain finger protein). Both complexes have repressive features where Rpd3L targets histones at promoter regions, Rpd3S deacetylates transcribed regions to suppress intragenic transcription initiation (Yang and Seto, 2008).

RING (Really interesting new gene) finger protein Snt2 is a SANT, BAH/PHD domain-containing DNA-binding E3 ubiquitin-protein ligase in yeast *S. cerevisiae* (Baker et al., 2013). The RING domain is a characteristic structure for most E3 ligases which contain a cysteine-rich sequence motif that can bind two zinc atoms. As previously mentioned, Snt2 physically interacts with Rpd3 and demethylase Ecm5, forming the Rpd3μ complex and it is required for oxidative stress responses in yeast (Baker et al., 2013). This

thesis is the first evidence presenting the KdmB-EcoA-RpdA-SntB association forming the KERS complex in *A. nidulans* (Chapter 3) and *A. flavus* (Chapter 4) which was not shown to form tetrameric complex previously.

5.2 KERS complex has a dual role in fungal development: KdmB-EcoA are negative regulators of sexual development while RpdA-SntB are positive-regulators

Interestingly, cohesin acetyltransferase-encoding *ecoA* gene could not be disrupted in *A. nidulans* and *A. flavus,* suggesting that *ecoA* is also essential for viability in filamentous fungi, similar to the yeast *eco1* ortholog. Surprisingly, the *kdmB*Δ strain displayed higher (40% increase in dark, Figure 3.7) fruiting body formation and lower conidiation (40% decrease in light, Figure 3.8) with respect to WT which was not described in previous KdmB studies. This might be as a result of the *ve1 A. nidulans* strain being used previously (Gacek-Matthews et al., 2016). A similar pattern with more drastic change was seen in the *ecoA* knock-down strain where conidiation in the presence of light was reduced by 70% and cleistothecia formation in dark was increased by 400%. These data strongly suggest that KdmB and EcoA act in a similar manner during the asexual and sexual life cycles as opposed to RpdA-SntB. *sntB*Δ and *rpdA* knock-downs completely abolished sexual cleistothecia formation. Strikingly, asexual sporulation was drastically reduced in both strains (90% decrease). Previous research done on the *sntB* mutant showed that SntB is required for sclerotia production and *A. flavus* pathogenicity (Pfannenstiel et al., 2018). The *sntB*Δ effect seems to be similar to previous work done in *N. crassa* and *F. oxysporum,* where SntB depletion strains impaired fungal pathogenicity (Denisov et al., 2011). The role of SntB may likely be conserved across filamentous fungi. Interestingly, *kdmB* disruption did not alter the *sntB*Δ phenotype, suggesting that SntB is epistatic to KdmB (Figure 3.8).

*Jhd2*Δ was not lethal and did not have any phenotypic effect in yeast (Huang et al., 2015). Although *kdmB* deletion in *A. nidulans* and yeast is not lethal, *Drosophila* KDM5 and mouse KDM5B are essential genes for survival (Li et al., 2010, Catchpole et al., 2011). Lid depletion leads to reduced proliferation and flies with developmental defects wing formation (Gajan et al., 2016). Mutations in Eco1 cause lethality and a human homolog ESCO2 mutation results in Roberts Syndrome and SC Phocomelia (Guacci et al., 2015, Lu et al., 2014). The lethal effect of Eco1 deletion can be suppressed by substituting Smc3 K112/113 to other residues mimicking acetylated lysine. Additionally, deleting WPL1/RAD61 was shown to suppress the lethal effect of the Eco1 mutation (Rolef Ben-Shahar et al., 2008, Sutani et al., 2009, Onn et al., 2008). In our work, SudA acetylation (K106/107) was impaired in an EcoA knock-down, however, this did not affect the viability of the strain, suggesting that a similar mechanism may not be conserved in filamentous fungi. Furthermore, acetylation of DNA polymerase V by Eso1 is essential for *S. pombe* viability (Chen et al., 2017). Class I histone deacetylase RpdA is essential for viability in *A. nidulans*, *A. fumigatus* and *Cochliobolus carbonum*, however, the RpdA homolog Rpd3 is not vital in yeast *S. cerevisiae,* making it a good candidate to study the *rpdA*Δ effect. It was discovered that the C-terminal part of the RpdA protein is crucial for survival which contains its catalytic activity for acetyl removal from histone tails (Bauer et al., 2016). Interestingly, *A. fumigatus* and *C. carbonum* RpdA could complement *A. nidulans rpdA*Δ, but not higher eukaryote HDACs. RpdA was shown to contribute to promoting fungal pathogenicity, thus making it an ideal target for HDAC inhibitors such as TSA. RpdA can remove acetyl modifications from all core histone residues signifying its role as a global chromatin remodeling enzyme which can also function as a histone chaperone and a chromatin stabilizing factor (Bauer et al., 2016). *rpdA* was deleted in *A. flavus* and confirmed by Southern blot analysis as well as RT-qPCR (Figures 2.3, 2.4, 4.2). Successful generation of *rpdA*Δ suggests that *A. flavus* RpdA may functionally be more closely related to yeast Rpd3.

Snt2 depletion prevents histone degradation and causes sensitivity to histone overexpression in yeast (Singh et al., 2012). KERS complex might also be involved in the regulation of histone proteins since several subunits of HIR complex required for repression of histone genes outside of S-phase were consistently detected at higher peptide numbers in *A. flavus* KdmB purifications (Appendix A, B). However, this requires further studies to show mechanistic interdependency between KERS and HIR complexes. Snt2 depletion impaired pathogenicity, asexual sporulation and hyphal growth in asexual soil-borne fungus *Fusarium oxysporum*. Similarly, an *snt-2*Δ strain displayed a lack of sexual development, reduction in asexual sporulation as well as hyphal growth in *Neurospora crassa* (Denisov et al., 2011). The *sntB*Δ phenotype in this study is in parallel to previous work done in other filamentous fungi which signifies its evolutionary conserved functions.

Chromatin modifier enzymes play fundamental roles in several distinct cellular response pathways. While *ecm5*Δ was shown to be sensitive to oxidative stress, *rpd3*Δ and *snt2*Δ strains were resistant, emphasizing their opposing roles in yeast stress responses (Baker et al., 2013). Unlike *S. cerevisiae rpd3*Δ and *snt2*Δ, *A. nidulans kdmB*, *ecoA*, *rpdA,* and *sntB* mutant strains did not have any significant impacts in the response to oxidative stress agents (Data not presented). The high-osmolarity glycerol (HOG) MAPK pathway is a widely studied topic in *A. nidulans* and is an essential mechanism for transmitting environmental osmotic signals (Ma and Li, 2013). Asexual conidiation was found to be up-regulated in *kdmB*, *ecoA*, *rpdA,* and *sntB* mutants (Figure 3.10). This suggests that genes involved in the HOG MAPK pathway such as *sln1*, *skn7*, *sho1*, *pbs2* and *hog1* may be direct targets of the KERS complex. KERS mutants resulted in sensitivity during cell-wall stress (Figure 3.12) and amino-acid starvation (Figure 3.13), suggesting that complex subunits equally contribute against certain stress response agents and are required for the regulation of various stress response pathways.

5.3 The tetrameric KERS complex is assembled via association of the heterodimers KdmB-EcoA and RpdA-SntB

Complex association interdependency analysis suggested that EcoA is recruited by KdmB to form the tetrameric KERS complex (Table 3.3). Likewise, RpdA was shown to be recruited by SntB for KERS assembly. In yeast, the KdmB homolog Jhd2 is thought to act alone during the removal of methyl groups from H3K4me3 residues and it was shown to be involved in the regulation of mitotic rDNA condensation (Ryu and Ahn, 2014). Eco1 was found to mediate the coordination of rDNA replication and transcription (Lu et al., 2014). It requires further research to answer if KdmB can act alone to shape the chromatin structure or if the KERS assembly is required for demethylase activity. Nevertheless, it is clear that KdmB is essential for the recruitment of EcoA to the RpdA-SntB heterodimer. Highly conserved SANT domain-containing protein motifs, such as Snt2, N-CoR and SMRT stimulate Rpd3 deacetylase activity, which are subunits of histone HDAC complexes (Yang and Seto, 2008). Not only SANT motifs are associated with HDACs, but also it was demonstrated that SANT domain-containing proteins are subunits of HATs such as ADA and SAGA (Spt–Ada–Gcn5-acetyltransferase) complexes (Boyer et al., 2004). Surprisingly, according to the *in vitro* HDAC activity assay, it is evident that RpdA deacetylase activity is not KdmB or SntB-dependent which is controversial to previous findings where Class I HDACs were shown to require SANT-domain subunits for H3K9ac deacetylase activity (Figure 3.14). It remains to be answered if SntB directs RpdA to certain chromatin regions for the control of transcription of gene clusters. ChIP-seq analyses could elucidate chromatin binding patterns of KERS complex in future studies.

5.4 SntB mediates EcoA-proteasomal degradation while KdmB protects its nuclear stability to promote the establishment of chromatid cohesion

In *S. cerevisiae*, the Eco1 degradation process is initiated by phosphorylation of serine 99 by Cdk1. Dbf4-Cdc7 then phosphorylates the adjacent S98 residue which further promotes phosphorylation of the T94 residue by another kinase Mck1. Such phosphorylation cascades result in ubiquitination by SCF^{Cdc4}, leading to Eco1 destruction by the proteasome (Lyons et al., 2013, Lyons and Morgan, 2011, Seoane and Morgan, 2017). These processes are essential for ceasing cohesion establishment after S phase. Protein immunoblotting and nuclear localization assays suggest that KdmB is a positive-regulator for EcoA stability while SntB directly or indirectly may be involved in targeting EcoA for proteasomal degradation (Figures 3.12, 3.13). This phenomenon can be supported by the fact that additional phosphorylated residues were detected when KdmB was absent on S41/45. These phosphorylated residues disappeared in the *kdmBΔ/sntBΔ* strain (Figure 3.13F). Hence, SntB most likely targets EcoA for phosphorylation-dependent ubiquitination which leads to proteasomal degradation. Ubiquitination could not be detected in mass spectrometry analysis possibly due to the fact that dephosphorylation-ubiquitination are transient processes resulting in prompt EcoA degradation. Recently, ESCO2 protein stability was shown to be controlled by E3 ubiquitin ligase CUL4-DDB1-VPRBP and MCM complexes (Minamino et al., 2018). It was discovered that MCM-ESCO2 physical interaction prevents ESCO2 proteasomal degradation during DNA replication and cell cycle while CUL4-DDB1-VPRBP promotes ESCO2 degradation during late S phase to suppress cohesion formation. It is unknown if SntB is associated with other kinases for EcoA degradation. Although orthologs of these proteins are conserved in *A. nidulans*, EcoA purifications and mass spectrometry analyses could not identify such proteins. Therefore, SntB might have a similar role to CUL4-DDB1-VPRBP which regulates ESCO2 degradation during late S phase to suppress cohesion formation (Minamino et al., 2018), while KdmB might act as

MCM complex preventing EcoA proteasomal degradation. EcoA nuclear levels are likely controlled by KdmB and SntB during specific cell-cycle mitotic phases of *A. nidulans* when cohesion establishment is necessary.

Establishment of sister chromatid cohesion occurs through Eco1 acetylating Smc3 on two conserved tandem lysine residues which contributes to the processes of chromosome segregation, DNA replication, chromosome condensation and DNA damage repair (Guacci et al., 2015). In yeast, these acetylations can be removed by deacetylase Hos1 (Xiong et al., 2010). In humans, Eco1 has two orthologs, namely ESCO1 and ESCO2 respectively, both of which can acetylate the evolutionary conserved Smc3 subunit K106/107 (Whelan et al., 2012, Nishiyama et al., 2010). Ortholog analysis revealed that *A. nidulans* EcoA is 28% identical to human ESCO1/2 (Table 3.2), suggesting that their functional roles may be conserved from filamentous fungi to human. The cohesin complex is composed of four subunits: Smc1, Smc3, Rad21 and SA1 or SA2 which are essential for cell-cycle pathways and Eco1 plays a crucial role in aiding the cohesion establishment during S phase which connects sister chromatids by encircling them as molecular rings (Onn et al., 2008, Zhang et al., 2008). The positions of *A. nidulans* SudA (yeast Smc3 ortholog) conserved lysine residues are the same as those in humans at K106/107 positions rather than yeast Smc3 K112/113 (Figure 3.16B). It is thought that Eco1 deletion is lethal due to unacetylated lysine residues of the Smc3 protein. Hence, the up-regulation of sexual development in EcoA knock-down strain might be as a result of SudA lacking acetylated K106/107 residues. In human, ESCO2 has additional functions other than acetylating Smc3. Additionally, Eco1 also was shown to acetylate Mcd1 (Rad21) which is required to establish cohesion during S phase (Choi et al., 2010, Kim et al., 2002). However, Mcd1 acetylation was not affected in EcoA down-regulation in *A. nidulans,* suggesting that a different mechanism may be involved during Mcd1 acetylation. It was emphasized that not only is ESCO2 capable of acetylating Smc3 and Mcd1 but also it is involved in HPTM by acetylating H4K16 residues

both *in vivo* and *in vitro* which is essential for Spindle Assembly Checkpoint (SAC) activity and kinetochore functions during mouse oocyte meiosis (Lu et al., 2017). In this work, it was shown that SudA recruited all cohesin complex components emphasizing that the multimeric complex is conserved in *A. nidulans*. Although EcoA could not be detected in mass spectrometry analysis in a SudA purification, it is shown that K105/106 acetylation residues were abolished in an EcoA knock-down strain. Interestingly, KdmB depletion does not seem to have any effect on SudA K106/107 acetylation (Figure 3.16).

To summarize, findings presented in *A. nidulans* demonstrate the first characterised tetrameric demethylase KERS complex involved in fungal development, stress responses and cohesin acetylation. The KERS complex links cohesion establishment to fungal development and possibly regulates the transcriptional activities of gene clusters required for asexual conidiation, sexual development and stress responses (Figure 5.2). Ortholog analysis suggests that KERS subunits are highly conserved from lower to higher eukaryotes, thus similar protein complexes could be present in other eukaryotes involved in cellular pathways controlling development and disease.

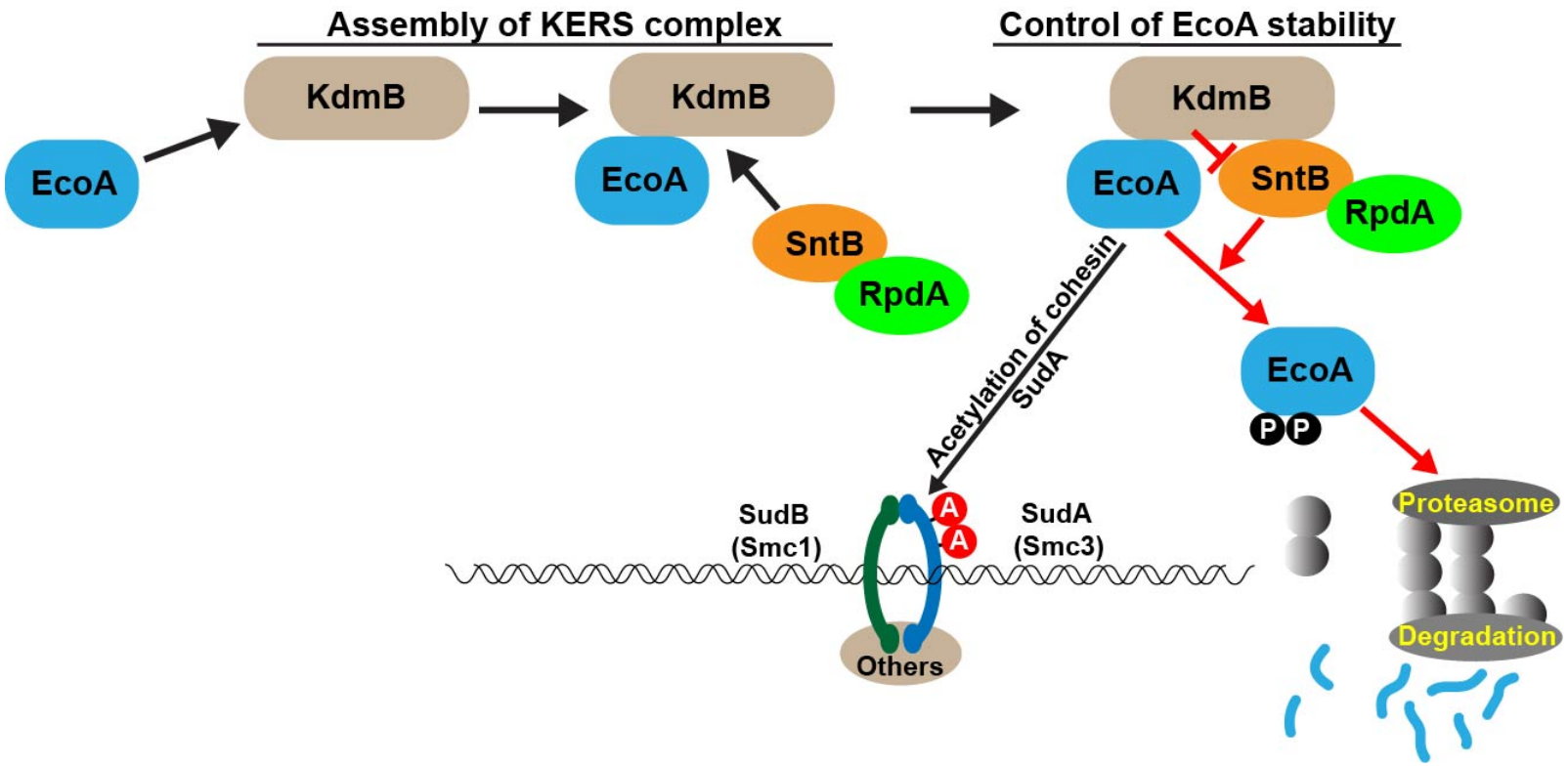

Figure 5.2. Schematic representation of the roles of the tetrameric KERS complex in *A. nidulans*. KdmB recruits EcoA to the heterodimer RpdA-SntB to form the tetrameric KERS complex. SntB targets EcoA for proteasomal degradation, while KdmB represses SntB function to maintain EcoA nuclear levels which are required for cohesin acetylation and possibly transcriptional regulation of various cellular pathways involved in fungal development, stress responses and secondary metabolite production.

5.5 KERS complex is conserved in the pathogenic fungus *Aspergillus flavus* with distinctive roles

KdmB::GFP and KdmB::3xHA purifications revealed that the KERS complex is recruited and conserved in the plant pathogen *A. flavus* (Figure 4.1). Ortholog analysis revealed that the KERS complex may be conserved in other plant and human pathogenic fungi such as *A. fumigatus* or *Magnaporthe oryzae,* making it a good candidate to study the epigenetic regulation of fungal chromatin and pathogenicity. In particular, KERS complex subunits sequence similarities were found to be quite high in human pathogen *A. fumigatus* (Figure 4.1E). It would be interesting to investigate the possible roles of this complex in the regulation of aspergillosis.

It is worth noting that KdmB and RpdA are chromatin modifier catalytic enzymes which could potentially influence histone PTMs genome-wide levels affecting development, SM production and pathogenicity. This hypothesis is further supported by the fact that both *kdmB* and *rpdA* deletions resulted in the lack of sclerotia formation (Figures 4.2A, 4.4C, 4.4D). Sclerotia regulating genes *nsdC* and *nsdD* were drastically reduced in mutant strains (Figure 4.2D), suggesting that the KERS complex is involved in positive regulation of *A. flavus* sclerotia development through *nsdC* and *nsdD* regulation while KdmB-EcoA were shown to be negative regulators of sexual development in *A. nidulans* (Figure 3.8). The *sntB* mutant strain was previously shown to lack sclerotia formation (Pfannenstiel et al., 2018), suggesting that KERS complex subunits are equally important for sclerotia development.

5.6 KdmB and RpdA have opposing roles in the regulation of light-induced development

In addition to sclerotia shut-down, conidiation was significantly reduced in the *rpdA* mutant strain (Figure 4.2B), coherent with the *rpdA* knock-down strain in *A. nidulans*. Gene expression analysis suggests that RpdA is likely regulating conidiation by targeting and positively regulating *abaA* and upstream conidia regulator *flbA* expression (Figure 4.2C). As opposed to *rpdA*Δ, conidiation is increased in the *kdmB* mutant indicating opposite functions of KdmB and RpdA during light-induced sporulation (Figure 4.2B). Furthermore, *kdmB* and *rpdA* mutants show sensitivity against topoisomerase inhibitor CPT, while the *kdmB* mutant was more resistant to menadione mediated oxidative stress (Figure 2G), emphasizing their critical roles against stress response agents. In yeast, *ecm5*Δ was shown to be sensitive towards oxidative stress (Baker et al., 2013). As opposed to yeast *ecm5*Δ, *kdmB* depletion resulted in increased resistance toward menadione mediated oxidative stress but did not have any effect against hydrogen peroxide suggesting functional differences of KdmB and Ecm5 which are not conserved. Therefore, the sensitivity of *kdmB* and *rpdA* against topoisomerase inhibitor might stem from EcoA functions on cohesins and genome integrity.

5.7 KERS complex is required for the induction of aflatoxin through the *afl* biosynthetic cluster

In previous studies, HPLC-MS/MS analyses suggested that sterigmatocystin, orsellinic acid and emericellamides C and D were reduced while emodin and its derivatives were increased in a *kdmB*Δ strain (Gacek-Matthews et al., 2016). Interestingly, aflatoxin production is completely abolished in *kdmB* and *rpdA* mutants which were confirmed by HPLC analysis performed from aflatoxin inducing agar media and *A. flavus* infected peanut samples (Figures 4.4A, 4.4E). This is consistent with the previous study with the *sntB* mutant which

was shown to be unable to produce aflatoxin in *A. flavus* as well as sterigmatocystin in *A. nidulans* (Pfannenstiel et al., 2017), suggesting KERS chromatin modifiers are equally essential for aflatoxin production. Furthermore, loss of aflatoxin production was shown to be as a result of the aflatoxin cluster biosynthetic genes *aflC*, *aflD*, *aflM* and *aflR* being significantly down-regulated (Figure 4.4B) in the KERS mutants. Hence, the chromatin modifier KERS complex most likely controls aflatoxin production by targeting *afl* biosynthetic gene clusters.

5.8 KdmB and RpdA are global regulators of secondary metabolism most likely mediated by their *in vivo* HDMA and HDAC activities

Having observed the profound effects of KdmB and RpdA in aflatoxin production, it became vital to elucidate if KdmB and RpdA-dependent regulation of secondary metabolism extended beyond aflatoxin production in *A. flavus*. Notably, transcription levels of nearly 80% of SM backbone genes are affected in *kdmB* and/or *rpdA* deletions, indicating their roles as global secondary metabolism regulators in *A. flavus* (Figure 4.6). Nuclear enrichment immunoblotting assays using HPTM antibodies show that *kdmB* and *rpdA* mutants have increased trimethylation on histone H3K4me3 and H3K9me3 sites. Unlike the *kdmB* mutant, *rpdA*Δ presented increased tri-methylation at the H3K36 residue. It remains unknown if RpdA can be associated with other chromatin readers, writers and erasers such as methyltransferases, demethylases or heterochromatin protein. The *rpdA* deletion resulted in a significant increase in H3K14 acetylation levels (Figure 4.7A). SntB was shown to be responsible for the regulation of H3 acetylation levels as well as *A. flavus* pathogenicity (Pfannenstiel et al., 2018). Similarly, in a recent study in *M. oryzae*, it was shown that SntB ortholog MoSnt2 interacts with histone deacetylase Hos2 (*A. nidulans* HosA ortholog) to mediate H3 deacetylation and plant infection (He et al., 2018). The impact of *A. flavus* SntB

in the H3 acetylation is most likely as a result of its association with RpdA. In the previous studies, histone enriched LC-MS/MS analysis revealed that global H3 N-terminal lysine acetylation (H3K9ac/K14ac) was increased by almost 20% in the *kdmB*Δ strain in *A. nidulans* (Gacek-Matthews et al., 2016). Furthermore, it was recently emphasized that the yeast KdmB homolog Jhd2 is a negative regulator of the Rpd3S complex which controls the function of Rpd3S through Eaf3 and Rco1 subunits (Lee et al., 2018b). However, there seems to be no change in histone K9ac or K14ac acetylation levels in the *kdmB*Δ strain, suggesting the inhibition of RpdA HDAC activity in KdmB depletion may not be conserved in *A. flavus* (Figure 4.7A). Nevertheless, it is evident that the KERS complex is conserved in the aflatoxin producer pathogenic fungus, however, it is possible that the mechanistic function of this complex might differ from the model organism *A. nidulans*.

Findings in this thesis provide strong evidence on how chromatin modifier protein complexes can have a broad effect on growth, development and natural product biosynthesis by controlling epigenetic marks (Figure 5.3). Demethylase KERS complex is not only involved in the establishment of sister chromatid cohesion by regulating acetylation of cohesin subunit but also regulates asexual sporulation, fruiting body formation, sclerotia development, aflatoxin production and seed contamination. It has been revealed in this thesis that KERS is essential for aflatoxin production and fungal pathogenicity. Because the KERS complex exhibits a broad influence on the development and SM production, it could be a good target not only for novel drug discovery but also to understand the epigenetic mechanisms contributing to fungal pathogenicity. These results suggest that similar epigenetic mechanisms mediated by KERS complex is probably conserved in other eukaryotes.

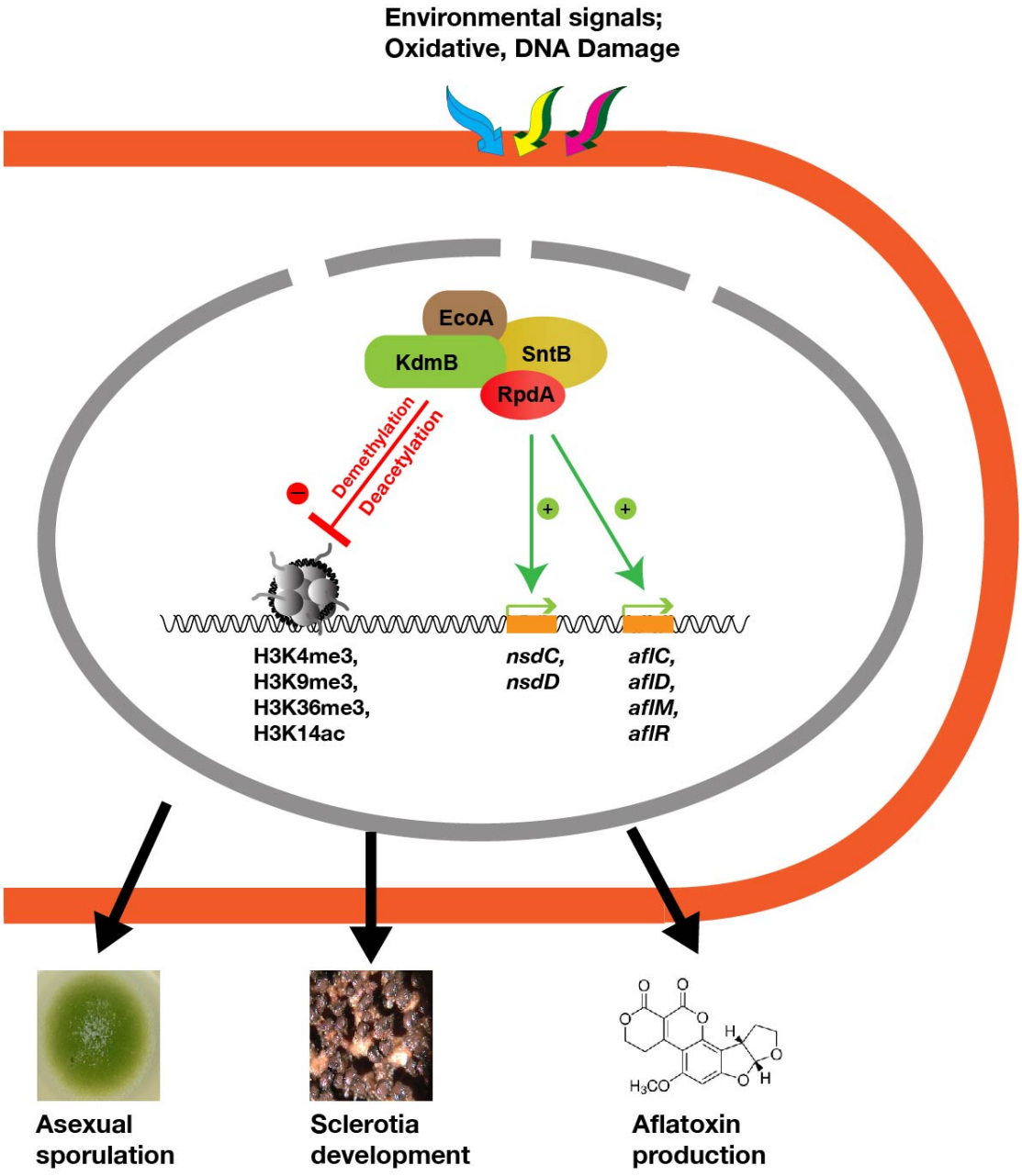

Figure 5.3. The schematic model representing the roles of the tetrameric chromatin modifier KERS complex in fungal development and secondary metabolite production in *A. flavus*. The KERS complex negatively affects H3K4m3, H3K9me3, H3K36me3 methylation levels. RpdA significantly repressed H3K14 acetylation. KdmB and RpdA are positive regulators of sclerotia development and aflatoxin biosynthesis through regulation of *nsdC*, *nsdD* and *afl* pathways respectively.

Reference:

.

ADAMS, T. H., BOYLAN, M. T. & TIMBERLAKE, W. E. 1988. brlA is necessary and sufficient to direct conidiophore development in Aspergillus nidulans. *Cell,* 54**,** 353-62.

ADAMS, T. H., WIESER, J. K. & YU, J. H. 1998. Asexual sporulation in Aspergillus nidulans. *Microbiol Mol Biol Rev,* 62**,** 35-54.

AHN, J. H. & WALTON, J. D. 1997. A fatty acid synthase gene in Cochliobolus carbonum required for production of HC-toxin, cyclo(D-prolyl-L-alanyl-D-alanyl-L-2-amino-9, 10-epoxi-8-oxodecanoyl). *Mol Plant Microbe Interact,* 10**,** 207-14.

ALAZI, E. & RAM, A. F. J. 2018. Modulating Transcriptional Regulation of Plant Biomass Degrading Enzyme Networks for Rational Design of Industrial Fungal Strains. *Front Bioeng Biotechnol,* 6**,** 133.

ALCAZAR-FUOLI, L. 2016. Amino acid biosynthetic pathways as antifungal targets for fungal infections. *Virulence,* 7**,** 376-8.

ALKHAYYAT, F., CHANG KIM, S. & YU, J. H. 2015. Genetic control of asexual development in aspergillus fumigatus. *Adv Appl Microbiol,* 90**,** 93-107.

ALLSHIRE, R. C. & EKWALL, K. 2015. Epigenetic Regulation of Chromatin States in Schizosaccharomyces pombe. *Cold Spring Harb Perspect Biol,* 7**,** a018770.

ALOMER, R. M., DA SILVA, E. M. L., CHEN, J., PIEKARZ, K. M., MCDONALD, K., SANSAM, C. G., SANSAM, C. L. & RANKIN, S. 2017. Esco1 and Esco2 regulate distinct cohesin functions during cell cycle progression. *Proc Natl Acad Sci U S A,* 114**,** 9906-9911.

AMAIKE, S. & KELLER, N. P. 2009. Distinct roles for VeA and LaeA in development and pathogenesis of Aspergillus flavus. *Eukaryot Cell,* 8**,** 1051-60.

AMARE, M. G. & KELLER, N. P. 2014. Molecular mechanisms of Aspergillus flavus secondary metabolism and development. *Fungal Genet Biol,* 66**,** 11-8.

ANDERSEN, M. R., NIELSEN, J. B., KLITGAARD, A., PETERSEN, L. M., ZACHARIASEN, M., HANSEN, T. J., BLICHER, L. H., GOTFREDSEN, C. H., LARSEN, T. O., NIELSEN, K. F. & MORTENSEN, U. H. 2013. Accurate prediction of secondary metabolite gene clusters in filamentous fungi. *Proc Natl Acad Sci U S A,* 110**,** E99-107.

ANDRIANOPOULOS, A. & TIMBERLAKE, W. E. 1994. The Aspergillus nidulans abaA gene encodes a transcriptional activator that acts as a genetic switch to control development. *Mol Cell Biol,* 14**,** 2503-15.

ATOUI, A., BAO, D., KAUR, N., GRAYBURN, W. S. & CALVO, A. M. 2008. Aspergillus nidulans natural product biosynthesis is regulated by mpkB, a putative pheromone response mitogen-activated protein kinase. *Appl Environ Microbiol,* 74**,** 3596-600.

AUSIO, J. 2006. Histone variants--the structure behind the function. *Brief Funct Genomic Proteomic,* 5**,** 228-43.

BABA, A., OHTAKE, F., OKUNO, Y., YOKOTA, K., OKADA, M., IMAI, Y., NI, M., MEYER, C. A., IGARASHI, K., KANNO, J., BROWN, M. & KATO, S. 2011. PKA-dependent regulation of the histone lysine demethylase complex PHF2-ARID5B. *Nat Cell Biol,* 13**,** 668-75.

BAIDYAROY, D., BROSCH, G., AHN, J. H., GRAESSLE, S., WEGENER, S., TONUKARI, N. J., CABALLERO, O., LOIDL, P. & WALTON, J. D. 2001. A gene related to yeast HOS2 histone deacetylase affects extracellular depolymerase expression and virulence in a plant pathogenic fungus. *Plant Cell,* 13**,** 1609-24.

BAKER, L. A., UEBERHEIDE, B. M., DEWELL, S., CHAIT, B. T., ZHENG, D. & ALLIS, C. D. 2013. The yeast Snt2 protein coordinates the transcriptional response to hydrogen peroxide-mediated oxidative stress. *Mol Cell Biol,* 33**,** 3735-48.
BANNISTER, A. J. & KOUZARIDES, T. 2011. Regulation of chromatin by histone modifications. *Cell Res,* 21**,** 381-95.
BAUER, I., VARADARAJAN, D., PIDRONI, A., GROSS, S., VERGEINER, S., FABER, B., HERMANN, M., TRIBUS, M., BROSCH, G. & GRAESSLE, S. 2016. A Class 1 Histone Deacetylase with Potential as an Antifungal Target. *MBio,* 7.
BAYRAM, O., BAYRAM, O. S., VALERIUS, O., JOHNK, B. & BRAUS, G. H. 2012. Identification of protein complexes from filamentous fungi with tandem affinity purification. *Methods Mol Biol,* 944**,** 191-205.
BAYRAM, O., BIESEMANN, C., KRAPPMANN, S., GALLAND, P. & BRAUS, G. H. 2008a. More than a repair enzyme: Aspergillus nidulans photolyase-like CryA is a regulator of sexual development. *Mol Biol Cell,* 19**,** 3254-62.
BAYRAM, O. & BRAUS, G. H. 2012. Coordination of secondary metabolism and development in fungi: the velvet family of regulatory proteins. *FEMS Microbiol Rev,* 36**,** 1-24.
BAYRAM, O., KRAPPMANN, S., NI, M., BOK, J. W., HELMSTAEDT, K., VALERIUS, O., BRAUS-STROMEYER, S., KWON, N. J., KELLER, N. P., YU, J. H. & BRAUS, G. H. 2008b. VelB/VeA/LaeA complex coordinates light signal with fungal development and secondary metabolism. *Science,* 320**,** 1504-6.
BAYRAM, O., SARI, F., BRAUS, G. H. & IRNIGER, S. 2009. The protein kinase ImeB is required for light-mediated inhibition of sexual development and for mycotoxin production in Aspergillus nidulans. *Mol Microbiol,* 71**,** 1278-95.
BENNETT, J. W. & KLICH, M. 2003. Mycotoxins. *Clin Microbiol Rev,* 16**,** 497-516.
BILLS, G. F. & GLOER, J. B. 2016. Biologically Active Secondary Metabolites from the Fungi. *Microbiol Spectr,* 4.
BOK, J. W., CHIANG, Y. M., SZEWCZYK, E., REYES-DOMINGUEZ, Y., DAVIDSON, A. D., SANCHEZ, J. F., LO, H. C., WATANABE, K., STRAUSS, J., OAKLEY, B. R., WANG, C. C. & KELLER, N. P. 2009. Chromatin-level regulation of biosynthetic gene clusters. *Nat Chem Biol,* 5**,** 462-4.
BOK, J. W. & KELLER, N. P. 2004. LaeA, a regulator of secondary metabolism in Aspergillus spp. *Eukaryot Cell,* 3**,** 527-35.
BOK, J. W., NOORDERMEER, D., KALE, S. P. & KELLER, N. P. 2006. Secondary metabolic gene cluster silencing in Aspergillus nidulans. *Mol Microbiol,* 61**,** 1636-45.
BOYER, L. A., LATEK, R. R. & PETERSON, C. L. 2004. The SANT domain: a unique histone-tail-binding module? *Nat Rev Mol Cell Biol,* 5**,** 158-63.
BRAKHAGE, A. A. 2013. Regulation of fungal secondary metabolism. *Nat Rev Microbiol,* 11**,** 21-32.
BROOKS, F. T. 1949. Fungi and their economic importance. *Adv Sci,* 5**,** 329-34.
BURGESS, R. J. & ZHANG, Z. 2013. Histone chaperones in nucleosome assembly and human disease. *Nat Struct Mol Biol,* 20**,** 14-22.
CALVO, A. M., BOK, J., BROOKS, W. & KELLER, N. P. 2004. veA is required for toxin and sclerotial production in Aspergillus parasiticus. *Appl Environ Microbiol,* 70**,** 4733-9.
CALVO, A. M., WILSON, R. A., BOK, J. W. & KELLER, N. P. 2002. Relationship between secondary metabolism and fungal development. *Microbiol Mol Biol Rev,* 66**,** 447-59, table of contents.
CARY, J. W., GR, O. B., NIELSEN, D. M., NIERMAN, W., HARRIS-COWARD, P., YU, J., BHATNAGAR, D., CLEVELAND, T. E., PAYNE, G. A. & CALVO, A. M. 2007. Elucidation of veA-dependent genes associated with aflatoxin and

sclerotial production in Aspergillus flavus by functional genomics. *Appl Microbiol Biotechnol,* 76**,** 1107-18.

CARY, J. W., HARRIS-COWARD, P., SCHARFENSTEIN, L., MACK, B. M., CHANG, P. K., WEI, Q., LEBAR, M., CARTER-WIENTJES, C., MAJUMDAR, R., MITRA, C., BANERJEE, S. & CHANDA, A. 2017. The Aspergillus flavus Homeobox Gene, hbx1, is Required for Development and Aflatoxin Production. *Toxins (Basel),* 9.

CARY, J. W., UKA, V., HAN, Z., BUYST, D., HARRIS-COWARD, P. Y., EHRLICH, K. C., WEI, Q., BHATNAGAR, D., DOWD, P. F., MARTENS, S. L., CALVO, A. M., MARTINS, J. C., VANHAECKE, L., COENYE, T., DE SAEGER, S. & DI MAVUNGU, J. D. 2015. An Aspergillus flavus secondary metabolic gene cluster containing a hybrid PKS-NRPS is necessary for synthesis of the 2-pyridones, leporins. *Fungal Genet Biol,* 81**,** 88-97.

CATCHPOLE, S., SPENCER-DENE, B., HALL, D., SANTANGELO, S., ROSEWELL, I., GUENATRI, M., BEATSON, R., SCIBETTA, A. G., BURCHELL, J. M. & TAYLOR-PAPADIMITRIOU, J. 2011. PLU-1/JARID1B/KDM5B is required for embryonic survival and contributes to cell proliferation in the mammary gland and in ER+ breast cancer cells. *Int J Oncol,* 38**,** 1267-77.

CHANDLER, S. & WOLFFE, A. P. 1999. Analysis of linker histone binding to mono- and dinucleosomes. *Methods Mol Biol,* 119**,** 103-12.

CHANG, P. K., SCHARFENSTEIN, L. L., LI, P. & EHRLICH, K. C. 2013. Aspergillus flavus VelB acts distinctly from VeA in conidiation and may coordinate with FluG to modulate sclerotial production. *Fungal Genet Biol,* 58-59**,** 71-9.

CHANG, P. K., SCHARFENSTEIN, L. L., LI, R. W., ARROYO-MANZANARES, N., DE SAEGER, S. & DIANA DI MAVUNGU, J. 2017. Aspergillus flavus aswA, a gene homolog of Aspergillus nidulans oefC, regulates sclerotial development and biosynthesis of sclerotium-associated secondary metabolites. *Fungal Genet Biol,* 104**,** 29-37.

CHANG, P. K., SCHARFENSTEIN, L. L., MACK, B. & EHRLICH, K. C. 2012. Deletion of the Aspergillus flavus orthologue of A. nidulans fluG reduces conidiation and promotes production of sclerotia but does not abolish aflatoxin biosynthesis. *Appl Environ Microbiol,* 78**,** 7557-63.

CHAVEZ, R., FIERRO, F., GARCIA-RICO, R. O. & VACA, I. 2015. Filamentous fungi from extreme environments as a promising source of novel bioactive secondary metabolites. *Front Microbiol,* 6**,** 903.

CHEN, T. & DENT, S. Y. 2014. Chromatin modifiers and remodellers: regulators of cellular differentiation. *Nat Rev Genet,* 15**,** 93-106.

CHEN, Y., LIU, X., LI, Y., QUAN, C., ZHENG, L. & HUANG, K. 2018. Lung Cancer Therapy Targeting Histone Methylation: Opportunities and Challenges. *Comput Struct Biotechnol J,* 16**,** 211-223.

CHEN, Z., CAO, H., LU, Y., REN, Q. & SUN, L. 2017. DNA polymerase 5 acetylation by Eso1 is essential for Schizosaccharomyces pombe viability. *Int J Mol Med,* 40**,** 1907-1913.

CHIOU, C. H., MILLER, M., WILSON, D. L., TRAIL, F. & LINZ, J. E. 2002. Chromosomal location plays a role in regulation of aflatoxin gene expression in Aspergillus parasiticus. *Appl Environ Microbiol,* 68**,** 306-15.

CHO, Y. W., HONG, T., HONG, S., GUO, H., YU, H., KIM, D., GUSZCZYNSKI, T., DRESSLER, G. R., COPELAND, T. D., KALKUM, M. & GE, K. 2007. PTIP associates with MLL3- and MLL4-containing histone H3 lysine 4 methyltransferase complex. *J Biol Chem,* 282**,** 20395-406.

CHOI, H. K., KIM, B. J., SEO, J. H., KANG, J. S., CHO, H. & KIM, S. T. 2010. Cohesion establishment factor, Eco1 represses transcription via association with histone demethylase, LSD1. *Biochem Biophys Res Commun,* 394**,** 1063-8.
CHOI, J. & KIM, S. H. 2017. A genome Tree of Life for the Fungi kingdom. *Proc Natl Acad Sci U S A,* 114**,** 9391-9396.
CHRISTENSEN, J., AGGER, K., CLOOS, P. A., PASINI, D., ROSE, S., SENNELS, L., RAPPSILBER, J., HANSEN, K. H., SALCINI, A. E. & HELIN, K. 2007. RBP2 belongs to a family of demethylases, specific for tri-and dimethylated lysine 4 on histone 3. *Cell,* 128**,** 1063-76.
CHRISTENSEN, S., BORREGO, E., SHIM, W. B., ISAKEIT, T. & KOLOMIETS, M. 2012. Quantification of fungal colonization, sporogenesis, and production of mycotoxins using kernel bioassays. *J Vis Exp*.
CLAYTON, A. L., ROSE, S., BARRATT, M. J. & MAHADEVAN, L. C. 2000. Phosphoacetylation of histone H3 on c-fos- and c-jun-associated nucleosomes upon gene activation. *EMBO J,* 19**,** 3714-26.
CLOOS, P. A., CHRISTENSEN, J., AGGER, K., MAIOLICA, A., RAPPSILBER, J., ANTAL, T., HANSEN, K. H. & HELIN, K. 2006. The putative oncogene GASC1 demethylates tri- and dimethylated lysine 9 on histone H3. *Nature,* 442**,** 307-11.
CLUTTERBUCK, A. J. 1969. A mutational analysis of conidial development in Aspergillus nidulans. *Genetics,* 63**,** 317-27.
CONNOLLY, L. R., SMITH, K. M. & FREITAG, M. 2013. The Fusarium graminearum histone H3 K27 methyltransferase KMT6 regulates development and expression of secondary metabolite gene clusters. *PLoS Genet,* 9**,** e1003916.
DANG, C. K., CHAUVET, E. & GESSNER, M. O. 2005. Magnitude and variability of process rates in fungal diversity-litter decomposition relationships. *Ecol Lett,* 8**,** 1129-37.
DECKERT, J. & STRUHL, K. 2001. Histone acetylation at promoters is differentially affected by specific activators and repressors. *Mol Cell Biol,* 21**,** 2726-35.
DEHENNAUT, V., LEPRINCE, D. & LEFEBVRE, T. 2014. O-GlcNAcylation, an Epigenetic Mark. Focus on the Histone Code, TET Family Proteins, and Polycomb Group Proteins. *Front Endocrinol (Lausanne),* 5**,** 155.
DENISOV, Y., FREEMAN, S. & YARDEN, O. 2011. Inactivation of Snt2, a BAH/PHD-containing transcription factor, impairs pathogenicity and increases autophagosome abundance in Fusarium oxysporum. *Mol Plant Pathol,* 12**,** 449-61.
DIMITROVA, E., TURBERFIELD, A. H. & KLOSE, R. J. 2015. Histone demethylases in chromatin biology and beyond. *EMBO Rep,* 16**,** 1620-39.
DYER, P. S. & O'GORMAN, C. M. 2012. Sexual development and cryptic sexuality in fungi: insights from Aspergillus species. *FEMS Microbiol Rev,* 36**,** 165-92.
DYNESEN, J. & NIELSEN, J. 2003. Branching is coordinated with mitosis in growing hyphae of Aspergillus nidulans. *Fungal Genet Biol,* 40**,** 15-24.
EBERHARTER, A., JOHN, S., GRANT, P. A., UTLEY, R. T. & WORKMAN, J. L. 1998. Identification and analysis of yeast nucleosomal histone acetyltransferase complexes. *Methods,* 15**,** 315-21.
ECKERT, S. E., HOFFMANN, B., WANKE, C. & BRAUS, G. H. 1999. Sexual development of Aspergillus nidulans in tryptophan auxotrophic strains. *Arch Microbiol,* 172**,** 157-66.
FAUSTINELLI, P. C., WANG, X. M., PALENCIA, E. R. & ARIAS, R. S. 2016. Genome Sequences of Eight Aspergillus flavus spp. and One A. parasiticus sp., Isolated from Peanut Seeds in Georgia. *Genome Announc,* 4.
FENG, Q., WANG, H., NG, H. H., ERDJUMENT-BROMAGE, H., TEMPST, P., STRUHL, K. & ZHANG, Y. 2002. Methylation of H3-lysine 79 is mediated by a new family of HMTases without a SET domain. *Curr Biol,* 12**,** 1052-8.

FERNANDES, M., KELLER, N. P. & ADAMS, T. H. 1998. Sequence-specific binding by Aspergillus nidulans AflR, a C6 zinc cluster protein regulating mycotoxin biosynthesis. *Mol Microbiol,* 28**,** 1355-65.
FINCH, J. T., NOLL, M. & KORNBERG, R. D. 1975. Electron microscopy of defined lengths of chromatin. *Proc Natl Acad Sci U S A,* 72**,** 3320-2.
FOLEY, K., FAZIO, G., JENSEN, A. B. & HUGHES, W. O. 2014. The distribution of Aspergillus spp. opportunistic parasites in hives and their pathogenicity to honey bees. *Vet Microbiol,* 169**,** 203-10.
FORNERIS, F., BINDA, C., DALL'AGLIO, A., FRAAIJE, M. W., BATTAGLIOLI, E. & MATTEVI, A. 2006. A highly specific mechanism of histone H3-K4 recognition by histone demethylase LSD1. *J Biol Chem,* 281**,** 35289-95.
FORTUNY, A. & POLO, S. E. 2018. The response to DNA damage in heterochromatin domains. *Chromosoma,* 127**,** 291-300.
FRANZKE, B., NEUBAUER, O. & WAGNER, K. H. 2015. Super DNAging-New insights into DNA integrity, genome stability and telomeres in the oldest old. *Mutat Res Rev Mutat Res,* 766**,** 48-57.
GACEK, A. & STRAUSS, J. 2012. The chromatin code of fungal secondary metabolite gene clusters. *Appl Microbiol Biotechnol,* 95**,** 1389-404.
GACEK-MATTHEWS, A., BERGER, H., SASAKI, T., WITTSTEIN, K., GRUBER, C., LEWIS, Z. A. & STRAUSS, J. 2016. KdmB, a Jumonji Histone H3 Demethylase, Regulates Genome-Wide H3K4 Trimethylation and Is Required for Normal Induction of Secondary Metabolism in Aspergillus nidulans. *PLoS Genet,* 12**,** e1006222.
GACEK-MATTHEWS, A., NOBLE, L. M., GRUBER, C., BERGER, H., SULYOK, M., MARCOS, A. T., STRAUSS, J. & ANDRIANOPOULOS, A. 2015. KdmA, a histone H3 demethylase with bipartite function, differentially regulates primary and secondary metabolism in Aspergillus nidulans. *Mol Microbiol,* 96**,** 839-60.
GAJAN, A., BARNES, V. L., LIU, M., SAHA, N. & PILE, L. A. 2016. The histone demethylase dKDM5/LID interacts with the SIN3 histone deacetylase complex and shares functional similarities with SIN3. *Epigenetics Chromatin,* 9**,** 4.
GALLAGHER, R. T. & WILSON, B. J. 1979. Aflatrem, the tremorgenic mycotoxin from Aspergillus flavus. *Mycopathologia,* 66**,** 183-5.
GERKE, J. & BRAUS, G. H. 2014. Manipulation of fungal development as source of novel secondary metabolites for biotechnology. *Appl Microbiol Biotechnol,* 98**,** 8443-55.
GILDEA, J. J., LOPEZ, R. & SHEARN, A. 2000. A screen for new trithorax group genes identified little imaginal discs, the Drosophila melanogaster homologue of human retinoblastoma binding protein 2. *Genetics,* 156**,** 645-63.
GILLETTE, T. G. & HILL, J. A. 2015. Readers, writers, and erasers: chromatin as the whiteboard of heart disease. *Circ Res,* 116**,** 1245-53.
GOLDMAN, G. H. & KAFER, E. 2004. Aspergillus nidulans as a model system to characterize the DNA damage response in eukaryotes. *Fungal Genet Biol,* 41**,** 428-42.
GOTTESFELD, J. M. & CAREY, M. F. 2018. Introduction to the Thematic Minireview Series: Chromatin and transcription. *J Biol Chem,* 293**,** 13775-13777.
GRAESSLE, S., DANGL, M., HAAS, H., MAIR, K., TROJER, P., BRANDTNER, E. M., WALTON, J. D., LOIDL, P. & BROSCH, G. 2000. Characterization of two putative histone deacetylase genes from Aspergillus nidulans. *Biochim Biophys Acta,* 1492**,** 120-6.
GRUNSTEIN, M. & GASSER, S. M. 2013. Epigenetics in Saccharomyces cerevisiae. *Cold Spring Harb Perspect Biol,* 5.

GU, W., SZAUTER, P. & LUCCHESI, J. C. 1998. Targeting of MOF, a putative histone acetyl transferase, to the X chromosome of Drosophila melanogaster. *Dev Genet,* 22**,** 56-64.

GUACCI, V., STRICKLIN, J., BLOOM, M. S., GUO, X., BHATTER, M. & KOSHLAND, D. 2015. A novel mechanism for the establishment of sister chromatid cohesion by the ECO1 acetyltransferase. *Mol Biol Cell,* 26**,** 117-33.

HAN, X., GUI, B., XIONG, C., ZHAO, L., LIANG, J., SUN, L., YANG, X., YU, W., SI, W., YAN, R., YI, X., ZHANG, D., LI, W., LI, L., YANG, J., WANG, Y., SUN, Y. E., ZHANG, D., MENG, A. & SHANG, Y. 2014. Destabilizing LSD1 by Jade-2 promotes neurogenesis: an antibraking system in neural development. *Mol Cell,* 55**,** 482-94.

HE, M., XU, Y., CHEN, J., LUO, Y., LV, Y., SU, J., KERSHAW, M. J., LI, W., WANG, J., YIN, J., ZHU, X., LIU, X., CHERN, M., MA, B., WANG, J., QIN, P., CHEN, W., WANG, Y., WANG, W., REN, Z., WU, X., LI, P., LI, S., PENG, Y., LIN, F., TALBOT, N. J. & CHEN, X. 2018. MoSnt2-dependent deacetylation of histone H3 mediates MoTor-dependent autophagy and plant infection by the rice blast fungus Magnaporthe oryzae. *Autophagy,* 14**,** 1543-1561.

HEDAYATI, M. T., PASQUALOTTO, A. C., WARN, P. A., BOWYER, P. & DENNING, D. W. 2007. Aspergillus flavus: human pathogen, allergen and mycotoxin producer. *Microbiology,* 153**,** 1677-92.

HEITMAN, J. 2011. Microbial Pathogens in the Fungal Kingdom. *Fungal Biol Rev,* 25**,** 48-60.

HELMSCHROTT, C., SASSE, A., SAMANTARAY, S., KRAPPMANN, S. & WAGENER, J. 2013. Upgrading fungal gene expression on demand: improved systems for doxycycline-dependent silencing in Aspergillus fumigatus. *Appl Environ Microbiol,* 79**,** 1751-4.

HICKS, J. K., YU, J. H., KELLER, N. P. & ADAMS, T. H. 1997. Aspergillus sporulation and mycotoxin production both require inactivation of the FadA G alpha protein-dependent signaling pathway. *EMBO J,* 16**,** 4916-23.

HORN, B. W., GELL, R. M., SINGH, R., SORENSEN, R. B. & CARBONE, I. 2016. Sexual Reproduction in Aspergillus flavus Sclerotia: Acquisition of Novel Alleles from Soil Populations and Uniparental Mitochondrial Inheritance. *PLoS One,* 11**,** e0146169.

HORN, B. W., MOORE, G. G. & CARBONE, I. 2009. Sexual reproduction in Aspergillus flavus. *Mycologia,* 101**,** 423-9.

HORN, B. W., SORENSEN, R. B., LAMB, M. C., SOBOLEV, V. S., OLARTE, R. A., WORTHINGTON, C. J. & CARBONE, I. 2014. Sexual reproduction in Aspergillus flavus sclerotia naturally produced in corn. *Phytopathology,* 104**,** 75-85.

HSU, I. C., METCALF, R. A., SUN, T., WELSH, J. A., WANG, N. J. & HARRIS, C. C. 1991. Mutational hotspot in the p53 gene in human hepatocellular carcinomas. *Nature,* 350**,** 427-8.

HUANG, F., CHANDRASEKHARAN, M. B., CHEN, Y. C., BHASKARA, S., HIEBERT, S. W. & SUN, Z. W. 2010. The JmjN domain of Jhd2 is important for its protein stability, and the plant homeodomain (PHD) finger mediates its chromatin association independent of H3K4 methylation. *J Biol Chem,* 285**,** 24548-61.

HUANG, F., RAMAKRISHNAN, S., POKHREL, S., PFLUEGER, C., PARNELL, T. J., KASTEN, M. M., CURRIE, S. L., BHACHECH, N., HORIKOSHI, M., GRAVES, B. J., CAIRNS, B. R., BHASKARA, S. & CHANDRASEKHARAN, M. B. 2015. Interaction of the Jhd2 Histone H3 Lys-4 Demethylase with Chromatin Is

Controlled by Histone H2A Surfaces and Restricted by H2B Ubiquitination. *J Biol Chem,* 290**,** 28760-77.
HUANG, J. & BERGER, S. L. 2008. The emerging field of dynamic lysine methylation of non-histone proteins. *Curr Opin Genet Dev,* 18**,** 152-8.
HUANG, J., SENGUPTA, R., ESPEJO, A. B., LEE, M. G., DORSEY, J. A., RICHTER, M., OPRAVIL, S., SHIEKHATTAR, R., BEDFORD, M. T., JENUWEIN, T. & BERGER, S. L. 2007. p53 is regulated by the lysine demethylase LSD1. *Nature,* 449**,** 105-8.
ISSAEVA, I., ZONIS, Y., ROZOVSKAIA, T., ORLOVSKY, K., CROCE, C. M., NAKAMURA, T., MAZO, A., EISENBACH, L. & CANAANI, E. 2007. Knockdown of ALR (MLL2) reveals ALR target genes and leads to alterations in cell adhesion and growth. *Mol Cell Biol,* 27**,** 1889-903.
JOHN, S., HOWE, L., TAFROV, S. T., GRANT, P. A., STERNGLANZ, R. & WORKMAN, J. L. 2000. The something about silencing protein, Sas3, is the catalytic subunit of NuA3, a yTAF(II)30-containing HAT complex that interacts with the Spt16 subunit of the yeast CP (Cdc68/Pob3)-FACT complex. *Genes Dev,* 14**,** 1196-208.
JONES, R. S. & GELBART, W. M. 1993. The Drosophila Polycomb-group gene Enhancer of zeste contains a region with sequence similarity to trithorax. *Mol Cell Biol,* 13**,** 6357-66.
JUNG, B., KIM, S. & LEE, J. 2014. Microcyle conidiation in filamentous fungi. *Mycobiology,* 42**,** 1-5.
KATO, N., BROOKS, W. & CALVO, A. M. 2003. The expression of sterigmatocystin and penicillin genes in Aspergillus nidulans is controlled by veA, a gene required for sexual development. *Eukaryot Cell,* 2**,** 1178-86.
KIDDER, B. L., HU, G. & ZHAO, K. 2014. KDM5B focuses H3K4 methylation near promoters and enhancers during embryonic stem cell self-renewal and differentiation. *Genome Biol,* 15**,** R32.
KIM, S. A., CHATTERJEE, N., JENNINGS, M. J., BARTHOLOMEW, B. & TAN, S. 2015. Extranucleosomal DNA enhances the activity of the LSD1/CoREST histone demethylase complex. *Nucleic Acids Res,* 43**,** 4868-80.
KIM, S. T., XU, B. & KASTAN, M. B. 2002. Involvement of the cohesin protein, Smc1, in Atm-dependent and independent responses to DNA damage. *Genes Dev,* 16**,** 560-70.
KIM, Y. J., YU, Y. M. & MAENG, P. J. 2017. Differential Control of Asexual Development and Sterigmatocystin Biosynthesis by a Novel Regulator in Aspergillus nidulans. *Sci Rep,* 7**,** 46340.
KLEIN, B. J., PIAO, L., XI, Y., RINCON-ARANO, H., ROTHBART, S. B., PENG, D., WEN, H., LARSON, C., ZHANG, X., ZHENG, X., CORTAZAR, M. A., PENA, P. V., MANGAN, A., BENTLEY, D. L., STRAHL, B. D., GROUDINE, M., LI, W., SHI, X. & KUTATELADZE, T. G. 2014. The histone-H3K4-specific demethylase KDM5B binds to its substrate and product through distinct PHD fingers. *Cell Rep,* 6**,** 325-35.
KLOSE, R. J., KALLIN, E. M. & ZHANG, Y. 2006. JmjC-domain-containing proteins and histone demethylation. *Nat Rev Genet,* 7**,** 715-27.
KOBAYASHI, T., ABE, K., ASAI, K., GOMI, K., JUVVADI, P. R., KATO, M., KITAMOTO, K., TAKEUCHI, M. & MACHIDA, M. 2007. Genomics of Aspergillus oryzae. *Biosci Biotechnol Biochem,* 71**,** 646-70.
KONTAKI, H. & TALIANIDIS, I. 2010. Lysine methylation regulates E2F1-induced cell death. *Mol Cell,* 39**,** 152-60.

KUMAR, P., MAHATO, D. K., KAMLE, M., MOHANTA, T. K. & KANG, S. G. 2016. Aflatoxins: A Global Concern for Food Safety, Human Health and Their Management. *Front Microbiol,* 7**,** 2170.

KWON, D. W. & AHN, S. H. 2011. Role of yeast JmjC-domain containing histone demethylases in actively transcribed regions. *Biochem Biophys Res Commun,* 410**,** 614-9.

KWON, S. H. & WORKMAN, J. L. 2011. The changing faces of HP1: From heterochromatin formation and gene silencing to euchromatic gene expression: HP1 acts as a positive regulator of transcription. *Bioessays,* 33**,** 280-9.

LAURENT, B., RUITU, L., MURN, J., HEMPEL, K., FERRAO, R., XIANG, Y., LIU, S., GARCIA, B. A., WU, H., WU, F., STEEN, H. & SHI, Y. 2015. A specific LSD1/KDM1A isoform regulates neuronal differentiation through H3K9 demethylation. *Mol Cell,* 57**,** 957-970.

LEE, B. N. & ADAMS, T. H. 1994. Overexpression of flbA, an early regulator of Aspergillus asexual sporulation, leads to activation of brlA and premature initiation of development. *Mol Microbiol,* 14**,** 323-34.

LEE, B. N. & ADAMS, T. H. 1996. FluG and flbA function interdependently to initiate conidiophore development in Aspergillus nidulans through brlA beta activation. *EMBO J,* 15**,** 299-309.

LEE, K. Y., CHEN, Z., JIANG, R. & MENEGHINI, M. D. 2018a. H3K4 Methylation Dependent and Independent Chromatin Regulation by JHD2 and SET1 in Budding Yeast. *G3 (Bethesda),* 8**,** 1829-1839.

LEE, K. Y., RANGER, M. & MENEGHINI, M. D. 2018b. Combinatorial Genetic Control of Rpd3S Through Histone H3K4 and H3K36 Methylation in Budding Yeast. *G3 (Bethesda)*.

LI, B., GOGOL, M., CAREY, M., LEE, D., SEIDEL, C. & WORKMAN, J. L. 2007. Combined action of PHD and chromo domains directs the Rpd3S HDAC to transcribed chromatin. *Science,* 316**,** 1050-4.

LI, L., GREER, C., EISENMAN, R. N. & SECOMBE, J. 2010. Essential functions of the histone demethylase lid. *PLoS Genet,* 6**,** e1001221.

LIANG, S. H., WU, T. S., LEE, R., CHU, F. S. & LINZ, J. E. 1997. Analysis of mechanisms regulating expression of the ver-1 gene, involved in aflatoxin biosynthesis. *Appl Environ Microbiol,* 63**,** 1058-65.

LIBERTINI, L. J., AUSIO, J., VAN HOLDE, K. E. & SMALL, E. W. 1988. Histone hyperacetylation. Its effects on nucleosome core particle transitions. *Biophys J,* 53**,** 477-87.

LINDSAY, S. 2007. Chromatin control of gene expression: the simplest model. *Biophys J,* 92**,** 1113.

LITT, M. D., SIMPSON, M., GASZNER, M., ALLIS, C. D. & FELSENFELD, G. 2001. Correlation between histone lysine methylation and developmental changes at the chicken beta-globin locus. *Science,* 293**,** 2453-5.

LIU, X., GREER, C. & SECOMBE, J. 2014. KDM5 interacts with Foxo to modulate cellular levels of oxidative stress. *PLoS Genet,* 10**,** e1004676.

LU, S., LEE, K. K., HARRIS, B., XIONG, B., BOSE, T., SARAF, A., HATTEM, G., FLORENS, L., SEIDEL, C. & GERTON, J. L. 2014. The cohesin acetyltransferase Eco1 coordinates rDNA replication and transcription. *EMBO Rep,* 15**,** 609-17.

LU, Y., DAI, X., ZHANG, M., MIAO, Y., ZHOU, C., CUI, Z. & XIONG, B. 2017. Cohesin acetyltransferase Esco2 regulates SAC and kinetochore functions via maintaining H4K16 acetylation during mouse oocyte meiosis. *Nucleic Acids Res,* 45**,** 9388-9397.

LUGER, K., MADER, A. W., RICHMOND, R. K., SARGENT, D. F. & RICHMOND, T. J. 1997. Crystal structure of the nucleosome core particle at 2.8 A resolution. *Nature,* 389**,** 251-60.
LYONS, N. A., FONSLOW, B. R., DIEDRICH, J. K., YATES, J. R., 3RD & MORGAN, D. O. 2013. Sequential primed kinases create a damage-responsive phosphodegron on Eco1. *Nat Struct Mol Biol,* 20**,** 194-201.
LYONS, N. A. & MORGAN, D. O. 2011. Cdk1-dependent destruction of Eco1 prevents cohesion establishment after S phase. *Mol Cell,* 42**,** 378-89.
MA, D. & LI, R. 2013. Current understanding of HOG-MAPK pathway in Aspergillus fumigatus. *Mycopathologia,* 175**,** 13-23.
MAEDA, K., IZAWA, M., NAKAJIMA, Y., JIN, Q., HIROSE, T., NAKAMURA, T., KOSHINO, H., KANAMARU, K., OHSATO, S., KAMAKURA, T., KOBAYASHI, T., YOSHIDA, M. & KIMURA, M. 2017. Increased metabolite production by deletion of an HDA1-type histone deacetylase in the phytopathogenic fungi, Magnaporthe oryzae (Pyricularia oryzae) and Fusarium asiaticum. *Lett Appl Microbiol,* 65**,** 446-452.
MANFIOLLI, A. O., DE CASTRO, P. A., DOS REIS, T. F., DOLAN, S., DOYLE, S., JONES, G., RIANO PACHON, D. M., ULAS, M., NOBLE, L. M., MATTERN, D. J., BRAKHAGE, A. A., VALIANTE, V., SILVA-ROCHA, R., BAYRAM, O. & GOLDMAN, G. H. 2017. Aspergillus fumigatus protein phosphatase PpzA is involved in iron assimilation, secondary metabolite production, and virulence. *Cell Microbiol,* 19.
MCMAHON, S. B., WOOD, M. A. & COLE, M. D. 2000. The essential cofactor TRRAP recruits the histone acetyltransferase hGCN5 to c-Myc. *Mol Cell Biol,* 20**,** 556-62.
MEIER, K. & BREHM, A. 2014. Chromatin regulation: how complex does it get? *Epigenetics,* 9**,** 1485-95.
MENG, L., MOHAN, R., KWOK, B. H., ELOFSSON, M., SIN, N. & CREWS, C. M. 1999. Epoxomicin, a potent and selective proteasome inhibitor, exhibits in vivo antiinflammatory activity. *Proc Natl Acad Sci U S A,* 96**,** 10403-8.
MESSNER, S. & HOTTIGER, M. O. 2011. Histone ADP-ribosylation in DNA repair, replication and transcription. *Trends Cell Biol,* 21**,** 534-42.
METZGER, E., WISSMANN, M., YIN, N., MULLER, J. M., SCHNEIDER, R., PETERS, A. H., GUNTHER, T., BUETTNER, R. & SCHULE, R. 2005. LSD1 demethylates repressive histone marks to promote androgen-receptor-dependent transcription. *Nature,* 437**,** 436-9.
MEYER, E., CARSS, K. J., RANKIN, J., NICHOLS, J. M., GROZEVA, D., JOSEPH, A. P., MENCACCI, N. E., PAPANDREOU, A., NG, J., BARRAL, S., NGOH, A., BEN-PAZI, H., WILLEMSEN, M. A., ARKADIR, D., BARNICOAT, A., BERGMAN, H., BHATE, S., BOYS, A., DARIN, N., FOULDS, N., GUTOWSKI, N., HILLS, A., HOULDEN, H., HURST, J. A., ISRAEL, Z., KAMINSKA, M., LIMOUSIN, P., LUMSDEN, D., MCKEE, S., MISRA, S., MOHAMMED, S. S., NAKOU, V., NICOLAI, J., NILSSON, M., PALL, H., PEALL, K. J., PETERS, G. B., PRABHAKAR, P., REUTER, M. S., RUMP, P., SEGEL, R., SINNEMA, M., SMITH, M., TURNPENNY, P., WHITE, S. M., WIECZOREK, D., WIETHOFF, S., WILSON, B. T., WINTER, G., WRAGG, C., POPE, S., HEALES, S. J., MORROGH, D., CONSORTIUM, U. K., DECIPHERING DEVELOPMENTAL DISORDERS, S., CONSORTIUM, N. B. R. D., PITTMAN, A., CARR, L. J., PEREZ-DUENAS, B., LIN, J. P., REIS, A., GAHL, W. A., TORO, C., BHATIA, K. P., WOOD, N. W., KAMSTEEG, E. J., CHONG, W. K., GISSEN, P., TOPF, M., DALE, R. C., CHUBB, J. R., RAYMOND, F. L. & KURIAN, M. A. 2017. Mutations in the histone methyltransferase gene KMT2B cause complex early-onset dystonia. *Nat Genet,* 49**,** 223-237.

MEYER, V. 2008. Genetic engineering of filamentous fungi--progress, obstacles and future trends. *Biotechnol Adv,* 26**,** 177-85.
MINAMINO, M., TEI, S., NEGISHI, L., KANEMAKI, M. T., YOSHIMURA, A., SUTANI, T., BANDO, M. & SHIRAHIGE, K. 2018. Temporal Regulation of ESCO2 Degradation by the MCM Complex, the CUL4-DDB1-VPRBP Complex, and the Anaphase-Promoting Complex. *Curr Biol*.
MISHIMA, Y., WATANABE, M., KAWAKAMI, T., JAYASINGHE, C. D., OTANI, J., KIKUGAWA, Y., SHIRAKAWA, M., KIMURA, H., NISHIMURA, O., AIMOTO, S., TAJIMA, S. & SUETAKE, I. 2013. Hinge and chromoshadow of HP1alpha participate in recognition of K9 methylated histone H3 in nucleosomes. *J Mol Biol,* 425**,** 54-70.
MITCHELL, N. J., BOWERS, E., HURBURGH, C. & WU, F. 2016. Potential economic losses to the US corn industry from aflatoxin contamination. *Food Addit Contam Part A Chem Anal Control Expo Risk Assess,* 33**,** 540-50.
MOCHIZUKI, K., HARIYA, N., HONMA, K. & GODA, T. 2017. Relationship between epigenetic regulation, dietary habits, and the developmental origins of health and disease theory. *Congenit Anom (Kyoto),* 57**,** 184-190.
MONTGOMERY, R. L., DAVIS, C. A., POTTHOFF, M. J., HABERLAND, M., FIELITZ, J., QI, X., HILL, J. A., RICHARDSON, J. A. & OLSON, E. N. 2007. Histone deacetylases 1 and 2 redundantly regulate cardiac morphogenesis, growth, and contractility. *Genes Dev,* 21**,** 1790-802.
MURRAY, K. 1964. The Occurrence of Epsilon-N-Methyl Lysine in Histones. *Biochemistry,* 3**,** 10-5.
NATHAN, D., INGVARSDOTTIR, K., STERNER, D. E., BYLEBYL, G. R., DOKMANOVIC, M., DORSEY, J. A., WHELAN, K. A., KRSMANOVIC, M., LANE, W. S., MELUH, P. B., JOHNSON, E. S. & BERGER, S. L. 2006. Histone sumoylation is a negative regulator in Saccharomyces cerevisiae and shows dynamic interplay with positive-acting histone modifications. *Genes Dev,* 20**,** 966-76.
NEBBIOSO, A., TAMBARO, F. P., DELL'AVERSANA, C. & ALTUCCI, L. 2018. Cancer epigenetics: Moving forward. *PLoS Genet,* 14**,** e1007362.
NISHIBUCHI, G., SHIBATA, Y., HAYAKAWA, T., HAYAKAWA, N., OHTANI, Y., SINMYOZU, K., TAGAMI, H. & NAKAYAMA, J. 2014. Physical and functional interactions between the histone H3K4 demethylase KDM5A and the nucleosome remodeling and deacetylase (NuRD) complex. *J Biol Chem,* 289**,** 28956-70.
NISHIYAMA, T., LADURNER, R., SCHMITZ, J., KREIDL, E., SCHLEIFFER, A., BHASKARA, V., BANDO, M., SHIRAHIGE, K., HYMAN, A. A., MECHTLER, K. & PETERS, J. M. 2010. Sororin mediates sister chromatid cohesion by antagonizing Wapl. *Cell,* 143**,** 737-49.
NOBILE, C. J. & JOHNSON, A. D. 2015. Candida albicans Biofilms and Human Disease. *Annu Rev Microbiol,* 69**,** 71-92.
ONN, I., HEIDINGER-PAULI, J. M., GUACCI, V., UNAL, E. & KOSHLAND, D. E. 2008. Sister chromatid cohesion: a simple concept with a complex reality. *Annu Rev Cell Dev Biol,* 24**,** 105-29.
OSBOURN, A. 2010. Secondary metabolic gene clusters: evolutionary toolkits for chemical innovation. *Trends Genet,* 26**,** 449-57.
OUTCHKOUROV, N. S., MUINO, J. M., KAUFMANN, K., VAN IJCKEN, W. F., GROOT KOERKAMP, M. J., VAN LEENEN, D., DE GRAAF, P., HOLSTEGE, F. C., GROSVELD, F. G. & TIMMERS, H. T. 2013. Balancing of histone H3K4 methylation states by the Kdm5c/SMCX histone demethylase modulates promoter and enhancer function. *Cell Rep,* 3**,** 1071-9.

OUYANG, J., SHI, Y., VALIN, A., XUAN, Y. & GILL, G. 2009. Direct binding of CoREST1 to SUMO-2/3 contributes to gene-specific repression by the LSD1/CoREST1/HDAC complex. *Mol Cell,* 34**,** 145-54.

PALMER, J. M., BOK, J. W., LEE, S., DAGENAIS, T. R. T., ANDES, D. R., KONTOYIANNIS, D. P. & KELLER, N. P. 2013. Loss of CclA, required for histone 3 lysine 4 methylation, decreases growth but increases secondary metabolite production in Aspergillus fumigatus. *PeerJ,* 1**,** e4.

PAOLETTI, M., SEYMOUR, F. A., ALCOCER, M. J., KAUR, N., CALVO, A. M., ARCHER, D. B. & DYER, P. S. 2007. Mating type and the genetic basis of self-fertility in the model fungus Aspergillus nidulans. *Curr Biol,* 17**,** 1384-9.

PARK, H. S., NAM, T. Y., HAN, K. H., KIM, S. C. & YU, J. H. 2014. VelC positively controls sexual development in Aspergillus nidulans. *PLoS One,* 9**,** e89883.

PARRISH, F. W., WILEY, B. J., SIMMONS, E. G. & LONG, L., JR. 1966. Production of aflatoxins and kojic acid by species of Aspergillus and Penicillium. *Appl Microbiol,* 14**,** 139.

PEDERSEN, M. T. & HELIN, K. 2010. Histone demethylases in development and disease. *Trends Cell Biol,* 20**,** 662-71.

PFANNENSTIEL, B. T., GRECO, C., SUKOWATY, A. T. & KELLER, N. P. 2018. The epigenetic reader SntB regulates secondary metabolism, development and global histone modifications in Aspergillus flavus. *Fungal Genet Biol*.

PFANNENSTIEL, B. T., ZHAO, X., WORTMAN, J., WIEMANN, P., THROCKMORTON, K., SPRAKER, J. E., SOUKUP, A. A., LUO, X., LINDNER, D. L., LIM, F. Y., KNOX, B. P., HAAS, B., FISCHER, G. J., CHOERA, T., BUTCHKO, R. A. E., BOK, J. W., AFFELDT, K. J., KELLER, N. P. & PALMER, J. M. 2017. Revitalization of a Forward Genetic Screen Identifies Three New Regulators of Fungal Secondary Metabolism in the Genus Aspergillus. *MBio,* 8.

PILOTTO, S., SPERANZINI, V., TORTORICI, M., DURAND, D., FISH, A., VALENTE, S., FORNERIS, F., MAI, A., SIXMA, T. K., VACHETTE, P. & MATTEVI, A. 2015. Interplay among nucleosomal DNA, histone tails, and corepressor CoREST underlies LSD1-mediated H3 demethylation. *Proc Natl Acad Sci U S A,* 112**,** 2752-7.

PITKIN, J. W., NIKOLSKAYA, A., AHN, J. H. & WALTON, J. D. 2000. Reduced virulence caused by meiotic instability of the TOX2 chromosome of the maize pathogen Cochliobolus carbonum. *Mol Plant Microbe Interact,* 13**,** 80-7.

POWERS-FLETCHER, M. V., KENDALL, B. A., GRIFFIN, A. T. & HANSON, K. E. 2016. Filamentous Fungi. *Microbiol Spectr,* 4.

RAM, A. F., ARENTSHORST, M., DAMVELD, R. A., VANKUYK, P. A., KLIS, F. M. & VAN DEN HONDEL, C. A. 2004. The cell wall stress response in Aspergillus niger involves increased expression of the glutamine : fructose-6-phosphate amidotransferase-encoding gene (gfaA) and increased deposition of chitin in the cell wall. *Microbiology,* 150**,** 3315-26.

RAM, A. F. & KLIS, F. M. 2006. Identification of fungal cell wall mutants using susceptibility assays based on Calcofluor white and Congo red. *Nat Protoc,* 1**,** 2253-6.

RAMAKRISHNAN, S., POKHREL, S., PALANI, S., PFLUEGER, C., PARNELL, T. J., CAIRNS, B. R., BHASKARA, S. & CHANDRASEKHARAN, M. B. 2016. Counteracting H3K4 methylation modulators Set1 and Jhd2 co-regulate chromatin dynamics and gene transcription. *Nat Commun,* 7**,** 11949.

RAMIREZ-PRADO, J. H., MOORE, G. G., HORN, B. W. & CARBONE, I. 2008. Characterization and population analysis of the mating-type genes in Aspergillus flavus and Aspergillus parasiticus. *Fungal Genet Biol,* 45**,** 1292-9.

REA, S., EISENHABER, F., O'CARROLL, D., STRAHL, B. D., SUN, Z. W., SCHMID, M., OPRAVIL, S., MECHTLER, K., PONTING, C. P., ALLIS, C. D. & JENUWEIN, T. 2000. Regulation of chromatin structure by site-specific histone H3 methyltransferases. *Nature,* 406**,** 593-9.

REYES-DOMINGUEZ, Y., BOK, J. W., BERGER, H., SHWAB, E. K., BASHEER, A., GALLMETZER, A., SCAZZOCCHIO, C., KELLER, N. & STRAUSS, J. 2010. Heterochromatic marks are associated with the repression of secondary metabolism clusters in Aspergillus nidulans. *Mol Microbiol,* 76**,** 1376-86.

ROKAS, A., PAYNE, G., FEDOROVA, N. D., BAKER, S. E., MACHIDA, M., YU, J., GEORGIANNA, D. R., DEAN, R. A., BHATNAGAR, D., CLEVELAND, T. E., WORTMAN, J. R., MAITI, R., JOARDAR, V., AMEDEO, P., DENNING, D. W. & NIERMAN, W. C. 2007. What can comparative genomics tell us about species concepts in the genus Aspergillus? *Stud Mycol,* 59**,** 11-7.

ROKAS, A., WISECAVER, J. H. & LIND, A. L. 2018. The birth, evolution and death of metabolic gene clusters in fungi. *Nat Rev Microbiol*.

ROLEF BEN-SHAHAR, T., HEEGER, S., LEHANE, C., EAST, P., FLYNN, H., SKEHEL, M. & UHLMANN, F. 2008. Eco1-dependent cohesin acetylation during establishment of sister chromatid cohesion. *Science,* 321**,** 563-6.

ROSE, N. R. & KLOSE, R. J. 2014. Understanding the relationship between DNA methylation and histone lysine methylation. *Biochim Biophys Acta,* 1839**,** 1362-72.

ROSSETTO, D., AVVAKUMOV, N. & COTE, J. 2012. Histone phosphorylation: a chromatin modification involved in diverse nuclear events. *Epigenetics,* 7**,** 1098-108.

RUGER-HERREROS, C., RODRIGUEZ-ROMERO, J., FERNANDEZ-BARRANCO, R., OLMEDO, M., FISCHER, R., CORROCHANO, L. M. & CANOVAS, D. 2011. Regulation of conidiation by light in Aspergillus nidulans. *Genetics,* 188**,** 809-22.

RYU, H. Y. & AHN, S. 2014. Yeast histone H3 lysine 4 demethylase Jhd2 regulates mitotic rDNA condensation. *BMC Biol,* 12**,** 75.

SARIKAYA BAYRAM, O., BAYRAM, O., VALERIUS, O., PARK, H. S., IRNIGER, S., GERKE, J., NI, M., HAN, K. H., YU, J. H. & BRAUS, G. H. 2010. LaeA control of velvet family regulatory proteins for light-dependent development and fungal cell-type specificity. *PLoS Genet,* 6**,** e1001226.

SARIKAYA-BAYRAM, O., BAYRAM, O., FEUSSNER, K., KIM, J. H., KIM, H. S., KAEVER, A., FEUSSNER, I., CHAE, K. S., HAN, D. M., HAN, K. H. & BRAUS, G. H. 2014. Membrane-bound methyltransferase complex VapA-VipC-VapB guides epigenetic control of fungal development. *Dev Cell,* 29**,** 406-20.

SARIKAYA-BAYRAM, O., PALMER, J. M., KELLER, N., BRAUS, G. H. & BAYRAM, O. 2015. One Juliet and four Romeos: VeA and its methyltransferases. *Front Microbiol,* 6**,** 1.

SCHEU, S. & SIMMERLING, F. 2004. Growth and reproduction of fungal feeding Collembola as affected by fungal species, melanin and mixed diets. *Oecologia,* 139**,** 347-53.

SCULLY, L. R. & BIDOCHKA, M. J. 2005. Serial passage of the opportunistic pathogen Aspergillus flavus through an insect host yields decreased saprobic capacity. *Can J Microbiol,* 51**,** 185-9.

SEOANE, A. I. & MORGAN, D. O. 2017. Firing of Replication Origins Frees Dbf4-Cdc7 to Target Eco1 for Destruction. *Curr Biol,* 27**,** 2849-2855 e2.

SETO, E. & YOSHIDA, M. 2014. Erasers of histone acetylation: the histone deacetylase enzymes. *Cold Spring Harb Perspect Biol,* 6**,** a018713.

SHAABAN, M., PALMER, J. M., EL-NAGGAR, W. A., EL-SOKKARY, M. A., HABIB EL, S. E. & KELLER, N. P. 2010. Involvement of transposon-like elements in penicillin gene cluster regulation. *Fungal Genet Biol,* 47**,** 423-32.

SHI, Y., LAN, F., MATSON, C., MULLIGAN, P., WHETSTINE, J. R., COLE, P. A., CASERO, R. A. & SHI, Y. 2004. Histone demethylation mediated by the nuclear amine oxidase homolog LSD1. *Cell,* 119**,** 941-53.

SHIIO, Y. & EISENMAN, R. N. 2003. Histone sumoylation is associated with transcriptional repression. *Proc Natl Acad Sci U S A,* 100**,** 13225-30.

SHIMIZU, K., HICKS, J. K., HUANG, T. P. & KELLER, N. P. 2003. Pka, Ras and RGS protein interactions regulate activity of AflR, a Zn(II)2Cys6 transcription factor in Aspergillus nidulans. *Genetics,* 165**,** 1095-104.

SHWAB, E. K., BOK, J. W., TRIBUS, M., GALEHR, J., GRAESSLE, S. & KELLER, N. P. 2007. Histone deacetylase activity regulates chemical diversity in Aspergillus. *Eukaryot Cell,* 6**,** 1656-64.

SINGH, G., SINGH, V. & SCHNEIDER, J. S. 2018. Post-translational histone modifications and their interaction with sex influence normal brain development and elaboration of neuropsychiatric disorders. *Biochim Biophys Acta Mol Basis Dis*.

SINGH, R. K., GONZALEZ, M., KABBAJ, M. H. & GUNJAN, A. 2012. Novel E3 ubiquitin ligases that regulate histone protein levels in the budding yeast Saccharomyces cerevisiae. *PLoS One,* 7**,** e36295.

SON, H., FU, M., LEE, Y., LIM, J. Y., MIN, K., KIM, J. C., CHOI, G. J. & LEE, Y. W. 2016. A novel transcription factor gene FHS1 is involved in the DNA damage response in Fusarium graminearum. *Sci Rep,* 6**,** 21572.

SOUKUP, A. & KELLER, N. P. 2013. Western Analysis of Histone Modifications (Aspergillus nidulans). *Bio Protoc,* 3.

STEGER, D. J., UTLEY, R. T., GRANT, P. A., JOHN, S., EBERHARTER, A., COTE, J., OWEN-HUGHES, T., IKEDA, K. & WORKMAN, J. L. 1998. Regulation of transcription by multisubunit complexes that alter nucleosome structure. *Cold Spring Harb Symp Quant Biol,* 63**,** 483-91.

STINNETT, S. M., ESPESO, E. A., COBENO, L., ARAUJO-BAZAN, L. & CALVO, A. M. 2007. Aspergillus nidulans VeA subcellular localization is dependent on the importin alpha carrier and on light. *Mol Microbiol,* 63**,** 242-55.

SUGUI, J. A., PARDO, J., CHANG, Y. C., MULLBACHER, A., ZAREMBER, K. A., GALVEZ, E. M., BRINSTER, L., ZERFAS, P., GALLIN, J. I., SIMON, M. M. & KWON-CHUNG, K. J. 2007. Role of laeA in the Regulation of alb1, gliP, Conidial Morphology, and Virulence in Aspergillus fumigatus. *Eukaryot Cell,* 6**,** 1552-61.

SUTANI, T., KAWAGUCHI, T., KANNO, R., ITOH, T. & SHIRAHIGE, K. 2009. Budding yeast Wpl1(Rad61)-Pds5 complex counteracts sister chromatid cohesion-establishing reaction. *Curr Biol,* 19**,** 492-7.

TRAVERS, A. A., VAILLANT, C., ARNEODO, A. & MUSKHELISHVILI, G. 2012. DNA structure, nucleosome placement and chromatin remodelling: a perspective. *Biochem Soc Trans,* 40**,** 335-40.

TRIBUS, M., BAUER, I., GALEHR, J., RIESER, G., TROJER, P., BROSCH, G., LOIDL, P., HAAS, H. & GRAESSLE, S. 2010. A novel motif in fungal class 1 histone deacetylases is essential for growth and development of Aspergillus. *Mol Biol Cell,* 21**,** 345-53.

TRIEVEL, R. C. 2004. Structure and function of histone methyltransferases. *Crit Rev Eukaryot Gene Expr,* 14**,** 147-69.

TROJER, P., BRANDTNER, E. M., BROSCH, G., LOIDL, P., GALEHR, J., LINZMAIER, R., HAAS, H., MAIR, K., TRIBUS, M. & GRAESSLE, S. 2003. Histone deacetylases in fungi: novel members, new facts. *Nucleic Acids Res,* 31**,** 3971-81.

TSCHIERSCH, B., HOFMANN, A., KRAUSS, V., DORN, R., KORGE, G. & REUTER, G. 1994. The protein encoded by the Drosophila position-effect variegation

suppressor gene Su(var)3-9 combines domains of antagonistic regulators of homeotic gene complexes. *EMBO J,* 13**,** 3822-31.
TSUKADA, Y., FANG, J., ERDJUMENT-BROMAGE, H., WARREN, M. E., BORCHERS, C. H., TEMPST, P. & ZHANG, Y. 2006. Histone demethylation by a family of JmjC domain-containing proteins. *Nature,* 439**,** 811-6.
TVARDOVSKIY, A., WRZESINSKI, K., SIDOLI, S., FEY, S. J., ROGOWSKA-WRZESINSKA, A. & JENSEN, O. N. 2015. Top-down and Middle-down Protein Analysis Reveals that Intact and Clipped Human Histones Differ in Post-translational Modification Patterns. *Mol Cell Proteomics,* 14**,** 3142-53.
UMEMURA, M., KOIKE, H., NAGANO, N., ISHII, T., KAWANO, J., YAMANE, N., KOZONE, I., HORIMOTO, K., SHIN-YA, K., ASAI, K., YU, J., BENNETT, J. W. & MACHIDA, M. 2013. MIDDAS-M: motif-independent de novo detection of secondary metabolite gene clusters through the integration of genome sequencing and transcriptome data. *PLoS One,* 8**,** e84028.
VAN DER LINDEN, J. W., CAMPS, S. M., KAMPINGA, G. A., ARENDS, J. P., DEBETS-OSSENKOPP, Y. J., HAAS, P. J., RIJNDERS, B. J., KUIJPER, E. J., VAN TIEL, F. H., VARGA, J., KARAWAJCZYK, A., ZOLL, J., MELCHERS, W. J. & VERWEIJ, P. E. 2013. Aspergillosis due to voriconazole highly resistant Aspergillus fumigatus and recovery of genetically related resistant isolates from domiciles. *Clin Infect Dis,* 57**,** 513-20.
VAN OEVELEN, C., WANG, J., ASP, P., YAN, Q., KAELIN, W. G., JR., KLUGER, Y. & DYNLACHT, B. D. 2008. A role for mammalian Sin3 in permanent gene silencing. *Mol Cell,* 32**,** 359-70.
VAN RECHEM, C., BLACK, J. C., ABBAS, T., ALLEN, A., RINEHART, C. A., YUAN, G. C., DUTTA, A. & WHETSTINE, J. R. 2011. The SKP1-Cul1-F-box and leucine-rich repeat protein 4 (SCF-FbxL4) ubiquitin ligase regulates lysine demethylase 4A (KDM4A)/Jumonji domain-containing 2A (JMJD2A) protein. *J Biol Chem,* 286**,** 30462-70.
VENKATESH, S. & WORKMAN, J. L. 2015. Histone exchange, chromatin structure and the regulation of transcription. *Nat Rev Mol Cell Biol,* 16**,** 178-89.
VIENKEN, K. & FISCHER, R. 2006. The Zn(II)2Cys6 putative transcription factor NosA controls fruiting body formation in Aspergillus nidulans. *Mol Microbiol,* 61**,** 544-54.
VIGNALI, M., HASSAN, A. H., NEELY, K. E. & WORKMAN, J. L. 2000a. ATP-dependent chromatin-remodeling complexes. *Mol Cell Biol,* 20**,** 1899-910.
VIGNALI, M., STEGER, D. J., NEELY, K. E. & WORKMAN, J. L. 2000b. Distribution of acetylated histones resulting from Gal4-VP16 recruitment of SAGA and NuA4 complexes. *EMBO J,* 19**,** 2629-40.
VOSS, A. K. & THOMAS, T. 2018. Histone Lysine and Genomic Targets of Histone Acetyltransferases in Mammals. *Bioessays,* 40**,** e1800078.
VU, L. D., GEVAERT, K. & DE SMET, I. 2018. Protein Language: Post-Translational Modifications Talking to Each Other. *Trends Plant Sci*.
WANG, J., QIU, Z. & WU, Y. 2018. Ubiquitin Regulation: The Histone Modifying Enzyme's Story. *Cells,* 7.
WEAKE, V. M. & WORKMAN, J. L. 2008. Histone ubiquitination: triggering gene activity. *Mol Cell,* 29**,** 653-63.
WEAVER, T. M., MORRISON, E. A. & MUSSELMAN, C. A. 2018. Reading More than Histones: The Prevalence of Nucleic Acid Binding among Reader Domains. *Molecules,* 23.
WHELAN, G., KREIDL, E., PETERS, J. M. & EICHELE, G. 2012. The non-redundant function of cohesin acetyltransferase Esco2: some answers and new questions. *Nucleus,* 3**,** 330-4.

WHETSTINE, J. R., NOTTKE, A., LAN, F., HUARTE, M., SMOLIKOV, S., CHEN, Z., SPOONER, E., LI, E., ZHANG, G., COLAIACOVO, M. & SHI, Y. 2006. Reversal of histone lysine trimethylation by the JMJD2 family of histone demethylases. *Cell,* 125**,** 467-81.

XIE, Q., BAI, Y., WU, J., SUN, Y., WANG, Y., ZHANG, Y., MEI, P. & YUAN, Z. 2011. Methylation-mediated regulation of E2F1 in DNA damage-induced cell death. *J Recept Signal Transduct Res,* 31**,** 139-46.

XIONG, B., LU, S. & GERTON, J. L. 2010. Hos1 is a lysine deacetylase for the Smc3 subunit of cohesin. *Curr Biol,* 20**,** 1660-5.

YAMAMOTO, K. & SONODA, M. 2003. Self-interaction of heterochromatin protein 1 is required for direct binding to histone methyltransferase, SUV39H1. *Biochem Biophys Res Commun,* 301**,** 287-92.

YANG, X. J. & SETO, E. 2003. Collaborative spirit of histone deacetylases in regulating chromatin structure and gene expression. *Curr Opin Genet Dev,* 13**,** 143-53.

YANG, X. J. & SETO, E. 2008. The Rpd3/Hda1 family of lysine deacetylases: from bacteria and yeast to mice and men. *Nat Rev Mol Cell Biol,* 9**,** 206-18.

YANG, Y., HUANG, W., QIU, R., LIU, R., ZENG, Y., GAO, J., ZHENG, Y., HOU, Y., WANG, S., YU, W., LENG, S., FENG, D. & WANG, Y. 2018. LSD1 coordinates with the SIN3A/HDAC complex and maintains sensitivity to chemotherapy in breast cancer. *Journal of Molecular Cell Biology***,** mjy021-mjy021.

YAO, H. W. & LI, J. 2015. Epigenetic modifications in fibrotic diseases: implications for pathogenesis and pharmacological targets. *J Pharmacol Exp Ther,* 352**,** 2-13.

YEHESKELY-HAYON, D., KOTLER, A., STARK, M., HASHIMSHONY, T., SAGEE, S. & KASSIR, Y. 2013. The roles of the catalytic and noncatalytic activities of Rpd3L and Rpd3S in the regulation of gene transcription in yeast. *PLoS One,* 8**,** e85088.

YU, J. H. 2010. Regulation of Development in Aspergillus nidulans and Aspergillus fumigatus. *Mycobiology,* 38**,** 229-37.

YU, J. H., BUTCHKO, R. A., FERNANDES, M., KELLER, N. P., LEONARD, T. J. & ADAMS, T. H. 1996. Conservation of structure and function of the aflatoxin regulatory gene aflR from Aspergillus nidulans and A. flavus. *Curr Genet,* 29**,** 549-55.

YU, J. H. & KELLER, N. 2005. Regulation of secondary metabolism in filamentous fungi. *Annu Rev Phytopathol,* 43**,** 437-58.

ZHANG, D., LI, Y., ZHANG, X., ZHA, P. & LIN, R. 2017. The SWI2/SNF2 Chromatin-Remodeling ATPase BRAHMA Regulates Chlorophyll Biosynthesis in Arabidopsis. *Mol Plant,* 10**,** 155-167.

ZHANG, J., SHI, X., LI, Y., KIM, B. J., JIA, J., HUANG, Z., YANG, T., FU, X., JUNG, S. Y., WANG, Y., ZHANG, P., KIM, S. T., PAN, X. & QIN, J. 2008. Acetylation of Smc3 by Eco1 is required for S phase sister chromatid cohesion in both human and yeast. *Mol Cell,* 31**,** 143-51.

ZHOU, Y., XU, J., ZHU, Y., DUAN, Y. & ZHOU, M. 2016. Mechanism of Action of the Benzimidazole Fungicide on Fusarium graminearum: Interfering with Polymerization of Monomeric Tubulin But Not Polymerized Microtubule. *Phytopathology,* 106**,** 807-13.

ZHUANG, Z., LOHMAR, J. M., SATTERLEE, T., CARY, J. W. & CALVO, A. M. 2016. The Master Transcription Factor mtfA Governs Aflatoxin Production, Morphological Development and Pathogenicity in the Fungus Aspergillus flavus. *Toxins (Basel),* 8.

ZIAEE, A., ZIA, M. & GOLI, M. 2018. Identification of saprophytic and allergenic fungi in indoor and outdoor environments. *Environ Monit Assess,* 190**,** 574.

Appendix A

LC-MS^2 protein lists combined from two biological replicates of KdmB::GFP purification. Non-specific peptide contaminants were filtered out by using WT as a negative control. KERS complex subunits are represented in bold letters.

Accession	Description	Score	Coverage	# Unique Peptides
CADAFLAP00010689	pep:known supercontig:JCVI-afl1-v2.0:EQ963482:1685104:1690608:-1 gene:CADAFLAG00010689 transcript:CADAFLAT00010689 description: PHD transcription factor, putative	799.99	63.62	90
CADAFLAP00002374	pep:known supercontig:JCVI-afl1-v2.0:EQ963473:1948258:1953549:1 gene:CADAFLAG00002374 transcript:CADAFLAT00002374 description: PHD finger and BAH domain protein (Snt2), putative	322.06	50.90	62
CADAFLAP00003973	pep:known supercontig:JCVI-afl1-v2.0:EQ963474:2204554:2210905:-1 gene:CADAFLAG00003973 transcript:CADAFLAT00003973 description: Transcriptional corepressor of histone genes (Hir3), putative	156.00	26.47	36
CADAFLAP00003996	pep:known supercontig:JCVI-afl1-v2.0:EQ963474:2276434:2279944:-1 gene:CADAFLAG00003996 transcript:CADAFLAT00003996 description: Histone transcription regulator Hir1, putative	146.67	39.22	28
CADAFLAP00003012	pep:known supercontig:JCVI-afl1-v2.0:EQ963473:3679184:3681492:-1 gene:CADAFLAG00003012 transcript:CADAFLAT00003012 description: Phosphoenolpyruvate carboxykinase AcuF	120.61	51.67	20

CADAFLAP00004614	pep:known supercontig:JCVI-afl1-v2.0:EQ963475:1215660:1217220:-1 gene:CADAFLAG00004614 transcript:CADAFLAT00004614 description: Aldehyde dehydrogenase AldA, putative	98.83	55.33	19
CADAFLAP00008921	pep:known supercontig:JCVI-afl1-v2.0:EQ963480:874863:877102:1 gene:CADAFLAG00008921 transcript:CADAFLAT00008921 description: Histone deacetylase RpdA/Rpd3	85.71	43.07	20
CADAFLAP00008853	pep:known supercontig:JCVI-afl1-v2.0:EQ963480:687870:689811:1 gene:CADAFLAG00008853 transcript:CADAFLAT00008853 description: Putative uncharacterized protein Has domain(s) with predicted cell outer membrane, integral component of membrane localization	83.76	57.36	16
CADAFLAP00000902	pep:known supercontig:JCVI-afl1-v2.0:EQ963472:2412375:2414764:1 gene:CADAFLAG00000902 transcript:CADAFLAT00000902 description: ARS binding protein Abp2, putative	80.14	31.84	15
CADAFLAP00002780	pep:known supercontig:JCVI-afl1-v2.0:EQ963473:3053401:3056239:-1 gene:CADAFLAG00002780 transcript:CADAFLAT00002780 description: Mitochondrial aconitate hydratase, putative	77.62	39.62	21
CADAFLAP00011231	pep:known supercontig:JCVI-afl1-v2.0:EQ963483:1281340:1283202:-1 gene:CADAFLAG00011231 transcript:CADAFLAT00011231 description: Isocitrate lyase	72.12	45.54	16
CADAFLAP00005809	pep:known supercontig:JCVI-afl1-v2.0:EQ963476:1776812:1778528:1 gene:CADAFLAG00005809 transcript:CADAFLAT00005809 description: Glucose-6-phosphate isomerase	57.54	30.56	10
CADAFLAP00010931	pep:known supercontig:JCVI-afl1-v2.0:EQ963483:417154:418937:1 gene:CADAFLAG00010931 transcript:CADAFLAT00010931 description: Malate synthase	55.49	31.17	14

CADAFLAP00004946	pep:known supercontig:JCVI-afl1-v2.0:EQ963475:2095220:2099094:-1 gene:CADAFLAG00004946 transcript:CADAFLAT00004946 description: Pyruvate carboxylase	55.23	17.77	14
CADAFLAP00012083	pep:known supercontig:JCVI-afl1-v2.0:EQ963484:1638349:1640768:1 gene:CADAFLAG00012083 transcript:CADAFLAT00012083 description: Histone promoter control protein, putative	54.18	19.44	9
CADAFLAP00001859	pep:known supercontig:JCVI-afl1-v2.0:EQ963473:491941:493962:-1 gene:CADAFLAG00001859 transcript:CADAFLAT00001859 description: Putative uncharacterized protein	50.45	26.00	9
CADAFLAP00005963	pep:known supercontig:JCVI-afl1-v2.0:EQ963476:2187122:2194103:1 gene:CADAFLAG00005963 transcript:CADAFLAT00005963 description: Acetyl-CoA carboxylase, putative	49.75	10.07	16
CADAFLAP00010106	pep:known supercontig:JCVI-afl1-v2.0:EQ963481:2006011:2007476:-1 gene:CADAFLAG00010106 transcript:CADAFLAT00010106 description: Replication protein A 70 kDa DNA-binding subunit	48.69	36.00	11
CADAFLAP00005003	pep:known supercontig:JCVI-afl1-v2.0:EQ963475:2257383:2260906:-1 gene:CADAFLAG00005003 transcript:CADAFLAT00005003 description: ATP dependent RNA helicase (Dob1), putative	46.89	16.94	14
CADAFLAP00007478	pep:known supercontig:JCVI-afl1-v2.0:EQ963478:1359100:1361580:-1 gene:CADAFLAG00007478 transcript:CADAFLAT00007478 description: Putative uncharacterized protein	46.53	20.03	10
CADAFLAP00004824	pep:known supercontig:JCVI-afl1-v2.0:EQ963475:1801208:1804231:1 gene:CADAFLAG00004824 transcript:CADAFLAT00004824 description: Putative uncharacterized protein ??????	46.44	13.68	12

CADAFLAP00000442	pep:known supercontig:JCVI-afl1-v2.0:EQ963472:1149017:1152795:1 gene:CADAFLAG00000442 transcript:CADAFLAT00000442 description: Translation elongation factor eEF-3, putative	46.23	22.40	13
CADAFLAP00002446	pep:known supercontig:JCVI-afl1-v2.0:EQ963473:2146910:2148707:-1 gene:CADAFLAG00002446 transcript:CADAFLAT00002446 description: Phosphoglucomutase PgmA	44.92	34.23	13
CADAFLAP00004947	pep:known supercontig:JCVI-afl1-v2.0:EQ963475:2101733:2110515:-1 gene:CADAFLAG00004947 transcript:CADAFLAT00004947 description: Clathrin heavy chain	43.69	11.46	11
CADAFLAP00010065	pep:known supercontig:JCVI-afl1-v2.0:EQ963481:1890958:1892981:1 gene:CADAFLAG00010065 transcript:CADAFLAT00010065 description: Hexokinase Kxk, putative	43.37	32.65	10
CADAFLAP00008160	pep:known supercontig:JCVI-afl1-v2.0:EQ963479:837390:838972:-1 gene:CADAFLAG00008160 transcript:CADAFLAT00008160 description: Elongation factor Tu	42.55	34.47	10
CADAFLAP00012073	pep:known supercontig:JCVI-afl1-v2.0:EQ963484:1615136:1616293:1 gene:CADAFLAG00012073 transcript:CADAFLAT00012073 description: Sister chromatid cohesion acetyltransferase Eco1, putative	42.13	32.21	11
CADAFLAP00012077	pep:known supercontig:JCVI-afl1-v2.0:EQ963484:1621938:1624159:1 gene:CADAFLAG00012077 transcript:CADAFLAT00012077 description: Eukaryotic translation initiation factor subunit eIF2A, putative	40.66	27.42	12
CADAFLAP00011721	pep:known supercontig:JCVI-afl1-v2.0:EQ963484:724131:727328:-1 gene:CADAFLAG00011721 transcript:CADAFLAT00011721 description: Putative uncharacterized protein	40.41	18.23	10

CADAFLAP00000620	pep:known supercontig:JCVI-afl1-v2.0:EQ963472:1615903:1617653:-1 gene:CADAFLAG00000620 transcript:CADAFLAT00000620 description: Acetyl-coA hydrolase Ach1, putative	39.98	27.24	7
CADAFLAP00003677	pep:known supercontig:JCVI-afl1-v2.0:EQ963474:1386461:1388119:-1 gene:CADAFLAG00003677 transcript:CADAFLAT00003677 description: Spermidine synthase	39.71	34.71	7
CADAFLAP00008520	pep:known supercontig:JCVI-afl1-v2.0:EQ963479:1855567:1858665:1 gene:CADAFLAG00008520 transcript:CADAFLAT00008520 description: Involucrin, putative	39.27	17.28	6
CADAFLAP00000450	pep:known supercontig:JCVI-afl1-v2.0:EQ963472:1182111:1184111:1 gene:CADAFLAG00000450 transcript:CADAFLAT00000450 description: Pyruvate dehydrogenase complex, dihydrolipoamide acetyltransferase	37.96	32.16	9
CADAFLAP00010521	pep:known supercontig:JCVI-afl1-v2.0:EQ963482:1155676:1158179:-1 gene:CADAFLAG00010521 transcript:CADAFLAT00010521 description: Vacuolar dynamin-like GTPase VpsA, putative	37.92	24.06	11
CADAFLAP00005479	pep:known supercontig:JCVI-afl1-v2.0:EQ963476:876078:877741:1 gene:CADAFLAG00005479 transcript:CADAFLAT00005479 description: Chromosome segregation protein (Pcs1), putative	36.54	29.48	9
CADAFLAP00010101	pep:known supercontig:JCVI-afl1-v2.0:EQ963481:1995326:1996965:-1 gene:CADAFLAG00010101 transcript:CADAFLAT00010101 description: Putative uncharacterized protein	35.32	27.31	9
CADAFLAP00009067	pep:known supercontig:JCVI-afl1-v2.0:EQ963480:1291839:1292342:-1 gene:CADAFLAG00009067 transcript:CADAFLAT00009067 description: SsDNA binding protein Ssb3, putative	35.26	50.41	4

CADAFLAP00008523	pep:known supercontig:JCVI-afl1-v2.0:EQ963479:1865471:1866979:-1 gene:CADAFLAG00008523 transcript:CADAFLAT00008523 description: UTP-glucose-1-phosphate uridylyltransferase Ugp1, putative	33.98	24.10	9
CADAFLAP00011019	pep:known supercontig:JCVI-afl1-v2.0:EQ963483:679089:680918:-1 gene:CADAFLAG00011019 transcript:CADAFLAT00011019 description: Conserved lysine-rich protein, putative	33.92	30.67	11
CADAFLAP00006051	pep:known supercontig:JCVI-afl1-v2.0:EQ963476:2499774:2501537:1 gene:CADAFLAG00006051 transcript:CADAFLAT00006051 description: Cystathionine beta-synthase, putative	33.62	24.39	7
CADAFLAP00002820	pep:known supercontig:JCVI-afl1-v2.0:EQ963473:3150116:3152402:1 gene:CADAFLAG00002820 transcript:CADAFLAT00002820 description: WD repeat protein	33.43	23.68	6
CADAFLAP00008812	pep:known supercontig:JCVI-afl1-v2.0:EQ963480:570126:572169:-1 gene:CADAFLAG00008812 transcript:CADAFLAT00008812 description: Fumarate hydratase, putative	33.39	23.10	7
CADAFLAP00005638	pep:known supercontig:JCVI-afl1-v2.0:EQ963476:1282856:1284624:1 gene:CADAFLAG00005638 transcript:CADAFLAT00005638 description: Dihydrolipoyl dehydrogenase	33.32	22.46	7
CADAFLAP00003019	pep:known supercontig:JCVI-afl1-v2.0:EQ963473:3702311:3703864:1 gene:CADAFLAG00003019 transcript:CADAFLAT00003019 description: Alanine aminotransferase, putative	33.27	27.11	7
CADAFLAP00005046	pep:known supercontig:JCVI-afl1-v2.0:EQ963475:2384512:2385823:-1 gene:CADAFLAG00005046 transcript:CADAFLAT00005046 description: GPI-anchored cell wall organization protein Ecm33	32.28	20.60	7

CADAFLAP00008895	pep:known supercontig:JCVI-afl1-v2.0:EQ963480:806443:808343:1 gene:CADAFLAG00008895 transcript:CADAFLAT00008895 description: Inosine-5'-monophosphate dehydrogenase	32.23	23.63	6
CADAFLAP00003559	pep:known supercontig:JCVI-afl1-v2.0:EQ963474:1042720:1044510:1 gene:CADAFLAG00003559 transcript:CADAFLAT00003559 description: Putative uncharacterized protein	32.23	20.24	8
CADAFLAP00000131	pep:known supercontig:JCVI-afl1-v2.0:EQ963472:324198:324959:1 gene:CADAFLAG00000131 transcript:CADAFLAT00000131 description: Tropomyosin, putative	32.06	50.93	7
CADAFLAP00004653	pep:known supercontig:JCVI-afl1-v2.0:EQ963475:1327837:1328832:-1 gene:CADAFLAG00004653 transcript:CADAFLAT00004653 description: Possible replication factor-a protein	31.81	33.33	6
CADAFLAP00005725	pep:known supercontig:JCVI-afl1-v2.0:EQ963476:1524272:1525447:-1 gene:CADAFLAG00005725 transcript:CADAFLAT00005725 description: Mannitol-1-phosphate dehydrogenase	31.52	31.71	9
CADAFLAP00005268	pep:known supercontig:JCVI-afl1-v2.0:EQ963476:350558:351379:1 gene:CADAFLAG00005268 transcript:CADAFLAT00005268 description: Cell wall serine-threonine-rich galactomannoprotein Mp1	29.99	34.07	5
CADAFLAP00002082	pep:known supercontig:JCVI-afl1-v2.0:EQ963473:1126458:1128842:-1 gene:CADAFLAG00002082 transcript:CADAFLAT00002082 description: Acetyl-coenzyme A synthetase FacA	27.99	13.80	10
CADAFLAP00002110	pep:known supercontig:JCVI-afl1-v2.0:EQ963473:1209310:1211142:-1 gene:CADAFLAG00002110 transcript:CADAFLAT00002110 description: Saccharopine dehydrogenase Lys9, putative	27.77	27.56	7

CADAFLAP00010921	pep:known supercontig:JCVI-afl1-v2.0:EQ963483:390873:392389:-1 gene:CADAFLAG00010921 transcript:CADAFLAT00010921 description: Citrate synthase	27.43	29.12	10
CADAFLAP00009911	pep:known supercontig:JCVI-afl1-v2.0:EQ963481:1452511:1454454:-1 gene:CADAFLAG00009911 transcript:CADAFLAT00009911 description: Delta-1-pyrroline-5-carboxylate dehydrogenase PrnC	27.24	23.34	6
CADAFLAP00009281	pep:known supercontig:JCVI-afl1-v2.0:EQ963480:1839860:1842354:1 gene:CADAFLAG00009281 transcript:CADAFLAT00009281 description: Hsp70 chaperone Hsp88	27.00	14.87	8
CADAFLAP00001737	pep:known supercontig:JCVI-afl1-v2.0:EQ963473:199571:199957:1 gene:CADAFLAG00001737 transcript:CADAFLAT00001737 description: Putative uncharacterized protein	26.85	55.47	5
CADAFLAP00008873	pep:known supercontig:JCVI-afl1-v2.0:EQ963480:744729:746663:1 gene:CADAFLAG00008873 transcript:CADAFLAT00008873 description: Septin AspA, putative	26.84	28.50	8
CADAFLAP00010333	pep:known supercontig:JCVI-afl1-v2.0:EQ963482:579999:582032:1 gene:CADAFLAG00010333 transcript:CADAFLAT00010333 description: Curved DNA-binding protein (42 kDa protein)	26.45	20.39	7
CADAFLAP00004546	pep:known supercontig:JCVI-afl1-v2.0:EQ963475:1032320:1033870:1 gene:CADAFLAG00004546 transcript:CADAFLAT00004546 description: Argininosuccinate synthase	25.84	22.78	7
CADAFLAP00010089	pep:known supercontig:JCVI-afl1-v2.0:EQ963481:1962393:1964153:-1 gene:CADAFLAG00010089 transcript:CADAFLAT00010089 description: Protein disulfide isomerase Pdi1, putative	25.08	21.94	8

CADAFLAP00002148	pep:known supercontig:JCVI-afl1-v2.0:EQ963473:1347555:1348597:1 gene:CADAFLAG00002148 transcript:CADAFLAT00002148 description: Glycerol dehydrogenase (GldB), putative	25.00	32.31	6
CADAFLAP00002106	pep:known supercontig:JCVI-afl1-v2.0:EQ963473:1197615:1198758:-1 gene:CADAFLAG00002106 transcript:CADAFLAT00002106 description: Fructose-1,6-bisphosphatase Fbp1, putative	24.97	26.76	6
CADAFLAP00001031	pep:known supercontig:JCVI-afl1-v2.0:EQ963472:2741596:2742394:1 gene:CADAFLAG00001031 transcript:CADAFLAT00001031 description: TCTP family protein	24.71	40.46	5
CADAFLAP00010767	pep:known supercontig:JCVI-afl1-v2.0:EQ963482:1879404:1881039:-1 gene:CADAFLAG00010767 transcript:CADAFLAT00010767 description: Homocysteine synthase CysD	24.68	22.53	6
CADAFLAP00010303	pep:known supercontig:JCVI-afl1-v2.0:EQ963482:501187:504449:-1 gene:CADAFLAG00010303 transcript:CADAFLAT00010303 description: Cell division control protein Cdc48	24.60	10.23	6
CADAFLAP00004794	pep:known supercontig:JCVI-afl1-v2.0:EQ963475:1707091:1710083:-1 gene:CADAFLAG00004794 transcript:CADAFLAT00004794 description: Aminopeptidase	24.44	11.55	8
CADAFLAP00002090	pep:known supercontig:JCVI-afl1-v2.0:EQ963473:1149241:1150080:-1 gene:CADAFLAG00002090 transcript:CADAFLAT00002090 description: Cell division control protein Cdc31, putative	24.40	44.18	6
CADAFLAP00004949	pep:known supercontig:JCVI-afl1-v2.0:EQ963475:2114609:2116687:-1 gene:CADAFLAG00004949 transcript:CADAFLAT00004949	24.24	22.52	9

	description: Phosphoribosylaminoimidazolecarboxamide formyltransferase/IMP			
CADAFLAP00011638	pep:known supercontig:JCVI-afl1-v2.0:EQ963484:473407:474791:-1 gene:CADAFLAG00011638 transcript:CADAFLAT00011638 description: Superoxide dismutase	24.21	51.95	4
CADAFLAP00002560	pep:known supercontig:JCVI-afl1-v2.0:EQ963473:2456211:2460173:-1 gene:CADAFLAG00002560 transcript:CADAFLAT00002560 description: Clustered mitochondria protein homolog	23.83	7.69	4
CADAFLAP00002845	pep:known supercontig:JCVI-afl1-v2.0:EQ963473:3215149:3217086:1 gene:CADAFLAG00002845 transcript:CADAFLAT00002845 description: Transcription factor RfeD, putative	23.78	21.26	7
CADAFLAP00008603	pep:known supercontig:JCVI-afl1-v2.0:EQ963480:36079:41772:1 gene:CADAFLAG00008603 transcript:CADAFLAT00008603 description: Fatty acid synthase alpha subunit FasA	23.54	6.79	9
CADAFLAP00010002	pep:known supercontig:JCVI-afl1-v2.0:EQ963481:1693935:1695761:1 gene:CADAFLAG00010002 transcript:CADAFLAT00010002 description: 1,3-beta-glucanosyltransferase, putative	23.32	15.99	6
CADAFLAP00001419	pep:known supercontig:JCVI-afl1-v2.0:EQ963472:3778580:3780973:-1 gene:CADAFLAG00001419 transcript:CADAFLAT00001419 description: Isocitrate dehydrogenase	22.73	19.84	8
CADAFLAP00003053	pep:known supercontig:JCVI-afl1-v2.0:EQ963473:3803535:3805320:1 gene:CADAFLAG00003053 transcript:CADAFLAT00003053 description: Putative uncharacterized protein	22.11	14.36	6
CADAFLAP00002146	pep:known supercontig:JCVI-afl1-v2.0:EQ963473:1342058:1342917:1 gene:CADAFLAG00002146	21.75	33.73	5

	transcript:CADAFLAT00002146 description: Peptidyl-prolyl cis-trans isomerase			
CADAFLAP00003646	pep:known supercontig:JCVI-afl1-v2.0:EQ963474:1277816:1278470:-1 gene:CADAFLAG00003646 transcript:CADAFLAT00003646 description: Histone H3	21.74	35.29	3
CADAFLAP00001659	pep:known supercontig:JCVI-afl1-v2.0:EQ963472:4442484:4444810:-1 gene:CADAFLAG00001659 transcript:CADAFLAT00001659 description: Glycerol-3-phosphate dehydrogenase, mitochondrial	21.71	13.80	6
CADAFLAP00007065	pep:known supercontig:JCVI-afl1-v2.0:EQ963478:237548:238102:1 gene:CADAFLAG00007065 transcript:CADAFLAT00007065 description: Putative uncharacterized protein	21.55	50.45	6
CADAFLAP00000624	pep:known supercontig:JCVI-afl1-v2.0:EQ963472:1631080:1633180:-1 gene:CADAFLAG00000624 transcript:CADAFLAT00000624 description: Fumarate reductase Osm1, putative	21.50	17.22	9
CADAFLAP00008409	pep:known supercontig:JCVI-afl1-v2.0:EQ963479:1516901:1517936:-1 gene:CADAFLAG00008409 transcript:CADAFLAT00008409 description: Glycerol dehydrogenase Gcy1, putative	21.47	34.56	6
CADAFLAP00007432	pep:known supercontig:JCVI-afl1-v2.0:EQ963478:1225665:1226685:-1 gene:CADAFLAG00007432 transcript:CADAFLAT00007432 description: ATP synthase oligomycin sensitivity conferral protein, putative	21.06	28.76	7
CADAFLAP00011184	pep:known supercontig:JCVI-afl1-v2.0:EQ963483:1159648:1161930:-1 gene:CADAFLAG00011184 transcript:CADAFLAT00011184 description: Glutamine synthetase	20.96	25.20	6

CADAFLAP00011749	pep:known supercontig:JCVI-afl1-v2.0:EQ963484:800622:801017:-1 gene:CADAFLAG00011749 transcript:CADAFLAT00011749 description: Putative uncharacterized protein	20.81	35.11	3
CADAFLAP00008502	pep:known supercontig:JCVI-afl1-v2.0:EQ963479:1791721:1793654:-1 gene:CADAFLAG00008502 transcript:CADAFLAT00008502 description: Acetamidase, putative	20.75	16.58	5
CADAFLAP00008125	pep:known supercontig:JCVI-afl1-v2.0:EQ963479:760440:763107:1 gene:CADAFLAG00008125 transcript:CADAFLAT00008125 description: Carnitine acetyl transferase	20.53	12.14	7
CADAFLAP00000389	pep:known supercontig:JCVI-afl1-v2.0:EQ963472:1003830:1005519:1 gene:CADAFLAG00000389 transcript:CADAFLAT00000389 description: Septin AspB	20.52	11.85	3
CADAFLAP00003039	pep:known supercontig:JCVI-afl1-v2.0:EQ963473:3770596:3772369:1 gene:CADAFLAG00003039 transcript:CADAFLAT00003039 description: PH domain protein	20.23	23.62	7
CADAFLAP00010853	pep:known supercontig:JCVI-afl1-v2.0:EQ963483:190843:192496:-1 gene:CADAFLAG00010853 transcript:CADAFLAT00010853 description: Succinyl-CoA synthetase alpha subunit, putative	20.05	22.42	6
CADAFLAP00000614	pep:known supercontig:JCVI-afl1-v2.0:EQ963472:1603161:1605021:-1 gene:CADAFLAG00000614 transcript:CADAFLAT00000614 description: Probable beta-glucosidase btgE	19.42	12.62	5
CADAFLAP00004055	pep:known supercontig:JCVI-afl1-v2.0:EQ963474:2432289:2433508:1 gene:CADAFLAG00004055 transcript:CADAFLAT00004055 description: Aminotransferase, class V, putative	19.30	11.66	4
CADAFLAP00000634	pep:known supercontig:JCVI-afl1-v2.0:EQ963472:1661701:1663028:-1	19.03	29.63	6

	gene:CADAFLAG00000634 transcript:CADAFLAT00000634 description: Mitochondrial ATPase subunit ATP4, putative			
CADAFLAP00000427	pep:known supercontig:JCVI-afl1-v2.0:EQ963472:1105368:1106555:1 gene:CADAFLAG00000427 transcript:CADAFLAT00000427 description: Electron transfer flavoprotein alpha subunit, putative	18.82	18.16	4
CADAFLAP00010763	pep:known supercontig:JCVI-afl1-v2.0:EQ963482:1866457:1868062:1 gene:CADAFLAG00010763 transcript:CADAFLAT00010763 description: Ubiquinol-cytochrome C reductase complex core protein 2, putative	18.70	27.04	5
CADAFLAP00005925	pep:known supercontig:JCVI-afl1-v2.0:EQ963476:2078558:2081418:-1 gene:CADAFLAG00005925 transcript:CADAFLAT00005925 description: Probable dipeptidyl-peptidase 5	18.65	9.44	5
CADAFLAP00009844	pep:known supercontig:JCVI-afl1-v2.0:EQ963481:1249119:1250065:1 gene:CADAFLAG00009844 transcript:CADAFLAT00009844 description: 60S acidic ribosomal protein P1	18.56	24.36	3
CADAFLAP00000784	pep:known supercontig:JCVI-afl1-v2.0:EQ963472:2077201:2078611:-1 gene:CADAFLAG00000784 transcript:CADAFLAT00000784 description: ATP synthase subunit gamma	18.46	17.51	4
CADAFLAP00003586	pep:known supercontig:JCVI-afl1-v2.0:EQ963474:1129063:1130937:1 gene:CADAFLAG00003586 transcript:CADAFLAT00003586 description: Mitochondrial processing peptidase beta subunit, putative	18.31	17.12	4
CADAFLAP00005829	pep:known supercontig:JCVI-afl1-v2.0:EQ963476:1814509:1816071:-1 gene:CADAFLAG00005829 transcript:CADAFLAT00005829 description: Aspartate aminotransferase	18.23	18.06	5

CADAFLAP00004007	pep:known supercontig:JCVI-afl1-v2.0:EQ963474:2307637:2310084:1 gene:CADAFLAG00004007 transcript:CADAFLAT00004007 description: tRNA ligase	18.21	4.54	3
CADAFLAP00012165	pep:known supercontig:JCVI-afl1-v2.0:EQ963485:51761:52235:1 gene:CADAFLAG00012165 transcript:CADAFLAT00012165 description: Putative uncharacterized protein	17.98	44.68	4
CADAFLAP00004424	pep:known supercontig:JCVI-afl1-v2.0:EQ963475:714186:715377:-1 gene:CADAFLAG00004424 transcript:CADAFLAT00004424 description: Aldehyde reductase (AKR1), putative	17.84	30.12	5
CADAFLAP00004139	pep:known supercontig:JCVI-afl1-v2.0:EQ963474:2663109:2665249:-1 gene:CADAFLAG00004139 transcript:CADAFLAT00004139 description: Cupin domain protein	17.79	10.92	4
CADAFLAP00002319	pep:known supercontig:JCVI-afl1-v2.0:EQ963473:1782398:1783642:-1 gene:CADAFLAG00002319 transcript:CADAFLAT00002319 description: NADH-cytochrome b5 reductase, putative	17.77	22.29	4
CADAFLAP00003581	pep:known supercontig:JCVI-afl1-v2.0:EQ963474:1115753:1118605:1 gene:CADAFLAG00003581 transcript:CADAFLAT00003581 description: Acetylglutamate kinase, putative	17.55	7.17	5
CADAFLAP00003740	pep:known supercontig:JCVI-afl1-v2.0:EQ963474:1563476:1566818:1 gene:CADAFLAG00003740 transcript:CADAFLAT00003740 description: Glycogen phosphorylase GlpV/Gph1, putative	17.37	12.06	6
CADAFLAP00001304	pep:known supercontig:JCVI-afl1-v2.0:EQ963472:3514361:3517540:-1 gene:CADAFLAG00001304 transcript:CADAFLAT00001304 description: RNA binding protein, putative	17.26	8.07	4

CADAFLAP00005736	pep:known supercontig:JCVI-afl1-v2.0:EQ963476:1559843:1561676:1 gene:CADAFLAG00005736 transcript:CADAFLAT00005736 description: Uricase	17.24	22.85	6
CADAFLAP00005038	pep:known supercontig:JCVI-afl1-v2.0:EQ963475:2359587:2360927:-1 gene:CADAFLAG00005038 transcript:CADAFLAT00005038 description: Outer mitochondrial membrane protein porin	17.20	15.90	5
CADAFLAP00001420	pep:known supercontig:JCVI-afl1-v2.0:EQ963472:3782147:3785518:-1 gene:CADAFLAG00001420 transcript:CADAFLAT00001420 description: C1 tetrahydrofolate synthase, putative	17.15	7.10	5
CADAFLAP00008251	pep:known supercontig:JCVI-afl1-v2.0:EQ963479:1070022:1071114:1 gene:CADAFLAG00008251 transcript:CADAFLAT00008251 description: Putative uncharacterized protein	17.11	32.93	3
CADAFLAP00011052	pep:known supercontig:JCVI-afl1-v2.0:EQ963483:776604:778253:1 gene:CADAFLAG00011052 transcript:CADAFLAT00011052 description: Betaine-aldehyde dehydrogenase, putative	16.97	14.29	4
CADAFLAP00001977	pep:known supercontig:JCVI-afl1-v2.0:EQ963473:814386:815950:1 gene:CADAFLAG00001977 transcript:CADAFLAT00001977 description: Calmodulin	16.82	22.15	3
CADAFLAP00010561	pep:known supercontig:JCVI-afl1-v2.0:EQ963482:1284518:1285438:-1 gene:CADAFLAG00010561 transcript:CADAFLAT00010561 description: Cytochrome c oxidase subunit Va, putative	16.57	30.38	3
CADAFLAP00003105	pep:known supercontig:JCVI-afl1-v2.0:EQ963473:3958971:3959867:-1 gene:CADAFLAG00003105 transcript:CADAFLAT00003105 description: Rho GTPase Rho1	16.40	39.90	5
CADAFLAP00003295	pep:known supercontig:JCVI-afl1-v2.0:EQ963474:339614:340434:1 gene:CADAFLAG00003295	16.33	72.48	4

	transcript:CADAFLAT00003295 description: Putative uncharacterized protein			
CADAFLAP00013435	pep:known supercontig:JCVI-afl1-v2.0:EQ963487:256722:258530:-1 gene:CADAFLAG00013435 transcript:CADAFLAT00013435 description: Succinyl-CoA synthetase beta subunit, putative	16.26	14.05	6
CADAFLAP00008024	pep:known supercontig:JCVI-afl1-v2.0:EQ963479:459507:460852:-1 gene:CADAFLAG00008024 transcript:CADAFLAT00008024 description: BZIP transcription factor, putative	16.23	14.08	3
CADAFLAP00006143	pep:known supercontig:JCVI-afl1-v2.0:EQ963477:199613:200217:1 gene:CADAFLAG00006143 transcript:CADAFLAT00006143 description: Centromere protein Cse4, putative	16.01	21.14	3
CADAFLAP00007163	pep:known supercontig:JCVI-afl1-v2.0:EQ963478:472774:474322:-1 gene:CADAFLAG00007163 transcript:CADAFLAT00007163 description: Arp2/3 complex subunit (Arp3), putative	15.97	21.48	5
CADAFLAP00008845	pep:known supercontig:JCVI-afl1-v2.0:EQ963480:671061:672149:-1 gene:CADAFLAG00008845 transcript:CADAFLAT00008845 description: Nascent polypeptide-associated complex (NAC) subunit, putative	15.80	22.47	3
CADAFLAP00010758	pep:known supercontig:JCVI-afl1-v2.0:EQ963482:1848914:1850659:1 gene:CADAFLAG00010758 transcript:CADAFLAT00010758 description: NTF2 and RRM domain protein	15.78	11.50	4
CADAFLAP00002147	pep:known supercontig:JCVI-afl1-v2.0:EQ963473:1344392:1345852:-1 gene:CADAFLAG00002147 transcript:CADAFLAT00002147 description: Phosphatidyl synthase	15.74	10.29	4
CADAFLAP00011640	pep:known supercontig:JCVI-afl1-v2.0:EQ963484:488554:490163:1 gene:CADAFLAG00011640	15.65	13.54	4

	transcript:CADAFLAT00011640 description: Autophagic serine protease Alp2			
CADAFLAP00008018	pep:known supercontig:JCVI-afl1-v2.0:EQ963479:440115:440614:1 gene:CADAFLAG00008018 transcript:CADAFLAT00008018 description: Glyoxalase family protein	15.64	37.50	3
CADAFLAP00007020	pep:known supercontig:JCVI-afl1-v2.0:EQ963478:107244:108734:1 gene:CADAFLAG00007020 transcript:CADAFLAT00007020 description: Eukaryotic translation initiation factor 3 subunit M	15.62	15.88	4
CADAFLAP00010410	pep:known supercontig:JCVI-afl1-v2.0:EQ963482:799044:801434:1 gene:CADAFLAG00010410 transcript:CADAFLAT00010410 description: Translation initiation factor 4B	15.57	13.39	4
CADAFLAP00002028	pep:known supercontig:JCVI-afl1-v2.0:EQ963473:981877:983504:1 gene:CADAFLAG00002028 transcript:CADAFLAT00002028 description: Homocitrate synthase	15.30	12.53	4
CADAFLAP00012505	pep:known supercontig:JCVI-afl1-v2.0:EQ963485:949613:950359:-1 gene:CADAFLAG00012505 transcript:CADAFLAT00012505 description: Glutathione-S-transferase theta, GST, putative	15.21	39.52	6
CADAFLAP00002378	pep:known supercontig:JCVI-afl1-v2.0:EQ963473:1966313:1969575:1 gene:CADAFLAG00002378 transcript:CADAFLAT00002378 description: Eukaryotic translation initiation factor 3 subunit A	14.82	6.49	4
CADAFLAP00007278	pep:known supercontig:JCVI-afl1-v2.0:EQ963478:779419:781271:1 gene:CADAFLAG00007278 transcript:CADAFLAT00007278 description: Secretory pathway gdp dissociation inhibitor	14.81	14.35	4
CADAFLAP00009793	pep:known supercontig:JCVI-afl1-v2.0:EQ963481:1098410:1100420:-1	14.79	6.30	2

	gene:CADAFLAG00009793 transcript:CADAFLAT00009793 description: N-acetylglucosamine-phosphate mutase			
CADAFLAP00002582	pep:known supercontig:JCVI-afl1-v2.0:EQ963473:2526005:2526658:-1 gene:CADAFLAG00002582 transcript:CADAFLAT00002582 description: Mitochondrial F1F0 ATP synthase subunit Atp14, putative	14.72	23.75	3
CADAFLAP00002876	pep:known supercontig:JCVI-afl1-v2.0:EQ963473:3300713:3301277:1 gene:CADAFLAG00002876 transcript:CADAFLAT00002876 description: Small nuclear ribonucleoprotein SmD1, putative	14.57	45.53	3
CADAFLAP00001079	pep:known supercontig:JCVI-afl1-v2.0:EQ963472:2875147:2876318:-1 gene:CADAFLAG00001079 transcript:CADAFLAT00001079 description: MIND kinetochore complex component Mtw1, putative	14.56	16.07	3
CADAFLAP00001519	pep:known supercontig:JCVI-afl1-v2.0:EQ963472:4054449:4055909:-1 gene:CADAFLAG00001519 transcript:CADAFLAT00001519 description: Histone deacetylase HosA	14.49	16.46	4
CADAFLAP00010764	pep:known supercontig:JCVI-afl1-v2.0:EQ963482:1868909:1870647:-1 gene:CADAFLAG00010764 transcript:CADAFLAT00010764 description: Mitochondrial DNA replication protein (Yhm2), putative	14.47	9.21	2
CADAFLAP00010702	pep:known supercontig:JCVI-afl1-v2.0:EQ963482:1718556:1720986:-1 gene:CADAFLAG00010702 transcript:CADAFLAT00010702 description: Glutamyl-tRNA synthetase	14.24	8.98	4
CADAFLAP00002925	pep:known supercontig:JCVI-afl1-v2.0:EQ963473:3427036:3428461:1 gene:CADAFLAG00002925	14.20	47.45	3

	transcript:CADAFLAT00002925 description: Cytochrome b5, putative			
CADAFLAP00010777	pep:known supercontig:JCVI-afl1-v2.0:EQ963482:1903512:1906994:-1 gene:CADAFLAG00010777 transcript:CADAFLAT00010777 description: Aminopeptidase, putative	14.04	9.76	5
CADAFLAP00001478	pep:known supercontig:JCVI-afl1-v2.0:EQ963472:3932110:3934557:-1 gene:CADAFLAG00001478 transcript:CADAFLAT00001478 description: Cell wall protein, putative	13.96	6.01	4
CADAFLAP00010727	pep:known supercontig:JCVI-afl1-v2.0:EQ963482:1782647:1785024:-1 gene:CADAFLAG00010727 transcript:CADAFLAT00010727 description: Spindle pole body associated protein SnaD, putative	13.80	8.24	5
CADAFLAP00001155	pep:known supercontig:JCVI-afl1-v2.0:EQ963472:3083165:3086306:-1 gene:CADAFLAG00001155 transcript:CADAFLAT00001155 description: Importin beta-1 subunit	13.65	6.88	4
CADAFLAP00006244	pep:known supercontig:JCVI-afl1-v2.0:EQ963477:476121:478024:1 gene:CADAFLAG00006244 transcript:CADAFLAT00006244 description: 2-methylcitrate dehydratase, putative	13.50	10.38	3
CADAFLAP00007141	pep:known supercontig:JCVI-afl1-v2.0:EQ963478:416585:417464:-1 gene:CADAFLAG00007141 transcript:CADAFLAT00007141 description: Rho-gdp dissociation inhibitor	13.46	29.44	3
CADAFLAP00011804	pep:known supercontig:JCVI-afl1-v2.0:EQ963484:943553:945457:-1 gene:CADAFLAG00011804 transcript:CADAFLAT00011804 description: ATP sulphurylase	13.45	10.87	4
CADAFLAP00007538	pep:known supercontig:JCVI-afl1-v2.0:EQ963478:1531723:1532637:-1	13.41	24.70	5

	gene:CADAFLAG00007538 transcript:CADAFLAT00007538 description: GrpE protein homolog			
CADAFLAP00009007	pep:known supercontig:JCVI-afl1-v2.0:EQ963480:1126513:1129940:1 gene:CADAFLAG00009007 transcript:CADAFLAT00009007 description: Ran-specific GTPase-activating protein 1, putative	13.29	12.53	4
CADAFLAP00011296	pep:known supercontig:JCVI-afl1-v2.0:EQ963483:1474009:1474914:-1 gene:CADAFLAG00011296 transcript:CADAFLAT00011296 description: Peroxiredoxin 5, prdx5, putative	13.26	24.78	3
CADAFLAP00005048	pep:known supercontig:JCVI-afl1-v2.0:EQ963475:2393680:2394488:-1 gene:CADAFLAG00005048 transcript:CADAFLAT00005048 description: Cytochrome b-c1 complex subunit 7	13.25	46.34	3
CADAFLAP00003168	pep:known supercontig:JCVI-afl1-v2.0:EQ963473:4131777:4132735:-1 gene:CADAFLAG00003168 transcript:CADAFLAT00003168 description: 6,7-dimethyl-8-ribityllumazine synthase	13.14	32.69	3
CADAFLAP00010900	pep:known supercontig:JCVI-afl1-v2.0:EQ963483:340611:341885:-1 gene:CADAFLAG00010900 transcript:CADAFLAT00010900 description: Biotin synthase, putative	12.98	17.01	3
CADAFLAP00000821	pep:known supercontig:JCVI-afl1-v2.0:EQ963472:2194851:2195651:1 gene:CADAFLAG00000821 transcript:CADAFLAT00000821 description: 6-phosphogluconolactonase, putative	12.95	19.17	2
CADAFLAP00004132	pep:known supercontig:JCVI-afl1-v2.0:EQ963474:2642668:2643673:-1 gene:CADAFLAG00004132 transcript:CADAFLAT00004132 description: Adenylate kinase, putative	12.86	17.83	3
CADAFLAP00011127	pep:known supercontig:JCVI-afl1-v2.0:EQ963483:994025:997698:1 gene:CADAFLAG00011127	12.70	6.56	5

	transcript:CADAFLAT00011127 description: Putative uncharacterized protein			
CADAFLAP00010876	pep:known supercontig:JCVI-afl1-v2.0:EQ963483:263704:265682:1 gene:CADAFLAG00010876 transcript:CADAFLAT00010876 description: Adenosine kinase, putative	12.59	14.45	3
CADAFLAP00000615	pep:known supercontig:JCVI-afl1-v2.0:EQ963472:1608276:1609022:-1 gene:CADAFLAG00000615 transcript:CADAFLAT00000615 description: Putative uncharacterized protein	12.59	35.44	2
CADAFLAP00010522	pep:known supercontig:JCVI-afl1-v2.0:EQ963482:1158813:1161211:-1 gene:CADAFLAG00010522 transcript:CADAFLAT00010522 description: Vacuolar ATP synthase catalytic subunit A, putative	12.56	7.88	4
CADAFLAP00001654	pep:known supercontig:JCVI-afl1-v2.0:EQ963472:4430385:4431686:1 gene:CADAFLAG00001654 transcript:CADAFLAT00001654 description: Septin	12.43	17.14	2
CADAFLAP00005666	pep:known supercontig:JCVI-afl1-v2.0:EQ963476:1355059:1357376:-1 gene:CADAFLAG00005666 transcript:CADAFLAT00005666 description: Hsp70 chaperone (BiP), putative	12.35	6.56	2
CADAFLAP00007133	pep:known supercontig:JCVI-afl1-v2.0:EQ963478:393076:393514:-1 gene:CADAFLAG00007133 transcript:CADAFLAT00007133 description: Thioredoxin	12.32	56.36	4
CADAFLAP00003090	pep:known supercontig:JCVI-afl1-v2.0:EQ963473:3915922:3916963:-1 gene:CADAFLAG00003090 transcript:CADAFLAT00003090 description: Thiamine thiazole synthase	12.22	15.29	3
CADAFLAP00001172	pep:known supercontig:JCVI-afl1-v2.0:EQ963472:3128262:3129740:-1 gene:CADAFLAG00001172 transcript:CADAFLAT00001172 description: Adenylosuccinate synthetase	12.17	13.92	3

CADAFLAP00005511	pep:known supercontig:JCVI-afl1-v2.0:EQ963476:970387:973645:-1 gene:CADAFLAG00005511 transcript:CADAFLAT00005511 description: Glycine dehydrogenase	12.14	4.70	4
CADAFLAP00008169	pep:known supercontig:JCVI-afl1-v2.0:EQ963479:854304:854984:-1 gene:CADAFLAG00008169 transcript:CADAFLAT00008169 description: Glycine cleavage system H protein	11.91	21.97	3
CADAFLAP00004803	pep:known supercontig:JCVI-afl1-v2.0:EQ963475:1739599:1740743:-1 gene:CADAFLAG00004803 transcript:CADAFLAT00004803 description: Cytochrome c peroxidase Ccp1, putative	11.88	17.68	5
CADAFLAP00011329	pep:known supercontig:JCVI-afl1-v2.0:EQ963483:1576033:1577407:-1 gene:CADAFLAG00011329 transcript:CADAFLAT00011329 description: GPI-anchored cell wall beta-1,3-endoglucanase EglC	11.72	12.00	3
CADAFLAP00003123	pep:known supercontig:JCVI-afl1-v2.0:EQ963473:4012526:4014367:-1 gene:CADAFLAG00003123 transcript:CADAFLAT00003123 description: 14-3-3 protein sigma, gamma, zeta, beta/alpha, putative	11.49	14.93	2
CADAFLAP00007231	pep:known supercontig:JCVI-afl1-v2.0:EQ963478:656101:659152:-1 gene:CADAFLAG00007231 transcript:CADAFLAT00007231 description: Coatomer subunit gamma	11.40	7.76	4
CADAFLAP00002125	pep:known supercontig:JCVI-afl1-v2.0:EQ963473:1267436:1269626:-1 gene:CADAFLAG00002125 transcript:CADAFLAT00002125 description: Mannose-1-phosphate guanylyltransferase	11.27	12.64	3
CADAFLAP00004476	pep:known supercontig:JCVI-afl1-v2.0:EQ963475:852712:854356:1 gene:CADAFLAG00004476	11.19	10.09	4

	transcript:CADAFLAT00004476 description: Putative uncharacterized protein			
CADAFLAP00006550	pep:known supercontig:JCVI-afl1-v2.0:EQ963477:1254389:1256272:-1 gene:CADAFLAG00006550 transcript:CADAFLAT00006550 description: Lysophospholipase Plb3	10.98	6.86	2
CADAFLAP00006846	pep:known supercontig:JCVI-afl1-v2.0:EQ963477:2049774:2051918:-1 gene:CADAFLAG00006846 transcript:CADAFLAT00006846 description: Mitochondrial outer membrane translocase receptor (TOM70), putative	10.94	8.78	3
CADAFLAP00009916	pep:known supercontig:JCVI-afl1-v2.0:EQ963481:1465611:1466733:-1 gene:CADAFLAG00009916 transcript:CADAFLAT00009916 description: NADH-ubiquinone oxidoreductase 304 kDa subunit	10.92	11.93	3
CADAFLAP00003443	pep:known supercontig:JCVI-afl1-v2.0:EQ963474:746114:746914:-1 gene:CADAFLAG00003443 transcript:CADAFLAT00003443 description: Sorbitol/xylulose reductase Sou1-like, putative	10.90	15.04	3
CADAFLAP00010529	pep:known supercontig:JCVI-afl1-v2.0:EQ963482:1182356:1183466:1 gene:CADAFLAG00010529 transcript:CADAFLAT00010529 description: Farnesyl-pyrophosphate synthetase	10.84	14.45	3
CADAFLAP00012537	pep:known supercontig:JCVI-afl1-v2.0:EQ963485:1037267:1038033:1 gene:CADAFLAG00012537 transcript:CADAFLAT00012537 description: Cytochrome c oxidase subunit V	10.82	19.80	3
CADAFLAP00009819	pep:known supercontig:JCVI-afl1-v2.0:EQ963481:1185002:1185702:-1 gene:CADAFLAG00009819 transcript:CADAFLAT00009819 description: High expression lethality protein Hel10, putative	10.74	19.52	2

CADAFLAP00010152	pep:known supercontig:JCVI-afl1-v2.0:EQ963482:105553:107622:1 gene:CADAFLAG00010152 transcript:CADAFLAT00010152 description: Tripeptidyl peptidase A	10.66	7.24	3
CADAFLAP00001225	pep:known supercontig:JCVI-afl1-v2.0:EQ963472:3269096:3271882:1 gene:CADAFLAG00001225 transcript:CADAFLAT00001225 description: Heat shock protein Hsp98/Hsp104/ClpA, putative	10.62	4.96	3
CADAFLAP00001441	pep:known supercontig:JCVI-afl1-v2.0:EQ963472:3840027:3842016:-1 gene:CADAFLAG00001441 transcript:CADAFLAT00001441 description: Glucose-6-phosphate 1-dehydrogenase	10.51	7.19	3
CADAFLAP00011162	pep:known supercontig:JCVI-afl1-v2.0:EQ963483:1090790:1092713:1 gene:CADAFLAG00011162 transcript:CADAFLAT00011162 description: Histidyl-tRNA synthetase, mitochondrial	10.50	8.67	3
CADAFLAP00000900	pep:known supercontig:JCVI-afl1-v2.0:EQ963472:2408387:2408762:1 gene:CADAFLAG00000900 transcript:CADAFLAT00000900 description: Putative uncharacterized protein	10.41	21.70	2
CADAFLAP00001377	pep:known supercontig:JCVI-afl1-v2.0:EQ963472:3693037:3694319:-1 gene:CADAFLAG00001377 transcript:CADAFLAT00001377 description: Regulatory protein SUAPRGA1	10.29	15.48	2
CADAFLAP00000112	pep:known supercontig:JCVI-afl1-v2.0:EQ963472:278577:279866:-1 gene:CADAFLAG00000112 transcript:CADAFLAT00000112 description: Phospho-2-dehydro-3-deoxyheptonate aldolase	10.27	14.84	3
CADAFLAP00006606	pep:known supercontig:JCVI-afl1-v2.0:EQ963477:1393864:1394858:-1 gene:CADAFLAG00006606 transcript:CADAFLAT00006606 description: Short-chain dehydrogenase, putative	10.17	11.29	2

CADAFLAP00002908	pep:known supercontig:JCVI-afl1-v2.0:EQ963473:3381094:3383319:1 gene:CADAFLAG00002908 transcript:CADAFLAT00002908 description: Translation release factor eRF3, putative	10.00	5.26	3
CADAFLAP00004961	pep:known supercontig:JCVI-afl1-v2.0:EQ963475:2145208:2146877:-1 gene:CADAFLAG00004961 transcript:CADAFLAT00004961 description: Translation initiation factor EF-2 gamma subunit, putative	10.00	7.21	2
CADAFLAP00005782	pep:known supercontig:JCVI-afl1-v2.0:EQ963476:1687295:1691114:-1 gene:CADAFLAG00005782 transcript:CADAFLAT00005782 description: Carbamoyl-phosphate synthase, large subunit	9.94	4.00	3
CADAFLAP00003913	pep:known supercontig:JCVI-afl1-v2.0:EQ963474:2040098:2040947:-1 gene:CADAFLAG00003913 transcript:CADAFLAT00003913 description: Glycolipid transfer protein HET-C2, putative	9.93	21.36	4
CADAFLAP00004054	pep:known supercontig:JCVI-afl1-v2.0:EQ963474:2429854:2430648:-1 gene:CADAFLAG00004054 transcript:CADAFLAT00004054 description: Vacuolar protein sorting 29, putative	9.76	15.08	3
CADAFLAP00002255	pep:known supercontig:JCVI-afl1-v2.0:EQ963473:1611987:1612752:1 gene:CADAFLAG00002255 transcript:CADAFLAT00002255 description: Eukaryotic translation initiation factor eIF-5A	9.74	18.87	2
CADAFLAP00001169	pep:known supercontig:JCVI-afl1-v2.0:EQ963472:3121243:3122277:-1 gene:CADAFLAG00001169 transcript:CADAFLAT00001169 description: Oxidoreductase, zinc-binding dehydrogenase family, putative	9.73	13.37	2
CADAFLAP00010782	pep:known supercontig:JCVI-afl1-v2.0:EQ963482:1923985:1926988:1 gene:CADAFLAG00010782	9.62	7.46	3

	transcript:CADAFLAT00010782 description: NADH-ubiquinone oxidoreductase, subunit G, putative			
CADAFLAP00011168	pep:known supercontig:JCVI-afl1-v2.0:EQ963483:1109402:1110828:1 gene:CADAFLAG00011168 transcript:CADAFLAT00011168 description: Thioredoxin reductase	9.56	11.05	3
CADAFLAP00005370	pep:known supercontig:JCVI-afl1-v2.0:EQ963476:605539:607474:1 gene:CADAFLAG00005370 transcript:CADAFLAT00005370 description: Tripeptidyl-peptidase (TppA), putative	9.52	10.30	3
CADAFLAP00010894	pep:known supercontig:JCVI-afl1-v2.0:EQ963483:323423:324843:1 gene:CADAFLAG00010894 transcript:CADAFLAT00010894 description: Acyl-CoA dehydrogenase family protein	9.38	12.37	4
CADAFLAP00012536	pep:known supercontig:JCVI-afl1-v2.0:EQ963485:1035656:1036394:1 gene:CADAFLAG00012536 transcript:CADAFLAT00012536 description: Cofilin	9.28	21.71	2
CADAFLAP00005517	pep:known supercontig:JCVI-afl1-v2.0:EQ963476:985490:987320:1 gene:CADAFLAG00005517 transcript:CADAFLAT00005517 description: Amidase family protein	9.20	6.07	2
CADAFLAP00008397	pep:known supercontig:JCVI-afl1-v2.0:EQ963479:1487900:1488990:1 gene:CADAFLAG00008397 transcript:CADAFLAT00008397 description: HMG box protein, putative	9.02	9.94	3
CADAFLAP00006294	pep:known supercontig:JCVI-afl1-v2.0:EQ963477:608184:609203:-1 gene:CADAFLAG00006294 transcript:CADAFLAT00006294 description: Electron transfer flavoprotein, beta subunit, putative	9.01	17.24	2
CADAFLAP00003002	pep:known supercontig:JCVI-afl1-v2.0:EQ963473:3651138:3653277:1 gene:CADAFLAG00003002	9.00	5.30	2

	transcript:CADAFLAT00003002 description: Lysine--tRNA ligase			
CADAFLAP00003408	pep:known supercontig:JCVI-afl1-v2.0:EQ963474:642407:646201:-1 gene:CADAFLAG00003408 transcript:CADAFLAT00003408 description: Poly(A)+ RNA transport protein (UbaA), putative	8.93	3.87	2
CADAFLAP00001560	pep:known supercontig:JCVI-afl1-v2.0:EQ963472:4189783:4191067:-1 gene:CADAFLAG00001560 transcript:CADAFLAT00001560 description: Cell wall integrity signaling protein Lsp1/Pil1, putative	8.91	13.26	4
CADAFLAP00000955	pep:known supercontig:JCVI-afl1-v2.0:EQ963472:2537554:2539608:1 gene:CADAFLAG00000955 transcript:CADAFLAT00000955 description: T-complex protein 1, beta subunit, putative	8.88	8.54	3
CADAFLAP00012054	pep:known supercontig:JCVI-afl1-v2.0:EQ963484:1559155:1559949:-1 gene:CADAFLAG00012054 transcript:CADAFLAT00012054 description: Cytochrome c oxidase subunit 6A, mitochondrial	8.81	23.57	3
CADAFLAP00001610	pep:known supercontig:JCVI-afl1-v2.0:EQ963472:4319148:4320367:-1 gene:CADAFLAG00001610 transcript:CADAFLAT00001610 description: Protein phosphatase 2C, putative	8.79	19.23	4
CADAFLAP00010841	pep:known supercontig:JCVI-afl1-v2.0:EQ963483:149516:150784:-1 gene:CADAFLAG00010841 transcript:CADAFLAT00010841 description: Eukaryotic translation initiation factor 6	8.73	13.36	2
CADAFLAP00008897	pep:known supercontig:JCVI-afl1-v2.0:EQ963480:810638:811224:1 gene:CADAFLAG00008897 transcript:CADAFLAT00008897 description: 40S ribosomal protein S21	8.71	31.82	2

CADAFLAP00010809	pep:known supercontig:JCVI-afl1-v2.0:EQ963483:53550:55891:1 gene:CADAFLAG00010809 transcript:CADAFLAT00010809 description: Peptide chain release factor eRF/aRF, subunit 1	8.70	6.91	2
CADAFLAP00007535	pep:known supercontig:JCVI-afl1-v2.0:EQ963478:1523778:1525000:1 gene:CADAFLAG00007535 transcript:CADAFLAT00007535 description: Cytochrome c	8.66	28.57	4
CADAFLAP00006797	pep:known supercontig:JCVI-afl1-v2.0:EQ963477:1919835:1920884:-1 gene:CADAFLAG00006797 transcript:CADAFLAT00006797 description: Pyridoxine biosynthesis protein	8.58	11.94	3
CADAFLAP00005750	pep:known supercontig:JCVI-afl1-v2.0:EQ963476:1592217:1593782:-1 gene:CADAFLAG00005750 transcript:CADAFLAT00005750 description: Eukaryotic translation initiation factor 3 subunit L	8.54	10.29	2
CADAFLAP00006296	pep:known supercontig:JCVI-afl1-v2.0:EQ963477:612587:613087:-1 gene:CADAFLAG00006296 transcript:CADAFLAT00006296 description: Putative uncharacterized protein	8.53	29.91	2
CADAFLAP00003656	pep:known supercontig:JCVI-afl1-v2.0:EQ963474:1321916:1325271:1 gene:CADAFLAG00003656 transcript:CADAFLAT00003656 description: Isoleucyl-tRNA synthetase ,cytoplasmic	8.52	3.25	3
CADAFLAP00008958	pep:known supercontig:JCVI-afl1-v2.0:EQ963480:972854:976241:1 gene:CADAFLAG00008958 transcript:CADAFLAT00008958 description: 26S proteasome regulatory subunit Mts4, putative	8.38	4.08	2
CADAFLAP00003396	pep:known supercontig:JCVI-afl1-v2.0:EQ963474:610392:614120:1 gene:CADAFLAG00003396 transcript:CADAFLAT00003396 description: Putative uncharacterized protein	8.36	3.46	2
CADAFLAP00003711	pep:known supercontig:JCVI-afl1-v2.0:EQ963474:1483345:1484037:1 gene:CADAFLAG00003711	8.29	40.66	3

	transcript:CADAFLAT00003711 description: DUF543 domain protein			
CADAFLAP00004474	pep:known supercontig:JCVI-afl1-v2.0:EQ963475:845682:847178:1 gene:CADAFLAG00004474 transcript:CADAFLAT00004474 description: PWWP domain protein	8.29	8.33	2
CADAFLAP00000466	pep:known supercontig:JCVI-afl1-v2.0:EQ963472:1225891:1226959:1 gene:CADAFLAG00000466 transcript:CADAFLAT00000466 description: Proteasome subunit alpha type	8.20	13.98	2
CADAFLAP00001306	pep:known supercontig:JCVI-afl1-v2.0:EQ963472:3519922:3522070:-1 gene:CADAFLAG00001306 transcript:CADAFLAT00001306 description: T-complex protein 1, zeta subunit, putative	8.17	7.22	2
CADAFLAP00003920	pep:known supercontig:JCVI-afl1-v2.0:EQ963474:2057962:2059092:1 gene:CADAFLAG00003920 transcript:CADAFLAT00003920 description: Translation initiation factor 2 alpha subunit, putative	8.16	11.04	2
CADAFLAP00002078	pep:known supercontig:JCVI-afl1-v2.0:EQ963473:1113350:1115227:1 gene:CADAFLAG00002078 transcript:CADAFLAT00002078 description: NADH-ubiquinone oxidoreductase, subunit F, putative	8.10	8.27	3
CADAFLAP00011816	pep:known supercontig:JCVI-afl1-v2.0:EQ963484:968882:970564:1 gene:CADAFLAG00011816 transcript:CADAFLAT00011816 description: Proteasome regulatory particle subunit (RpnE), putative	8.09	10.44	5
CADAFLAP00004126	pep:known supercontig:JCVI-afl1-v2.0:EQ963474:2631558:2632519:1 gene:CADAFLAG00004126 transcript:CADAFLAT00004126 description: Coproporphyrinogen III oxidase, putative	8.05	17.01	3
CADAFLAP00007673	pep:known supercontig:JCVI-afl1-v2.0:EQ963478:1896694:1899127:-1	8.04	4.80	3

	gene:CADAFLAG00007673 transcript:CADAFLAT00007673 description: Arginyl-tRNA synthetase			
CADAFLAP00004367	pep:known supercontig:JCVI-afl1-v2.0:EQ963475:561390:562542:-1 gene:CADAFLAG00004367 transcript:CADAFLAT00004367 description: Chaperonin, putative	7.94	33.65	2
CADAFLAP00003018	pep:known supercontig:JCVI-afl1-v2.0:EQ963473:3699245:3700840:1 gene:CADAFLAG00003018 transcript:CADAFLAT00003018 description: Proteasome regulatory particle subunit (RpnG), putative	7.91	7.54	2
CADAFLAP00006424	pep:known supercontig:JCVI-afl1-v2.0:EQ963477:963504:965147:1 gene:CADAFLAG00006424 transcript:CADAFLAT00006424 description: Myo-inositol-phosphate synthase, putative	7.83	4.33	2
CADAFLAP00008304	pep:known supercontig:JCVI-afl1-v2.0:EQ963479:1226718:1228096:-1 gene:CADAFLAG00008304 transcript:CADAFLAT00008304 description: Vacuolar ATP synthase subunit c	7.83	6.98	2
CADAFLAP00005800	pep:known supercontig:JCVI-afl1-v2.0:EQ963476:1758125:1759528:-1 gene:CADAFLAG00005800 transcript:CADAFLAT00005800 description: Oxidoreductase, 2-nitropropane dioxygenase family, putative	7.75	17.55	3
CADAFLAP00008571	pep:known supercontig:JCVI-afl1-v2.0:EQ963479:2005255:2005977:-1 gene:CADAFLAG00008571 transcript:CADAFLAT00008571 description: Adenine phosphoribosyltransferase 1	7.73	15.35	2
CADAFLAP00010797	pep:known supercontig:JCVI-afl1-v2.0:EQ963483:26281:28266:1 gene:CADAFLAG00010797 transcript:CADAFLAT00010797 description: Nucleosome assembly protein Nap1, putative	7.72	7.56	2
CADAFLAP00000159	pep:known supercontig:JCVI-afl1-v2.0:EQ963472:399440:404950:1 gene:CADAFLAG00000159	7.69	2.16	2

	transcript:CADAFLAT00000159 description: DNA mismatch repair protein Msh3			
CADAFLAP00012069	pep:known supercontig:JCVI-afl1-v2.0:EQ963484:1600944:1604823:1 gene:CADAFLAG00012069 transcript:CADAFLAT00012069 description: Glutaryl-CoA dehydrogenase, putative	7.56	7.16	2
CADAFLAP00001396	pep:known supercontig:JCVI-afl1-v2.0:EQ963472:3729553:3730457:1 gene:CADAFLAG00001396 transcript:CADAFLAT00001396 description: Proteasome regulatory particle subunit (RpnL), putative	7.54	11.79	2
CADAFLAP00003954	pep:known supercontig:JCVI-afl1-v2.0:EQ963474:2145939:2148377:-1 gene:CADAFLAG00003954 transcript:CADAFLAT00003954 description: Extracellular serine-threonine rich protein	7.51	3.60	2
CADAFLAP00010793	pep:known supercontig:JCVI-afl1-v2.0:EQ963483:12255:14350:1 gene:CADAFLAG00010793 transcript:CADAFLAT00010793 description: Seryl-tRNA synthetase	7.44	7.59	2
CADAFLAP00009049	pep:known supercontig:JCVI-afl1-v2.0:EQ963480:1237178:1238343:1 gene:CADAFLAG00009049 transcript:CADAFLAT00009049 description: U6 small nuclear ribonucleoprotein (Lsm3), putative	7.39	19.79	2
CADAFLAP00011080	pep:known supercontig:JCVI-afl1-v2.0:EQ963483:847581:849011:-1 gene:CADAFLAG00011080 transcript:CADAFLAT00011080 description: GTP binding protein, putative	7.32	8.29	2
CADAFLAP00011733	pep:known supercontig:JCVI-afl1-v2.0:EQ963484:767101:768632:1 gene:CADAFLAG00011733 transcript:CADAFLAT00011733 description: Argininosuccinate lyase	7.31	9.91	3
CADAFLAP00003945	pep:known supercontig:JCVI-afl1-v2.0:EQ963474:2120397:2123780:1 gene:CADAFLAG00003945	7.25	2.93	2

	transcript:CADAFLAT00003945 description: AT DNA binding protein, putative			
CADAFLAP00003436	pep:known supercontig:JCVI-afl1-v2.0:EQ963474:729033:729625:1 gene:CADAFLAG00003436 transcript:CADAFLAT00003436 description: Small nuclear ribonucleoprotein SmF, putative	7.21	27.27	2
CADAFLAP00007209	pep:known supercontig:JCVI-afl1-v2.0:EQ963478:598013:601062:-1 gene:CADAFLAG00007209 transcript:CADAFLAT00007209 description: Putative uncharacterized protein	7.19	5.60	4
CADAFLAP00011085	pep:known supercontig:JCVI-afl1-v2.0:EQ963483:864750:867278:1 gene:CADAFLAG00011085 transcript:CADAFLAT00011085 description: Phenylalanyl-tRNA synthetase, beta subunit	7.11	7.33	4
CADAFLAP00001521	pep:known supercontig:JCVI-afl1-v2.0:EQ963472:4060096:4061067:1 gene:CADAFLAG00001521 transcript:CADAFLAT00001521 description: Allergen Asp F4	7.11	8.98	2
CADAFLAP00003465	pep:known supercontig:JCVI-afl1-v2.0:EQ963474:823210:823787:1 gene:CADAFLAG00003465 transcript:CADAFLAT00003465 description: DUF636 domain protein	7.10	27.41	2
CADAFLAP00011105	pep:known supercontig:JCVI-afl1-v2.0:EQ963483:925817:928707:1 gene:CADAFLAG00011105 transcript:CADAFLAT00011105 description: Probable beta-glucosidase A	7.09	3.25	2
CADAFLAP00009242	pep:known supercontig:JCVI-afl1-v2.0:EQ963480:1737558:1740029:-1 gene:CADAFLAG00009242 transcript:CADAFLAT00009242 description: RNA annealing protein Yra1, putative	7.08	12.55	2
CADAFLAP00010024	pep:known supercontig:JCVI-afl1-v2.0:EQ963481:1758485:1759513:1 gene:CADAFLAG00010024	6.82	24.75	2

	transcript:CADAFLAT00010024 description: Mitochondrial F1F0 ATP synthase subunit F (Atp17), putative			
CADAFLAP00004517	pep:known supercontig:JCVI-afl1-v2.0:EQ963475:958618:959261:1 gene:CADAFLAG00004517 transcript:CADAFLAT00004517 description: Heterogeneous nuclear ribonucleoprotein G, putative	6.74	25.60	2
CADAFLAP00012790	pep:known supercontig:JCVI-afl1-v2.0:EQ963485:1639564:1641913:1 gene:CADAFLAG00012790 transcript:CADAFLAT00012790 description: Putative uncharacterized protein	6.65	4.34	2
CADAFLAP00003985	pep:known supercontig:JCVI-afl1-v2.0:EQ963474:2246125:2248381:1 gene:CADAFLAG00003985 transcript:CADAFLAT00003985 description: Putative uncharacterized protein	6.64	8.65	4
CADAFLAP00006819	pep:known supercontig:JCVI-afl1-v2.0:EQ963477:1971753:1973048:-1 gene:CADAFLAG00006819 transcript:CADAFLAT00006819 description: HAD superfamily hydrolase, putative	6.63	11.33	2
CADAFLAP00008134	pep:known supercontig:JCVI-afl1-v2.0:EQ963479:782915:783817:1 gene:CADAFLAG00008134 transcript:CADAFLAT00008134 description: Mitochondrial hypoxia responsive domain protein	6.51	12.26	2
CADAFLAP00002649	pep:known supercontig:JCVI-afl1-v2.0:EQ963473:2694524:2696851:-1 gene:CADAFLAG00002649 transcript:CADAFLAT00002649 description: Transcription factor TFIID	6.50	10.65	2
CADAFLAP00007021	pep:known supercontig:JCVI-afl1-v2.0:EQ963478:109179:109826:-1 gene:CADAFLAG00007021 transcript:CADAFLAT00007021 description: Uridylate kinase Ura6	6.50	19.07	3
CADAFLAP00002988	pep:known supercontig:JCVI-afl1-v2.0:EQ963473:3602772:3604380:1 gene:CADAFLAG00002988	6.47	5.85	2

	transcript:CADAFLAT00002988 description: 14-alpha sterol demethylase Cyp51A			
CADAFLAP00000923	pep:known supercontig:JCVI-afl1-v2.0:EQ963472:2466299:2468724:-1 gene:CADAFLAG00000923 transcript:CADAFLAT00000923 description: Eukaryotic translation initiation factor 3 subunit B	6.41	5.53	2
CADAFLAP00002839	pep:known supercontig:JCVI-afl1-v2.0:EQ963473:3197281:3198884:-1 gene:CADAFLAG00002839 transcript:CADAFLAT00002839 description: Aminopeptidase Y, putative	6.36	7.46	2
CADAFLAP00007137	pep:known supercontig:JCVI-afl1-v2.0:EQ963478:407120:408702:1 gene:CADAFLAG00007137 transcript:CADAFLAT00007137 description: Ndc80 complex component Nuf2, putative	6.27	5.62	2
CADAFLAP00001407	pep:known supercontig:JCVI-afl1-v2.0:EQ963472:3753100:3753739:-1 gene:CADAFLAG00001407 transcript:CADAFLAT00001407 description: NADH-ubiquinone oxidoreductase subunit GRIM-19, putative	6.15	24.37	2
CADAFLAP00002744	pep:known supercontig:JCVI-afl1-v2.0:EQ963473:2952676:2953540:-1 gene:CADAFLAG00002744 transcript:CADAFLAT00002744 description: 60S ribosomal protein L31e	6.14	24.39	3
CADAFLAP00004630	pep:known supercontig:JCVI-afl1-v2.0:EQ963475:1251452:1261685:-1 gene:CADAFLAG00004630 transcript:CADAFLAT00004630 description: Bifunctional pyrimidine biosynthesis protein (PyrABCN), putative	6.10	1.38	2
CADAFLAP00004086	pep:known supercontig:JCVI-afl1-v2.0:EQ963474:2523604:2524029:-1 gene:CADAFLAG00004086 transcript:CADAFLAT00004086 description: Cyclin, putative	6.07	14.89	2

CADAFLAP00000806	pep:known supercontig:JCVI-afl1-v2.0:EQ963472:2150666:2151679:1 gene:CADAFLAG00000806 transcript:CADAFLAT00000806 description: ATP synthase delta chain, mitochondrial, putative	6.02	15.76	2
CADAFLAP00012531	pep:known supercontig:JCVI-afl1-v2.0:EQ963485:1024395:1025389:1 gene:CADAFLAG00012531 transcript:CADAFLAT00012531 description: Cytochrome b-c1 complex subunit Rieske, mitochondrial	5.99	9.70	2
CADAFLAP00008416	pep:known supercontig:JCVI-afl1-v2.0:EQ963479:1543060:1544660:1 gene:CADAFLAG00008416 transcript:CADAFLAT00008416 description: GTP-binding protein YchF	5.98	7.61	3
CADAFLAP00004407	pep:known supercontig:JCVI-afl1-v2.0:EQ963475:666658:667423:1 gene:CADAFLAG00004407 transcript:CADAFLAT00004407 description: Putative uncharacterized protein	5.86	18.56	2
CADAFLAP00001442	pep:known supercontig:JCVI-afl1-v2.0:EQ963472:3844806:3845594:1 gene:CADAFLAG00001442 transcript:CADAFLAT00001442 description: 60S ribosomal protein L35Ae	5.81	20.18	2
CADAFLAP00009833	pep:known supercontig:JCVI-afl1-v2.0:EQ963481:1221618:1223919:-1 gene:CADAFLAG00009833 transcript:CADAFLAT00009833 description: T-complex protein 1, eta subunit, putative	5.76	4.96	2
CADAFLAP00012842	pep:known supercontig:JCVI-afl1-v2.0:EQ963485:1779350:1781866:-1 gene:CADAFLAG00012842 transcript:CADAFLAT00012842 description: Dynamin-like GTPase Dnm1, putative	5.62	7.25	3
CADAFLAP00003000	pep:known supercontig:JCVI-afl1-v2.0:EQ963473:3645119:3646581:-1 gene:CADAFLAG00003000 transcript:CADAFLAT00003000 description: GDP-mannose pyrophosphorylase A	5.47	4.55	2

CADAFLAP00000446	pep:known supercontig:JCVI-afl1-v2.0:EQ963472:1168101:1171036:-1 gene:CADAFLAG00000446 transcript:CADAFLAT00000446 description: Phospholipase PldA, putative	5.33	3.48	2
CADAFLAP00012129	pep:known supercontig:JCVI-afl1-v2.0:EQ963484:1770107:1771836:1 gene:CADAFLAG00012129 transcript:CADAFLAT00012129 description: Glutamate carboxypeptidase, putative	5.31	6.69	2
CADAFLAP00010794	pep:known supercontig:JCVI-afl1-v2.0:EQ963483:14880:16652:1 gene:CADAFLAG00010794 transcript:CADAFLAT00010794 description: D-3-phosphoglycerate dehydrogenase	5.27	10.14	3
CADAFLAP00005919	pep:known supercontig:JCVI-afl1-v2.0:EQ963476:2058659:2059803:1 gene:CADAFLAG00005919 transcript:CADAFLAT00005919 description: Prohibitin, putative	5.19	6.45	2
CADAFLAP00007321	pep:known supercontig:JCVI-afl1-v2.0:EQ963478:905684:906783:-1 gene:CADAFLAG00007321 transcript:CADAFLAT00007321 description: Very-long-chain 3-oxoacyl-CoA reductase	5.16	8.09	2
CADAFLAP00012136	pep:known supercontig:JCVI-afl1-v2.0:EQ963484:1789263:1791559:-1 gene:CADAFLAG00012136 transcript:CADAFLAT00012136 description: Dihydrolipoamide succinyltransferase, putative	5.16	7.34	2
CADAFLAP00008525	pep:known supercontig:JCVI-afl1-v2.0:EQ963479:1879017:1880919:-1 gene:CADAFLAG00008525 transcript:CADAFLAT00008525 description: Heat shock protein (Sti1), putative	5.15	7.25	2
CADAFLAP00002511	pep:known supercontig:JCVI-afl1-v2.0:EQ963473:2306586:2309501:1 gene:CADAFLAG00002511 transcript:CADAFLAT00002511 description: Proteasome component Prs2, putative	5.08	5.26	3
CADAFLAP00004416	pep:known supercontig:JCVI-afl1-v2.0:EQ963475:691946:693316:1 gene:CADAFLAG00004416	4.90	8.11	2

	transcript:CADAFLAT00004416 description: Guanine deaminase, putative			
CADAFLAP00011623	pep:known supercontig:JCVI-afl1-v2.0:EQ963484:427912:434348:1 gene:CADAFLAG00011623 transcript:CADAFLAT00011623 description: Putative uncharacterized protein	4.87	8.14	2
CADAFLAP00008254	pep:known supercontig:JCVI-afl1-v2.0:EQ963479:1076124:1077159:1 gene:CADAFLAG00008254 transcript:CADAFLAT00008254 description: 1,3-beta-glucanosyltransferase Bgt1	4.86	9.54	3
CADAFLAP00005631	pep:known supercontig:JCVI-afl1-v2.0:EQ963476:1265724:1267122:-1 gene:CADAFLAG00005631 transcript:CADAFLAT00005631 description: Peptidyl-prolyl cis-trans isomerase Cpr7, putative	4.74	6.47	2
CADAFLAP00002464	pep:known supercontig:JCVI-afl1-v2.0:EQ963473:2188043:2189750:1 gene:CADAFLAG00002464 transcript:CADAFLAT00002464 description: Saccharopine dehydrogenase	4.66	5.11	2
CADAFLAP00011248	pep:known supercontig:JCVI-afl1-v2.0:EQ963483:1342686:1344281:1 gene:CADAFLAG00011248 transcript:CADAFLAT00011248 description: MAP kinase MpkA	4.58	7.33	2
CADAFLAP00005043	pep:known supercontig:JCVI-afl1-v2.0:EQ963475:2371632:2372231:-1 gene:CADAFLAG00005043 transcript:CADAFLAT00005043 description: Putative uncharacterized protein	4.53	14.29	2
CADAFLAP00001573	pep:known supercontig:JCVI-afl1-v2.0:EQ963472:4234480:4235839:-1 gene:CADAFLAG00001573 transcript:CADAFLAT00001573 description: Isocitrate dehydrogenase LysB	4.36	5.71	2
CADAFLAP00001461	pep:known supercontig:JCVI-afl1-v2.0:EQ963472:3885396:3886384:-1 gene:CADAFLAG00001461 transcript:CADAFLAT00001461	4.31	11.34	2

	description: Pyruvate dehydrogenase complex component Pdx1, putative			
CADAFLAP00007346	pep:known supercontig:JCVI-afl1-v2.0:EQ963478:977556:978845:1 gene:CADAFLAG00007346 transcript:CADAFLAT00007346 description: Probable DNA-binding protein creA	3.96	12.82	2
CADAFLAP00009247	pep:known supercontig:JCVI-afl1-v2.0:EQ963480:1747029:1748679:1 gene:CADAFLAG00009247 transcript:CADAFLAT00009247 description: CCCH finger DNA binding protein, putative	3.92	6.80	2
CADAFLAP00002119	pep:known supercontig:JCVI-afl1-v2.0:EQ963473:1241406:1244748:1 gene:CADAFLAG00002119 transcript:CADAFLAT00002119 description: Aminotransferase, classes I and II, putative	3.75	3.43	2
CADAFLAP00002472	pep:known supercontig:JCVI-afl1-v2.0:EQ963473:2209434:2210639:-1 gene:CADAFLAG00002472 transcript:CADAFLAT00002472 description: Homoserine dehydrogenase	2.86	10.57	2
CADAFLAP00010316	pep:known supercontig:JCVI-afl1-v2.0:EQ963482:539641:540869:1 gene:CADAFLAG00010316 transcript:CADAFLAT00010316 description: Succinate:fumarate antiporter (Acr1), putative	2.57	6.97	2
CADAFLAP00002339	pep:known supercontig:JCVI-afl1-v2.0:EQ963473:1828986:1829568:1 gene:CADAFLAG00002339 transcript:CADAFLAT00002339 description: Dynein light chain type 1, putative	2.38	15.96	2
CADAFLAP00003653	pep:known supercontig:JCVI-afl1-v2.0:EQ963474:1308050:1312938:-1 gene:CADAFLAG00003653 transcript:CADAFLAT00003653 description: Pentafunctional AROM polypeptide 3-dehydroquinate synthase 3-phosphoshikimate 1-carboxyvinyltransferase Shikimate kinase 3-dehydroquinate dehydratase Shikimate dehydrogenase	2.04	1.39	2

CADAFLAP00005860	pep:known supercontig:JCVI-afl1-v2.0:EQ963476:1897595:1902056:1 gene:CADAFLAG00005860 transcript:CADAFLAT00005860 description: Eukaryotic translation initiation factor subunit eIF-4F, putative	1.94	1.67	2
CADAFLAP00005727	pep:known supercontig:JCVI-afl1-v2.0:EQ963476:1529946:1532654:-1 gene:CADAFLAG00005727 transcript:CADAFLAT00005727 description: COPI vesicle coat beta' subunit, putative	1.65	3.05	2
CADAFLAP00002504	pep:known supercontig:JCVI-afl1-v2.0:EQ963473:2288550:2290147:1 gene:CADAFLAG00002504 transcript:CADAFLAT00002504 description: Eukaryotic translation initiation factor 3 subunit E	0.00	5.32	2
CADAFLAP00004910	pep:known supercontig:JCVI-afl1-v2.0:EQ963475:2021359:2023179:1 gene:CADAFLAG00004910 transcript:CADAFLAT00004910 description: Putative uncharacterized protein	0.00	5.31	2

Appendix B

LC-MS^2 protein lists combined from two biological replicates of KdmB::3xHA purification. Non-specific peptide contaminants were filtered out by using WT as a negative control. Green color represents KdmB and yellow color represents EcoA, RpdA, and SntB interacting partners.

Accession	Description	Score	Coverage	# Unique Peptides
CADAFLAP00010689	pep:known supercontig:JCVI-afl1-v2.0:EQ963482:1685104:1690608:-1 gene:CADAFLAG00010689 transcript:CADAFLAT00010689 description: PHD transcription factor, putative	614.53	61.97	77
CADAFLAP00002374	pep:known supercontig:JCVI-afl1-v2.0:EQ963473:1948258:1953549:1 gene:CADAFLAG00002374 transcript:CADAFLAT00002374 description: PHD finger and BAH domain protein (Snt2), putative	285.81	43.90	56
CADAFLAP00003996	pep:known supercontig:JCVI-afl1-v2.0:EQ963474:2276434:2279944:-1 gene:CADAFLAG00003996 transcript:CADAFLAT00003996 description: Histone transcription regulator Hir1, putative	232.61	53.69	39
CADAFLAP00003973	pep:known supercontig:JCVI-afl1-v2.0:EQ963474:2204554:2210905:-1 gene:CADAFLAG00003973 transcript:CADAFLAT00003973 description: Transcriptional corepressor of histone genes (Hir3), putative	216.88	30.84	47
CADAFLAP00000902	pep:known supercontig:JCVI-afl1-v2.0:EQ963472:2412375:2414764:1 gene:CADAFLAG00000902 transcript:CADAFLAT00000902 description: ARS binding protein Abp2, putative	123.93	32.61	16

CADAFLAP00010106	pep:known supercontig:JCVI-afl1-v2.0:EQ963481:2006011:2007476:-1 gene:CADAFLAG00010106 transcript:CADAFLAT00010106 description: Replication protein A 70 kDa DNA-binding subunit	83.08	53.07	18
CADAFLAP00001488	pep:known supercontig:JCVI-afl1-v2.0:EQ963472:3956565:3958794:-1 gene:CADAFLAG00001488 transcript:CADAFLAT00001488 description: C6 transcription factor (OTam), putative	81.59	32.21	14
CADAFLAP00008520	pep:known supercontig:JCVI-afl1-v2.0:EQ963479:1855567:1858665:1 gene:CADAFLAG00008520 transcript:CADAFLAT00008520 description: Involucrin, putative	71.21	18.61	8
CADAFLAP00003053	pep:known supercontig:JCVI-afl1-v2.0:EQ963473:3803535:3805320:1 gene:CADAFLAG00003053 transcript:CADAFLAT00003053 description: Putative uncharacterized protein	70.41	20.04	11
CADAFLAP00010727	pep:known supercontig:JCVI-afl1-v2.0:EQ963482:1782647:1785024:-1 gene:CADAFLAG00010727 transcript:CADAFLAT00010727 description: Spindle pole body associated protein SnaD, putative	67.50	35.94	21
CADAFLAP00004824	pep:known supercontig:JCVI-afl1-v2.0:EQ963475:1801208:1804231:1 gene:CADAFLAG00004824 transcript:CADAFLAT00004824 description: Putative uncharacterized protein	65.83	20.68	16
CADAFLAP00010101	pep:known supercontig:JCVI-afl1-v2.0:EQ963481:1995326:1996965:-1 gene:CADAFLAG00010101 transcript:CADAFLAT00010101 description: Putative uncharacterized protein	63.69	35.56	14
CADAFLAP00003012	pep:known supercontig:JCVI-afl1-v2.0:EQ963473:3679184:3681492:-1 gene:CADAFLAG00003012 transcript:CADAFLAT00003012 description: Phosphoenolpyruvate carboxykinase AcuF	60.23	29.17	12

CADAFLAP00012083	pep:known supercontig:JCVI-afl1-v2.0:EQ963484:1638349:1640768:1 gene:CADAFLAG00012083 transcript:CADAFLAT00012083 description: Histone promoter control protein, putative	51.63	12.71	7
CADAFLAP00002050	pep:known supercontig:JCVI-afl1-v2.0:EQ963473:1030614:1032169:-1 gene:CADAFLAG00002050 transcript:CADAFLAT00002050 description: AAA family ATPase Pontin, putative	50.53	37.42	12
CADAFLAP00002780	pep:known supercontig:JCVI-afl1-v2.0:EQ963473:3053401:3056239:-1 gene:CADAFLAG00002780 transcript:CADAFLAT00002780 description: Mitochondrial aconitate hydratase, putative	47.27	20.76	11
CADAFLAP00004614	pep:known supercontig:JCVI-afl1-v2.0:EQ963475:1215660:1217220:-1 gene:CADAFLAG00004614 transcript:CADAFLAT00004614 description: Aldehyde dehydrogenase AldA, putative	46.73	36.02	14
CADAFLAP00004139	pep:known supercontig:JCVI-afl1-v2.0:EQ963474:2663109:2665249:-1 gene:CADAFLAG00004139 transcript:CADAFLAT00004139 description: Cupin domain protein	42.26	24.49	10
CADAFLAP00008921	pep:known supercontig:JCVI-afl1-v2.0:EQ963480:874863:877102:1 gene:CADAFLAG00008921 transcript:CADAFLAT00008921 description: Histone deacetylase RpdA/Rpd3	41.32	25.84	12
CADAFLAP00000885	pep:known supercontig:JCVI-afl1-v2.0:EQ963472:2377479:2379339:-1 gene:CADAFLAG00000885 transcript:CADAFLAT00000885 description: AAA family ATPase Rvb2/Reptin, putative	38.25	26.17	10
CADAFLAP00012073	pep:known supercontig:JCVI-afl1-v2.0:EQ963484:1615136:1616293:1 gene:CADAFLAG00012073 transcript:CADAFLAT00012073 description: Sister chromatid cohesion acetyltransferase Eco1, putative	37.94	35.32	9

CADAFLAP00004653	pep:known supercontig:JCVI-afl1-v2.0:EQ963475:1327837:1328832:-1 gene:CADAFLAG00004653 transcript:CADAFLAT00004653 description: Possible replication factor-a protein	37.23	38.41	7
CADAFLAP00001307	pep:known supercontig:JCVI-afl1-v2.0:EQ963472:3522383:3524067:1 gene:CADAFLAG00001307 transcript:CADAFLAT00001307 description: Pre-rRNA processing nucleolar protein Sik1, putative	35.75	25.48	9
CADAFLAP00010931	pep:known supercontig:JCVI-afl1-v2.0:EQ963483:417154:418937:1 gene:CADAFLAG00010931 transcript:CADAFLAT00010931 description: Malate synthase	35.51	27.64	12
CADAFLAP00002022	pep:known supercontig:JCVI-afl1-v2.0:EQ963473:970805:972428:-1 gene:CADAFLAG00002022 transcript:CADAFLAT00002022 description: Aspartate aminotransferase	34.79	26.81	9
CADAFLAP00009067	pep:known supercontig:JCVI-afl1-v2.0:EQ963480:1291839:1292342:-1 gene:CADAFLAG00009067 transcript:CADAFLAT00009067 description: SsDNA binding protein Ssb3, putative	34.55	47.97	4
CADAFLAP00006154	pep:known supercontig:JCVI-afl1-v2.0:EQ963477:230152:231761:-1 gene:CADAFLAG00006154 transcript:CADAFLAT00006154 description: Translation elongation factor eEF-1 subunit gamma, putative	33.00	28.78	9
CADAFLAP00008559	pep:known supercontig:JCVI-afl1-v2.0:EQ963479:1964301:1965959:1 gene:CADAFLAG00008559 transcript:CADAFLAT00008559 description: UDP-N-acetylglucosamine pyrophosphorylase	32.24	20.16	8
CADAFLAP00002641	pep:known supercontig:JCVI-afl1-v2.0:EQ963473:2674101:2676382:1 gene:CADAFLAG00002641 transcript:CADAFLAT00002641 description: HEC/Ndc80p family protein	31.29	13.86	7

CADAFLAP00008024	pep:known supercontig:JCVI-afl1-v2.0:EQ963479:459507:460852:-1 gene:CADAFLAG00008024 transcript:CADAFLAT00008024 description: BZIP transcription factor, putative	30.30	28.52	7
CADAFLAP00001316	pep:known supercontig:JCVI-afl1-v2.0:EQ963472:3544382:3548054:1 gene:CADAFLAG00001316 transcript:CADAFLAT00001316 description: Spindle-pole body protein (Pcp1), putative	28.95	14.61	6
CADAFLAP00002106	pep:known supercontig:JCVI-afl1-v2.0:EQ963473:1197615:1198758:-1 gene:CADAFLAG00002106 transcript:CADAFLAT00002106 description: Fructose-1,6-bisphosphatase Fbp1, putative	26.44	29.01	6
CADAFLAP00013326	pep:known supercontig:JCVI-afl1-v2.0:EQ963486:1259924:1261388:-1 gene:CADAFLAG00013326 transcript:CADAFLAT00013326 description: Acetyl-CoA acetyltransferase, putative	26.14	26.82	5
CADAFLAP00008602	pep:known supercontig:JCVI-afl1-v2.0:EQ963480:27030:33372:-1 gene:CADAFLAG00008602 transcript:CADAFLAT00008602 description: Fatty acid synthase beta subunit, putative	25.94	6.12	8
CADAFLAP00011231	pep:known supercontig:JCVI-afl1-v2.0:EQ963483:1281340:1283202:-1 gene:CADAFLAG00011231 transcript:CADAFLAT00011231 description: Isocitrate lyase	25.73	18.96	6
CADAFLAP00002554	pep:known supercontig:JCVI-afl1-v2.0:EQ963473:2435324:2436960:-1 gene:CADAFLAG00002554 transcript:CADAFLAT00002554 description: BZIP transcription factor (MeaB), putative	24.76	18.09	6
CADAFLAP00006051	pep:known supercontig:JCVI-afl1-v2.0:EQ963476:2499774:2501537:1 gene:CADAFLAG00006051 transcript:CADAFLAT00006051 description: Cystathionine beta-synthase, putative	23.34	17.39	5
CADAFLAP00005963	pep:known supercontig:JCVI-afl1-v2.0:EQ963476:2187122:2194103:1 gene:CADAFLAG00005963	22.77	5.13	8

	transcript:CADAFLAT00005963 description: Acetyl-CoA carboxylase, putative			
CADAFLAP00012165	pep:known supercontig:JCVI-afl1-v2.0:EQ963485:51761:52235:1 gene:CADAFLAG00012165 transcript:CADAFLAT00012165 description: Putative uncharacterized protein	22.23	51.77	4
CADAFLAP00009109	pep:known supercontig:JCVI-afl1-v2.0:EQ963480:1402310:1404536:1 gene:CADAFLAG00009109 transcript:CADAFLAT00009109 description: Putative uncharacterized protein	21.98	20.10	8
CADAFLAP00003873	pep:known supercontig:JCVI-afl1-v2.0:EQ963474:1917046:1918987:1 gene:CADAFLAG00003873 transcript:CADAFLAT00003873 description: Mis12-Mtw1 family protein	21.72	11.43	4
CADAFLAP00004946	pep:known supercontig:JCVI-afl1-v2.0:EQ963475:2095220:2099094:-1 gene:CADAFLAG00004946 transcript:CADAFLAT00004946 description: Pyruvate carboxylase	21.66	9.39	7
CADAFLAP00002146	pep:known supercontig:JCVI-afl1-v2.0:EQ963473:1342058:1342917:1 gene:CADAFLAG00002146 transcript:CADAFLAT00002146 description: Peptidyl-prolyl cis-trans isomerase	21.53	31.93	4
CADAFLAP00000620	pep:known supercontig:JCVI-afl1-v2.0:EQ963472:1615903:1617653:-1 gene:CADAFLAG00000620 transcript:CADAFLAT00000620 description: Acetyl-coA hydrolase Ach1, putative	21.45	20.38	6
CADAFLAP00000131	pep:known supercontig:JCVI-afl1-v2.0:EQ963472:324198:324959:1 gene:CADAFLAG00000131 transcript:CADAFLAT00000131 description: Tropomyosin, putative	21.43	32.92	4
CADAFLAP00002389	pep:known supercontig:JCVI-afl1-v2.0:EQ963473:2002547:2003611:-1 gene:CADAFLAG00002389 transcript:CADAFLAT00002389 description: 60S ribosomal protein P0	21.18	25.56	6

CADAFLAP00000730	pep:known supercontig:JCVI-afl1-v2.0:EQ963472:1925515:1927778:1 gene:CADAFLAG00000730 transcript:CADAFLAT00000730 description: Oligopeptidase family protein	20.75	14.48	7
CADAFLAP00002478	pep:known supercontig:JCVI-afl1-v2.0:EQ963473:2228907:2231489:1 gene:CADAFLAG00002478 transcript:CADAFLAT00002478 description: Putative uncharacterized protein	20.10	9.86	6
CADAFLAP00008160	pep:known supercontig:JCVI-afl1-v2.0:EQ963479:837390:838972:-1 gene:CADAFLAG00008160 transcript:CADAFLAT00008160 description: Elongation factor Tu	19.67	17.23	5
CADAFLAP00004546	pep:known supercontig:JCVI-afl1-v2.0:EQ963475:1032320:1033870:1 gene:CADAFLAG00004546 transcript:CADAFLAT00004546 description: Argininosuccinate synthase	19.59	20.38	7
CADAFLAP00003945	pep:known supercontig:JCVI-afl1-v2.0:EQ963474:2120397:2123780:1 gene:CADAFLAG00003945 transcript:CADAFLAT00003945 description: AT DNA binding protein, putative	19.01	10.47	8
CADAFLAP00001079	pep:known supercontig:JCVI-afl1-v2.0:EQ963472:2875147:2876318:-1 gene:CADAFLAG00001079 transcript:CADAFLAT00001079 description: MIND kinetochore complex component Mtw1, putative	18.91	20.24	4
CADAFLAP00005046	pep:known supercontig:JCVI-afl1-v2.0:EQ963475:2384512:2385823:-1 gene:CADAFLAG00005046 transcript:CADAFLAT00005046 description: GPI-anchored cell wall organization protein Ecm33	18.70	11.56	3
CADAFLAP00010065	pep:known supercontig:JCVI-afl1-v2.0:EQ963481:1890958:1892981:1 gene:CADAFLAG00010065 transcript:CADAFLAT00010065 description: Hexokinase Kxk, putative	18.64	14.90	4

CADAFLAP00011019	pep:known supercontig:JCVI-afl1-v2.0:EQ963483:679089:680918:-1 gene:CADAFLAG00011019 transcript:CADAFLAT00011019 description: Conserved lysine-rich protein, putative	18.33	14.50	7
CADAFLAP00002082	pep:known supercontig:JCVI-afl1-v2.0:EQ963473:1126458:1128842:-1 gene:CADAFLAG00002082 transcript:CADAFLAT00002082 description: Acetyl-coenzyme A synthetase FacA	18.06	8.59	6
CADAFLAP00001419	pep:known supercontig:JCVI-afl1-v2.0:EQ963472:3778580:3780973:-1 gene:CADAFLAG00001419 transcript:CADAFLAT00001419 description: Isocitrate dehydrogenase	17.86	14.63	6
CADAFLAP00010884	pep:known supercontig:JCVI-afl1-v2.0:EQ963483:289969:292077:-1 gene:CADAFLAG00010884 transcript:CADAFLAT00010884 description: C6 finger domain protein, putative	17.83	9.70	4
CADAFLAP00004474	pep:known supercontig:JCVI-afl1-v2.0:EQ963475:845682:847178:1 gene:CADAFLAG00004474 transcript:CADAFLAT00004474 description: PWWP domain protein	17.69	12.62	3
CADAFLAP00002937	pep:known supercontig:JCVI-afl1-v2.0:EQ963473:3466835:3469020:-1 gene:CADAFLAG00002937 transcript:CADAFLAT00002937 description: Hsp70 chaperone BiP/Kar2, putative	17.40	9.97	5
CADAFLAP00008224	pep:known supercontig:JCVI-afl1-v2.0:EQ963479:1001496:1002390:-1 gene:CADAFLAG00008224 transcript:CADAFLAT00008224 description: Ribosomal protein	16.86	18.43	3
CADAFLAP00007209	pep:known supercontig:JCVI-afl1-v2.0:EQ963478:598013:601062:-1 gene:CADAFLAG00007209 transcript:CADAFLAT00007209 description: Putative uncharacterized protein	16.43	7.68	5

CADAFLAP00002306	pep:known supercontig:JCVI-afl1-v2.0:EQ963473:1745130:1746774:1 gene:CADAFLAG00002306 transcript:CADAFLAT00002306 description: Alcohol dehydrogenase, zinc-containing, putative	16.26	18.21	4
CADAFLAP00003958	pep:known supercontig:JCVI-afl1-v2.0:EQ963474:2165407:2166459:-1 gene:CADAFLAG00003958 transcript:CADAFLAT00003958 description: Putative uncharacterized protein	16.21	37.36	6
CADAFLAP00006333	pep:known supercontig:JCVI-afl1-v2.0:EQ963477:706525:708010:-1 gene:CADAFLAG00006333 transcript:CADAFLAT00006333 description: RNP domain protein	15.92	13.42	4
CADAFLAP00000159	pep:known supercontig:JCVI-afl1-v2.0:EQ963472:399440:404950:1 gene:CADAFLAG00000159 transcript:CADAFLAT00000159 description: DNA mismatch repair protein Msh3	15.27	4.11	4
CADAFLAP00010702	pep:known supercontig:JCVI-afl1-v2.0:EQ963482:1718556:1720986:-1 gene:CADAFLAG00010702 transcript:CADAFLAT00010702 description: Glutamyl-tRNA synthetase	15.01	10.46	4
CADAFLAP00003923	pep:known supercontig:JCVI-afl1-v2.0:EQ963474:2070956:2072222:1 gene:CADAFLAG00003923 transcript:CADAFLAT00003923 description: Stomatin family protein	14.92	13.66	4
CADAFLAP00002510	pep:known supercontig:JCVI-afl1-v2.0:EQ963473:2303025:2306093:1 gene:CADAFLAG00002510 transcript:CADAFLAT00002510 description: Spindle pole body component (Alp6), putative	14.84	7.65	4
CADAFLAP00002148	pep:known supercontig:JCVI-afl1-v2.0:EQ963473:1347555:1348597:1 gene:CADAFLAG00002148 transcript:CADAFLAT00002148 description: Glycerol dehydrogenase (GldB), putative	14.48	20.31	4

CADAFLAP00002110	pep:known supercontig:JCVI-afl1-v2.0:EQ963473:1209310:1211142:-1 gene:CADAFLAG00002110 transcript:CADAFLAT00002110 description: Saccharopine dehydrogenase Lys9, putative	14.45	12.67	3
CADAFLAP00005906	pep:known supercontig:JCVI-afl1-v2.0:EQ963476:2027181:2027781:-1 gene:CADAFLAG00005906 transcript:CADAFLAT00005906 description: 60S ribosomal protein L30, putative	14.11	29.25	2
CADAFLAP00011702	pep:known supercontig:JCVI-afl1-v2.0:EQ963484:653933:656439:-1 gene:CADAFLAG00011702 transcript:CADAFLAT00011702 description: Woronin body major protein, putative	14.06	8.92	4
CADAFLAP00006639	pep:known supercontig:JCVI-afl1-v2.0:EQ963477:1480422:1481624:1 gene:CADAFLAG00006639 transcript:CADAFLAT00006639 description: Ketol-acid reductoisomerase	14.01	19.00	5
CADAFLAP00005736	pep:known supercontig:JCVI-afl1-v2.0:EQ963476:1559843:1561676:1 gene:CADAFLAG00005736 transcript:CADAFLAT00005736 description: Uricase	13.92	21.52	6
CADAFLAP00004947	pep:known supercontig:JCVI-afl1-v2.0:EQ963475:2101733:2110515:-1 gene:CADAFLAG00004947 transcript:CADAFLAT00004947 description: Clathrin heavy chain	13.83	2.67	3
CADAFLAP00000924	pep:known supercontig:JCVI-afl1-v2.0:EQ963472:2469367:2470837:1 gene:CADAFLAG00000924 transcript:CADAFLAT00000924 description: SWIB/MDM2 domain protein	13.62	19.86	3
CADAFLAP00006772	pep:known supercontig:JCVI-afl1-v2.0:EQ963477:1838042:1838891:-1 gene:CADAFLAG00006772 transcript:CADAFLAT00006772 description: Single-stranded DNA-binding protein	13.36	31.25	4

CADAFLAP00008502	pep:known supercontig:JCVI-afl1-v2.0:EQ963479:1791721:1793654:-1 gene:CADAFLAG00008502 transcript:CADAFLAT00008502 description: Acetamidase, putative	12.78	11.57	4
CADAFLAP00010089	pep:known supercontig:JCVI-afl1-v2.0:EQ963481:1962393:1964153:-1 gene:CADAFLAG00010089 transcript:CADAFLAT00010089 description: Protein disulfide isomerase Pdi1, putative	12.73	11.07	4
CADAFLAP00010073	pep:known supercontig:JCVI-afl1-v2.0:EQ963481:1916427:1918943:1 gene:CADAFLAG00010073 transcript:CADAFLAT00010073 description: NAD+ dependent glutamate dehydrogenase, putative	12.45	6.13	3
CADAFLAP00000877	pep:known supercontig:JCVI-afl1-v2.0:EQ963472:2350263:2352028:-1 gene:CADAFLAG00000877 transcript:CADAFLAT00000877 description: Origin recognition complex subunit Orc5, putative	12.01	12.41	5
CADAFLAP00000442	pep:known supercontig:JCVI-afl1-v2.0:EQ963472:1149017:1152795:1 gene:CADAFLAG00000442 transcript:CADAFLAT00000442 description: Translation elongation factor eEF-3, putative	12.01	5.25	4
CADAFLAP00010457	pep:known supercontig:JCVI-afl1-v2.0:EQ963482:957762:961135:-1 gene:CADAFLAG00010457 transcript:CADAFLAT00010457 description: Nuclear condensin complex subunit 3, putative	11.99	4.25	4
CADAFLAP00010921	pep:known supercontig:JCVI-afl1-v2.0:EQ963483:390873:392389:-1 gene:CADAFLAG00010921 transcript:CADAFLAT00010921 description: Citrate synthase	11.93	10.71	5
CADAFLAP00002649	pep:known supercontig:JCVI-afl1-v2.0:EQ963473:2694524:2696851:-1 gene:CADAFLAG00002649 transcript:CADAFLAT00002649 description: Transcription factor TFIID	11.68	10.65	2
CADAFLAP00002125	pep:known supercontig:JCVI-afl1-v2.0:EQ963473:1267436:1269626:-1 gene:CADAFLAG00002125	11.52	13.46	3

	transcript:CADAFLAT00002125 description: Mannose-1-phosphate guanylyltransferase			
CADAFLAP00010829	pep:known supercontig:JCVI-afl1-v2.0:EQ963483:112627:114814:1 gene:CADAFLAG00010829 transcript:CADAFLAT00010829 description: Glycyl-tRNA synthetase	11.35	6.07	4
CADAFLAP00008169	pep:known supercontig:JCVI-afl1-v2.0:EQ963479:854304:854984:-1 gene:CADAFLAG00008169 transcript:CADAFLAT00008169 description: Glycine cleavage system H protein	10.93	23.70	3
CADAFLAP00007538	pep:known supercontig:JCVI-afl1-v2.0:EQ963478:1531723:1532637:-1 gene:CADAFLAG00007538 transcript:CADAFLAT00007538 description: GrpE protein homolog	10.76	24.70	5
CADAFLAP00008603	pep:known supercontig:JCVI-afl1-v2.0:EQ963480:36079:41772:1 gene:CADAFLAG00008603 transcript:CADAFLAT00008603 description: Fatty acid synthase alpha subunit FasA	10.47	3.23	6
CADAFLAP00004055	pep:known supercontig:JCVI-afl1-v2.0:EQ963474:2432289:2433508:1 gene:CADAFLAG00004055 transcript:CADAFLAT00004055 description: Aminotransferase, class V, putative	10.42	7.51	3
CADAFLAP00007137	pep:known supercontig:JCVI-afl1-v2.0:EQ963478:407120:408702:1 gene:CADAFLAG00007137 transcript:CADAFLAT00007137 description: Ndc80 complex component Nuf2, putative	10.26	8.42	3
CADAFLAP00003685	pep:known supercontig:JCVI-afl1-v2.0:EQ963474:1410977:1412928:-1 gene:CADAFLAG00003685 transcript:CADAFLAT00003685 description: Tubulin gamma chain	10.17	10.56	3
CADAFLAP00008251	pep:known supercontig:JCVI-afl1-v2.0:EQ963479:1070022:1071114:1 gene:CADAFLAG00008251 transcript:CADAFLAT00008251 description: Putative uncharacterized protein	10.00	32.93	3

CADAFLAP00003090	pep:known supercontig:JCVI-afl1-v2.0:EQ963473:3915922:3916963:-1 gene:CADAFLAG00003090 transcript:CADAFLAT00003090 description: Thiamine thiazole synthase	9.99	12.84	2
CADAFLAP00006797	pep:known supercontig:JCVI-afl1-v2.0:EQ963477:1919835:1920884:-1 gene:CADAFLAG00006797 transcript:CADAFLAT00006797 description: Pyridoxine biosynthesis protein	9.92	9.35	2
CADAFLAP00008228	pep:known supercontig:JCVI-afl1-v2.0:EQ963479:1012754:1013553:1 gene:CADAFLAG00008228 transcript:CADAFLAT00008228 description: ADP-ribosylation factor, putative	9.76	24.59	3
CADAFLAP00003677	pep:known supercontig:JCVI-afl1-v2.0:EQ963474:1386461:1388119:-1 gene:CADAFLAG00003677 transcript:CADAFLAT00003677 description: Spermidine synthase	9.64	10.29	3
CADAFLAP00008827	pep:known supercontig:JCVI-afl1-v2.0:EQ963480:607657:609968:-1 gene:CADAFLAG00008827 transcript:CADAFLAT00008827 description: ATP dependent RNA helicase (Sub2), putative	9.62	12.47	5
CADAFLAP00006823	pep:known supercontig:JCVI-afl1-v2.0:EQ963477:1985186:1986763:1 gene:CADAFLAG00006823 transcript:CADAFLAT00006823 description: RNA binding protein, putative	9.56	9.63	2
CADAFLAP00009793	pep:known supercontig:JCVI-afl1-v2.0:EQ963481:1098410:1100420:-1 gene:CADAFLAG00009793 transcript:CADAFLAT00009793 description: N-acetylglucosamine-phosphate mutase	9.40	7.78	3
CADAFLAP00010853	pep:known supercontig:JCVI-afl1-v2.0:EQ963483:190843:192496:-1 gene:CADAFLAG00010853 transcript:CADAFLAT00010853 description: Succinyl-CoA synthetase alpha subunit, putative	9.40	12.12	3

CADAFLAP00005638	pep:known supercontig:JCVI-afl1-v2.0:EQ963476:1282856:1284624:1 gene:CADAFLAG00005638 transcript:CADAFLAT00005638 description: Dihydrolipoyl dehydrogenase	9.20	8.01	3
CADAFLAP00002346	pep:known supercontig:JCVI-afl1-v2.0:EQ963473:1849065:1853452:-1 gene:CADAFLAG00002346 transcript:CADAFLAT00002346 description: Proliferating cell nuclear antigen	9.12	4.43	2
CADAFLAP00008895	pep:known supercontig:JCVI-afl1-v2.0:EQ963480:806443:808343:1 gene:CADAFLAG00008895 transcript:CADAFLAT00008895 description: Inosine-5'-monophosphate dehydrogenase	8.98	6.04	2
CADAFLAP00003123	pep:known supercontig:JCVI-afl1-v2.0:EQ963473:4012526:4014367:-1 gene:CADAFLAG00003123 transcript:CADAFLAT00003123 description: 14-3-3 protein sigma, gamma, zeta, beta/alpha, putative	8.79	12.44	2
CADAFLAP00003581	pep:known supercontig:JCVI-afl1-v2.0:EQ963474:1115753:1118605:1 gene:CADAFLAG00003581 transcript:CADAFLAT00003581 description: Acetylglutamate kinase, putative	8.76	4.86	3
CADAFLAP00004949	pep:known supercontig:JCVI-afl1-v2.0:EQ963475:2114609:2116687:-1 gene:CADAFLAG00004949 transcript:CADAFLAT00004949 description: Phosphoribosylaminoimidazolecarboxamide formyltransferase/IMP	8.69	8.24	4
CADAFLAP00005080	pep:known supercontig:JCVI-afl1-v2.0:EQ963475:2489130:2490544:1 gene:CADAFLAG00005080 transcript:CADAFLAT00005080 description: CHL4 family chromosome segregation protein, putative	8.69	12.68	3
CADAFLAP00008125	pep:known supercontig:JCVI-afl1-v2.0:EQ963479:760440:763107:1 gene:CADAFLAG00008125 transcript:CADAFLAT00008125 description: Carnitine acetyl transferase	8.55	4.51	2

CADAFLAP00000955	pep:known supercontig:JCVI-afl1-v2.0:EQ963472:2537554:2539608:1 gene:CADAFLAG00000955 transcript:CADAFLAT00000955 description: T-complex protein 1, beta subunit, putative	8.50	6.23	2
CADAFLAP00001135	pep:known supercontig:JCVI-afl1-v2.0:EQ963472:3035909:3037632:1 gene:CADAFLAG00001135 transcript:CADAFLAT00001135 description: Coatomer subunit delta, putative	8.43	7.75	2
CADAFLAP00010764	pep:known supercontig:JCVI-afl1-v2.0:EQ963482:1868909:1870647:-1 gene:CADAFLAG00010764 transcript:CADAFLAT00010764 description: Mitochondrial DNA replication protein (Yhm2), putative	8.32	9.21	2
CADAFLAP00010793	pep:known supercontig:JCVI-afl1-v2.0:EQ963483:12255:14350:1 gene:CADAFLAG00010793 transcript:CADAFLAT00010793 description: Seryl-tRNA synthetase	8.30	6.96	2
CADAFLAP00005511	pep:known supercontig:JCVI-afl1-v2.0:EQ963476:970387:973645:-1 gene:CADAFLAG00005511 transcript:CADAFLAT00005511 description: Glycine dehydrogenase	8.27	4.89	3
CADAFLAP00007278	pep:known supercontig:JCVI-afl1-v2.0:EQ963478:779419:781271:1 gene:CADAFLAG00007278 transcript:CADAFLAT00007278 description: Secretory pathway gdp dissociation inhibitor	8.25	7.28	2
CADAFLAP00011296	pep:known supercontig:JCVI-afl1-v2.0:EQ963483:1474009:1474914:-1 gene:CADAFLAG00011296 transcript:CADAFLAT00011296 description: Peroxiredoxin 5, prdx5, putative	8.23	15.93	2
CADAFLAP00001172	pep:known supercontig:JCVI-afl1-v2.0:EQ963472:3128262:3129740:-1 gene:CADAFLAG00001172 transcript:CADAFLAT00001172 description: Adenylosuccinate synthetase	8.02	11.32	2

CADAFLAP00010333	pep:known supercontig:JCVI-afl1-v2.0:EQ963482:579999:582032:1 gene:CADAFLAG00010333 transcript:CADAFLAT00010333 description: Curved DNA-binding protein (42 kDa protein)	7.84	6.88	3
CADAFLAP00006090	pep:known supercontig:JCVI-afl1-v2.0:EQ963477:48816:51858:-1 gene:CADAFLAG00006090 transcript:CADAFLAT00006090 description: Transcriptional repressor TupA/RocA, putative	7.79	4.95	2
CADAFLAP00000806	pep:known supercontig:JCVI-afl1-v2.0:EQ963472:2150666:2151679:1 gene:CADAFLAG00000806 transcript:CADAFLAT00000806 description: ATP synthase delta chain, mitochondrial, putative	7.76	15.76	2
CADAFLAP00002809	pep:known supercontig:JCVI-afl1-v2.0:EQ963473:3126914:3127908:-1 gene:CADAFLAG00002809 transcript:CADAFLAT00002809 description: 40S ribosomal protein S10b	7.58	14.36	2
CADAFLAP00009007	pep:known supercontig:JCVI-afl1-v2.0:EQ963480:1126513:1129940:1 gene:CADAFLAG00009007 transcript:CADAFLAT00009007 description: Ran-specific GTPase-activating protein 1, putative	7.55	8.92	3
CADAFLAP00002245	pep:known supercontig:JCVI-afl1-v2.0:EQ963473:1587194:1588291:-1 gene:CADAFLAG00002245 transcript:CADAFLAT00002245 description: Ubiquitin UbiA, putative	7.36	16.03	2
CADAFLAP00011072	pep:known supercontig:JCVI-afl1-v2.0:EQ963483:825280:826322:1 gene:CADAFLAG00011072 transcript:CADAFLAT00011072 description: 40S ribosomal protein S12	7.35	14.00	2
CADAFLAP00007521	pep:known supercontig:JCVI-afl1-v2.0:EQ963478:1485534:1487876:-1 gene:CADAFLAG00007521 transcript:CADAFLAT00007521 description: V-type ATPase, B subunit, putative	7.27	5.91	2

CADAFLAP00008018	pep:known supercontig:JCVI-afl1-v2.0:EQ963479:440115:440614:1 gene:CADAFLAG00008018 transcript:CADAFLAT00008018 description: Glyoxalase family protein	7.21	21.32	2
CADAFLAP00011640	pep:known supercontig:JCVI-afl1-v2.0:EQ963484:488554:490163:1 gene:CADAFLAG00011640 transcript:CADAFLAT00011640 description: Autophagic serine protease Alp2	7.20	7.47	3
CADAFLAP00003465	pep:known supercontig:JCVI-afl1-v2.0:EQ963474:823210:823787:1 gene:CADAFLAG00003465 transcript:CADAFLAT00003465 description: DUF636 domain protein	7.17	25.19	2
CADAFLAP00006244	pep:known supercontig:JCVI-afl1-v2.0:EQ963477:476121:478024:1 gene:CADAFLAG00006244 transcript:CADAFLAT00006244 description: 2-methylcitrate dehydratase, putative	7.06	4.47	2
CADAFLAP00011623	pep:known supercontig:JCVI-afl1-v2.0:EQ963484:427912:434348:1 gene:CADAFLAG00011623 transcript:CADAFLAT00011623 description: Putative uncharacterized protein	6.99	13.08	3
CADAFLAP00010303	pep:known supercontig:JCVI-afl1-v2.0:EQ963482:501187:504449:-1 gene:CADAFLAG00010303 transcript:CADAFLAT00010303 description: Cell division control protein Cdc48	6.84	3.53	2
CADAFLAP00003366	pep:known supercontig:JCVI-afl1-v2.0:EQ963474:531301:533670:1 gene:CADAFLAG00003366 transcript:CADAFLAT00003366 description: Prolyl-tRNA synthetase	6.78	8.13	3
CADAFLAP00012536	pep:known supercontig:JCVI-afl1-v2.0:EQ963485:1035656:1036394:1 gene:CADAFLAG00012536 transcript:CADAFLAT00012536 description: Cofilin	6.78	22.37	2

CADAFLAP00012537	pep:known supercontig:JCVI-afl1-v2.0:EQ963485:1037267:1038033:1 gene:CADAFLAG00012537 transcript:CADAFLAT00012537 description: Cytochrome c oxidase subunit V	6.27	13.20	2
CADAFLAP00007535	pep:known supercontig:JCVI-afl1-v2.0:EQ963478:1523778:1525000:1 gene:CADAFLAG00007535 transcript:CADAFLAT00007535 description: Cytochrome c	6.20	19.64	2
CADAFLAP00001438	pep:known supercontig:JCVI-afl1-v2.0:EQ963472:3827471:3829494:-1 gene:CADAFLAG00001438 transcript:CADAFLAT00001438 description: Transcription factor smp1, putative	6.19	3.82	2
CADAFLAP00002501	pep:known supercontig:JCVI-afl1-v2.0:EQ963473:2278690:2280209:-1 gene:CADAFLAG00002501 transcript:CADAFLAT00002501 description: Proteasome regulatory particle subunit Rpt3, putative	6.18	6.02	2
CADAFLAP00003657	pep:known supercontig:JCVI-afl1-v2.0:EQ963474:1326199:1329523:1 gene:CADAFLAG00003657 transcript:CADAFLAT00003657 description: Centrin-binding protein Sfi1, putative	6.16	4.24	5
CADAFLAP00002908	pep:known supercontig:JCVI-afl1-v2.0:EQ963473:3381094:3383319:1 gene:CADAFLAG00002908 transcript:CADAFLAT00002908 description: Translation release factor eRF3, putative	6.10	3.46	2
CADAFLAP00013435	pep:known supercontig:JCVI-afl1-v2.0:EQ963487:256722:258530:-1 gene:CADAFLAG00013435 transcript:CADAFLAT00013435 description: Succinyl-CoA synthetase beta subunit, putative	6.09	4.48	2
CADAFLAP00003913	pep:known supercontig:JCVI-afl1-v2.0:EQ963474:2040098:2040947:-1 gene:CADAFLAG00003913 transcript:CADAFLAT00003913 description: Glycolipid transfer protein HET-C2, putative	6.01	14.56	3

CADAFLAP00002925	pep:known supercontig:JCVI-afl1-v2.0:EQ963473:3427036:3428461:1 gene:CADAFLAG00002925 transcript:CADAFLAT00002925 description: Cytochrome b5, putative	5.96	18.25	2
CADAFLAP00010845	pep:known supercontig:JCVI-afl1-v2.0:EQ963483:166386:167774:1 gene:CADAFLAG00010845 transcript:CADAFLAT00010845 description: E3 ubiquitin ligase complex SCF subunit sconC	5.94	11.80	2
CADAFLAP00011733	pep:known supercontig:JCVI-afl1-v2.0:EQ963484:767101:768632:1 gene:CADAFLAG00011733 transcript:CADAFLAT00011733 description: Argininosuccinate lyase	5.93	6.90	2
CADAFLAP00012072	pep:known supercontig:JCVI-afl1-v2.0:EQ963484:1610402:1611266:-1 gene:CADAFLAG00012072 transcript:CADAFLAT00012072 description: RNA processing protein Emg1, putative	5.91	9.54	2
CADAFLAP00001492	pep:known supercontig:JCVI-afl1-v2.0:EQ963472:3967032:3968093:-1 gene:CADAFLAG00001492 transcript:CADAFLAT00001492 description: Putative uncharacterized protein	5.76	6.97	2
CADAFLAP00007012	pep:known supercontig:JCVI-afl1-v2.0:EQ963478:92963:94948:1 gene:CADAFLAG00007012 transcript:CADAFLAT00007012 description: C2H2 zinc finger protein	5.67	7.26	3
CADAFLAP00001560	pep:known supercontig:JCVI-afl1-v2.0:EQ963472:4189783:4191067:-1 gene:CADAFLAG00001560 transcript:CADAFLAT00001560 description: Cell wall integrity signaling protein Lsp1/Pil1, putative	5.59	4.90	2
CADAFLAP00010646	pep:known supercontig:JCVI-afl1-v2.0:EQ963482:1574390:1576351:-1 gene:CADAFLAG00010646 transcript:CADAFLAT00010646 description: Septin	5.50	5.73	2
CADAFLAP00003378	pep:known supercontig:JCVI-afl1-v2.0:EQ963474:563341:564663:1 gene:CADAFLAG00003378	5.44	5.91	2

	transcript:CADAFLAT00003378 description: Cofactor for methionyl-and glutamyl-tRNA synthetase, putative			
CADAFLAP00002464	pep:known supercontig:JCVI-afl1-v2.0:EQ963473:2188043:2189750:1 gene:CADAFLAG00002464 transcript:CADAFLAT00002464 description: Saccharopine dehydrogenase	5.39	5.91	2
CADAFLAP00004909	pep:known supercontig:JCVI-afl1-v2.0:EQ963475:2019328:2020275:1 gene:CADAFLAG00004909 transcript:CADAFLAT00004909 description: RAB GTPase Ypt5, putative	5.34	10.55	2
CADAFLAP00011248	pep:known supercontig:JCVI-afl1-v2.0:EQ963483:1342686:1344281:1 gene:CADAFLAG00011248 transcript:CADAFLAT00011248 description: MAP kinase MpkA	5.25	4.96	2
CADAFLAP00002511	pep:known supercontig:JCVI-afl1-v2.0:EQ963473:2306586:2309501:1 gene:CADAFLAG00002511 transcript:CADAFLAT00002511 description: Proteasome component Prs2, putative	5.24	5.71	3
CADAFLAP00004844	pep:known supercontig:JCVI-afl1-v2.0:EQ963475:1867986:1869228:1 gene:CADAFLAG00004844 transcript:CADAFLAT00004844 description: Mitochondrial peroxiredoxin Prx1, putative	4.74	5.54	2
CADAFLAP00011804	pep:known supercontig:JCVI-afl1-v2.0:EQ963484:943553:945457:-1 gene:CADAFLAG00011804 transcript:CADAFLAT00011804 description: ATP sulphurylase	4.68	4.08	2
CADAFLAP00002378	pep:known supercontig:JCVI-afl1-v2.0:EQ963473:1966313:1969575:1 gene:CADAFLAG00002378 transcript:CADAFLAT00002378 description: Eukaryotic translation initiation factor 3 subunit A	4.37	3.72	2
CADAFLAP00004390	pep:known supercontig:JCVI-afl1-v2.0:EQ963475:616809:618259:-1 gene:CADAFLAG00004390 transcript:CADAFLAT00004390 description: Putative uncharacterized protein	4.33	6.80	3

CADAFLAP00003586	pep:known supercontig:JCVI-afl1-v2.0:EQ963474:1129063:1130937:1 gene:CADAFLAG00003586 transcript:CADAFLAT00003586 description: Mitochondrial processing peptidase beta subunit, putative	4.16	3.76	2
CADAFLAP00007133	pep:known supercontig:JCVI-afl1-v2.0:EQ963478:393076:393514:-1 gene:CADAFLAG00007133 transcript:CADAFLAT00007133 description: Thioredoxin	4.14	21.82	2
CADAFLAP00008320	pep:known supercontig:JCVI-afl1-v2.0:EQ963479:1262791:1264357:1 gene:CADAFLAG00008320 transcript:CADAFLAT00008320 description: Vacuolar ATP synthase subunit H, putative	4.09	5.25	2
CADAFLAP00002319	pep:known supercontig:JCVI-afl1-v2.0:EQ963473:1782398:1783642:-1 gene:CADAFLAG00002319 transcript:CADAFLAT00002319 description: NADH-cytochrome b5 reductase, putative	3.77	10.84	2
CADAFLAP00003696	pep:known supercontig:JCVI-afl1-v2.0:EQ963474:1435622:1437321:-1 gene:CADAFLAG00003696 transcript:CADAFLAT00003696 description: BZIP transcription factor, putative	3.19	6.48	2
CADAFLAP00004803	pep:known supercontig:JCVI-afl1-v2.0:EQ963475:1739599:1740743:-1 gene:CADAFLAG00004803 transcript:CADAFLAT00004803 description: Cytochrome c peroxidase Ccp1, putative	3.13	9.94	3
CADAFLAP00013316	pep:known supercontig:JCVI-afl1-v2.0:EQ963486:1226650:1228407:-1 gene:CADAFLAG00013316 transcript:CADAFLAT00013316 description: Choline oxidase (CodA), putative	2.91	8.67	2
CADAFLAP00007673	pep:known supercontig:JCVI-afl1-v2.0:EQ963478:1896694:1899127:-1 gene:CADAFLAG00007673 transcript:CADAFLAT00007673 description: Arginyl-tRNA synthetase	2.87	3.24	2

CADAFLAP00010775	pep:known supercontig:JCVI-afl1-v2.0:EQ963482:1901307:1902958:-1 gene:CADAFLAG00010775 transcript:CADAFLAT00010775 description: Secretion related GTPase SrgB/Ypt1	2.85	9.45	2
CADAFLAP00005925	pep:known supercontig:JCVI-afl1-v2.0:EQ963476:2078558:2081418:-1 gene:CADAFLAG00005925 transcript:CADAFLAT00005925 description: Probable dipeptidyl-peptidase 5	2.82	3.97	2
CADAFLAP00003985	pep:known supercontig:JCVI-afl1-v2.0:EQ963474:2246125:2248381:1 gene:CADAFLAG00003985 transcript:CADAFLAT00003985 description: Putative uncharacterized protein	2.63	3.38	2
CADAFLAP00007043	pep:known supercontig:JCVI-afl1-v2.0:EQ963478:172369:174644:-1 gene:CADAFLAG00007043 transcript:CADAFLAT00007043 description: HLH transcription factor (Hpa3), putative	2.43	5.31	2
CADAFLAP00001441	pep:known supercontig:JCVI-afl1-v2.0:EQ963472:3840027:3842016:-1 gene:CADAFLAG00001441 transcript:CADAFLAT00001441 description: Glucose-6-phosphate 1-dehydrogenase	2.37	4.39	2
CADAFLAP00001306	pep:known supercontig:JCVI-afl1-v2.0:EQ963472:3519922:3522070:-1 gene:CADAFLAG00001306 transcript:CADAFLAT00001306 description: T-complex protein 1, zeta subunit, putative	2.21	4.44	2
CADAFLAP00012559	pep:known supercontig:JCVI-afl1-v2.0:EQ963485:1104434:1105465:1 gene:CADAFLAG00012559 transcript:CADAFLAT00012559 description: Iron-sulfur protein subunit of succinate dehydrogenase Sdh2, putative	1.73	6.12	2

Appendix C

A. flavus Secondary metabolite gene clusters identified by Secondary Metabolite Unique Regions Finder (SMURF)

Cluster:1

Backbone_gene_id	Gene_id	Gene_positions		Chromosome-Contig		Gene_order	5'end	3'end	Gene_distance	Domain_score	Annotated_gene_function
AFLA_002900	AFLA_002920	-2	1569	252	648825	650784	727	1			Cytochrome P450 family protein
AFLA_002900	AFLA_002910	-1	1569	251	647376	648098	546	0			hypothetical protein
AFLA_002900	AFLA_002900	0	1569	250	646830	639511	0	0			polyketide synthase, putative

Cluster:2

Backbone_gene_id	Gene_id	Gene_positions		Chromosome-Contig		Gene_order	5'end	3'end	Gene_distance	Domain_score	Annotated_gene_function
AFLA_004450	AFLA_004450	0	1569	405	1115175	1131702	0	1			nonribosomal peptide synthase, putative
AFLA_004450	AFLA_004440	1	1569	404	1113845	1109751	1330	1			ABC transporter family protein
AFLA_004450	AFLA_004430	2	1569	403	1108599	1106632	1152	0			hypothetical protein
AFLA_004450	AFLA_004420	3	1569	402	1103238	1102369	3394	0			hypothetical protein
AFLA_004450	AFLA_004410	4	1569	401	1100003	1099638	2366	0			hypothetical protein
AFLA_004450	AFLA_004400	5	1569	400	1098417	1098812	826	0			Trypsin Inhibitor like cysteine rich domain containing protein
AFLA_004450	AFLA_004390	6	1569	399	1095738	1096878	1539	0			conserved hypothetical protein
AFLA_004450	AFLA_004380	7	1569	398	1095120	1092880	618	0			glycosyl hydrolase, family 43 protein
AFLA_004450	AFLA_004370	8	1569	397	1090139	1088155	2741	1			Cytochrome P450 family protein
AFLA_004450	AFLA_004360	9	1569	396	1087391	1085996	764	1			oxidoreductase, zinc-binding dehydrogenase family protein

Cluster:3

Backbone_gene_id	Gene_id	Gene_positions		Chromosome-Contig		Gene_order	5'end	3'end	Gene_distance	Domain_score	Annotated_gene_function

AFLA_005320	AFLA_005360	-4	1569	495	1422063	1423775	2082	1	hypothetical protein
AFLA_005320	AFLA_005350	-3	1569	494	1419712	1419981	2147	0	hypothetical protein
AFLA_005320	AFLA_005340	-2	1569	493	1417565	1416530	1297	0	conserved hypothetical protein
AFLA_005320	AFLA_005330	-1	1569	492	1414409	1415233	631	0	hypothetical protein
AFLA_005320	AFLA_005320	0	1569	491	1413778	1405582	0	1	polyketide synthase, putative
AFLA_005320	AFLA_005310	1	1569	490	1404510	1401884	1072	0	V-type ATPase, C subunit family protein
AFLA_005320	AFLA_005300	2	1569	489	1400018	1397292	1866	0	hypothetical protein
AFLA_005320	AFLA_005290	3	1569	488	1394180	1396515	777	1	New cDNA-based gene: (AO_CDS_042706, novel, updateIDs: 352, [gene: novel_gene_57, model: novel_model_57])

Cluster:4

Backbone_gene_id	Gene_id	Gene_positions		Chromosome-Contig	Gene_order	5'end	3'end	Gene_distance	Domain_score	Annotated_gene_function
AFLA_005440	AFLA_005520	-8	1569	511	1475253	1473372	650	1	hypothetical protein	
AFLA_005440	AFLA_005510	-7	1569	510	1470936	1472722	6	1	hypothetical protein	
AFLA_005440	AFLA_005500	-6	1569	509	1470462	1470930	2446	0	hypothetical protein	
AFLA_005440	AFLA_005490	-5	1569	508	1468016	1467296	52	0	hypothetical protein	
AFLA_005440	AFLA_005480	-4	1569	507	1467244	1464173	1492	0	mitochondrial nicotinamide nucleotide transhydrogenase subunit, putative	
AFLA_005440	AFLA_005470	-3	1569	506	1462681	1456979	1959	0	hypothetical protein	
AFLA_005440	AFLA_005460	-2	1569	505	1455020	1454392	1793	0	cytochrome P450 monooxygenase SirB-like, putative	
AFLA_005440	AFLA_005450	-1	1569	504	1452599	1451477	1252	1	conserved protein; similar to SLR0865 Synechocystis sp. and other bacteria; no apparent S. cerevisiae ortholog-related	
AFLA_005440	AFLA_005440	0	1569	503	1450225	1442264	0	0	nonribosomal peptide synthase, putative	
AFLA_005440	AFLA_005430	1	1569	502	1439576	1440704	1560	0	conserved hypothetical protein	
AFLA_005440	AFLA_005420	2	1569	501	1437084	1437629	1947	0	conserved hypothetical protein	
AFLA_005440	AFLA_005410	3	1569	500	1436220	1432677	864	0	Protein kinase domain containing protein	
AFLA_005440	AFLA_005400	4	1569	499	1432543	1431949	134	0	hypothetical protein	

AFLA_005440	AFLA_005390	5	1569	498	1429687	1428285	2262	0	hypothetical protein
AFLA_005440	AFLA_005380	6	1569	497	1426512	1425756	1773	0	hypothetical protein
AFLA_005440	AFLA_005370	7	1569	496	1424685	1423861	1071	0	hypothetical protein
AFLA_005440	AFLA_005360	8	1569	495	1422063	1423775	86	1	hypothetical protein

Cluster:5

Backbone_gene_id	Gene_id	Gene_positions		Chromosome-Contig	Gene_order	5'end	3'end	Gene_distance	Domain_score	Annotated_gene_function
AFLA_006170	AFLA_006230	-6	1569	582	1683111	1684316	458	1		1-aminocyclopropane-1-carboxylate deaminase, putative
AFLA_006170	AFLA_006220	-5	1569	581	1682653	1681265	612	0		hypothetical protein
AFLA_006170	AFLA_006210	-4	1569	580	1676835	1680653	628	0		Variant SH3 domain containing protein
AFLA_006170	AFLA_006200	-3	1569	579	1676207	1675887	1050	0		New cDNA-based gene: (AO_CDS_042706, novel, updateIDs: 417, [gene: novel_gene_73, model: novel_model_73])
AFLA_006170	AFLA_006190	-2	1569	578	1674837	1674196	2	0		hypothetical protein
AFLA_006170	AFLA_006180	-1	1569	577	1674194	1672714	1462	0		conidial pigment biosynthesis oxidase Abr1/brown 1
AFLA_006170	AFLA_006170	0	1569	576	1671252	1664602	0	0		polyketide synthetase PksP

Cluster:6

Backbone_gene_id	Gene_id	Gene_positions		Chromosome-Contig	Gene_order	5'end	3'end	Gene_distance	Domain_score	Annotated_gene_function
AFLA_008770	AFLA_008770	0	1739	143	349578	333887	0	0		nonribosomal peptide synthase, putative
AFLA_008770	AFLA_008760	1	1739	142	332785	328544	1102	1		ABC transporter family protein
AFLA_008770	AFLA_008750	2	1739	141	327942	327354	602	0		hypothetical protein
AFLA_008770	AFLA_008740	3	1739	140	325659	324646	1695	1		oxidoreductase, short chain dehydrogenase/reductase family protein
AFLA_008770	AFLA_008730	4	1739	139	324248	323871	398	0		hypothetical protein
AFLA_008770	AFLA_008720	5	1739	138	323658	322531	213	0		Patatin-like phospholipase family protein

AFLA_008770	AFLA_008710	6	1739	137	320117	320587	1944	0	hypothetical protein
AFLA_008770	AFLA_008700	7	1739	136	318905	319923	194	0	hypothetical protein
AFLA_008770	AFLA_008690	8	1739	135	317335	317789	1116	0	hypothetical protein
AFLA_008770	AFLA_008680	9	1739	134	315538	316891	444	0	hypothetical protein
AFLA_008770	AFLA_008670	10	1739	133	313672	314862	676	0	hypothetical protein
AFLA_008770	AFLA_008660	11	1739	132	310965	312334	1338	0	hypothetical protein
AFLA_008770	AFLA_008650	12	1739	131	310570	309992	395	1	oxidoreductase, short chain dehydrogenase/reductase family protein

Cluster:7

Backbone_gene_id	Gene_id	Gene_positions		Chromosome-Contig	Gene_order	5'end	3'end	Gene_distance	Domain_score	Annotated_gene_function
AFLA_010010	AFLA_010030	-2	1739	269	705078	706213	554	1		hypothetical protein
AFLA_010010	AFLA_010020	-1	1739	268	704524	700414	744	0		nonribosomal peptide synthase, putative
AFLA_010010	AFLA_010010	0	1739	267	694790	699670	0	0		nonribosomal peptide synthase, putative
AFLA_010010	AFLA_010000	1	1739	266	687862	693859	931	0		polyketide synthase, putative
AFLA_010010	AFLA_009990	2	1739	265	686495	685466	1367	1		oxidoreductase, 2OG-Fe(II) oxygenase family, putative
AFLA_010010	AFLA_009980	3	1739	264	680721	684644	822	1		To ATP-binding cassette transporter protein YOR1, putative

Cluster:8

Backbone_gene_id	Gene_id	Gene_positions		Chromosome-Contig	Gene_order	5'end	3'end	Gene_distance	Domain_score	Annotated_gene_function
AFLA_010620	AFLA_010640	-2	1739	330	860965	862908	1008	1		MFS siderophore transporter, putative
AFLA_010620	AFLA_010630	-1	1739	329	859957	855974	827	1		ABC transporter, identical
AFLA_010620	AFLA_010620	0	1739	328	848792	855147	0	0		nonribosomal siderophore peptide synthase Sid2

AFLA_010620	AFLA_010610	1	1739	327	846539	847423	1369	0	enoyl-CoA hydratase/isomerase family protein
AFLA_010620	AFLA_010600	2	1739	326	846222	844747	317	0	acetylase, putative
AFLA_010620	AFLA_010590	3	1739	325	841108	840788	3639	0	siderophore biosynthesis lipase/esterase, putative
AFLA_010620	AFLA_010580	4	1739	324	815096	838441	2347	0	nonribosomal peptide synthase, putative
AFLA_010620	AFLA_010570	5	1739	323	814602	814191	494	0	hypothetical protein
AFLA_010620	AFLA_010560	6	1739	322	812044	811769	2147	0	hypothetical protein
AFLA_010620	AFLA_010550	7	1739	321	811536	810512	233	1	O-methyltransferase family protein

Cluster:9

Backbone_gene_id	Gene_id	Gene_positions		Chromosome-Contig	Gene_order	5'end	3'end	Gene_distance	Domain_score Annotated_gene_function
AFLA_017840	AFLA_017900	-6	1866	505	1378298	1381120	3094	1	Fungal specific transcription factor domain containing protein
AFLA_017840	AFLA_017890	-5	1866	504	1373490	1375204	299	0	SET domain protein, ,putative
AFLA_017840	AFLA_017880	-4	1866	503	1373191	1372394	103	0	hypothetical protein
AFLA_017840	AFLA_017870	-3	1866	502	1370500	1372497	2640	0	GTP-binding protein, putative
AFLA_017840	AFLA_017860	-2	1866	501	1367860	1367376	1201	0	hypothetical protein
AFLA_017840	AFLA_017850	-1	1866	500	1366175	1365370	883	0	hypothetical protein
AFLA_017840	AFLA_017840	0	1866	499	1361134	1364487	0	0	NRPS-like enzyme, putative
AFLA_017840	AFLA_017830	1	1866	498	1359214	1360086	1048	0	Ribosomal protein L7Ae containing protein
AFLA_017840	AFLA_017820	2	1866	497	1352556	1355626	3588	0	Fes/CIP4 homology domain containing protein
AFLA_017840	AFLA_017810	3	1866	496	1352033	1350671	523	0	Protein kinase domain containing protein
AFLA_017840	AFLA_017800	4	1866	495	1348575	1346497	2096	0	proline-rich SH3 domain protein, ,putative

AFLA_017840	AFLA_017790	5	1866	494	1346287	1345971	210	0	New cDNA-based gene: (AO_CDS_042706, novel, updateIDs: 1439, [gene: novel_gene_185, model: novel_model_185])
AFLA_017840	AFLA_017780	6	1866	493	1343225	1345672	299	0	oligonucleotide transporter, putative
AFLA_017840	AFLA_017770	7	1866	492	1341770	1342859	366	0	D-isomer specific 2-hydroxyacid dehydrogenase, NAD binding domain containing protein
AFLA_017840	AFLA_017760	8	1866	491	1339127	1341356	414	1	FAD binding domain containing protein

Cluster:10

Backbone_gene_id	Gene_id	Gene_positions		Chromosome-Contig	Gene_order	5'end	3'end	Gene_distance	Domain_score	Annotated_gene_function
AFLA_023020	AFLA_023050	-3	1918	16	42622	44123	601	1		Major Facilitator Superfamily protein
AFLA_023020	AFLA_023040	-2	1918	15	39903	42021	208	1		Fungal specific transcription factor domain containing protein
AFLA_023020	AFLA_023030	-1	1918	14	38036	39695	615	1		Cytochrome P450 family protein
AFLA_023020	AFLA_023020	0	1918	13	37421	34356	0	0		NRPS-like enzyme, putative
AFLA_023020	AFLA_023010	1	1918	12	32707	33814	542	0		hypothetical protein
AFLA_023020	AFLA_023000	2	1918	11	31125	30057	1582	0		hypothetical protein
AFLA_023020	AFLA_022990	3	1918	10	26396	27139	2918	0		hypothetical protein
AFLA_023020	AFLA_022880	4	1918	9	25237	22398	1159	1		POT family protein
AFLA_023020	AFLA_022870	5	1918	8	21929	20652	469	0		hypothetical protein
AFLA_023020	AFLA_022860	6	1918	7	20098	19673	554	0		hypothetical protein
AFLA_023020	AFLA_022850	7	1918	6	16942	17796	1877	0		Amidohydrolase family protein
AFLA_023020	AFLA_022840	8	1918	5	16614	15005	328	1		Major Facilitator Superfamily protein
AFLA_023020	AFLA_022830	9	1918	4	11750	13504	1501	0		hypothetical protein
AFLA_023020	AFLA_022820	10	1918	3	10959	7454	791	0		hypothetical protein
AFLA_023020	AFLA_022810	11	1918	2	4125	5886	1568	1		Sugar transporter family protein

Cluster:11

Backbone_gene_id	Gene_id	Gene_positions		Chromosome-Contig	Gene_order	5'end	3'end	Gene_distance	Domain_score	Annotated_gene_function

AFLA_028720	AFLA_028720	0	1918	582	1595382	1592347	0	0	NRPS-like enzyme, putative
AFLA_028720	AFLA_028710	1	1918	581	1590345	1591103	1244	1	oxidoreductase, short chain dehydrogenase/reductase family protein
AFLA_028720	AFLA_028700	2	1918	580	1588291	1587194	2054	0	ubiquitin (UbiA), putative
AFLA_028720	AFLA_028690	3	1918	579	1585925	1587022	172	0	Yip1 domain containing protein
AFLA_028720	AFLA_028680	4	1918	578	1584430	1585591	334	0	hypothetical protein
AFLA_028720	AFLA_028670	5	1918	577	1582838	1578892	1592	0	thermotolerance protein, putative
AFLA_028720	AFLA_028660	6	1918	576	1578642	1574431	250	0	Elongation factor Tu GTP binding domain containing protein
AFLA_028720	AFLA_028650	7	1918	575	1573422	1574996	565	0	Rhodanese-like domain containing protein
AFLA_028720	AFLA_028640	8	1918	574	1570900	1572733	689	1	cytochrome P450 sterol C-22 desaturase, putaitve, putative

Cluster:12

Backbone_gene_id	Gene_id	Gene_positions		Chromosome-Contig	Gene_order		5'end	3'end	Gene_distance	Domain_score	Annotated_gene_function
AFLA_038600	AFLA_038670	-7	2043	51	171097	173060	678	1	Major Facilitator Superfamily protein		
AFLA_038600	AFLA_038660	-6	2043	50	170125	170419	682	0	New cDNA-based gene: (AO_CDS_042706, novel, updateIDs: 3547, [gene: novel_gene_397, model: novel_model_397])		
AFLA_038600	AFLA_038650	-5	2043	49	168208	169443	510	0	Eukaryotic aspartyl protease family protein		
AFLA_038600	AFLA_038640	-4	2043	48	162029	167698	708	1	fatty acid synthase alpha subunit, putative		
AFLA_038600	AFLA_038630	-3	2043	47	161321	159465	659	1	Cytochrome P450 family protein		
AFLA_038600	AFLA_038620	-2	2043	46	156808	158806	85	0	aminotransferase, class IV family protein		
AFLA_038600	AFLA_038610	-1	2043	45	156723	155841	3400	0	hypothetical protein		
AFLA_038600	AFLA_038600	0	2043	44	152441	143335	0	0	nonribosomal peptide synthase, putative		

Cluster:13

Backbone_gene_id	Gene_id	Gene_positions		Chromosome-Contig		Gene_order	5'end	3'end	Gene_distance	Domain_score	Annotated_gene_function
AFLA_041610	AFLA_041610	0	2043	345	904196	901113	0	0			NRPS-like enzyme, putative
AFLA_041610	AFLA_041600	1	2043	344	898173	900320	793	0			hypothetical protein
AFLA_041610	AFLA_041590	2	2043	343	896003	897496	677	0			hypothetical protein
AFLA_041610	AFLA_041580	3	2043	342	894565	895281	722	1			short chain dehydrogenase/oxidoreductase, putative
AFLA_041610	AFLA_041570	4	2043	341	893539	892256	1026	0			conserved hypothetical protein
AFLA_041610	AFLA_041560	5	2043	340	890819	891815	441	0			hypothetical protein
AFLA_041610	AFLA_041550	6	2043	339	888719	890082	737	0			cystathionine beta-lyase family protein
AFLA_041610	AFLA_041540	7	2043	338	884862	888121	598	1			C6 transcription factor, putative

Cluster:14

Backbone_gene_id	Gene_id	Gene_positions		Chromosome-Contig		Gene_order	5'end	3'end	Gene_distance	Domain_score	Annotated_gene_function
AFLA_045490	AFLA_045560	-7	2043	740	1959838	1961722	25	1			sugar transporter family protein, putative
AFLA_045490	AFLA_045550	-6	2043	739	1959813	1959493	1529	0			hypothetical protein
AFLA_045490	AFLA_045540	-5	2043	738	1956126	1957964	456	1			cytochrome P450 monooxygenase, putative
AFLA_045490	AFLA_045530	-4	2043	737	1955281	1955670	311	0			hypothetical protein
AFLA_045490	AFLA_045520	-3	2043	736	1954480	1954970	363	0			hypothetical protein
AFLA_045490	AFLA_045510	-2	2043	735	1954117	1953325	790	0			hypothetical protein
AFLA_045490	AFLA_045500	-1	2043	734	1952535	1950597	983	1			cytochrome P450 monooxygenase, putative
AFLA_045490	AFLA_045490	0	2043	733	1949614	1948240	0	0			dimethylallyl tryptophan synthase, putative

Cluster:15

Backbone_gene_id	Gene_id	Gene_positions		Chromosome-Contig	Gene_order	5'end	3'end	Gene_distance	Domain_score	Annotated_gene_function
AFLA_053870	AFLA_053910	-4	2091	595	1703485	1705440	1070	1		Major Facilitator Superfamily protein
AFLA_053870	AFLA_053900	-3	2091	594	1701195	1702415	832	0		New cDNA-based gene: (AO_CDS_042706, novel, updateIDs: 4835, [gene: novel_gene_570, model: novel_model_570])
AFLA_053870	AFLA_053890	-2	2091	593	1700363	1698957	79	0		Carboxylesterase family protein
AFLA_053870	AFLA_053880	-1	2091	592	1698878	1698657	1154	0		hypothetical protein
AFLA_053870	AFLA_053870	0	2091	591	1697503	1688441	0	1		polyketide synthase, putative
AFLA_053870	AFLA_053860	1	2091	590	1686559	1687040	1401	0		New cDNA-based gene: (AO_CDS_042706, novel, updateIDs: 4833, [gene: novel_gene_569, model: novel_model_569])
AFLA_053870	AFLA_053850	2	2091	589	1685920	1686438	121	0		hypothetical protein
AFLA_053870	AFLA_053840	3	2091	588	1684405	1681736	1515	0		conserved hypothetical protein
AFLA_053870	AFLA_053830	4	2091	587	1679345	1681385	351	1		Major Facilitator Superfamily protein
AFLA_053870	AFLA_053820	5	2091	586	1676994	1678678	667	1		Flavin-binding monooxygenase-like family protein
AFLA_053870	AFLA_053810	6	2091	585	1676347	1675102	647	0		Taurine catabolism dioxygenase TauD, TfdA family protein
AFLA_053870	AFLA_053800	7	2091	584	1674145	1674690	412	0		New cDNA-based gene: (AO_CDS_042706, novel, updateIDs: 4829, [gene: novel_gene_568, model: novel_model_568])
AFLA_053870	AFLA_053790	8	2091	583	1673157	1672510	988	0		mas-related
AFLA_053870	AFLA_053780	9	2091	582	1672498	1671444	12	0		polyketide synthase-related
AFLA_053870	AFLA_053770	10	2091	581	1671364	1670504	80	0		polyketide synthase-related
AFLA_053870	AFLA_053760	11	2091	580	1667661	1669317	1187	1		hypothetical protein

Cluster:16

Backbone_gene_id	Gene_id	Gene_positions		Chromosome-Contig	Gene_order	5'end	3'end	Gene_distance	Domain_score	Annotated_gene_function
AFLA_054090	AFLA_054090	0	2091	613	1755004	1746910	0	1		polyketide synthase, putative
AFLA_054090	AFLA_054080	1	2091	612	1745043	1746458	452	0		Sodium/hydrogen exchanger family protein
AFLA_054090	AFLA_054070	2	2091	611	1743632	1744351	692	0		hypothetical protein

AFLA_054090	AFLA_054060	3	2091	610	1743152	1742205	480	0	ATP/GTP binding protein, putative
AFLA_054090	AFLA_054050	4	2091	609	1739456	1735124	2749	1	ABC-2 type transporter family protein
AFLA_054090	AFLA_054040	5	2091	608	1733389	1731120	1735	1	hypothetical protein

Cluster:17

Backbone_gene_id	Gene_id	Gene_positions		Chromosome-Contig	Gene_order		5'end	3'end	Gene_distance	Domain_score	Annotated_gene_function
AFLA_054270	AFLA_054390	-12	2091	643	1827371	1829206	84	1			Fungal specific transcription factor domain containing protein
AFLA_054270	AFLA_054380	-11	2091	642	1826952	1827287	2208	0			hypothetical protein
AFLA_054270	AFLA_054370	-10	2091	641	1823709	1824744	1348	1			oxidoreductase, short chain dehydrogenase/reductase family protein
AFLA_054270	AFLA_054360	-9	2091	640	1822361	1821491	923	0			conserved hypothetical protein
AFLA_054270	AFLA_054350	-8	2091	639	1819378	1820568	643	0			actin-binding protein fragmin, putative
AFLA_054270	AFLA_054340	-7	2091	638	1817631	1818735	433	0			NmrA-like family protein
AFLA_054270	AFLA_054330	-6	2091	637	1816477	1817198	450	0			hypothetical protein
AFLA_054270	AFLA_054320	-5	2091	636	1815250	1816027	2067	0			NPP1 domain protein, putative
AFLA_054270	AFLA_054310	-4	2091	635	1813183	1810986	309	1			Fungal specific transcription factor domain containing protein
AFLA_054270	AFLA_054300	-3	2091	634	1808950	1810677	807	1			Major Facilitator Superfamily protein
AFLA_054270	AFLA_054290	-2	2091	633	1808143	1807107	224	0			oxidoreductase, aldo/keto reductase family protein
AFLA_054270	AFLA_054280	-1	2091	632	1806437	1806883	1860	0			conserved hypothetical protein
AFLA_054270	AFLA_054270	0	2091	631	1804577	1800767	0	0			NRPS-like enzyme, putative
AFLA_054270	AFLA_054260	1	2091	630	1798533	1800305	462	1			Major Facilitator Superfamily protein

Cluster:18

Backbone_gene_id	Gene_id	Gene_positions		Chromosome-Contig		Gene_order	5'end	3'end	Gene_distance	Domain_score	Annotated_gene_function
AFLA_060020	AFLA_060090	-7	2258	545	1434636	1433008	979	1			Major Facilitator Superfamily protein
AFLA_060020	AFLA_060080	-6	2258	544	1432029	1426642	1080	1			ABC transporter family protein
AFLA_060020	AFLA_060070	-5	2258	543	1423650	1425562	839	0			hypothetical protein
AFLA_060020	AFLA_060060	-4	2258	542	1422811	1421139	1392	1			Major Facilitator Superfamily protein
AFLA_060020	AFLA_060050	-3	2258	541	1417975	1419747	693	1			Amino acid permease family protein
AFLA_060020	AFLA_060040	-2	2258	540	1417282	1415945	253	0			hypothetical protein
AFLA_060020	AFLA_060030	-1	2258	539	1413349	1415692	2716	0			hypothetical protein
AFLA_060020	AFLA_060020	0	2258	538	1406717	1410633	0	0			PKS-like enzyme, putative
AFLA_060020	AFLA_060010	1	2258	537	1404376	1406005	712	0			hypothetical protein
AFLA_060020	AFLA_060000	2	2258	536	1402360	1403600	776	1			metallo-beta-lactamase superfamily protein
AFLA_060020	AFLA_059990	3	2258	535	1401933	1398469	427	1			Tryptophan halogenase family protein
AFLA_060020	AFLA_059980	4	2258	534	1396349	1397996	473	0			GMC oxidoreductase family protein
AFLA_060020	AFLA_059970	5	2258	533	1394858	1393864	1491	1			NAD dependent epimerase/dehydratase family protein
AFLA_060020	AFLA_059960	6	2258	532	1392496	1393509	355	1			hypothetical protein
AFLA_060020	AFLA_059950	7	2258	531	1389270	1390926	1570	1			oxidoreductase, FAD-binding, putative

Cluster:19

Backbone_gene_id	Gene_id	Gene_positions		Chromosome-Contig		Gene_order	5'end	3'end	Gene_distance	Domain_score	Annotated_gene_function
AFLA_060680	AFLA_060760	-8	2258	612	1604191	1608539	1500	1			hypothetical protein
AFLA_060680	AFLA_060750	-7	2258	611	1602691	1600398	1360	0			Sec1 family protein

AFLA_060680	AFLA_060740	-6	2258	610	1599038	1597858	432	0	mating-type alpha-pheromone receptor PreB
AFLA_060680	AFLA_060730	-5	2258	609	1597426	1595566	532	0	conserved hypothetical protein
AFLA_060680	AFLA_060720	-4	2258	608	1593450	1595034	495	1	oxidoreductase, oxygen dependent, FAD-dependent protein-related
AFLA_060680	AFLA_060710	-3	2258	607	1591507	1592955	418	0	hydrolase, alpha/beta fold family protein
AFLA_060680	AFLA_060700	-2	2258	606	1588821	1591089	560	0	phenylalanine ammonia-lyase family protein
AFLA_060680	AFLA_060690	-1	2258	605	1586494	1588261	170	1	Cytochrome P450 family protein
AFLA_060680	AFLA_060680	0	2258	604	1586324	1584884	0	0	dimethylallyl tryptophan synthase, putative

Cluster:20

Backbone_gene_id	Gene_id	Gene_positions		Chromosome-Contig	Gene_order		5'end	3'end	Gene_distance	Domain_score	Annotated_gene_function
AFLA_062860	AFLA_062990	-13	2258	835	2205524	2206837	244	1	hypothetical protein		
AFLA_062860	AFLA_062980	-12	2258	834	2205280	2204236	691	0	enoyl-CoA hydratase/isomerase family protein		
AFLA_062860	AFLA_062970	-11	2258	833	2203545	2201302	918	0	Copper amine oxidase, enzyme domain containing protein		
AFLA_062860	AFLA_062960	-10	2258	832	2198253	2200384	365	1	hypothetical protein		
AFLA_062860	AFLA_062950	-9	2258	831	2197888	2197476	36	0	hypothetical protein		
AFLA_062860	AFLA_062940	-8	2258	830	2197440	2195885	1914	0	hypothetical protein		
AFLA_062860	AFLA_062930	-7	2258	829	2193971	2192936	1047	0	glycosyl hydrolase, family 43 protein		
AFLA_062860	AFLA_062920	-6	2258	828	2191254	2191889	356	0	hypothetical protein		
AFLA_062860	AFLA_062910	-5	2258	827	2188732	2190898	651	1	New cDNA-based gene: (AO_CDS_042706, novel, updateIDs: 5628, [gene: novel_gene_645, model: novel_model_645])		
AFLA_062860	AFLA_062900	-4	2258	826	2185955	2188081	2100	0	Acyltransferase family protein		
AFLA_062860	AFLA_062890	-3	2258	825	2183855	2183270	1476	0	hypothetical protein		

AFLA_062860	AFLA_062880	-2	2258	824	2181794	2180961	803	1	oxidoreductase, short chain dehydrogenase/reductase family protein
AFLA_062860	AFLA_062870	-1	2258	823	2179433	2180158	2391	0	hypothetical protein
AFLA_062860	AFLA_062860	0	2258	822	2170305	2177042	0	0	polyketide synthase, putative
AFLA_062860	AFLA_062850	1	2258	821	2169231	2167549	1074	0	Fatty acid desaturase family protein
AFLA_062860	AFLA_062840	2	2258	820	2165747	2166541	1008	0	conserved hypothetical protein
AFLA_062860	AFLA_062830	3	2258	819	2164703	2163155	1044	1	FAD binding domain containing protein
AFLA_062860	AFLA_062820	4	2258	818	2161415	2153493	1740	1	polyketide synthase, putative

Cluster:21

Backbone_gene_id	Gene_id	Gene_positions		Chromosome-Contig			Gene_order	5'end	3'end	Gene_distance	Domain_score	Annotated_gene_function
AFLA_064240	AFLA_064440	-20	2368	27	83972	81563	600	1	vacuolar ABC heavy metal transporter (Hmt1), putative			
AFLA_064240	AFLA_064430	-19	2368	26	79308	80963	904	1	Major Facilitator Superfamily protein			
AFLA_064240	AFLA_064420	-18	2368	25	78404	77944	1305	0	GliK-related			
AFLA_064240	AFLA_064410	-17	2368	24	76639	75158	104	0	hypothetical protein			
AFLA_064240	AFLA_064400	-16	2368	23	73235	75054	216	1	Cytochrome P450 family protein			
AFLA_064240	AFLA_064390	-15	2368	22	73019	71207	235	1	Cytochrome P450 family protein			
AFLA_064240	AFLA_064380	-14	2368	21	70972	68974	898	1	Tryptophan halogenase family protein			
AFLA_064240	AFLA_064370	-13	2368	20	65641	68076	743	1	Fungal specific transcription factor domain containing protein			
AFLA_064240	AFLA_064360	-12	2368	19	64898	60297	842	1	ABC transporter family protein			
AFLA_064240	AFLA_064350	-11	2368	18	57672	59455	1701	1	conserved hypothetical protein			
AFLA_064240	AFLA_064340	-10	2368	17	55971	55171	2098	0	haloacid dehalogenase, type II family protein			
AFLA_064240	AFLA_064330	-9	2368	16	53073	51418	427	0	hypothetical protein			
AFLA_064240	AFLA_064320	-8	2368	15	47758	50991	33	1	POT family protein			
AFLA_064240	AFLA_064310	-7	2368	14	47408	47725	444	0	di/tri peptide transporter 2-related			
AFLA_064240	AFLA_064300	-6	2368	13	46964	45453	267	0	FAD dependent oxidoreductase family protein			
AFLA_064240	AFLA_064290	-5	2368	12	45186	44443	427	0	O-methyltransferase family protein			

AFLA_064240	AFLA_064280	-4	2368	11	42851	44016	537	1	hypothetical protein
AFLA_064240	AFLA_064270	-3	2368	10	41154	42314	644	1	hypothetical protein
AFLA_064240	AFLA_064260	-2	2368	9	40510	38582	1480	0	MFS peptide transporter, putaitve, putative
AFLA_064240	AFLA_064250	-1	2368	8	36311	37102	920	1	FAD binding domain containing protein
AFLA_064240	AFLA_064240	0	2368	7	35391	25905	0	0	nonribosomal peptide synthase, putative

Cluster:22

Backbone_gene_id	Gene_id	Gene_positions		Chromosome-Contig	Gene_order		5'end	3'end	Gene_distance	Domain_score	Annotated_gene_function
AFLA_064560	AFLA_064610	-5	2368	44	116491	115109	798	1	oxidoreductase, short chain dehydrogenase/reductase family protein		
AFLA_064560	AFLA_064600	-4	2368	43	112870	114311	707	0	hypothetical protein		
AFLA_064560	AFLA_064590	-3	2368	42	112163	111281	263	1	O-methyltransferase family protein		
AFLA_064560	AFLA_064580	-2	2368	41	109800	111018	248	0	Oxidoreductase family, NAD-binding Rossmann fold containing protein		
AFLA_064560	AFLA_064570	-1	2368	40	109552	107693	804	0	permease, cytosine/purines, uracil, thiamine, allantoin family protein		
AFLA_064560	AFLA_064560	0	2368	39	106889	101963	0	0	nonribosomal peptide synthase, putative		
AFLA_064560	AFLA_064550	1	2368	38	100260	101660	303	1	Renal dipeptidase family protein		
AFLA_064560	AFLA_064540	2	2368	37	100034	98411	226	1	Cytochrome P450 family protein		
AFLA_064560	AFLA_064530	3	2368	36	97373	98280	131	1	Glutathione S-transferase, C-terminal domain containing protein		
AFLA_064560	AFLA_064520	4	2368	35	95877	97232	141	1	O-methyltransferase GliM-like, putative		
AFLA_064560	AFLA_064510	5	2368	34	95613	94556	264	1	GliT-related		
AFLA_064560	AFLA_064500	6	2368	33	93592	92595	964	1	pyridine nucleotide-disulphide oxidoreductase, class II-related		
AFLA_064560	AFLA_064490	7	2368	32	91098	92168	427	1	7alpha-cephem-methoxylase P8 chain, putative		
AFLA_064560	AFLA_064480	8	2368	31	90822	89773	276	1	GliT-related		
AFLA_064560	AFLA_064470	9	2368	30	89655	87729	118	1	Cytochrome P450 family protein		
AFLA_064560	AFLA_064460	10	2368	29	86181	87534	195	0	hypothetical protein		

AFLA_064560	AFLA_064450	11	2368	28	84795	86027	154	1	aminotransferase, classes I and II family protein
AFLA_064560	AFLA_064440	12	2368	27	83972	81563	823	1	vacuolar ABC heavy metal transporter (Hmt1), putative
AFLA_064560	AFLA_064430	13	2368	26	79308	80963	600	1	Major Facilitator Superfamily protein
AFLA_064560	AFLA_064420	14	2368	25	78404	77944	904	0	GliK-related
AFLA_064560	AFLA_064410	15	2368	24	76639	75158	1305	0	hypothetical protein
AFLA_064560	AFLA_064400	16	2368	23	73235	75054	104	1	Cytochrome P450 family protein
AFLA_064560	AFLA_064390	17	2368	22	73019	71207	216	1	Cytochrome P450 family protein
AFLA_064560	AFLA_064380	18	2368	21	70972	68974	235	1	Tryptophan halogenase family protein
AFLA_064560	AFLA_064370	19	2368	20	65641	68076	898	1	Fungal specific transcription factor domain containing protein
AFLA_064560	AFLA_064360	20	2368	19	64898	60297	743	1	ABC transporter family protein

Cluster:23

Backbone_gene_id	Gene_id	Gene_positions		Chromosome-Contig	Gene_order		5'end	3'end	Gene_distance	Domain_score	Annotated_gene_function
AFLA_066840	AFLA_066980	-14	2368	281	742432	749952	979	1			polyketide synthase, putative
AFLA_066840	AFLA_066970	-13	2368	280	741453	739298	487	0			conserved hypothetical protein
AFLA_066840	AFLA_066960	-12	2368	279	738385	738811	141	0			hypothetical protein
AFLA_066840	AFLA_066950	-11	2368	278	736840	738244	528	0			FAD binding domain containing protein
AFLA_066840	AFLA_066940	-10	2368	277	734919	736312	333	1			O-methyltransferase family protein
AFLA_066840	AFLA_066930	-9	2368	276	734586	732934	212	1			Cytochrome P450 family protein
AFLA_066840	AFLA_066920	-8	2368	275	731458	732722	237	0			ToxD-like zinc binding oxidoreductase, putative
AFLA_066840	AFLA_066910	-7	2368	274	731221	730081	715	0			hypothetical protein
AFLA_066840	AFLA_066900	-6	2368	273	726830	729366	2276	1			Fungal specific transcription factor domain containing protein
AFLA_066840	AFLA_066890	-5	2368	272	724554	722643	599	1			Cytochrome P450 family protein
AFLA_066840	AFLA_066880	-4	2368	271	720534	722044	633	1			Major Facilitator Superfamily protein

AFLA_066840	AFLA_066870	-3	2368	270	719901	719479	75	1	hypothetical protein
AFLA_066840	AFLA_066860	-2	2368	269	719404	717626	330	0	conserved hypothetical protein
AFLA_066840	AFLA_066850	-1	2368	268	716818	717296	285	0	hypothetical protein
AFLA_066840	AFLA_066840	0	2368	267	716533	704693	0	1	hybrid NRPS/PKS enzyme, putative
AFLA_066840	AFLA_066830	1	2368	266	703972	701610	721	1	Fungal specific transcription factor domain containing protein
AFLA_066840	AFLA_066820	2	2368	265	698602	699772	1838	1	oxidoreductase, zinc-binding dehydrogenase family protein
AFLA_066840	AFLA_066810	3	2368	264	696628	697948	654	0	hypothetical protein
AFLA_066840	AFLA_066800	4	2368	263	695070	694459	1558	0	hypothetical protein
AFLA_066840	AFLA_066790	5	2368	262	690975	693451	1008	0	hypothetical protein
AFLA_066840	AFLA_066780	6	2368	261	688382	690085	890	0	Polyprenyl synthetase family protein
AFLA_066840	AFLA_066770	7	2368	260	688074	686534	308	1	FAD dependent oxidoreductase, putative
AFLA_066840	AFLA_066760	8	2368	259	682176	685132	1402	0	unknown-related
AFLA_066840	AFLA_066750	9	2368	258	678960	681518	658	0	Glycosyl hydrolase family 3 C terminal domain containing protein
AFLA_066840	AFLA_066740	10	2368	257	676143	677540	1420	1	Major Facilitator Superfamily protein
AFLA_066840	AFLA_066730	11	2368	256	673317	674393	1750	1	oxidoreductase, zinc-binding dehydrogenase family protein
AFLA_066840	AFLA_066720	12	2368	255	655460	671802	1515	0	nonribosomal peptide synthase, putative
AFLA_066840	AFLA_066710	13	2368	254	655109	653979	351	1	hypothetical protein
AFLA_066840	AFLA_066700	14	2368	253	653630	652134	349	1	Cytochrome P450 family protein

Cluster:24

Backbone_gene_id	Gene_id	Gene_positions	Chromosome-Contig	Gene_order	5'end	3'end	Gene_distance	Domain_score	Annotated_gene_function

AFLA_069330	AFLA_069410	-8	2368	524	1399261	1396108	580	1	RNase L inhibitor of the ABC superfamily, putative
AFLA_069330	AFLA_069400	-7	2368	523	1392947	1395528	290	0	FF domain containing protein
AFLA_069330	AFLA_069390	-6	2368	522	1392657	1390724	691	0	hypothetical protein
AFLA_069330	AFLA_069380	-5	2368	521	1390033	1388908	831	0	Mpv17 / PMP22 family protein
AFLA_069330	AFLA_069370	-4	2368	520	1388077	1386692	189	0	phosphoglycerate kinase PgkA, putative
AFLA_069330	AFLA_069360	-3	2368	519	1385454	1386503	796	1	26 proteasome complex subunit Sem1, putative
AFLA_069330	AFLA_069350	-2	2368	518	1384658	1382210	980	0	conserved hypothetical protein
AFLA_069330	AFLA_069340	-1	2368	517	1381230	1379343	569	1	MSF drug transporter, putative
AFLA_069330	AFLA_069330	0	2368	516	1362826	1378774	0	0	nonribosomal peptide synthase Pes1

Cluster:25

Backbone_gene_id	Gene_id	Gene_positions		Chromosome-Contig		Gene_order	5'end	3'end	Gene_distance	Domain_score	Annotated_gene_function
AFLA_070920	AFLA_070980	-6	2368	681	1864430	1861877	932	1	C6 transcription factor, putative		
AFLA_070920	AFLA_070970	-5	2368	680	1860945	1858934	269	1	Fungal specific transcription factor domain containing protein		
AFLA_070920	AFLA_070960	-4	2368	679	1855567	1858665	1634	0	AT hook motif family protein		
AFLA_070920	AFLA_070950	-3	2368	678	1852565	1853933	1896	0	malate permease, ,putative		
AFLA_070920	AFLA_070940	-2	2368	677	1850669	1848985	322	0	extracellular rhamnogalacturonase, putative		
AFLA_070920	AFLA_070930	-1	2368	676	1848663	1846933	1152	1	membrane transporter; 11 predicted transmembrane helices, putative		
AFLA_070920	AFLA_070920	0	2368	675	1842755	1845781	0	0	NRPS-like enzyme, putative		
AFLA_070920	AFLA_070910	1	2368	674	1841501	1840100	1254	1	aminotransferase, classes I and II family protein		
AFLA_070920	AFLA_070900	2	2368	673	1838063	1838698	1402	0	hypothetical protein		
AFLA_070920	AFLA_070890	3	2368	672	1836192	1836995	1068	0	hypothetical protein		

AFLA_070920	AFLA_070880	4	2368	671	1833085	1834369	1823	1	Acyl-coenzyme A:6-aminopenicillanic-acid-acyltransferase precursor, putative
AFLA_070920	AFLA_070870	5	2368	670	1831356	1832351	734	1	New cDNA-based gene: (AO_CDS_042706, novel, updateIDs: 6373, [gene: novel_gene_717, model: novel_model_717])
AFLA_070920	AFLA_070860	6	2368	669	1830330	1819006	1026	0	nonribosomal peptide synthase, putative
AFLA_070920	AFLA_070850	7	2368	668	1818468	1817090	538	0	Phosphatidylserine decarboxylase, ,putative
AFLA_070920	AFLA_070840	8	2368	667	1815175	1816971	119	1	Major Facilitator Superfamily protein
AFLA_070920	AFLA_070830	9	2368	666	1809066	1814555	620	0	hypothetical protein
AFLA_070920	AFLA_070820	10	2368	665	1804776	1806633	2433	1	3-hydroxy-3-methylglutaryl-coenzyme A lyase/3-methylglutaconyl-coenzyme A hydratase, putative
AFLA_070920	AFLA_070810	11	2368	664	1801567	1799384	3209	0	Carboxylesterase family protein
AFLA_070920	AFLA_070800	12	2368	663	1797196	1798842	542	0	hypothetical protein
AFLA_070920	AFLA_070790	13	2368	662	1795038	1794436	2158	0	New cDNA-based gene: (AO_CDS_042706, novel, updateIDs: 6368, [gene: novel_gene_716, model: novel_model_716])
AFLA_070920	AFLA_070780	14	2368	661	1793654	1791721	782	0	Amidase family protein
AFLA_070920	AFLA_070770	15	2368	660	1788584	1786982	3137	0	hypothetical protein
AFLA_070920	AFLA_070760	16	2368	659	1784323	1786494	488	1	Major Facilitator Superfamily protein
AFLA_070920	AFLA_070750	17	2368	658	1781368	1781614	2709	0	New cDNA-based gene: (AO_CDS_042706, novel, updateIDs: 6365, [gene: novel_gene_715, model: novel_model_715])
AFLA_070920	AFLA_070740	18	2368	657	1780336	1779468	1032	0	hypothetical protein
AFLA_070920	AFLA_070730	19	2368	656	1774151	1777064	2404	1	hypothetical protein

Cluster:26

Backbone_gene_id	Gene_id	Gene_positions		Chromosome-Contig	Gene_order	5'end	3'end	Gene_distance	Domain_score	Annotated_gene_function
AFLA_079400	AFLA_079510	-11	2504	734	1932862	1930791	109	1	Major Facilitator Superfamily protein	
AFLA_079400	AFLA_079500	-10	2504	733	1929684	1930682	885	0	xylosidase, putative	

AFLA_079400	AFLA_079490	-9	2504	732	1928248	1928799	470	0	hypothetical protein
AFLA_079400	AFLA_079480	-8	2504	731	1925515	1927778	526	0	prolyl oligopeptidase family protein
AFLA_079400	AFLA_079470	-7	2504	730	1918357	1924989	611	0	pre-mRNA splicing helicase, putative
AFLA_079400	AFLA_079460	-6	2504	729	1917746	1914711	179	0	MutS domain III family protein
AFLA_079400	AFLA_079450	-5	2504	728	1913795	1914532	264	0	Ureidoglycolate hydrolase family protein
AFLA_079400	AFLA_079440	-4	2504	727	1912113	1913531	1038	1	Major Facilitator Superfamily protein
AFLA_079400	AFLA_079430	-3	2504	726	1911075	1910291	1926	0	glutamyl-tRNA(Gln) amidotransferase subunit A, putative
AFLA_079400	AFLA_079420	-2	2504	725	1908365	1907742	218	0	hypothetical protein
AFLA_079400	AFLA_079410	-1	2504	724	1905565	1907524	508	1	Major Facilitator Superfamily protein
AFLA_079400	AFLA_079400	0	2504	723	1901221	1905057	0	1	NRPS-like enzyme, putative
AFLA_079400	AFLA_079390	1	2504	722	1898598	1899094	2127	0	hypothetical protein
AFLA_079400	AFLA_079380	2	2504	721	1894656	1897651	947	0	NRPS-like enzyme, putative
AFLA_079400	AFLA_079370	3	2504	720	1894296	1894484	172	0	hypothetical protein
AFLA_079400	AFLA_079360	4	2504	719	1892994	1892237	1302	0	PKS-like enzyme, putative
AFLA_079400	AFLA_079350	5	2504	718	1890807	1890073	1430	0	hypothetical protein
AFLA_079400	AFLA_079340	6	2504	717	1886382	1887372	2701	0	Dienelactone hydrolase family protein
AFLA_079400	AFLA_079330	7	2504	716	1885259	1883652	1123	0	Transmembrane amino acid transporter protein
AFLA_079400	AFLA_079320	8	2504	715	1882763	1880467	889	1	Fungal specific transcription factor domain containing protein

Cluster:27

Backbone_gene_id	Gene_id	Gene_positions	Chromosome-Contig	Gene_order	5'end	3'end	Gene_distance	Domain_score	Annotated_gene_function

AFLA_082150	AFLA_082280	-13	2504	1011	2680129	2679227	189	1	Glutathione S-transferase, N-terminal domain containing protein
AFLA_082150	AFLA_082270	-12	2504	1010	2677008	2679038	554	0	UDP-glucose/GDP-mannose dehydrogenase family, UDP binding domain containing protein
AFLA_082150	AFLA_082260	-11	2504	1009	2676454	2675009	698	0	glycosyl transferase, group 1 family protein
AFLA_082150	AFLA_082250	-10	2504	1008	2674311	2672301	1400	0	GMC oxidoreductase family protein
AFLA_082150	AFLA_082240	-9	2504	1007	2670901	2669988	1635	0	hypothetical protein
AFLA_082150	AFLA_082230	-8	2504	1006	2668353	2666670	119	1	Major Facilitator Superfamily protein
AFLA_082150	AFLA_082220	-7	2504	1005	2664797	2666551	283	0	oxidoreductase-related
AFLA_082150	AFLA_082210	-6	2504	1004	2664514	2663441	776	0	hypothetical protein
AFLA_082150	AFLA_082200	-5	2504	1003	2662665	2660638	531	0	ATPase, AAA family protein
AFLA_082150	AFLA_082190	-4	2504	1002	2660107	2659280	856	0	hypothetical protein
AFLA_082150	AFLA_082180	-3	2504	1001	2658424	2658155	50	0	hypothetical protein
AFLA_082150	AFLA_082170	-2	2504	1000	2658105	2656834	1460	1	Major Facilitator Superfamily protein
AFLA_082150	AFLA_082160	-1	2504	999	2655374	2653373	536	1	Sugar transporter family protein
AFLA_082150	AFLA_082150	0	2504	998	2646293	2652837	0	0	polyketide synthase, putative

Cluster:28

Backbone_gene_id	Gene_id	Gene_positions		Chromosome-Contig	Gene_order		5'end	3'end	Gene_distance	Domain_score	Annotated_gene_function
AFLA_082480	AFLA_082480	0	2504	1031	2730816	2732067	0	1	NRPS-like enzyme, putative		
AFLA_082480	AFLA_082470	1	2504	1030	2730410	2728379	406	0	AMP-binding enzyme family protein		
AFLA_082480	AFLA_082460	2	2504	1029	2726731	2727646	733	0	Phosphatidylserine decarboxylase-related		
AFLA_082480	AFLA_082450	3	2504	1028	2726036	2724533	695	1	Major Facilitator Superfamily protein		
AFLA_082480	AFLA_082440	4	2504	1027	2723068	2723992	541	0	hypothetical protein		

AFLA_082480	AFLA_082430	5	2504	1026	2721452	2722705	363	1	hypothetical protein
AFLA_082480	AFLA_082420	6	2504	1025	2718976	2719365	2087	0	New cDNA-based gene: (AO_CDS_042706, novel, updateIDs: 7291, [gene: novel_gene_812, model: novel_model_812])
AFLA_082480	AFLA_082410	7	2504	1024	2718542	2717312	434	0	hypothetical protein
AFLA_082480	AFLA_082400	8	2504	1023	2716786	2712072	526	1	ABC transporter family protein

Cluster:29

Backbone_gene_id	Gene_id	Gene_positions		Chromosome-Contig	Gene_order	5'end	3'end	Gene_distance	Domain_score	Annotated_gene_function
AFLA_083250	AFLA_083330	-8	2504	1116	2962748	2959979	367	1		Fungal specific transcription factor domain containing protein
AFLA_083250	AFLA_083320	-7	2504	1115	2957830	2959612	1205	1		Sugar transporter family protein
AFLA_083250	AFLA_083310	-6	2504	1114	2956625	2955630	1556	0		Amidohydrolase family protein
AFLA_083250	AFLA_083300	-5	2504	1113	2951101	2954074	2515	0		Glycosyl hydrolases family 31 protein
AFLA_083250	AFLA_083290	-4	2504	1112	2948586	2947507	1194	0		conserved hypothetical protein
AFLA_083250	AFLA_083280	-3	2504	1111	2946313	2945832	1718	0		hypothetical protein
AFLA_083250	AFLA_083270	-2	2504	1110	2944114	2942091	935	1		Amino acid permease family protein
AFLA_083250	AFLA_083260	-1	2504	1109	2941156	2939989	1858	0		hypothetical protein
AFLA_083250	AFLA_083250	0	2504	1108	2938131	2936772	0	0		dimethylallyl tryptophan synthase, putative
AFLA_083250	AFLA_083240	1	2504	1107	2934533	2935740	1032	1		xylitol dehydrogenase LadA/XdhB

Cluster:30

Backbone_gene_id	Gene_id	Gene_positions		Chromosome-Contig	Gene_order	5'end	3'end	Gene_distance	Domain_score	Annotated_gene_function
AFLA_084080	AFLA_084210	-13	2504	1204	3200982	3200087	1137	1		hypothetical protein
AFLA_084080	AFLA_084200	-12	2504	1203	3198950	3197412	810	0		hypothetical protein
AFLA_084080	AFLA_084190	-11	2504	1202	3196602	3194506	152	0		hypothetical protein

AFLA_084080	AFLA_084180	-10	2504	1201	3194354	3193799	442	0	New cDNA-based gene: (AO_CDS_042706, novel, updateIDs: 7429, [gene: novel_gene_834, model: novel_model_834])
AFLA_084080	AFLA_084170	-9	2504	1200	3193357	3191475	885	0	Multicopper oxidase family protein
AFLA_084080	AFLA_084160	-8	2504	1199	3190590	3189654	461	0	conserved hypothetical protein
AFLA_084080	AFLA_084150	-7	2504	1198	3188069	3189193	863	0	peroxisome biogenesis factor, putative
AFLA_084080	AFLA_084140	-6	2504	1197	3187206	3185676	592	1	2-oxoglutarate dehydrogenase, E2 component, dihydrolipoamide succinyltransferase family protein
AFLA_084080	AFLA_084130	-5	2504	1196	3185084	3183580	60	1	2-oxoglutarate dehydrogenase E1 component, mitochondrial precursor-related
AFLA_084080	AFLA_084120	-4	2504	1195	3183520	3183068	53	1	2-oxoglutarate dehydrogenase E1 component, mitochondrial precursor-related
AFLA_084080	AFLA_084110	-3	2504	1194	3183015	3182578	141	1	2-oxoglutarate dehydrogenase E1 component, mitochondrial precursor, putative
AFLA_084080	AFLA_084100	-2	2504	1193	3182437	3181824	90	1	2-oxoglutarate dehydrogenase E1 component, mitochondrial precursor-related
AFLA_084080	AFLA_084090	-1	2504	1192	3179694	3181734	696	1	Fungal specific transcription factor domain containing protein
AFLA_084080	AFLA_084080	0	2504	1191	3177863	3178998	0	0	dimethylallyl tryptophan synthase, putative

Cluster:31

Backbone_gene_id	Gene_id	Gene_positions		Chromosome-Contig	Gene_order		5'end	3'end	Gene_distance	Domain_score	Annotated_gene_function
AFLA_090200	AFLA_090210	-1	2541	115	309444	307780	344	1	Amino acid permease family protein		
AFLA_090200	AFLA_090200	0	2541	114	302181	307436	0	0	nonribosomal peptide synthase, putative		
AFLA_090200	AFLA_090190	1	2541	113	300318	298721	1863	0	dimethylallyl tryptophan synthase, putative		

AFLA_090200	AFLA_090180	2	2541	112	298048	297158	673	0	hydrolase, alpha/beta fold family protein
AFLA_090200	AFLA_090170	3	2541	111	294013	295717	1441	1	Sugar transporter family protein

Cluster:32

Backbone_gene_id	Gene_id	Gene_positions		Chromosome-Contig	Gene_order		5'end	3'end	Gene_distance	Domain_score	Annotated_gene_function
AFLA_096770	AFLA_096770	0	2541	771	2022113	2025146	0	0			polyketide synthase, putative
AFLA_096770	AFLA_096760	1	2541	770	2019179	2020813	1300	1			Major Facilitator Superfamily protein
AFLA_096770	AFLA_096750	2	2541	769	2018354	2017183	825	1			Cytochrome P450 family protein
AFLA_096770	AFLA_096740	3	2541	768	2016237	2014725	946	1			FAD binding domain containing protein

Cluster:33

Backbone_gene_id	Gene_id	Gene_positions		Chromosome-Contig	Gene_order		5'end	3'end	Gene_distance	Domain_score	Annotated_gene_function
AFLA_101700	AFLA_101740	-4	2634	467	1211563	1209968	357	1			major facilitator superfamily protein
AFLA_101700	AFLA_101730	-3	2634	466	1207868	1209611	694	1			Cytochrome P450 family protein
AFLA_101700	AFLA_101720	-2	2634	465	1207174	1205421	1529	1			Cytochrome P450 family protein
AFLA_101700	AFLA_101710	-1	2634	464	1202775	1203892	685	0			NmrA-like family protein
AFLA_101700	AFLA_101700	0	2634	463	1202090	1198962	0	0			NRPS-like enzyme, putative
AFLA_101700	AFLA_101690	1	2634	462	1197753	1195973	1209	1			oxidoreductase, zinc-binding dehydrogenase family protein

Cluster:34

Backbone_gene_id	Gene_id	Gene_positions		Chromosome-Contig	Gene_order		5'end	3'end	Gene_distance	Domain_score	Annotated_gene_function
AFLA_104210	AFLA_104250	-4	2689	7	24095	26449	354	1			conserved hypothetical protein
AFLA_104210	AFLA_104240	-3	2689	6	22682	23741	601	0			PKS-like enzyme, putative
AFLA_104210	AFLA_104230	-2	2689	5	22081	20244	240	1			Major Facilitator Superfamily protein

AFLA_104210	AFLA_104220	-1	2689	4	17820	20004	1125	1	Fungal specific transcription factor domain containing protein
AFLA_104210	AFLA_104210	0	2689	3	16695	14187	0	0	PKS-like enzyme, putative

Cluster:35

Backbone_gene_id	Gene_id	Gene_positions		Chromosome-Contig	Gene_order		5'end	3'end	Gene_distance	Domain_score	Annotated_gene_function
AFLA_105190	AFLA_105300	-11	2689	112	297517	298524	660	1	metallo-beta-lactamase superfamily protein		
AFLA_105190	AFLA_105290	-10	2689	111	296857	296367	1380	0	hypothetical protein		
AFLA_105190	AFLA_105280	-9	2689	110	293919	294987	1692	0	hypothetical protein		
AFLA_105190	AFLA_105270	-8	2689	109	292227	291730	888	0	hypothetical protein		
AFLA_105190	AFLA_105260	-7	2689	108	290842	290185	407	0	hypothetical protein		
AFLA_105190	AFLA_105250	-6	2689	107	289778	289009	1229	0	hypothetical protein		
AFLA_105190	AFLA_105240	-5	2689	106	287341	287780	2368	0	hypothetical protein		
AFLA_105190	AFLA_105230	-4	2689	105	284973	283497	447	0	hypothetical protein		
AFLA_105190	AFLA_105220	-3	2689	104	283050	282265	78	1	oxidoreductase, short chain dehydrogenase/reductase family protein		
AFLA_105190	AFLA_105210	-2	2689	103	282187	281052	2666	0	enoyl-CoA hydratase/isomerase family protein		
AFLA_105190	AFLA_105200	-1	2689	102	278386	276383	598	0	GPI anchored glucanase, putative		
AFLA_105190	AFLA_105190	0	2689	101	272459	275785	0	0	NRPS-like enzyme, putative		
AFLA_105190	AFLA_105180	1	2689	100	270065	269796	2394	0	hypothetical protein		
AFLA_105190	AFLA_105170	2	2689	99	269020	267559	776	1	O-methyltransferase family protein		
AFLA_105190	AFLA_105160	3	2689	98	264930	265400	2159	0	hypothetical protein		
AFLA_105190	AFLA_105150	4	2689	97	263456	264876	54	0	Carboxylesterase family protein		
AFLA_105190	AFLA_105140	5	2689	96	262532	262940	516	0	hypothetical protein		
AFLA_105190	AFLA_105130	6	2689	95	260881	261653	879	0	hypothetical protein		
AFLA_105190	AFLA_105120	7	2689	94	259615	260166	715	1	hypothetical protein		
AFLA_105190	AFLA_105110	8	2689	93	259414	258906	201	0	hypothetical protein		
AFLA_105190	AFLA_105100	9	2689	92	256537	258553	353	0	conserved hypothetical protein		

AFLA_105190 AFLA_105090 10 2689 91 256083 254102 454 1 New cDNA-based gene: (AO_CDS_042706, novel, updateIDs: 9638, [gene: novel_gene_1014, model: novel_model_1014])

Cluster:36

Backbone_gene_id	Gene_id	Gene_positions		Chromosome-Contig	Gene_order	5'end	3'end	Gene_distance	Domain_score	Annotated_gene_function
AFLA_105450	AFLA_105450	0	2689	127	336825	345056	0	1		polyketide synthase, putative
AFLA_105450	AFLA_105440	1	2689	126	335722	334376	1103	1		Cytochrome P450 family protein

Cluster:37

Backbone_gene_id	Gene_id	Gene_positions		Chromosome-Contig	Gene_order	5'end	3'end	Gene_distance	Domain_score	Annotated_gene_function
AFLA_108550	AFLA_108610	-6	2689	443	1165381	1166754	3305	1		Cytochrome P450 family protein
AFLA_108550	AFLA_108600	-5	2689	442	1162076	1161182	112	1		acetyltransferase, GNAT family protein
AFLA_108550	AFLA_108590	-4	2689	441	1160173	1161070	2919	0		hypothetical protein
AFLA_108550	AFLA_108580	-3	2689	440	1157254	1155495	612	1		hypothetical protein
AFLA_108550	AFLA_108570	-2	2689	439	1154883	1153809	584	0		hypothetical protein
AFLA_108550	AFLA_108560	-1	2689	438	1151758	1153225	1551	1		O-methyltransferase family protein
AFLA_108550	AFLA_108550	0	2689	437	1150207	1144762	0	0		polyketide synthase, putative

Cluster:38

Backbone_gene_id	Gene_id	Gene_positions		Chromosome-Contig	Gene_order	5'end	3'end	Gene_distance	Domain_score	Annotated_gene_function
AFLA_109430	AFLA_109430	0	2689	525	1416093	1401753	0	0		nonribosomal siderophore peptide synthase SidC
AFLA_109430	AFLA_109420	1	2689	524	1398897	1401293	460	0		predicted protein
AFLA_109430	AFLA_109410	2	2689	523	1395653	1397964	933	0		UV-endonuclease uvde family protein
AFLA_109430	AFLA_109400	3	2689	522	1394651	1393611	1002	0		hypothetical protein
AFLA_109430	AFLA_109390	4	2689	521	1390969	1391828	1783	0		conserved hypothetical protein

AFLA_109430	AFLA_109380	5	2689	520	1388586	1389948	1021	1	oxidoreductase, zinc-binding dehydrogenase family protein

Cluster:39

Backbone_gene_id	Gene_id	Gene_positions		Chromosome-Contig	Gene_order	5'end	3'end	Gene_distance	Domain_score Annotated_gene_function
AFLA_112840	AFLA_112890	-5	2689	871	2323499	2325296	520	1	Major Facilitator Superfamily protein
AFLA_112840	AFLA_112880	-4	2689	870	2322979	2320865	135	1	FAD binding domain containing protein
AFLA_112840	AFLA_112870	-3	2689	869	2318738	2320730	191	1	FAD dependent oxidoreductase family protein
AFLA_112840	AFLA_112860	-2	2689	868	2318547	2317464	752	0	hypothetical protein
AFLA_112840	AFLA_112850	-1	2689	867	2316712	2315306	507	1	O-methyltransferase family protein
AFLA_112840	AFLA_112840	0	2689	866	2307795	2314799	0	0	polyketide synthase, putative
AFLA_112840	AFLA_112830	1	2689	865	2304569	2306866	929	1	Fungal specific transcription factor domain containing protein
AFLA_112840	AFLA_112820	2	2689	864	2300919	2299817	3650	1	NAD dependent epimerase/dehydratase family protein

Cluster:40

Backbone_gene_id	Gene_id	Gene_positions		Chromosome-Contig	Gene_order	5'end	3'end	Gene_distance	Domain_score Annotated_gene_function
AFLA_114820	AFLA_114820	0	2802	63	153643	159213	0	1	polyketide synthase, putative
AFLA_114820	AFLA_114810	1	2802	62	151713	149890	1930	1	Cytochrome P450 family protein

Cluster:41

Backbone_gene_id	Gene_id	Gene_positions		Chromosome-Contig	Gene_order	5'end	3'end	Gene_distance	Domain_score Annotated_gene_function
AFLA_116220	AFLA_116330	-11	2842	61	148002	149287	596	1	O-methyltransferase family protein

AFLA_116220	AFLA_116320	-10	2842	60	146401	147406	2482	0	hypothetical protein
AFLA_116220	AFLA_116310	-9	2842	59	142284	143919	124	0	conserved hypothetical protein
AFLA_116220	AFLA_116300	-8	2842	58	142160	141351	433	1	oxidoreductase, short chain dehydrogenase/reductase family protein
AFLA_116220	AFLA_116290	-7	2842	57	140918	140597	474	0	hypothetical protein
AFLA_116220	AFLA_116280	-6	2842	56	140123	138135	319	0	Dehydratase family protein
AFLA_116220	AFLA_116270	-5	2842	55	136575	137816	775	0	hypothetical protein
AFLA_116220	AFLA_116260	-4	2842	54	134791	135800	424	0	N-acetyltransferase family protein
AFLA_116220	AFLA_116250	-3	2842	53	133302	134367	775	0	conserved hypothetical protein
AFLA_116220	AFLA_116240	-2	2842	52	132527	131580	1094	0	conserved hypothetical protein
AFLA_116220	AFLA_116230	-1	2842	51	129644	130486	1335	0	hypothetical protein
AFLA_116220	AFLA_116220	0	2842	50	121844	128309	0	0	polyketide synthase, putative
AFLA_116220	AFLA_116210	1	2842	49	119733	121105	739	1	O-methyltransferase family protein
AFLA_116220	AFLA_116200	2	2842	48	118012	118518	1215	0	hypothetical protein
AFLA_116220	AFLA_116190	3	2842	47	116560	110436	1452	0	hypothetical protein
AFLA_116220	AFLA_116180	4	2842	46	108807	109508	928	0	hypothetical protein
AFLA_116220	AFLA_116170	5	2842	45	108373	107985	434	0	hypothetical protein
AFLA_116220	AFLA_116160	6	2842	44	105722	104504	2263	1	oxidoreductase, zinc-binding dehydrogenase family protein
AFLA_116220	AFLA_116150	7	2842	43	103586	104193	311	0	hypothetical protein
AFLA_116220	AFLA_116140	8	2842	42	102202	100917	1384	0	hypothetical protein
AFLA_116220	AFLA_116130	9	2842	41	99530	100198	719	0	hypothetical protein
AFLA_116220	AFLA_116120	10	2842	40	97549	94432	1981	0	conserved hypothetical protein
AFLA_116220	AFLA_116110	11	2842	39	92279	94315	117	1	Fungal specific transcription factor domain containing protein
AFLA_116220	AFLA_116100	12	2842	38	91917	90391	362	1	Major Facilitator Superfamily protein
AFLA_116220	AFLA_116090	13	2842	37	88277	90102	289	1	Sugar transporter family protein

Cluster:42

Backbone_gene_id	Gene_id	Gene_positions		Chromosome-Contig	Gene_order	5'end	3'end	Gene_distance	Domain_score	Annotated_gene_function
AFLA_116600	AFLA_116600	0	2842	88	206389	207845	0	0		dimethylallyl tryptophan synthase, putative
AFLA_116600	AFLA_116590	1	2842	87	205225	204489	1164	0		CRAL/TRIO domain containing protein
AFLA_116600	AFLA_116580	2	2842	86	203716	202349	773	1		3-beta hydroxysteroid dehydrogenase/isomerase family protein
AFLA_116600	AFLA_116570	3	2842	85	201402	201920	429	0		DUF636 domain protein, putative
AFLA_116600	AFLA_116560	4	2842	84	200998	200009	404	1		2-hydroxyisoflavone reductase, putative
AFLA_116600	AFLA_116550	5	2842	83	199601	199031	408	0		Phage lysozyme family protein
AFLA_116600	AFLA_116540	6	2842	82	197296	198006	1025	0		hypothetical protein
AFLA_116600	AFLA_116530	7	2842	81	194775	193219	2521	1		Cytochrome P450 family protein
AFLA_116600	AFLA_116520	8	2842	80	191867	193037	182	1		hypothetical protein
AFLA_116600	AFLA_116510	9	2842	79	191562	190351	305	0		hypothetical protein
AFLA_116600	AFLA_116500	10	2842	78	188716	190220	131	1		oxidoreductase, short chain dehydrogenase/reductase family protein
AFLA_116600	AFLA_116490	11	2842	77	187561	188037	679	0		hypothetical protein
AFLA_116600	AFLA_116480	12	2842	76	187194	186108	367	0		NAD dependent epimerase/dehydratase family protein
AFLA_116600	AFLA_116470	13	2842	75	185066	184224	1042	1		metallo-beta-lactamase superfamily protein
AFLA_116600	AFLA_116460	14	2842	74	182370	183151	1073	0		oxidoreductase-related
AFLA_116600	AFLA_116450	15	2842	73	180441	182039	331	1		FAD binding domain containing protein

Cluster:43

Backbone_gene_id	Gene_id	Gene_positions		Chromosome-Contig	Gene_order	5'end	3'end	Gene_distance	Domain_score	Annotated_gene_function

AFLA_116890	AFLA_116920	-3	2842	120	309649	316354	2049	1	oxidoreductase, short chain dehydrogenase/reductase family protein
AFLA_116890	AFLA_116910	-2	2842	119	307036	307600	1562	0	hypothetical protein
AFLA_116890	AFLA_116900	-1	2842	118	305474	304762	359	0	hypothetical protein
AFLA_116890	AFLA_116890	0	2842	117	296613	304403	0	0	polyketide synthase, putative
AFLA_116890	AFLA_116880	1	2842	116	294100	295920	693	1	New cDNA-based gene: (AO_CDS_042706, novel, updateIDs: 10705, [gene: novel_gene_1117, model: novel_model_1117])
AFLA_116890	AFLA_116870	2	2842	115	291683	290319	2417	1	Transferase family protein
AFLA_116890	AFLA_116860	3	2842	114	289659	287442	660	0	alpha-N-acetylglucosaminidase, putative
AFLA_116890	AFLA_116850	4	2842	113	287114	285858	328	0	hypothetical protein
AFLA_116890	AFLA_116840	5	2842	112	284401	282903	1457	1	FAD binding domain containing protein
AFLA_116890	AFLA_116830	6	2842	111	277662	282510	393	0	oxidoreductase, 2-nitropropane dioxygenase family protein
AFLA_116890	AFLA_116820	7	2842	110	274509	269808	3153	1	4'-phosphopantetheinyl transferase superfamily protein

Cluster:44

Backbone_gene_id	Gene_id	Gene_positions		Chromosome-Contig	Gene_order	5'end	3'end	Gene_distance	Domain_score	Annotated_gene_function
AFLA_118440	AFLA_118460	-2	2842	274	724528	717381	306	1		Major Facilitator Superfamily protein
AFLA_118440	AFLA_118450	-1	2842	273	717075	714970	1442	0		conserved hypothetical protein
AFLA_118440	AFLA_118440	0	2842	272	713528	710225	0	0		NRPS-like enzyme, putative

Cluster:45

Backbone_gene_id	Gene_id	Gene_positions		Chromosome-Contig	Gene_order	5'end	3'end	Gene_distance	Domain_score	Annotated_gene_function
AFLA_118940	AFLA_119000	-6	2842	328	864460	865900	1728	1		O-methyltransferase family protein

AFLA_118940	AFLA_118990	-5	2842	327	860771	862732	988	1	Major Facilitator Superfamily protein
AFLA_118940	AFLA_118980	-4	2842	326	859783	858715	128	0	Mitochondrial carrier protein
AFLA_118940	AFLA_118970	-3	2842	325	857064	858587	723	1	FAD dependent oxidoreductase family protein
AFLA_118940	AFLA_118960	-2	2842	324	856341	849580	317	0	polyketide synthase, putative
AFLA_118940	AFLA_118950	-1	2842	323	849263	848472	807	0	candidate tumor suppressor in ovarian cancer 2-related
AFLA_118940	AFLA_118940	0	2842	322	847665	840026	0	1	polyketide synthase, putative
AFLA_118940	AFLA_118930	1	2842	321	837504	837923	2103	0	hypothetical protein
AFLA_118940	AFLA_118920	2	2842	320	836981	837268	236	0	hypothetical protein
AFLA_118940	AFLA_118910	3	2842	319	835803	836674	307	0	hypothetical protein
AFLA_118940	AFLA_118900	4	2842	318	833331	834827	976	0	conserved hypothetical protein
AFLA_118940	AFLA_118890	5	2842	317	831650	832296	1035	0	translation initiation factor eIF-5A family protein
AFLA_118940	AFLA_118880	6	2842	316	829161	830552	1098	1	conserved hypothetical protein
AFLA_118940	AFLA_118870	7	2842	315	828567	828080	594	0	Endoribonuclease L-PSP family protein
AFLA_118940	AFLA_118860	8	2842	314	827637	827912	168	0	New cDNA-based gene: (AO_CDS_042706, novel, updateIDs: 10859, [gene: novel_gene_1135, model: novel_model_1135])
AFLA_118940	AFLA_118850	9	2842	313	826960	827451	186	0	hypothetical protein
AFLA_118940	AFLA_118840	10	2842	312	826054	824528	906	1	conserved hypothetical protein
AFLA_118940	AFLA_118830	11	2842	311	822272	824353	175	0	Zinc finger, C2H2 type family protein
AFLA_118940	AFLA_118820	12	2842	310	821202	820180	1070	1	oxidoreductase, short chain dehydrogenase/reductase family protein

Cluster:46

Backbone_gene_id	Gene_id	Gene_positions			Chromosome-Contig	Gene_order	5'end	3'end	Gene_distance	Domain_score	Annotated_gene_function
AFLA_119110	AFLA_119140	-3	2842	342	906069	906963	3131	1	NAD dependent epimerase/dehydratase family protein		

AFLA_119110	AFLA_119130	-2	2842	341	902211	902938	469	0	hypothetical protein
AFLA_119110	AFLA_119120	-1	2842	340	900338	901742	578	0	beta-lactamase family protein
AFLA_119110	AFLA_119110	0	2842	339	896447	899760	0	0	NRPS-like enzyme, putative
AFLA_119110	AFLA_119100	1	2842	338	896116	896393	54	0	New cDNA-based gene: (AO_CDS_042706, novel, updateIDs: 10881, [gene: novel_gene_1138, model: novel_model_1138])
AFLA_119110	AFLA_119090	2	2842	337	895578	894408	538	1	NAD dependent epimerase/dehydratase family protein

Cluster:47

Backbone_gene_id	Gene_id	Gene_positions		Chromosome-Contig	Gene_order	5'end	3'end	Gene_distance	Domain_score Annotated_gene_function
AFLA_121520	AFLA_121540	-2	2842	582	1485551	1487055	1301	1	Major Facilitator Superfamily protein
AFLA_121520	AFLA_121530	-1	2842	581	1483117	1484250	727	0	oxidoreductase, FAD/FMN-binding family protein
AFLA_121520	AFLA_121520	0	2842	580	1482390	1479298	0	0	NRPS-like enzyme, putative
AFLA_121520	AFLA_121510	1	2842	579	1477769	1476852	1529	0	methyltransferase LaeA-like, putative
AFLA_121520	AFLA_121500	2	2842	578	1474631	1476355	497	1	Cytochrome P450 family protein
AFLA_121520	AFLA_121490	3	2842	577	1474181	1472992	450	0	NmrA-like family protein
AFLA_121520	AFLA_121480	4	2842	576	1471814	1472787	205	1	hypothetical protein

Cluster:48

Backbone_gene_id	Gene_id	Gene_positions		Chromosome-Contig	Gene_order	5'end	3'end	Gene_distance	Domain_score Annotated_gene_function
AFLA_127090	AFLA_127110	-2	2856	408	1043171	1041460	182	1	Major Facilitator Superfamily protein
AFLA_127090	AFLA_127100	-1	2856	407	1040353	1041278	657	0	hypothetical protein
AFLA_127090	AFLA_127090	0	2856	406	1031825	1039696	0	0	polyketide synthase, putative
AFLA_127090	AFLA_127080	1	2856	405	1030106	1031122	703	0	NmrA-like family protein
AFLA_127090	AFLA_127070	2	2856	404	1029840	1028933	266	1	oxidoreductase, short chain dehydrogenase/reductase family protein

AFLA_127090	AFLA_127060	3	2856	403	1027377	1028585	348	0	hypothetical protein
AFLA_127090	AFLA_127050	4	2856	402	1026663	1026334	714	0	hypothetical protein
AFLA_127090	AFLA_127040	5	2856	401	1024714	1026015	319	1	To monocarboxylate transporter, putative
AFLA_127090	AFLA_127030	6	2856	400	1023836	1023033	878	0	unknown-related
AFLA_127090	AFLA_127020	7	2856	399	1022410	1020928	623	1	FAD binding domain containing protein
AFLA_127090	AFLA_127010	8	2856	398	1020241	1020699	229	0	hypothetical protein
AFLA_127090	AFLA_127000	9	2856	397	1019062	1019679	562	0	hypothetical protein
AFLA_127090	AFLA_126990	10	2856	396	1017582	1018880	182	1	Fungal specific transcription factor domain containing protein
AFLA_127090	AFLA_126980	11	2856	395	1014062	1015736	1846	0	hypothetical protein
AFLA_127090	AFLA_126970	12	2856	394	1012031	1013848	214	1	Amino acid permease family protein

Cluster:49

Backbone_gene_id	Gene_id	Gene_positions		Chromosome-Contig	Gene_order		5'end	3'end	Gene_distance	Domain_score	Annotated_gene_function
AFLA_128060	AFLA_128090	-3	2856	506	1328474	1330062	775	1	Cytochrome P450 family protein		
AFLA_128060	AFLA_128080	-2	2856	505	1326250	1327699	705	0	conserved hypothetical protein		
AFLA_128060	AFLA_128070	-1	2856	504	1325545	1324111	1112	0	conserved hypothetical protein		
AFLA_128060	AFLA_128060	0	2856	503	1314426	1322999	0	1	polyketide synthase, putative		
AFLA_128060	AFLA_128050	1	2856	502	1313485	1312404	941	0	DUF341 domain oxidoreductase, putative		
AFLA_128060	AFLA_128040	2	2856	501	1312172	1310950	232	1	Major Facilitator Superfamily protein		

Cluster:50

Backbone_gene_id	Gene_id	Gene_positions		Chromosome-Contig	Gene_order		5'end	3'end	Gene_distance	Domain_score	Annotated_gene_function
AFLA_128170	AFLA_128170	0	2856	514	1361595	1364900	0	1	NRPS-like enzyme, putative		

AFLA_128170	AFLA_128160	1	2856	513	1357969	1360564	1031	1	Fungal specific transcription factor domain containing protein
AFLA_128170	AFLA_128150	2	2856	512	1355550	1356233	1736	1	hypothetical protein

Cluster:51

Backbone_gene_id	Gene_id	Gene_positions		Chromosome-Contig	Gene_order		5'end	3'end	Gene_distance	Domain_score	Annotated_gene_function
AFLA_129930	AFLA_129930	0	2856	690	1853766	1855767	0	1	3-oxoacyl carrier protein synthase, putative		
AFLA_129930	AFLA_129920	1	2856	689	1853373	1852018	393	0	agmatinase, putative		
AFLA_129930	AFLA_129910	2	2856	688	1849649	1850619	1399	0	RAS small monomeric GTPase Rab6, putative		
AFLA_129930	AFLA_129900	3	2856	687	1845774	1847810	1839	1	MFS siderophore transporter, putative		

Cluster:52

Backbone_gene_id	Gene_id	Gene_positions		Chromosome-Contig	Gene_order		5'end	3'end	Gene_distance	Domain_score	Annotated_gene_function
AFLA_135490	AFLA_135490	0	2911	441	1209037	1212252	0	0	nonribosomal peptide synthase, putative		
AFLA_135490	AFLA_135480	1	2911	440	1207576	1208112	925	0	conserved hypothetical protein		
AFLA_135490	AFLA_135470	2	2911	439	1206763	1205330	813	0	Pyridoxal-dependent decarboxylase, pyridoxal binding domain containing protein		
AFLA_135490	AFLA_135460	3	2911	438	1204397	1203084	933	0	hypothetical protein		
AFLA_135490	AFLA_135450	4	2911	437	1200602	1201774	1310	0	hypothetical protein		
AFLA_135490	AFLA_135440	5	2911	436	1199997	1198143	605	1	Cytochrome P450 family protein		
AFLA_135490	AFLA_135430	6	2911	435	1197282	1195553	861	1	Cytochrome P450 family protein		
AFLA_135490	AFLA_135420	7	2911	434	1194144	1195202	351	0	NmrA-like family protein		
AFLA_135490	AFLA_135410	8	2911	433	1193172	1190701	972	0	conserved hypothetical protein		
AFLA_135490	AFLA_135400	9	2911	432	1187408	1185764	3293	1	hypothetical protein		

Cluster:53

Backbone_gene_id	Gene_id	Gene_positions		Chromosome-Contig	Gene_order		5'end	3'end	Gene_distance	Domain_score	Annotated_gene_function
AFLA_137870	AFLA_137920	-5	2911	684	1887924	1886127	244	1	Major Facilitator Superfamily protein		
AFLA_137870	AFLA_137910	-4	2911	683	1884679	1885883	2354	0	monooxygenase-related		
AFLA_137870	AFLA_137900	-3	2911	682	1881887	1882325	1427	0	hypothetical protein		
AFLA_137870	AFLA_137890	-2	2911	681	1879744	1880460	1736	0	hypothetical protein		
AFLA_137870	AFLA_137880	-1	2911	680	1876855	1878008	1382	0	Lipase family protein		
AFLA_137870	AFLA_137870	0	2911	679	1868122	1875473	0	1	polyketide synthase, putative		
AFLA_137870	AFLA_137860	1	2911	678	1865851	1867182	940	0	hypothetical protein		
AFLA_137870	AFLA_137850	2	2911	677	1864603	1863441	1248	0	hypothetical protein		
AFLA_137870	AFLA_137840	3	2911	676	1862418	1861633	1023	0	hypothetical protein		
AFLA_137870	AFLA_137830	4	2911	675	1861345	1860472	288	0	To negative acting factor		
AFLA_137870	AFLA_137820	5	2911	674	1857823	1859636	836	1	metallo-beta-lactamase superfamily protein, putative		
AFLA_137870	AFLA_137810	6	2911	673	1857270	1855677	553	1	Major Facilitator Superfamily protein		
AFLA_137870	AFLA_137800	7	2911	672	1854366	1855107	570	0	hypothetical protein		
AFLA_137870	AFLA_137790	8	2911	671	1853040	1853610	756	0	hypothetical protein		
AFLA_137870	AFLA_137780	9	2911	670	1850177	1852591	449	1	ABC-2 type transporter family protein		

Cluster:54

Backbone_gene_id	Gene_id	Gene_positions		Chromosome-Contig	Gene_order		5'end	3'end	Gene_distance	Domain_score	Annotated_gene_function
AFLA_139410	AFLA_139500	-9	2911	841	2278117	2279969	440	1	Fungal specific transcription factor domain containing protein		
AFLA_139410	AFLA_139490	-8	2911	840	2265957	2277677	979	1	hybrid PKS/NRPS enzyme, putative		
AFLA_139410	AFLA_139480	-7	2911	839	2264978	2263609	499	0	dimethylallyl tryptophan synthase, putative		
AFLA_139410	AFLA_139470	-6	2911	838	2261743	2263110	3110	0	hypothetical protein		

AFLA_139410	AFLA_139460	-5	2911	837	2258633	2257028	2329	1	major facilitator superfamily protein
AFLA_139410	AFLA_139450	-4	2911	836	2254023	2254699	921	0	New cDNA-based gene: (AO_CDS_042706, novel, updateIDs: 12573, [gene: novel_gene_1311, model: novel_model_1311])
AFLA_139410	AFLA_139440	-3	2911	835	2252340	2253102	18	0	aflF / norB / dehydrogenase
AFLA_139410	AFLA_139430	-2	2911	834	2252322	2250833	371	0	aflU / cypA / P450 monooxygenase
AFLA_139410	AFLA_139420	-1	2911	833	2250462	2248242	1659	1	aflT / aflT / transmembrane protein
AFLA_139410	AFLA_139410	0	2911	832	2239960	2246583	0	0	aflC / pksA / pksL1 / poleketide synthase
AFLA_139410	AFLA_139400	1	2911	831	2239550	2238777	410	0	aflCa / hypC / hypothetical protein
AFLA_139410	AFLA_139390	2	2911	830	2238324	2237281	453	1	aflD / nor-1 / reductase
AFLA_139410	AFLA_139380	3	2911	829	2230826	2235970	1311	1	aflA / fas-2 / hexA / fatty acid synthase alpha subunit
AFLA_139410	AFLA_139370	4	2911	828	2230136	2224290	690	0	aflB / fas-1 / fatty acid synthase beta subunit
AFLA_139410	AFLA_139360	5	2911	827	2221686	2223020	1270	1	aflR / apa-2 / afl-2 / transcription activator
AFLA_139410	AFLA_139340	6	2911	826	2220947	2219496	739	0	aflS/ pathway regulator
AFLA_139410	AFLA_139330	7	2911	825	2218928	2217954	568	1	aflH/ adhA/ short chain alcohol dehydrogenase
AFLA_139410	AFLA_139320	8	2911	824	2217172	2216171	782	0	aflJ/ estA/ esterase
AFLA_139410	AFLA_139310	9	2911	823	2215880	2214407	291	0	aflE/ norA/ aad/ adh-2/ NOR reductase/ dehydrogenase
AFLA_139410	AFLA_139300	10	2911	822	2213781	2212881	626	1	aflM/ ver-1/ dehydrogenase/ ketoreductase
AFLA_139410	AFLA_139290	11	2911	821	2212268	2212651	230	0	aflMa/ hypE/ hypothetical protein
AFLA_139410	AFLA_139280	12	2911	820	2212022	2210319	246	1	aflN/ verA/ monooxygenase

AFLA_139410	AFLA_139270	13	2911	819	2209882	2209493	437	0	aflNa/ hypD/ hypothetical protein
AFLA_139410	AFLA_139260	14	2911	818	2207673	2209264	229	1	aflG/ avnA/ ord-1/ cytochrome P450 monooxygenase
AFLA_139410	AFLA_139250	15	2911	817	2205644	2207305	368	1	aflL/ verB/ desaturase/ P450 monooxygenase
AFLA_139410	AFLA_139240	16	2911	816	2204914	2205455	189	0	aflLa/ hypB/ hypothetical protein
AFLA_139410	AFLA_139230	17	2911	815	2203883	2204843	71	0	aflI/ avfA/ cytochrome P450 monooxygenase
AFLA_139410	AFLA_139220	18	2911	814	2202376	2203709	174	1	aflO/ omtB/ dmtA/ O-methyltransferase B
AFLA_139410	AFLA_139210	19	2911	813	2199609	2201242	1134	1	aflP/ omtA/ omt-1/ O-methyltransferase A
AFLA_139410	AFLA_139200	20	2911	812	2198596	2196236	1013	1	aflQ/ ordA/ ord-1/ oxidoreductase/ cytochrome P450 monooxigenase

Cluster:55

Backbone_gene_id	Gene_id	Gene_positions		Chromosome-Contig	Gene_order		5'end	3'end	Gene_distance	Domain_score	Annotated_gene_function
AFLA_139670	AFLA_139660	1	2911	857	2328209	2328721	103	0	hypothetical protein		
AFLA_139670	AFLA_139650	2	2911	856	2326370	2326089	1839	0	hypothetical protein		
AFLA_139670	AFLA_139640	3	2911	855	2324840	2324460	1249	0	hypothetical protein		
AFLA_139670	AFLA_139630	4	2911	854	2320176	2324124	336	1	ABC multidrug transporter, putative		
AFLA_139670	AFLA_139620	5	2911	853	2316403	2318184	1992	1	Amino acid permease family protein		
AFLA_139670	AFLA_139610	6	2911	852	2314230	2311922	2173	0	conserved hypothetical protein		
AFLA_139670	AFLA_139600	7	2911	851	2310748	2311455	467	0	hypothetical protein		
AFLA_139670	AFLA_139590	8	2911	850	2309635	2310636	112	0	hypothetical protein		
AFLA_139670	AFLA_139580	9	2911	849	2307690	2306248	1945	1	gluconolactone oxidase, putative		
AFLA_139670	AFLA_139570	10	2911	848	2303196	2303633	2615	0	hypothetical protein		

AFLA_139670	AFLA_139560	11	2911	847	2302374	2300224	822	1	Fungal	specific	transcription	factor domain containing protein